SOURCE CHARACTERIZATION AND GEOCHEMICAL SIGNATURE OF TRACE METALS IN THE KERALA COAST AND ADJOINING CONTINENTAL SHELF OF SOUTHEASTERN ARABIAN SEA

Thesis submitted to
Cochin University of Science and Technology
in partial fulfilment of the requirements
for the degree of
Doctor of Philosophy
in
Marine Chemistry
Under the Faculty of Marine Sciences

by

ELDHOSE CHERIYAN
Reg. No. 4830

DEPARTMENT OF CHEMICAL OCEANOGRAPHY
SCHOOL OF MARINE SCIENCES
COCHIN UNIVERSITY OF SCIENCE AND TECHNOLOGY
COCHIN 682016

June 2017

Source Characterization and Geochemical Signature of Trace Metals in the Kerala Coast and Adjoining Continental Shelf of Southeastern Arabian Sea

Ph.D. Thesis under the Faculty of Marine Sciences

Author

Eldhose Cheriyan
Research Scholar
Department of Chemical Oceanography
School of Marine Sciences
Cochin University of Science and Technology
Cochin 682016
Email id: eldhosecheriyan@cusat.ac.in
eldhosecheriyanm@gmail.com

Supervising Guide

Dr. Sujatha C.H
Professor
Department of Chemical Oceanography
School of Marine Sciences
Cochin University of Science and Technology
Cochin 682016
Email id: drchsujatha@yahoo.co.in

Department of Chemical Oceanography
School of Marine Sciences
Cochin University of Science and Technology
Cochin 682016

June 2017

Cochin University of Science and Technology
School of Marine Sciences
Department of Chemical Oceanography

Dr. Sujatha C.H
Professor

Fine Arts Avenue
Cochin, Kerala - 682 016, India
Tel: +91 484 2382131 (0)
Mob: 9995991778
Fax: +91 484 2374164
E-mail: drchsujatha@yahoo.co.in

Certificate

This is to certify that the thesis entitled ***"Source Characterization and Geochemical Signature of Trace Metals in the Kerala Coast and Adjoining Continental Shelf of Southeastern Arabian Sea"*** *is an authentic record of the research work carried out by Mr. Eldhose Cheriyan, under my supervision and guidance at the Department of Chemical Oceanography, School of Marine Sciences, Cochin University of Science and Technology, Cochin 682016, in partial fulfilment of the requirements for Ph.D degree of Cochin University of Science and Technology and no part of this has been presented before for any degree in any university. All the relevant corrections and modifications suggested by the audience during the pre-synopsis seminar and recommendations by doctoral committee of the candidate have been incorporated in the thesis.*

Cochin 682016
June 2017

Dr. Sujatha C.H
(Supervising Guide)

Declaration

I hereby declare that the thesis entitled **"Source Characterization and Geochemical Signature of Trace Metals in the Kerala Coast and Adjoining Continental Shelf of Southeastern Arabian Sea"** is an authentic record of the research work carried out by me under the guidance and supervision of Dr. Sujatha C.H, Professor, Department of Chemical Oceanography, School of Marine Sciences, Cochin University of Science and Technology and no part of this has previously formed the basis of the award of any degree, diploma, associateship, fellowship or any other similar title or recognition from any University/Institution.

Cochin 682016
June 2017

Eldhose Cheriyan

Dedicated to
My beloved brothers and sisters

Acknowledgements

GLORY TO GOD...

The lord God made all this things possible.......

I am deeply grateful to my beloved supervising guide, Professor Dr. Sujatha C.H, who stood aside me as a teacher, mentor, friend and guide from the beginning of my research life. Her kindness and dearness, inspired me to continue my studies and also for expanding my aptitude to true research. I express my sincere gratitude for her patient supervision, warm relationship and understanding from the first day to the very last. Furthermore, I would like to thank her for giving me the opportunity to take part in research cruises in the course of the Ph.D.

I am thankful to Emeritus Professor Dr. N. Chandramohanakumar and Professor & Head Dr. S. Muraleedharan Nair for their support, advice and encouragement at each stage of my work. I also thank Dr. Habeeb Rahman K., Assistant Professor, Department of Chemical Oceanography for his help and support during the course of my research.

I greatly acknowledge the financial support by the Ministry of Earth Sciences (MoES), Government of India through the Centre for Marine Living Resources and Ecology (CMLRE), Kochi by grant number MoES/CMLRE/10-MMME/02/2012, as a JRF in the project entitled "Quantification of trace metals and its counter parts as an interlocking system for revealing the sediment/water/air status in the southern tip of peninsular India" during 2012-2015.

My parents always supported and motivated even in their hardships allowing me to choose the best in life. The moral support and prayers by my father and mother helped me to be peaceful, happy and healthy during the entire course of this research.

I am very much grateful to Mr. Binoy C. Nedumpuram and family, for their prayers as well as vital support and incitement throughout the years.

I am grateful to Dr. K. Sajan, Director, School of Marine sciences and Dr. A.N Balchand, Dean, Faculty of Marine sciences for the support and facilities provided for the study.

I am grateful to all the scientists and crews of FORV Sagar Sampada (Cruise No. 316, 318 and 332) and R/V King Fisher for their help in the sampling. I also acknowledge the services rendered by SAIF lab, STIC, Cochin for CHNS and metal analyses.

I want to greatly acknowledge the services, support and togetherness received from my fellow researchers Mr. Mrudulrag S.K and Mrs. Athira Sreekanth, during sampling, processing and analyses of samples.

I thank Dr. Shaiju P, Technical Assistant, Department of Chemical Oceanography who was always available when I needed advice and help.

Special thanks go to Dr. Manju P. Nair and Dr. Akhil P.S for sharing elementary ideas and the basics of many techniques involved in monitoring and analyses of environmental samples.

I express my gratitude to Dr. Salas P.M, Post Doctoral Fellow, Ms. Saritha S, Senior Research Fellow and Mrs. Ragi A.S, Senior Research Fellow, Department of Chemical Oceanography for their unconditional support, practical experimental tips, flaring smile and discussions.

I acknowledge Dr. Gireesh Kumar T.R, Scientist, NIO (RC), Kochi and Dr. Deepulal P.M, Post Doctoral Fellow, Department of Chemical Oceanography for sharing their ideas and comments without reservation.

I sincerely acknowledge the support of all the research scholars and my dear friends in the Chemical Oceanography department for their constant solace and encouragement. My heartfelt thanks to Dr. Sanil Kumar K.S, Dr. Ratheesh Kumar C.S, Dr. Pratheesh V.B, Dr. Renjith K.R, Dr. Manju Mary Joseph, Dr. Bindu K.R, Dr. Nebula Anilkumar, Jyothish Kumar T, Libin Baby, Dr. Gayathreedevi P.K, Dayala V.T, *Dr. Renjitha Raveenderan, Shibini Mol P.A, Dr. Byju K.P, Dr. Resmi P, Dr. Manju M.N, Movitha Mohandas, Leena P.P, Ramzi A Rahman, Sudheesh V, Renjith P.K, Dr. Prashob Peter K.J, Dr. Kala K. Jacob, Nisa K.G, Dibu Divakaran, Manu Mohan, Shameem K, Arsha Krishnan, Divya K.R, Moushmi K.S, Muhammed Akber, Jacob Joshuva, Jyoti Varier and Nisari A.R.*

I sincerely thank Mrs. Geetha Menon and other staffs of the Department of Chemical Oceanography and in the administration of Cochin University of Science and Technology for their careful and timely support during the period of my research. I thank the Librarian and staff, School of Marine Sciences Library for their valuable cooperation.

I am grateful to my beloved sister Ms. Anu Susan Cheriyan, my relatives and all my friends who supported and encouraged me in this venture.

I express my greatest gratitude to all the sisters and brothers in my church who are praying for my successful completion of research.

Eldhose Cheriyan

Preface

The time has changed, humans interpreted a lot in environmental research but the multitude of anthropogenic intervention is ever increasing. The wetlands, estuaries, watersheds and coastal zones holding high flux of ecological and socio-economic potential on the one hand and high rates of deterioration on the other hand are of a particular concern in this 21st century. Concern on planet is worth in the arena of scientific expeditions but the progress of our knowledge should help to improve the understanding of fundamental concepts regarding environment especially the marine environment. Environmental monitoring today became a symptom of greater environmental pollution especially in estuaries and coastal zones possessing remarkable economic potential and environmental background. Natural and anthropogenic stresses on environments all around the world are almost similar, but characterization of individual factors depending on geographical locations are quite essential for a quantitative evaluation of coastal ecosystems. External impacts on aquatic systems should not be represented as a single focal point as human induced hazards, but it should be distinguished and described in a much better level of source specific mode of disturbance, for example, flow regulation of river systems by use of dams or effluent inputs from industries, both have significant role in environmental settings. The scientific research on estuarine and coastal systems are complete and comprehend nevertheless, it pledges the credible effects and societal benefits on life and livelihoods in regional or rather in a global scenario.

Trace metals play an important role in oceanography as participants in and as tracers of processes of fundamental interest. They serve important roles as regulators of ocean processes, including marine ecosystem dynamics and carbon cycling. Among them a quite few in numbers viz., Fe, Zn, Mn and Cu serve as essential micronutrients, the availability of which influences the physiological state and, both on the biochemical and metabolic activity of marine organisms. Other trace elements (e.g., Cd, Pb and perhaps Hg) are influenced by global-scale anthropogenic emissions. Knowledge of these processes that control the transport and fate of these pollutants is an important aspect of protecting the ocean environment. Some of these are harmful to the natural and human environment due to their behaviour of toxicity and/or radioactivity. The large-scale distribution of these trace elements is, however, poorly known and represents a major barrier to understanding their biogeochemical role in the Earth system. Our understanding of the regional biogeochemical cycle of many trace elements has not advanced as much as might be expected as its type, and their functions that they perform. The various fluxes of trace metals in an aquatic ecosystem are controlled not only by physical forcing by the river discharge, tidal currents, resuspension and sedimentation, but also by the often high rates of biological and abiological degradation and remineralization patterns. In the present scenario, it has been not sufficient to think of trace elements simply as "conservative", "nutrient-like" or "scavenged" but there is a growing appreciation that more region specific geochemical process-based descriptions are required and the present study would highlight a strong correlation pattern with all these chemical identities. More significantly, the present study would provide a good knowledge of the spatial distribution of these distinguished conquering trace elements.

Coastal zone including the continental shelf are highly dynamic and complex by nature which may act as a major transition zone for upstream-downstream linkages effectively experience impacts both from the landward and the seaward side, resulting in source induced biogeochemistry and physico-chemical properties at the interface between land and sea. Investigation on the biogeochemistry of the continental shelf provides a better understanding of both the marine and terrestrial sources and helps to link the two together. Marine sediments are the fundamental data source for gathering information on seabed character, depositional history and environmental change. They provide raw data for a wide range of research findings including studies of global change, paleoceanography, oil exploration, pollution assessment and control. The Indian subcontinent is blessed with a long stretch of coastal zone that supports a variety of lowlands having lively fragile ecosystems. These ecosystems widely known as wetlands, backwaters, lagoons, estuaries are not significantly monitored considering its tangible economic diversity and are largely confronted with anthropogenic activities. The rapidly expanding human population, large-scale changes in land use/land covers, burgeoning development projects and improper use of watersheds have caused alterations in sources, composition and accumulation of trace elements in aquatic systems. The successive increase of chemical strength in rivers and other water bodies resulted from the enhanced discharge of industrial effluents and municipal waste water, which have become the major problem affecting the water quality of the aquatic system. Interestingly, the continental shelf along Southwest India is a major fishing zone with more than 300 species and monitoring of trace elements should be carried out due to metal toxicity, non-biodegradability and bioaccumulation. Our understanding of the chemical and physical oceanographic processes occurring in this type of ecosystem has increased from fragmentary elements during recent years, but only limited information is available regarding metal enrichment geochemistry towards South India especially in the marine environment bordering Kerala.

Following this, the thesis entitled "**Source Characterization and Geochemical Signature of Trace Metals in the Kerala Coast and Adjoining Continental Shelf of Southeastern Arabian Sea**" deals with the sources and geochemistry of metals in the shallow marine environment, from the coastal and estuarine region of Kerala extending to the continental shelf of Southeastern Arabian Sea. Therefore, the distribution of this constituent would appreciate the intercompartmental relationships between these elements with other physicochemical parameters. Besides, the study would contribute and encompass the sources of these elements and the biological processes regulating their distribution. The study endeavours to cover the significant sources and corresponding metal enrichment in the coastal and estuarine region through natural or anthropogenic disturbances. To fulfill this assignment, it has taken to the extent of a comparative assessment of metal interrelationships and normalization with different sediment backgrounds, to remark its geochemical influence in the present realm. However, the study utilized the combined implementation of geochemical indices and statistical methods to scientifically pinpoint the source characterization of trace metals for adopting better strategies in the conservation of coastal ecosystems. This regional study demonstrates the geochemical association of metal in terms of spatial variability in sources and concentration, carefully separated and interpreted to produce insightful findings on marine environmental research.

The thesis has been divided into six chapters. The following is a brief overview of each chapter in the thesis.

Chapter 1 introduces a general outline of the research on metals, the importance of monitoring the environment and its transport and fate in the marine realm. It also addresses the previous studies, significance, fundamental aims, objectives and scope of the present study.

Chapter 2 gives an overview of the study region and the methodology adopted for the analysis of water and sediment samples. It also describes the hydrological, geological and anthropogenic set up of the area. Further, it includes the precision and accuracy of metal analyses, statistical methods adopted for data interpretation, geochemical indices for assessing metal enrichment and ecological risk assessment methods.

Chapter 3 aims to determine the metal distribution background using sediment cores in the Kerala coast. It is essential to distinguish the anthropogenic perturbation from natural sources of metals by analyzing core sediments from the region. Hence, the distribution profile of trace metals in the core sediments retrieved from Cape Comorin and the Cochin estuary are presented in this chapter.

Chapter 4 describes the spatial variability, controlling factors and potential risk of selected metals in the coastal and estuarine sediments along the Kerala coast. The degree of metal contamination is assessed using geochemical indices by normalizing with background metal levels determined in the field observations. Statistical techniques such as principal component analysis were applied to find out the factors affecting the trace metal behaviour. Cluster analysis, which groups the sampling stations based on the metals and other geochemical variables, is also adopted in this chapter.

Chapter 5 describes the spatial variability and sources of trace elements in the shelf sediments of Southeastern Arabian Sea along Kerala coast. It also deals with the sources, nature and quality of sedimentary organic matter deposited from in situ biological production and terrestrial sources. Multivariate statistics are employed to ascertain the association of metals and for correlating the metal levels with bulk sediment properties.

Chapter 6 portrays the geochemistry of trace metal enrichment in the continental shelf sediments through a comparative approach. It discusses the authigenic and biogenic metal enrichment processes along with a comparative assessment of metal enrichment using different background levels with reference to Al normalization. Toxicity associated with metals in the sediment to the aquatic organisms is assessed using ecological risk assessment methods. This chapter also compares the toxic metal levels in the study region with other globally impacted coastal systems.

Finally, summary and conclusions comprise the salient features and major findings of the preceding chapters. Recommendation for areas of further research arising from this investigation is also detailed in this section.

References are provided at the end of each chapter. The publications are incorporated at the end following the summary and conclusions.

Contents

Chapter 3 Metal Distribution Background Using Sediment Cores --65-98

LIST OF ABBREVIATIONS

AAS	Atomic Absorption Spectrophotometer
Avg	Average
BDL	Below Detectable Level
BPC	Biopolymeric Carbon
BSA	Bovine Serum Albumin
HCA	Hierarchical Cluster Analysis
Carot	Carotenoids
CF	Contamination Factor
Chl-a	Chlorophyll-a
Chl-b	Chlorophyll-b
Chl-c	Chlorophyll-c
CHO	Carbohydrates
CTD	Conductivity Temperature Depth
DO	Dissolved Oxygen
EEZ	Exclusive Economic Zone
EF	Enrichment Factor
ERL	Effective Range Low
ERM	Effective Range Medium
FORV	Fisheries Oceanographic Research Vessel
ICP AES	Inductively Coupled Plasma Atomic Emission Spectroscopy
I_{geo}	Geoaccumulation Index
LIP	Lipids
MMME	Monitoring and Modelling of Marine Ecosystems
Min	Minimum
Max	Maximum
NA	Not Available
ND	Not Detectable

OMZ	Oxygen Minimum Zone
PCA	Principal Component Analysis
Phaeo	Phaeophytin
PLI	Pollution Load Index
PRT	Proteins
PVC	Poly-vinyl Chloride
SPSS	Statistical Package for Social Sciences
SQG	Sediment Quality Guidelines
TC	Total Carbon
TH	Total Hydrogen
TIC	Total Inorganic Carbon
TOC	Total Organic Carbon
TS	Total Sulphur

Chapter

1 INTRODUCTION

Contents

1.1 General Introduction

Coastal zone is an area that has been defined as the junction between two major ecosystems where the terrain links the ocean. It has been regarded as an area of intense hydraulic, depositional, chemical and biologically mediated activities since many processes in both environments are intensified at this boundary. Coastal plains and seas include the most taxonomically rich and productive ecosystems on the earth. A coastal region is thus a place of hectic human activity, followed by intense urbanization, resulting in human interference of rapid development. So the coastal ecosystems are now highly disturbed and very much threatened due to encountering problems like pollution, siltation, erosion, flooding, saltwater intrusion, storm surges and other activities. They are important reservoirs for many pollutant constituents including metals derived from geological weathering, untreated factory effluents, agricultural and sewage discharges, and rapid urbanization established during recent periods (Gu and Lin, 2016). These anthropogenic inputs cause excessive eutrophication (Sujatha et al., 2009) and resulted in an overall decline in the livability of the coastal regions (Prasanthan et al., 2011).

Marine sediments can act as potential sinks and provenance of pollutants and contaminants in aquatic environment because of their set up of variable lithogenic, mineralogical and chemical properties. Evaluation of metals in the surficial sediment besides sediment cores of an environmental setting is useful in the estimation of past record of pollution (Hornberger et al., 1999; Karbassi and Shankar, 2005; Priju and Narayana, 2007; Kumar and Edward, 2009; Sundararajan and Natesan, 2010; Heimbürger et al., 2012; Santos et al., 2013; Nair et al., 2014; Gao et al., 2016; Prajith et al., 2016), bioavailability of contaminants to marine biota (Vangronsveld and Cunnihgham, 1998; Raveenderan and Sujatha, 2011; Gao et al., 2014; ShibiniMol et al., 2015; Gu et al., 2016; Ragi et al., 2017), physical and diagenetical changes in the sedimentary environment (Al-Masri et al., 2002; Spencer et al., 2003; Robert et al., 2004; Audry et al., 2006), anthropogenic sources on the coast (Akcay et al., 2003; Prego et al., 2008; Costa et al., 2011; Huang et al., 2012; Dsikowitzky et al., 2014; Salas et al., 2017) and natural metal background in the sediments (Zhou et al., 2003; Marmolejo-Rodriguez et al., 2007; Guerra et al., 2011). In addition, trace metals have been recorded to trace ancient changes in productivity and dissolved oxygen content since, hypoxic events occurring during productivity induced organic matter flux plays a vital role in the chemical speciation of elements in the marine environment (Pailler et al., 2002; Van der Weijden et al., 2006; Muñoz et al., 2012; Acharya et al., 2015). In upwelling regions, several biologically essential trace elements (Cd, Co, Zn, Ni, etc.) can be enriched in the sediment surface as a result of primary production and subsequent export and sedimentation of organic rich biogenic particles (Böning et al., 2004, 2005, 2009, 2015; Calvert and Pedersen, 2007). Thus, the studies on sediment biogeochemistry help us to link the marine productivity with organic matter preservation and fate of various components in the ocean, remarkably the trace element budget.

1.2 Major Sources and Sinks Influencing Metal Variability in Coastal Systems

Two fundamental aspects affecting the sediment geochemistry in aquatic ecosystems are oxygen content of the overlying waters and their topographic peculiarities. The physiographic features of coastal ocean are such that they receive land inputs from the surrounding terrestrial catchments tolerating shipping activities, industrial sectors, agricultural and aquaculture territories, discharging materials through fluvial and airborne modes. The bottom sediments can be put forward as the final sink for all the particles/compounds entering or sustaining in the ocean. Thus, the ocean surface sediments can be judged as a combination of metal enriched detrital minerals as well as metal exported from solution associated with non-crystalline matrix. Coastal seas are repository of metals originated from river runoff, dry and wet atmospheric deposition, dissolution/precipitation due to diagenetic changes and upwelling juxtaposed with high biological production (Chester, 2000). The residence time of metals in the ocean depends on their morphology as ionic, complex form or as fraction of the mineral matrix (Wangersky, 1986). Rivers play a crucial role in transporting materials to the coastal margins that involve dissolved and particulate components derived from geological weathering, land runoff, organic matter degradation, atmospheric deposition and nowadays, inputs from different pollution sources.

1.2.1 Mineralogical and Detrital Sources

The weathering of crustal minerals leds to the dispersal of trace metals in the marine environment. These mineralogical phases exist in association with complex humic suspensions and hydrous oxide particulates in the sedimentary surfaces. Trace elements may undergo exchange for other metal cations in silicate and other mineral lattices resulted from chemical weathering and contribute for significant metal content in the surface sediments (Alloway, 1990). Also, the negatively charged clay mineral particles as by product of rock weathering bear large surface area for the adsorption of positively charged metal cations. Moreover, the tropical regions are vulnerable to weathering compared to arid areas and there is every chance of detrital enrichment of metals in deposited sediments (Whitten and Brooks, 1972).

1.2.2 Anthropogenic Sources

The important anthropogenic sources imparting metal pollution in the environment are described in Table 1.1. The paramount anthropogenic source of metal contamination is mining activity and smelting which have been increased at a rapid rate with the era of industrialization and development. During this industrial era, metals have been accounted as toxic environmental pollutants causing cytotoxic, mutagenic and carcinogenic effects posing severe threats to aquatic fauna and flora and may possibly transfer to higher trophic levels (More et al., 2003). However, the mobilization and bioavailability of toxic metal of interest depends on its distribution pattern and adsorption coefficients on a wide range of adsorbent medium (Vega et al., 2006; Vidal et al., 2009). Riverine and atmospheric input are considered predominant to intense tropical coastal plains bordered by industrial zones. Again, the direct riverine discharge of untreated/partially treated pollutants and effluents occur locally in several environments have been clearly accounted. Many researchers have extensively studied similar areas like Cochin backwaters (Balachandran et al., 2005; Deepulal et al., 2012; Shivaprasad et al., 2013; Akhil and Sujatha, 2014; Dsikowitzky et al., 2014; Ciji and Nandan, 2014; Bindu et al., 2015; Salas et al., 2017) and reported the local components influencing the hazardous organic/ inorganic contaminants discharged from significant economic and domestic sectors. Recently, many authors suggest that the bioavailability of metals to aquatic organisms is high in estuaries and adjoining shelf compared to the deep ocean due to the input of anthropogenic metals (Birch and Apostolatos, 2013; Lin et al., 2016). Post-depositional changes by bioturbation, seasonal floods, tidal currents, mining, etc. can result in sediment reworking and resuspension leading to the release of toxic contaminants into the water column, which may pose a serious ecological risk to the coastal marine ecosystem (Diagomanolin et al., 2004; Larrose et al., 2010; Morelli and Gasparon, 2015).

Table 1.1: Distribution, toxicity and major sources of anthropogenic metal pollution in the marine environment (Bashkin, 2006).

Metals	Anthropogenic sources	Distribution and toxicity
Cd	Mining and smelting, Metal finishing and Microelectronic industries, Fossil fuel combustion, Fertilizers	Very toxic and widely distributed
Cu	Pyrometallurgical industries, Agricultural manures, Wood preserving, Waste disposal viz., sewage sludge, scrapheaps, urban/industrial incineration plants	Very toxic and widely distributed
Co	Mining and processing of ores, Plastic industries, Phosphate fertilizers	Very toxic and widely distributed
Cr	Metal finishing industries, Wood processing units, Leather processing, Petrochemical refineries, Sewage sludge, Textile production	Very toxic and widely distributed
Fe	Waste disposal, Leachate from land fill, Dredging, Corrosion of metals	Low toxic and widely distributed
Mn	Pyrometallurgical industries, Fertilizers, Manures, Pesticides, Sewage sludge	-
Ni	Steel and iron industry, Metal finishing, Pyrometallurgical industries, Microelectronics, Sewage sludge	Very toxic and widely distributed
Pb	Atmospheric deposition, Mining and smelting, Waste disposal on land, Agriculture, Electronics, Oil and coal combustion plants	Very toxic and widely distributed
Zn	Rubber and plastic production, Discharge of domestic wastewaters, Coal-burning power plants, Fertilizers, Manures, Fungicides, Zinc-based anti-corrosion and anti-fouling paints	Very toxic and widely distributed

1.3 Geochemical Factors Affecting Trace Metal Cycling

In considering the cycling of most metals, the particulate and dissolved phases possess predominant control over the edges of ocean waters. The particulate phase includes suspended inorganic/organic matrix containing living and dead fractions in river channels and coastal waters, and aerosol particulate matter in the atmosphere. Most of particulate components reaching from the continents is retained in the estuaries and backwaters adjoining to the coastal ocean. Thus, estuaries act as geochemical reactors and the different physical oceanographic processes occurring within them determine the fate and transport of particulates to the sea. Further, the continental shelf retains most of particulates discharged into the sea and the dissolved metals are carried to the open ocean (Caccia and Millero, 2003). Moreover, the particulate fraction may record minimum in the water column supporting rapid advective processes due to degradation, as it sinks to the bottom sediments.

In marine settings, the sedimentary organic matter comprises the organic component in sediments derived mainly from various organisms at different degradation stages such as lipids, amino acids, carbohydrates, humus, black carbon, etc. (Kögel-Knabner, 2002). Organic matter deposition evolved from allochthonous and autochthonous sources depend on water column properties such as oxygen content, sedimentation rate, hydrodynamic balance of fine sediments and productivity enhanced biogenic matter. Noteworthy, the organic matter degradation indirectly controls the shift of trace elements in the oceans and eventually important in the movement of essential micronutrients. The oxygen consumption during organic matter diagenesis plays a principal role in metal mobility in the marine sector. The more reactive portion will be remineralized easily and the remaining refractory component is settled to the sediments. When remineralization dominates over organic matter preservation prior to deposition, less than 1% of total organic carbon produced is buried in the sediments. Hence, the quantification of trace metals in the sea shelf signals the biogeochemical processes accomplished through external fluvial and air borne particulates and internal circulation pathways, a factor of major geochemical cycles.

Generally, the internal geochemical processes viz., export flux of high marine productivity, residence time, hydrothermal sources and reaction of deep water circulations may superimpose the external environmental factors influencing trace element framework in the marine realm. The in situ chemical interactions have a crucial part in generating lithogenic materials composed of crustal rocks mainly quartz, feldspar, sulphides, humic particulates, clay minerals and hydrogenous forms such as Fe and Mn oxides (Turner and Millward, 2002). Hence, the metal mobility in the sediments is related to various geochemical constituents chiefly organic matter content, Fe/Mn oxyhydroxides, carbonates, sulphides and granulometric properties (Ho et al., 2013).

1.3.1 Importance of Upwelling Regimes

Upwelling regions are generally distinguished in terms of severe oxygen depletion; creates oxygen minimum zone, which is important at areas along the continental margins (Suess and Thiede, 1983). An upwelling zone like margins of Arabian Sea along west coast of India accounts for 5% of global primary production exhibiting periodical oscillations in nutrient sources, biological productivity rates and phytoplankton abundance (Qasim, 1982; Cowie, 2005; Habeebrehman et al., 2008). Phytoplankton photosynthesis generates vast amount of particulate biogenic matter in the sea surface utilizing dissolved inorganic carbon and other nutrient elements (Hupe and Karstensen, 2000). As a cycle, remineralization occurring in the sub-surface waters is the basis for the release of dissolved inorganic carbon and nutrients to the overlying surface layer. The externally produced particulates and internally generated particulates of primary production have strong controls in surface waters mainly in upwelling regimes. The water column movement and degradation of biogenic particles derived from primary productivity are the principal factors controlling the fate of trace elements in such environments. Biologically mediated chemical reactions occur during the transport of organic matter supply together with the presence of primary and secondary oxidants such as O_2, NO_3^{-}, Mn^{4+}, Fe^{3+} and SO_4^{2-}. The biological activity due to high primary production and subsequent rate of organic matter degradation, exceeds the rate of oxygen supply impinging suboxic/anoxic conditions in the water column and at the interface of sedimentary surfaces. Degradation of deposited organic matter by microorganisms utilizing oxidizing agents initiates early diagenetic processes. During diagenetic processes oxic environments are characterized by the consumption of dissolved oxygen as oxidant. On the other hand, suboxic and anoxic conditions are impinged through the utilization of secondary oxidants namely nitrate, Fe and Mn oxides, and sulphates (Alagarsamy et al., 2005). Therefore, the degradation index and sedimentation rate influence the transport and fate of chemical elements in the water column. Noteworthy, the sedimentary surface undergoes considerable sediment reworking and suspension during upwelling which have great a impact on the diffusion/precipitation of trace metals (especially Fe and Mn) and their corresponding enrichment/depletion in the sediments. For example, Mn is highly mobile in reducing environments and has been used to remodel past variation in bottom water oxygen conditions (Calvert and Pedersen, 1993; Lewis and Luther III, 2000). The microbial degradation of labile organic matter induces reduction of Mn(IV) to Mn(II) in the water column and surface sediment layers underlying areas of high primary productivity. Furthermore, the sedimentary components adsorb the organic particulates and subsequently found as organic layer, which is important in initiating biochemical reactions. Hence, the global significance of Arabian Sea is that, the seasonal upwelling, biological production and subsequent biogenic particle flux induce suboxic and anaerobic mechanisms in the water column (Naqvi et al., 2005; Cowie, 2005) which are considered as dominant in the cycling and accumulation of key trace elements and initiation of biogeochemical processes, stimulating substantial alteration in the geochemistry of oceans.

1.4 Trace Element Geochemistry in Marine Systems

The coastal areas are intermediate zones of physical, chemical and biological processes between terrestrial and freshwater environments which exerts significant influence on the transport and deposition of metals (Bianchi and Allison, 2009; Wu et al., 2011). Trace metals in the marine environment have the characteristics of enhanced concentration levels than their terrestrial counterparts mainly due to their involvement in complex physical, chemical and bio-cycling processes in the sea (Alagarsamy, 1997). As water column is concerned, the significant association of dissolved metals with biologically produced detritus especially in areas of high primary production, hydrogenous precipitates, etc. can boost its transport as settling particles to the ocean floor. Contrastingly, the sediment reworking effected through biogeochemical processes viz., upwelling as deep as 200 m depth, organic matter diagenesis, etc. can remarkably alter the state of sedimentary bound metal species and induce the transport to the overlying water column. As explained earlier, the geochemistry of elements in the ocean can be altered with respect to factors viz., river runoff, atmospheric deposition, diffusion from sedimentary column, etc. while the upwelling phenomenon also responsible in certain coastal ecosystems.

Cd shows nutrient type behaviour in the water column similar to labile nutrients such as phosphate, nitrate and organic carbon. Organic detritus produced during upwelling of cold nutrient subsurface waters adsorbs Cd which leds to its depletion in the surface water (van Geen et al., 1995; Dean et al., 2006). The sinking carrier phases may decompose/settles to the bottom thereby increasing the concentration of metal in the overlying waters and surface sediments (Knauer and Martin, 1981; McCorkle and Klinkhammer, 1991; Nameroff et al., 2002; Brumsack, 2006). In anoxic environments, the metal complexes with micro quantities of free sulphur precipitating as sulphides and get accumulated in the sediments (Rosenthal et al., 1995). No doubt, Cu is an essential micronutrient to marine organisms which take part in its metabolic activities. Primary productivity is the major source of metal to the surface waters and settling of scavenged metal to the bottom increases its concentration in the sediments. In anoxic sediments, Cu may preferably associate with sulphur and form insoluble sulphides to get transported to the sea floor whereas it is found as metal oxides in oxic conditions (Hellio and Yebra, 2009). Further, the abundance of specific metals viz., Cu and Zn in the sea water is sometimes concurrent with the metal accumulation in organic rich sediments (Goldschmidt, 1954).

Chromium normally exist under two oxidation states viz., Cr(III) and Cr(VI) and the oxidation of Cr species is effected by Mn oxyhydroxides (MnOOH) in the aquatic environment. However, Cr reduction is established as probably affected by redox reactions in oxygen depleted water layers (Graham and Bouwer, 2009). Although, Cr species is found to be stable at reducing environments; sub-surface scavenging deplete its concentration in waters while an enrichment in surface sediments with respect to organic matter accumulation. Fe poses nutrient and scavenging type properties in ocean waters and under certain circumstances this element can be mobile during diagenesis (Rubio et al., 2010, Álvarez-Iglesias and Rubio, 2012). Fe and Mn distribution is notably altered by in situ redox processes resulting from organic matter decomposition at the sediment water interface. Oxygen minimum zones in the ocean can cause depletion and diffusion of Mn out of the sedimentary surfaces while insoluble Fe sulphides get precipitated with regard to oxygen minima (Klinkhammer and Bender, 1980). Ni is nutrient type in the ocean exhibiting similarities to both phosphate and silicate fractions in the water column (Sclater et al., 1976). Recent study by Twining et al. (2012) and Böning et al. (2015) suggest that Ni cycling is preferably controlled by high concentrations in marine plankton viz., diatoms incorporating onto organic tissues and opaline frustrules. In contrast to other nutrient elements such as Cd, Cu and Zn, Ni does not complex with sulphides even under reducing conditions due to kinetic instability (Morse and Luther III, 1999) and earlier studies in different environment suggested that the element is brought to the bottom with settling biodetritus (Brumsack, 1989; Van der Weijden et al., 2006).

Pb input to the ocean surface has been attributed to aeolian inputs rather than fluvial mechanism (Echegoyen et al., 2014; Chen et al., 2016). For instance, it shows surface enrichment and depth depletion behaviour in the marine environment. Previous literature suggests that the intensity of atmospheric input of Pb is sufficient to cause surface enrichment in coastal margins. The metal may be removed from the water column through particle scavenging reaching the bottom sediments (Desenfant et al., 2006; Inoue and Tanimizu, 2008). Zn has been considered as marine refractory nutrient element having distribution similar to that of silicate in the water column (Conway and John, 2014; Zhao et al., 2014). The metal shows surface depletion caused by the adsorption to less labile fractions of marine plankton and enrichment in the deep sediment water interface (Lohan et al., 2002; John and Conway, 2014). However, the nutrient elements associated with biological plankton in high concentrations may not always found to bind with the organic fraction after burial in the sediments (Brumsack, 2006). Further, these elements as a result of organic matter degradation followed by bacterial sulphate reduction and production of H_2S form sulphides in the depositional environment (Zheng et al., 2000; Tribovillard et al., 2006).

1.5 Anomalies in Assessing Metal Enrichment

Enrichment factor (EF), geoaccumulation index (I_{geo}) and contamination factor (CF) are the widely used geochemical indices to assess trace metal contamination in various aquatic environments. Generally, the metal enrichment and contamination is characterized with respect to the corresponding background metal concentration estimated in similar environmental settings. To carefully assess the toxic metal enrichment pattern affected by local components, one should knows the regional background of the metal. Many authors have suggested that the determination of metal contamination of a region should be verified by normalizing the observed metal values with that of texturally and mineralogically equivalent unpolluted long sediment cores (Gibbs, 1993; Rubio et al., 2000; Caeiro et al., 2005; Yang et al., 2012; Zalewska et al., 2015). In several cases, the metal contamination in a particular environment computed using shale average, crustal abundance, etc. as reference baselines (Turekian and Wedepohl, 1961; Taylor, 1964) should be verified in terms of regional background (Table 1.2) or core sediment in the region (Covelli and Fontolan, 1997). It is difficult to reasonably explain the metal contamination in the surface sediments with a single normalization by crustal background since, it does not account for the local lithology and regional sediment properties (Abrahim and Parker, 2008). Therefore, it is essential to describe the regional sediment composition to judge effectively the metal enrichment of a particular area. Subsequently, a new set of geochemical normalization values can be generated using the regional metal composition to compare with the values of crustal background, average shale, etc.

Table 1.2: General background of metals adopted for calculation of geochemical indices and a regional background taken from a previous study conducted in the Western continental shelf of India.

Elements	Upper crustal abundance[1]	Average shale[2]	Crustal average[3]	Regional background[4]
mg kg^{-1}				
Cd	0.10	0.30	0.20	*NA
Co	10	19	25	10.38
Cr	35	90	100	99.59
Cu	25	45	55	29.3
Mn	600	850	950	430
Ni	20	68	75	45.4
Pb	20	20	12.50	11.81
Zn	71	95	70	68.67
Fe (%)	5.00	4.72	5.63	5.08
Al (%)	15.20	8.89	8.23	7.14

[1]Taylor and McLennan (1985), [2]Turekian and Wedepohl (1961), [3]Taylor (1964), [4]Varghese (2004)

*NA: not available

1.6 Aim and Objectives of the Study

The aim of the thesis is to assess the sources of trace metals and processes controlling the geochemistry of metal enrichment, as part of the

Monitoring and Modelling of Marine Ecosystems (MMME) programme in the Southeastern Arabian Sea, an exclusive economic zone (EEZ) of India. This region of Arabian Sea is interesting in that the summer and winter monsoons significantly alter the physical oceanography in the region, with the summer monsoon generating episodes of upwelling which promotes enhanced primary productivity. This productivity enhances the fishery reserve of the Indian EEZ. Globally, about 50% of the world fish catch comes from 0.1% of the upwelling zone reveals its importance (Ryther, 1969). The productivity induced suboxic zone in the water column has a major role in the associated biogeochemical processes. Further, the changes in redox conditions caused by oxygen depletion affects the transport mechanism of metals from the water column to the sediments and vice versa. There is also significant anthropogenic development in the coastal regions of Southwest India which may provide a source of trace metals to the sediments. Interestingly, the Southeastern Arabian Sea is a major commercial fishing zone that contributes 31.7% to annual marine fish production in India with more than 300 species (Vivekanandan et al., 2003; Abdurahiman et al., 2010; Suresh et al., 2015). Monitoring of trace elements is important due to metal toxicity, non-biodegradability and bioaccumulation since little monitoring of this type has been done over time in the region (Udayakumar et al., 2014). lnadequacies in the previous studies have been their proper addressing of the influence of oceanographic and sedimentary processes to the metal geochemistry. Further, such studies require increased density of sampling covering seasonal signals, which play an important role when coastal regions are considered. Therefore, an assessment approach on chemical pollutant constituent in an area is not complete unless it takes a serious concern in and around its portfolio since, these areas are important for business, trade and aquaculture.

Different sedimentary environments are considered to experience and show wide range of biogeochemical characteristics according to regional significance. Thus, the regional significance of this study is that the area has not been studied intensively so far and this data adds to the knowledge bias of monitoring studies carried out elsewhere in the Indian coast. Several researchers have reported the concentration of trace metals in the Cochin backwaters (Deepulal et al., 2012; Dsikowitzky et al., 2014; Bindu et al., 2015) but only a few have sampled the Kerala coast (Suresh et al., 2015) and used a regional background to assess the metal enrichment (Balachandran et al., 2003; Balachandran et al., 2005). Up to now, metal enrichment studies in the Southeastern Arabian Sea (Laluraj and Nair, 2006; Robin et al., 2012) as well as in the adjacent Kerala coast (Suresh et al., 2015; Peter et al., 2017) were based on only one numerical value pertained to crustal background such as average shale, upper continental crust, etc. and not on the regional background. If such data is available, it would be possible to evaluate the spatial variations and geochemistry of environmentally relevant toxic metal concentrations in upwelling regimes and the comparison with other upwelling regions elsewhere in the world may help to confirm the effects of metal contamination, pollution sources and geochemical behaviour. Indeed, the global significance is that the study reveals the factors controlling the enrichment of bioelements in the upwelling margin of Arabian Sea; similar areas have been extensively consolidated in different parts of the world Ocean, forms a part to support and validate the previous data explaining the geochemical signature of trace elements.

The present research includes the estimation of background metal level using sediment cores in the region, assessing the trace metal content in the estuarine and coastal regions of Kerala coast, evaluating the organic matter sources as a precursor for studying trace metal enrichment and determining the trace metal distribution in the continental shelf of Southeastern Arabian Sea adjacent to the Kerala coast during an upwelling period. The natural metal background concentrations are established, so it is possible to sort out the locations where metal enrichment is due to contamination processes. Therefore these background values now provide a baseline of information for future research on sediment contamination in the Kerala coast. Additionally, a comparative approach has been adopted to study the geochemistry of trace metal enrichment in the Arabian Sea off Kerala. The comparison and correlation of metal data set with organic carbon, textural properties and redox parameters may provide systematic information about the mechanism of deposition and transport phenomena existing among certain trace elements. Hence, determining the level of metals in the estuarine, coastal and shelf margins would provide a better understanding of possible sources, ecological risk and transport mechanism. Accordingly, this study represents a realistic approach to estimate the distribution, sources and geochemistry of trace metal enrichment in response to changes in climatic events and other biogeochemical processes occurring along the west coast of India. It is also an attempt to corroborate human disturbances impaired on the natural functioning of the ecosystem. The present study would provide baseline information necessary for developing strategies for future pollution control in the coastal environments of southwest coast of India.

In order to achieve the aim of this thesis, a series of objectives have been formulated. The objectives can be detailed as follows:

I. To evaluate the distribution profile of trace metals in specific core sediments along the Kerala coast to further estimate the background metal levels in the region. This data has been extended to evaluate the enrichment pattern of trace metals in the surface sediments of Kerala coast and adjoining continental shelf of the Southeastern Arabian Sea.

II. To assess the distribution, controlling factors and potential risk of trace metals in the coastal and estuarine sediments along the Kerala coast.

III. To survey the spatial changes in sources, nature, quality and diagenetical state of organic matter as a precursor to examine the trace metal enrichment, through elemental compositions (C, H, N and S), C/N, C/S and biochemical compositions in the continental shelf of Southeastern Arabian Sea.

IV. To investigate the sources of environmentally relevant trace elements in response to seasonal upwelling and typical oxygen minimum conditions in the Southeastern Arabian Sea, to the variation of texture and organic matter in the sediments. In addition, the total metal concentrations will be compared with those found in the sediment samples from a number of different geographical areas to elaborate the environmental characteristics.

V. To explore the geochemistry of trace metal enrichment based on applying Al normalization in the shelf sediments. It aimed at a comparison of different background parameters to set up a good agreement in interpreting the enrichment of major and trace elements.

VI. Ecological risk assessment factor of toxic metals is computed to assess the potential effects to biota in the shelf sediments.

VII. Geochemical indices such as EF, CF, I_{geo} and PLI are calculated to assess the contamination status, and the possible sources of these metals to the coastal environment are characterized using multivariate statistical methods.

References

Abdurahiman, K.P., Nayak, T.H., Zacharia, P.U., Mohamed, K.S., 2010. Trophic organisation and predatoreprey interactions among commercially exploited demersal finfishes in the coastal waters of the southeastern Arabian Sea. Estuarine Coastal and Shelf Science, 87, 601–610.

Abrahim, G.M.S., Parker, R.J., 2008. Assessment of heavy metal enrichment factors and the degree of contamination in marine sediments from Tamaki Estuary, Auckland, New Zealand. Environmental Monitoring and Assessment, 136, 227–238.

Acharya, S.S., Panigrahi, M.K., Gupta, A.K., Tripathy, S., 2015. Response of trace metal redox proxies in continental shelf environment: the Eastern Arabian Sea scenario. Continental Shelf Research, 106, 70−84.

Akcay, H., Oguz, A., Karapire, C., 2003. Study of heavy metal pollution and speciation in Buyak Menderes and Gediz river sediments. Water Research, 37, 813–822.

Akhil, P.S., Sujatha, C.H., 2014. Spatial budgetary evaluation of organochlorine contaminants in the sediments of Cochin Estuary, India. Marine Pollution Bulletin, 78, 246–251.

Alagarsamy, R., 1997. Trace metals and organic matter diagenesis at the Oman margin. University of Liverpool, Liverpool, England. (Ph.D. thesis).

Alagarsamy, R., Wolff, G.A., Chester, R., 2005. Partitioning and speciation of trace metal diagenesis in differing depositional environments in the sediments of the Oman Margin. Aquatic Geochemistry, 11, 195–213.

Alloway, B.J., 1990. Heavy metals in soils. Blackie and Son Ltd., London, UK.

Al-Masri, M.S., Aba, A., Khalil, H., Al-Hares, Z., 2002. Sedimentation rates and pollution history of a dried lake: Al-Oteibeh Lake. Science of the Total Environment, 293, 177–189.

Álvarez-Iglesias, P., Rubio, B., 2012. Trace metals in shallow marine sediments from the Ría de Vigo: sources, pollution, speciation and early diagenesis. INTECH Open Access Publisher. doi: 10.5772/32485.

Audry, S., Blanc, G., Schäfer, J., Chaillou, G., Robert, S., 2006. Early diagenesis of trace metals (Cd, Cu, Co, Ni, U, Mo, and V) in the freshwater reaches of a macrotidal estuary. Geochimica et Cosmochimica Acta, 70, 2264–2282.

Balachandran, K.K., Joseph, T., Nair, M., Sankaranarayanan, V.N., Kesavadas, V., Sheeba, P., 2003. Geochemistry of surficial sediments along the central southwest coast of India: Seasonal changes in regional distribution. Journal of Coastal Research, 19, 664–683.

Balachandran, K.K., Laluraj, C.M., Nair, M., Joseph, T., Sheeba, P., Venugopal, P., 2005. Heavy metal accumulation in a flow restricted, tropical estuary. Estuarine Coastal and Shelf Science, 65, 361–370.

Bashkin, V.N., 2006, Modern biogeochemistry: Environmental risk assessment. Springer, Dordrecht, The Netherlands.

Bianchi, T.S., Allison, M.A., 2009. Large-river delta-front estuaries as natural "recorders" of global environmental change. Proceedings of the National Academy of Sciences of the United States of America, 106, 8085–8092.

Bindu, K.R., Deepulal, P.M., Gireeshkumar, T.R., Chandramohanakumar, N., 2015. Evaluation of heavy metal enrichment in Cochin estuary and its adjacent coast: multivariate statistical approach. Environmental Monitoring and Assessment, 187, 519. doi: 10.1007/s10661-015-4749-2.

Birch, G.F., Apostolatos, C., 2013. Use of sedimentary metals to predict metal concentrations in black mussel (*Mytilus galloprovincialis*) tissue and risk to human health (Sydney estuary, Australia). Environmental Science and Pollution Research, 20, 5481–5491.

Böning, P., Brumsack, H.J., Böttcher, M.E., Schnetger, B., Kriete, C., Kallmeyer, J., Borchers, S.L., 2004. Geochemistry of Peruvian near-surface sediments. Geochimica et Cosmochimica Acta, 68, 4429–4451.

Böning, P., Cuypers, S., Grunwald, M., Schnetger, B., Brumsack, H.J., 2005. Geochemical characteristics of Chilean upwelling sediments at 36°S. Marine Geology, 220, 1–21.

Böning, P., Brumsack, H.J., Schnetger, B., Grunwald, M., 2009. Trace element signatures of Chilean upwelling sediments at 36°S. Marine Geology, 259, 112–121.

Böning, P., Shaw, T., Pahnke, K., Brumsack, H.J., 2015. Nickel as indicator of fresh organic matter in upwelling sediments. Geochimica et Cosmochimica Acta, 162, 99–108.

Brumsack, H.J., 1989. Geochemistry of recent TOC-rich sediments from the Gulf of California and the Black sea. Geologische Rundschau, 78, 851–882.

Brumsack, H.J., 2006. The trace metal content of recent organic carbon-rich sediments: Implications for Cretaceous black shale formation. Palaeogeography, Palaeoclimatology, Palaeoecology, 232, 344–361.

Caccia, V.G., Millero, F.J., 2003. The distribution and seasonal variation of dissolved trace metals in Florida Bay and adjacent waters. Aquatic Geochemistry, 9, 111–144.

Caeiro, S., Costa, M.H., Ramos, T.B., Fernandes, F., Silveira, N., Coimbra, A., Medeiros, G., Painho, M., 2005. Assessing heavy metal contamination in Sado Estuary sediment: An index analysis approach. Ecological Indicators, 5, 151–169.

Calvert, S.E., Pedersen, T.F., 1993. Geochemistry of recent oxic and anoxic marine sediments: Implications for the geological record. Marine Geology, 113, 67–88.

Calvert, S.E., Pedersen, T., 2007. Elemental proxies for palaeoclimatic and palaeoceanographic variability in marine sediments: interpretation and application. In: Hillaire-Marcel, C., Vernal, A. (Eds.), Developments in Marine Geology, Proxies in Late Cenozoic Paleoceanography, vol. 1. Elsevier B.V.

Chen, M., Goodkin, N.F., Boyle, E.A., Switzer, A.D., Bolton, A., 2016. Lead in the western South China Sea: Evidence of atmospheric deposition and upwelling. Geophysical Research Letters, 43, 4490–4499.

Chester, R., 2000. Marine geochemistry. Blackwell Science Ltd., Oxford.

Ciji, P.P., Nandan, S.B., 2014. Toxicity of copper and zinc to *Puntius parrah* (Day, 1865). Marine Environmental Research, 93, 38–46.

Conway, T.M., John, S.G., 2014. The biogeochemical cycling of zinc and zinc isotopes in the North Atlantic Ocean. Global Biogeochemical Cycles, 28, 1111–1128.

Costa, A.M., Mil-Homens, M., Lebreiro, S.M., Richter, T.O., de Stigter, H., Boer, W., Trancoso, M.A., Melo, Z., Mouro, F., Mateus, M., Canário, J., Branco V., Caetano, M., 2011. Origin and transport of trace metals deposited in the canyons off Lisboa and adjacent slopes (Portuguese Margin) in the last century. Marine Geology, 282,169–177.

Covelli, S., Fontonlan, G., 1997. Application of a normalisation procedure in determining regional geochemical baselines. Environmental Geology, 30, 34–45.

Cowie, G., 2005. The biogeochemistry of Arabian Sea surficial sediments: A review of recent studies. Progress in Oceanography, 65, 260–289.

Diagomanolin, V., Farhang, M., Ghazi-Khansari, M., Jafarzadeh, N., 2004. Heavy metals (Ni, Cr, Cu) in the Karoon waterway river, Iran. Toxicology Letters, 151, 63–67.

Dean, W.E., Zheng, Y., Ortiz, J.D., van Geen, A., 2006. Sediment Cd and Mo accumulation in the oxygen-minimum zone off western Baja California linked to global climate over the past 52 kyr. Paleoceanography, 21, PA4209. doi: 10.1029/2005PA001239.

Deepulal, P.M., Sujatha, C.H., George, R., 2012. Chemometric study on the trace metal accumulation in the sediments of the Cochin Estuary-Southwest coast of India. Environmental Monitoring and Assessment, 184, 6261–6279.

Desenfant, F., Veron, A.J., Camoin, G.F., Nyberg, J., 2006. Reconstruction of pollutant lead invasion into the tropical North Atlantic during the twentieth century. Coral Reefs, 25, 473–484.

Dsikowitzky, L., Nordhaus, I., Sujatha, C.H., Akhil, P.S., Soman, K., Schwarzbauer, J., 2014. A combined chemical and biological assessment of industrial contamination in an estuarine system in Kerala, India. Science of the Total Environment, 485, 348–362.

Echegoyen, Y., Boyle, E.A., Lee, J.M., Gamo, T., Obata, H., Norisuye, K., 2014. Recent distribution of lead in the Indian Ocean reflects the impact of regional emissions. Proceedings of the National Academy of Sciences, 111, 15328–15331.

Gao, X.L., Zhou, F.X., Chen, C-T.A., 2014. Pollution status of the Bohai Sea: an overview of the environmental quality assessment related trace metals. Environment International, 62, 12–30.

Gao, L., Wang, Z., Shan, J., Chen, J., Tang, C., Yi, M., Zhao, X., 2016. Distribution characteristics and sources of trace metals in sediment cores from a trans-boundary watercourse: An example from the Shima River, Pearl River Delta. Ecotoxicology and Environmental Safety, 134, 186–195.

Gibbs, R.J., 1993. Metals of the bottom muds in Townsville Harbor, Australia. Environmental Pollution, 81, 297–300.

Goldschmidt, V.M., 1954. Geochemistry. In: Muir, A. (Ed.), The international series of monographs on physics. Clarendon Press, Oxford.

Graham, A.M., Bouwer, E.J., 2009. Rates of hexavalent chromium reduction in anoxic estuarine sediments: pH effects and the role of acid volatile sulfides. Environmental Science & Technology, 44, 136–142.

Gu, Y-G., Lin, Q., 2016. Trace metals in a sediment core from the largest mariculture base of the eastern Guangdong coast, South China: Vertical distribution, speciation, and biological risk. Marine Pollution Bulletin, 113, 520–525.

Gu, Y-G., Gao, Y.P., Lin, Q., 2016. Contamination, bioaccessibility and human health risk of heavy metals in exposed-lawn soils from 28 urban parks in southern China's largest city, Guangzhou. Applied Geochemistry, 67, 52–58.

Guerra, R., Fetter, E., Ceschim, L.M., Martins, C.C., 2011. Trace metals in sediment cores from Deception and Penguin Islands (South Shetland Islands, Antarctica). Marine Pollution Bulletin, 62, 2571–2575.

Habeebrehman, H., Prabhakaran, M.P., Jacob, J., Sabu, P., Jayalakshmi, K.J., Achuthankutty, C.J., Revichandran, C., 2008. Variability in biological responses influenced by upwelling events in the Eastern Arabian Sea. Journal of Marine Systems, 74, 545–560.

Heimbürger, L., Cossa, D., Thibodeau, B., Khripounoff, A., Mas, V., Chiffoleau, J., Schmidt, S., Migon, C., 2012. Natural and anthropogenic trace metals in sediments of the Ligurian Sea (Northwestern Mediterranean). Chemical Geology, 291, 141–151.

Hellio, C., Yebra, D., 2009. Advances in marine antifouling coatings and technologies. Woodhead Publishing Ltd., Cambridge, UK.

Ho, H.H., Swennen, R., Cappuyns, V., Vassilieva, E., Gerven, T.V., Tran, T.V., 2013. Speciation and mobility of selected trace metals (As, Cu, Mn, Pb and Zn) in sediment with depth in Cam River-Mouth, Haiphong, Vietnam. Aquatic Geochemistry, 19, 57–75.

Hornberger, M.I., Luoma, S.N., van Geen, A., Fuller, C., Anima, R., 1999. Historical trends of metals in the sediments of San Francisco Bay, California. Marine Chemistry, 64, 39–55.

Huang, J., Ge, X., Wang, D., 2012. Distribution of heavy metals in the water column, suspended particulate matters and the sediment under hydrodynamic conditions using an annular flume. Journal of Environmental Sciences, 24, 2051–2059.

Hupe, A., Karstensen, J., 2000. Redfield stoichiometry in Arabian Sea subsurface waters. Global Biogeochemical Cycles, 14, 357–372.

Inoue, M., Tanimizu, M., 2008. Anthropogenic lead inputs to the western Pacific during the 20th century. Science of the Total Environment, 406, 123–130.

John, S.G., Conway, T.M., 2014. A role for scavenging in the marine biogeochemical cycling of zinc and zinc isotopes. Earth and Planetary Science Letters, 394, 159–167.

Karbassi, A.R., Shankar, R., 2005. Geochemistry of two sediment cores from the west coast of India. International Journal of Environmental Science and Technology, 1, 307–316.

Klinkhammer, G.P., Bender, M.L., 1980. The distribution of manganese in the Pacific Ocean. Earth and Planetary Science Letters, 46, 361– 384.

Knauer, G.A., Martin, J.H., 1981. Phosphorous-cadmium cycling in northeast Pacific waters. Journal of Marine Research, 39, 65–76.

Kögel-Knabner, I., 2002. The macromolecular organic composition of plant and microbial residues as inputs to soil organic matter. Soil Biology and Biochemistry, 34, 139–162.

Kumar, S.P., Edward, J.K.P., 2009. Assessment of metal concentration in the sediment cores of Manakudy estuary, south west coast of India. Indian Journal of Marine Sciences, 38, 235–248.

Larrose, A., Coynel, A., Schäfer, J., Blanc, G., Massé, L., Maneux, E., 2010. Assessing the current state of the Gironde Estuary by mapping priority contaminant distribution and risk potential in surface sediment. Applied Geochemistry, 25, 1912–1923.

Laluraj, C.M., Nair, S.M., 2006. Geochemical index of trace metals in the surficial sediments from the western continental shelf of India, Arabian Sea. Environmental Geochemistry and Health, 28, 509–518.

Lewis, B.L., Luther III, G.W., 2000. Processes controlling the distribution and cycling of manganese in the oxygen minimum zone of the Arabian Sea. Deep Sea Research Part II: Topical Studies in Oceanography, 47, 1541–1561.

Lin, Q., Liu, E., Zhang, E., Li, K., Shen, J., 2016. Spatial distribution, contamination and ecological risk assessment of heavy metals in surface sediments of Erhai Lake, a large eutrophic plateau lake in southwest China. Catena, 145, 193–203.

Lohan, M.C., Statham, P.J., Crawford D.W., 2002. Total dissolved zinc in the upper water column of the subarctic North East Pacific. Deep Sea Research Part II: Topical Studies in Oceanography, 49, 5793–5808.

Marmolejo-Rodriguez, A.J., Prego, R., Mayer-Willerer, A., Shumilin, E., Cobelo-Garcia, A., 2007. Total and labile metals in surface sediments of the tropical river-estuary system of Marabasco (Pacific coast of Mexico): Influence of an iron mine. Marine Pollution Bulletin, 55, 459–468.

McCorkle, D., Klinkhammer, G.P., 1991. Porewater cadmium geochemistry and the porewater cadmium: $\delta^{13}C$ relation. Geochimica et Cosmochimica Acta, 55, 161–168.

More, T.G., Rajput, R.A., Bandela, N.N., 2003. Impact of heavy metals on DNA content in the whole body of freshwater bivalve, Lamelleiden marginalis. Environmental Science and Pollution Research, 22, 605–616.

Morelli, G., Gasparon, M., 2015. Depositional variability of estuarine intertidal sediments and implications for metal distribution: An example from Moreton Bay (Australia). Continental Shelf Research, 108, 41–54.

Morse, J.W., Luther III, G.W., 1999. Chemical influences on trace metal-sulfide interactions in anoxic sediments. Geochimica et Cosmochimica Acta, 63, 3373–3378.

Muñoz, P., Dezileau, L., Lange, C., Cardenas, L., Sellanes, J., Salamanca, M.A., Maldonado, A., 2012. Evaluation of sediment trace metal records as paleoproductivity and paleoxygenation proxies in the upwelling center off Concepción, Chile (36°S). Progress in Oceanography, 92–95, 66–80.

Nair, M.P., Akhil, P.S., Sujatha, C.H., 2014. Toxic metal distribution in the core sediment of Cochin Estuarine System (CES). International Journal of Environmental Research, 8, 133–138.

Nameroff, T.J., Balistrieri, L.S., Murray, J.W., 2002. Suboxic trace metal geochemistry in the eastern tropical North Pacific. Geochimica et Cosmochimica Acta, 66, 1139–1158.

Naqvi, S.W.A., Bange, H.W., Gibb, S.W., Goyet, C., Hatton, A.D., Upstill-Goddard, R.C., 2005. Biogeochemical ocean-atmosphere transfers in the Arabian Sea. Progress in Oceanography, 65, 116–144.

Pailler, D., Bard, E., Rostek, F., Zheng, Y., Mortlock, R., van Geen, A., 2002. Burial of redox-sensitive metals and organic matter in the equatorial Indian Ocean linked to precession. Geochimica et Cosmochimica Acta, 66, 849–865.

Peter, T.S., Chandrasekar, N., Wilson, J.J., Selvakumar, S., Krishnakumar, S., Magesh, N.S., 2017. A baseline record of trace elements concentration along the beach placer mining areas of Kanyakumari coast, South India. Marine Pollution Bulletin, 119, 416–422.

Prajith, A., Rao, V.P., Chakraborty, P., 2016. Distribution, provenance and early diagenesis of major and trace metals in sediment cores from the Mandovi estuary, western India. Estuarine Coastal and Shelf Science, 170, 1–13.

Prasanthan, V., Udayakumar, P., Ouseph, P.P., 2011. Influence of abiotic environmental factors on the abundance and distribution of Vibrio species in coastal waters of Kerala, India. Indian Journal of Geo-Marine Sciences, 40, 587–592.

Prego, R., Filgueiras, A.V., Santos-Echeandia, J., 2008. Temporal and spatial changes of total and labile metal concentration in the surface sediments of the Vigo Ria (NW Iberian Peninsula): Influence of anthropogenic sources. Marine Pollution Bulletin, 56, 1022–1042.

Priju, C.P., Narayana, A.C., 2007. Heavy and trace metals in Vembanad lake sediments. International Journal of Environmental Research, 1, 280–289.

Qasim, S.Z., 1982. Oceanography of the northern Arabian Sea. Deep Sea Research Part A. Oceanographic Research Papers, 29, 1041–1068.

Ragi, A.S., Leena, P.P., Cheriyan, E., Nair, S.M., 2017. Heavy metal concentrations in some gastropods and bivalves collected from the fishing zone of South India. Marine Pollution Bulletin, 118, 452–458.

Raveenderan, R., Sujatha, C.H., 2011. Quantitation of specific trace metals in bivalve, *Villorita Cyprinoides* Var Cochinensis in the Cochin estuary. Indian Journal of Geo-Marine Science, 40, 424–429.

Robert, S., Blanc, G., Schafer, J., Lavaux, G., Abril, G., 2004. Metal mobilization in the Gironde Estuary (France): the role of the soft mud layer in the maximum turbidity zone. Marine Chemistry, 87, 1–13.

Robin, R.S., Muduli, P.R., Vardhan, K.V., Ganguly, D., Abhilash, K.R., Balasubramanian, T., 2012. Heavy metal contamination and risk assessment in the marine environment of Arabian Sea, along the southwest coast of India. American Journal of Chemistry, 2, 191–208.

Rosenthal, Y., Lam, P., Boyle, E.A., Thomson, J., 1995. Authigenic cadmium enrichments in suboxic sediments: Precipitation and postdepositional mobility. Earth and Planetary Science Letters, 132, 99–111.

Rubio, B., Nombela, M.A., Vilas, F., 2000. Geochemistry of major and trace elements in sediments of the Ria de Vigo (NW Spain): an assessment of metal pollution. Marine Pollution Bulletin, 40, 968–980.

Rubio, B., Álvarez-Iglesias, P., Vilas, F., 2010. Diagenesis and anthropogenesis of metals in the recent Holocene sedimentary record of the Ría de Vigo (NW Spain). Marine Pollution Bulletin, 60, 1122–1129.

Ryther, J.H., 1969. Photosynthesis and fish production in the sea. Science, 166, 72–80.

Salas, P.M., Sujatha, C.H., Kumar, C.S.R., Cheriyan, E., 2017. Heavy metal distribution and contamination status in the sedimentary environment of Cochin Estuary. Marine Pollution Bulletin, 119, 191–203.

Santos, I.S., Garcia, C.A.B., Passos, E.A., Alves, J.P.H., 2013. Distributions of trace metals in sediment cores from a hypertrophic reservoir in Northeast Brazil. Journal of the Brazilian Chemical Society, 24, 246–255.

Sclater, F.R., Boyle, E., Edmond, J.M., 1976. Marine geochemistry of nickel. Earth and Planetary Science Letters, 31, 119–128.

ShibiniMol, P.A., Raveendran, R., Sujatha, C.H., 2015. Elucidation of contaminant-induced toxic responses in the biota of Lake Vembanad, Kerala, India. Human and Ecological Risk Assessment: An International Journal, 21, 1576–1592.

Shivaprasad, A., Vinita, J., Revichandran, C., Reny, P.D., Deepak, M.P., Muraleedharan, K.R., Kumar, K.R.N., 2013. Seasonal stratification and property distributions in a tropical estuary (Cochin estuary, west coast, India). Hydrology and Earth System Sciences, 17, 187–199.

Spencer, K.L., Cundy, A.B., Croudace, I.W., 2003. Heavy metal distribution and early-diagenesis in salt marsh sediments from the Medway estuary, Kent, UK. Estuarine Coastal and Shelf Science, 57, 43–54.

Suess, E., Thiede, J., 1983. Coastal upwelling, its sediment record. NATO Conference Series. IV, Marine Sciences, vol. 10A-B. Plenum Press, New York.

Sujatha, C.H., Benny, N., Raveendran, R., Fanimol, C.L., Samantha, N.K., 2009. Nutrient dynamics in the two lakes of Kerala, India. Indian Journal of Geo-Marine Sciences, 38, 451–456.

Sundararajan, M., Natesan, U., 2010. Geochemistry of elements in core sediments near Point Claimere, the southeast coast of India. International Journal of Environmental Research, 4, 379–394.

Suresh, G., Ramasamy, V., Sundarrajan, M., Paramasivam, K., 2015. Spatial and vertical distributions of heavy metals and their potential toxicity levels in various beach sediments from high-background-radiation area, Kerala, India. Marine Pollution Bulletin, 91, 389–400.

Taylor, S.R., 1964. The abundance of chemical elements in the continental crust: a new table. Geochimica et Cosmochimica Acta, 28, 1273–1285.

Taylor, S.R., McLennan, S.M., 1985. The continental crust: Its composition and evolution. Blackwell, London.

Tribovillard, N., Algeo, T.J., Lyons, T., Riboulleau, A., 2006. Trace metals as paleoredox and paleoproductivity proxies: An update. Chemical Geology, 232, 12–32.

Turekian, K.K., Wedepohl, D.H., 1961. Distribution of the elements in some major units of the earth's crust. Bulletin Geological Society of America, 72, 175–192.

Turner, A., Millward, G.E., 2002. Suspended particles: Their role in estuarine biogeochemical cycles. Estuarine Coastal and Shelf Science, 55, 857–883.

Twining, B.S., Baines, S.B., Vogt, S., Nelson, D.M., 2012. Role of diatoms in nickel biogeochemistry in the ocean. Global Biogeochemical Cycles, 26. doi: 10.1029/2011GB004233.

Udayakumar, P., Jose, J.J., Krishnan, K.A., Kumar, C.S.R., Manju, M.N., Salas, P.M., 2014. Heavy metal accumulation in the surficial sediments along southwest coast of India. Environmental Earth Sciences, 72, 1887–1900.

Van der Weijden, C., Reichart, G., Vanos, B., 2006. Sedimentary trace element records over the last 200 kyr from within and below the northern Arabian Sea oxygen minimum zone. Marine Geology, 231, 68–88.

van Geen, A., McCorkle, D.C., Klinkhammer, G.P., 1995. Sensitivity of the phosphate-cadmium-carbon isotope relation in the ocean to cadmium removal by suboxic sediments. Paleoceanography, 10, 159–169.

Vangronsveld, J., Cunnihgham, S.D., 1998. Metal contaminated soils: In-situ inactivation and phytoremediation. Springer-Verlag, Berlin.

Varghese, S., 2004. Geochemistry of rare earth elements and trace metals along the western continental shelf of India. Cochin University of Science and Technology, Cochin, India. (Ph.D.thesis).

Vega, F.A., Covelo, E.F., Andrade, M.L., 2006. Competitive sorption and desorption of heavy metals in mine soils: Influence of mine soil characteristics. Journal of Colloid and Interface Science, 298, 582–592.

Vidal, M., Santos, M.J., Abroa, T., Rodriguez, J., Rigol, A., 2009. Modeling competitive metal sorption in a mineral soil. Geoderma, 149, 189–198.

Vivekanandan, E., Srinath, M., Pillai, V.N., Immanuel, S., Kurup, K.N., 2003. Marine fisheries along the southwest coast of India. In: Silvestre, G. (Ed.), Assessment, management and future directions for coastal fisheries in Asian countries, World Fish Center Conference Proceedings.

Wangersky, P.J., 1986. Biological control of trace metal residence time and speciation: A review and synthesis. Marine Chemistry, 18, 269–297.

Whitten, D.G.A., Brooks, J.R.V., 1972. The penguin dictionary of geology. Penguin Books Ltd., Middlesex, UK.

Wu, Z., He, M., Lin, C., Fan, Y., 2011. Distribution and speciation of four heavy metals (Cd, Cr, Mn and Ni) in the surficial sediments from estuary in Daliao River and Yingkou Bay. Environmental Earth Sciences, 63, 163–175.

Yang, Y., Chen, F., Zhang, L., Liu, J., Wu, S., Kang, M., 2012. Comprehensive assessment of heavy metal contamination in sediment of the Pearl River Estuary and adjacent shelf. Marine Pollution Bulletin, 64, 1947–1955.

Zalewska, T., Woroń, J., Danowska, B., Suplińska, M., 2015. Temporal changes in Hg, Pb, Cd and Zn environmental concentrations in the southern Baltic Sea sediments dated with ^{210}Pb method. Oceanologia, 57, 32–43.

Zhao, Y., Vance, D., Abouchami, W., De Baar, H.J.W., 2014. Biogeochemical cycling of zinc and its isotopes in the Southern Ocean. Geochimica et Cosmochimica Acta, 125, 653–672.

Zheng, Y., Anderson, R.F., Geen, A.V., Kuwabara, J., 2000. Authigenic molybdenum formation in marine sediments: a link to pore water sulfide in the Santa Barbara Basin. Geochimica et Cosmochimica Acta, 64, 4165–4178.

Zhou, J.L., Liu, Y.P., Abrahams, P.W., 2003. Trace metal behavior in the Conwy estuary, North Wales. Chemosphere, 51, 429–440.

Chapter

2 MATERIALS AND METHODS

Contents

2.1 Description of Study Area and Sampling

2.1.1 Southern Kerala Coast

The west coast of India is environmentally unique because it is bordering one of the sensitive ecosystems in the world, the Arabian Sea. The Kerala coastline extending up to 570 km in length is bordered prominently by beaches, ridges, riverine deposits and backwaters generally running parallel to the shoreline. Geologically, the major rock formations are precambrian crystalline rocks, sedimentary rocks, laterites, etc. The coastal land is characterized by paddy fields, coconut plantations and extensive network of backwaters inter-connected with rivers and canals in the landside. About 30% of the population of Kerala state lives in the coastal areas, resulting in very high density of more than 2000 persons per km^2. The coastal wetland systems occupying the Kerala coast are remarkably fed by perennial rivers and majority of them are characteristically river mouth estuaries linking the land and Sea (Nandan, 2005). According to the reports available, about 3000 medium and large scale and about 2000 small scale industries in the state discharge one lakh cubic metres of treated effluents per day directly into saline and fresh water bodies (Green Peace, 2003).

The southernmost geographical end is at Cape Comorin serving as the confluence of the three water-bodies–the Arabian Sea, the Bay of Bengal and the Indian Ocean. Towards central and southern coast of Kerala, the Vembanad and Kayamkulam backwaters form a beach ridge morphology which is separated from the Sea by long land barriers. The Cochin backwaters are opening out to the sea at Cochin harbour channel and at the Periyar river confluence. The bulk of the state's wood and clay based industries, fish processing plants, boat building yards, coir industries, etc. are situated in and around the Cochin backwaters area. A major port at Cochin (Cochin Port Trust) and 14 minor ports, International Container Transhipment Terminal (ICTT) and fishing harbours are situated in this coastal zone. Cochin estuary, the second largest estuarine system in India, is a part of the Vembanad-Kol wetlands, a Ramsar Site (No. 1214). Numerous large scale industries namely, Fertilisers and Chemicals Travancore Ltd. (FACT), Hindustan Insecticides Ltd. (HIL), Indian Rare Earths (IRE), Merchem, Sudchemie, Cochin Minerals and Rutiles Ltd. (CMRL), Binani Zinc Ltd. (BZL), Travancore Cochin Chemicals, BPCL Kochi Refinery, Hindustan Organic Chemicals Ltd. (HOCL), Cochin Shipyard, etc. are situated on the banks of major rivers finally draining into the Cochin estuary. The total percentage of river discharge to the estuary varies accordingly and can be estimated as 33% contribution from river Periyar, and the Muvattupuzha, Achenkovil, Pampa, Meenachil and Manimala rivers contribute 24.2%, 5.8%, 19.7%, 8.3% and 8.8% respectively (Srinivas et al., 2003). On the other hand, Ashtamudi lagoon, the second largest brackish water lake in Kerala has its axis perpendicular to the coast extending up to the foothill margin of the coastal terrain (Nandan, 2005). This lagoon opens to the Arabian Sea at Neendakara, an area of frequent sea erosion and one of the famous fish landing centres of Kerala, South India. The low lying plains of Alleppey are contrasting regions of onshore industries including traditional mariculture activities, tourism related establishments, domestic effluents, etc. Valapad in the central Kerala is heavily threatened by the discharge of sewage from Chettuva estuary, which is a major fishing port. The heavy marine traffic involving the operation of large scale oil tankers and numerous motorized fishing boats along with oil spills add to the problem of marine oil pollution in the coast.

2.1.1.1 Sampling Strategy

To generate background metal levels and to reveal different enrichment pattern with geographical anomalies, sediment cores were sampled from selected locations along the Southern Kerala, namely, Cape Comorin (CC1) and Cochin estuary (CE1) during February 2013 (Table 2.1/Fig. 2.1). CC1 is in the extreme south of the study area and exclusively representative of the coastal site. To date, there are no studies estimated the downcore metal content in the southern tip of peninsular India at Cape Comorin. On the other hand, CE1 lies in the southern arm of the Cochin estuary. The estuarine front is extensively an arena of maricultural activities along with the densely populated human settlement. A hand driven PVC (Poly-vinyl chloride) corer with an internal diameter of 6.2 cm was used for collecting the cores from the study sites. Core tubes were washed using deionized water to remove any dust adhered to the inner walls of the tubing during transport to the core site. A PVC corer of 54 cm and 93 cm long were obtained from Cape Comorin (CC1) and Cochin estuary (CE1) respectively. Sediment cores were sliced at 3 cm interval from the surface to bottom using clean techniques and were immediately transferred into polyethylene zip lock plastic bags. Samples were preserved at $-20^{\circ}C$, freeze dried and ground using agate mortar for further analyses.

Table 2.1: Location of core sediment sampling sites and sample codes.

Location code	Location name	Latitude	Longitude
		°N	°E
CC1	Cape Comorin	08°04.90'	77°33.09'
CE1	Cochin estuary	09°52.44'	76°19.38'

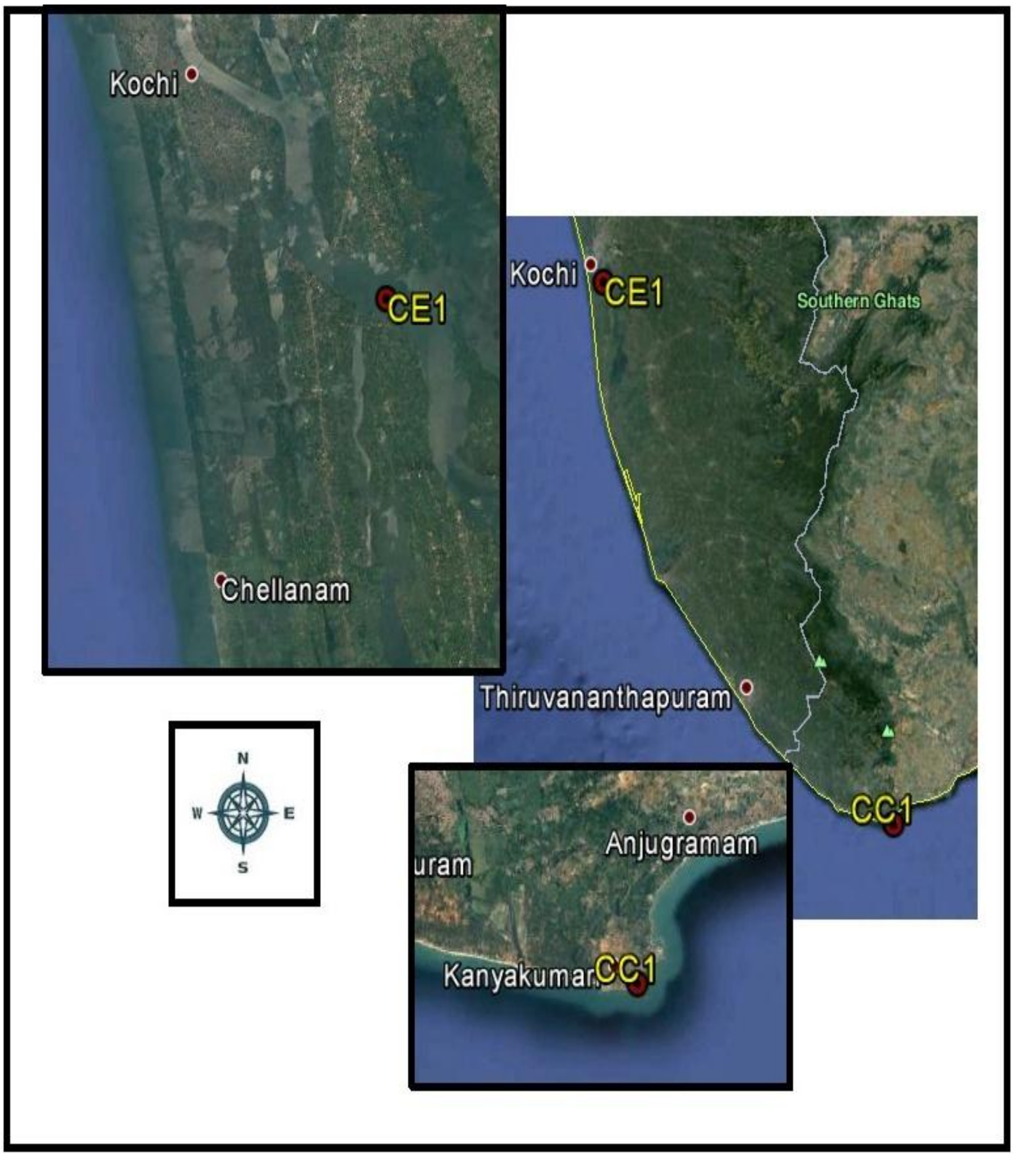

Fig. 2.1 Map showing sampling location of sediment cores in the Cape Comorin (CC1) and Cochin estuary (CE1).

Surface sampling sites were located on different geographical regions along the Southern Kerala coast, selected on the basis of pollution sources and different hydrogeochemical environments. Thirteen stations were considered for the collection of surface sediment and water samples along the southern region of Kerala extending from Chettuva in the central Kerala to Cape Comorin in the southern end (Table 2.2/Fig. 2.2). The stations selected are broadly confined to two zones along the coast representing the nearshore beach sites and estuarine sites with freshwater and marine water interactions respectively. The nearshore region includes Cape (C1 and C2), Kovalam (K3), Neendakara (N4), Purakkad (P8) and Nattika (N12). The estuarine stations are Ashtamudi (A5), Kayamkulam (K6), Kilimukkekadavu (K7), Aroorkutty (A9), Thevara (T10), Chennur (C11) and Chettuva (C13). The nearshore regions are major fishing zones experiencing ceaseless boat operations and also affected by tourism related establishments, fish processing industries and municipal activities. The estuarine region mainly Ashtamudi, Kayamkulam and Kilimukkekadavu are impacted by fishing operations, extensive mariculture activities, coconut husk retting, industrial and urban effluents. The stations Aroorkutty, Thevara and Chennur lie in the middle part of the Cochin estuary facing extreme anthropogenic pressures from different inceptions. The rapid industrialization and urbanization has created high volume of exogenic influence in the region which leds to the detioration of the quality of the estuary and further decline in the bioresources (Gopalan et al., 1983; Martin et al., 2011; Akhil and Sujatha, 2014; Dsikowitzky et al., 2014; Ciji and Nandan, 2014). The wide range backwater reclamation, harbour operations, dredging activities, untreated and partially treated effluents from the industrial zone, municipal effluents and motorized boat operations add to this detioration scenario (Bindu et al., 2015; Salas et al., 2017). The station Chettuva lies comparatively in a low polluted region but anthropogenic inputs are likely due to boat operations and urban sewages.

Water samples were collected using a Niskin sampler (GO-FLO, USA) and surface sediment samples were collected using a stainless steel Van Veen grab sampler (0.042 m^2). At each site, surface sediments were sub sampled using a plastic spatula without any metal contamination and transferred into polyethylene bags. Samples were preserved at −20°C, freeze dried and ground using agate mortar for further analyses.

Table 2.2: Location of surface sampling sites and sample codes.

Station code	Station name	Latitude	Longitude
		°N	°E
C1	Cape 1	08°04.90'	77°33.09'
C2	Cape 2	08°04.71'	77°33.07'
K3	Kovalam	08°23.81'	76°58.41'
N4	Neendakara	08°57.33'	76°31.95'
A5	Ashtamudi	08°57.70'	76°35.88'
K6	Kayamkulam	09°09.69'	76°27.97'
K7	Kilimukkekadavu	09°10.24'	76°28.67'
P8	Purakkad	09°20.48'	76°22.21'
A9	Aroorkutty	09°52.44'	76°19.38'
T10	Thevara	09°55.47'	76°18.28'
C11	Chennur	10°03.25'	76°16.04'
N12	Nattika	10°24.79'	76°05.08'
C13	Chettuva	10°31.91'	76°02.55'

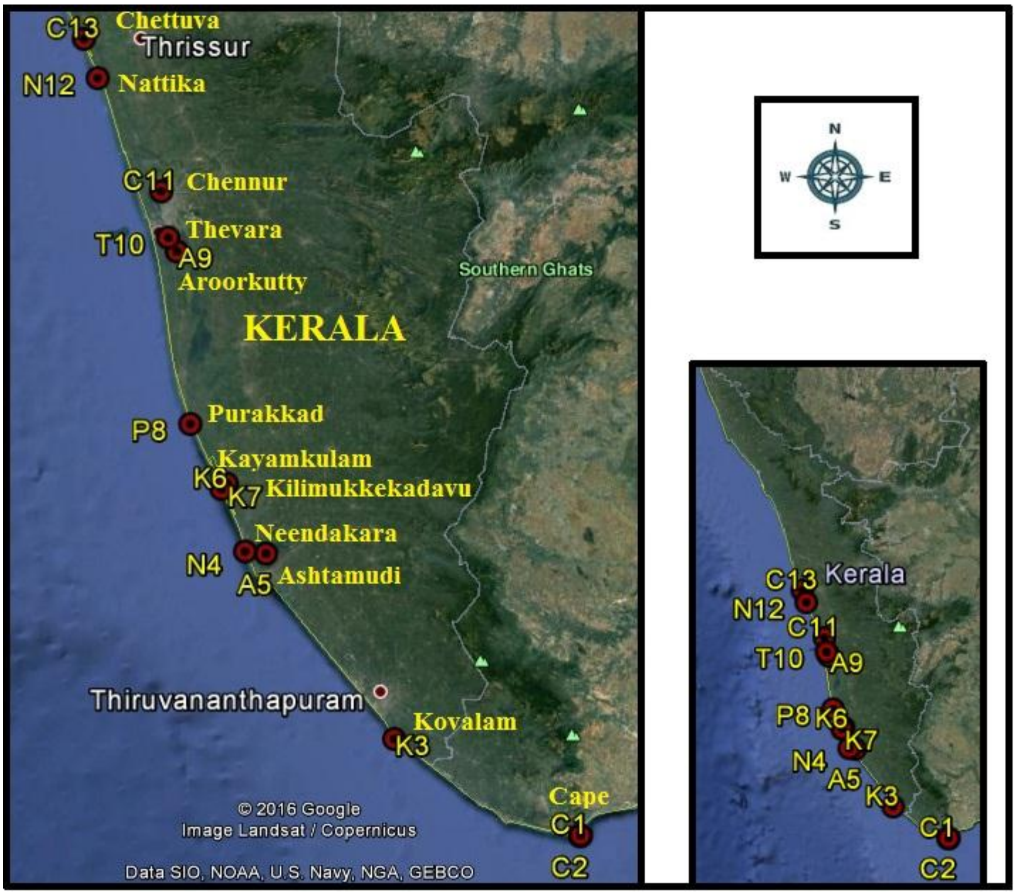

Fig. 2.2 Map showing study region and sampling locations along the Southern Kerala coast.

2.1.2 Southeastern Arabian Sea off Kerala

The Arabian Sea in the southeastern part bordering the Kerala coast experiences seasonal upwelling, which increases the marine productivity (Wiggert et al., 2005). It is characterized by the unique oceanographic set up of reversal of water circulation in response to seasonal monsoonal forcing which has a major role in the productivity induced biogeochemical changes and water column denitrification in the coastal environment (Babu et al., 2002; Marra and Barber, 2005). It is a region of negative water balance, where the evaporation far exceeds precipitation and runoff; consequently the upper layers in this region are highly saline and weakly stratified. Furthermore, this area hosts the core of the warm pool in north Indian Ocean prior to the onset of summer monsoon. These physical processes have profound influence on the biogeochemistry and Southeastern Arabian Sea is the only upwelling area where the upwelling occurs in conjunction with rainfall and intense fresh water influx. It stretches to a complex oceanic behaviour of eutrophic as well as oligotrophic biogeochemical conformation and a well developed oxygen minimum zone (Burkill et al., 1993; Hupe and Karstensen, 2000). This semi-enclosed water basin is bordered by coastal highlands along the western continental shelf of India. The continental shelf of the Arabian Sea is narrower towards the south and widened in the north along the west coast of India. The width of the continental shelf varies accordingly; about 120 km at the southern tip of India, off Cape Comorin while narrow off Cochin (80 km) and again wider off Ratnagiri (130 km; Rao and Rao, 1995). The shelf break occurs at about 120 km in the northern part and at about 80 km in the southern part (Thamban, 1998).

During the summer monsoon, the southwest monsoon currents (June-September) flow towards the equator and the coast (off Somalia, Oman and west coast of India) experiences upwelling, which increases the biological production (Wiggert et al., 2005) resulting in the export of organic matter to the ocean floor (Habeebrehman et al., 2008). Contrary to this, in winter (November-February), the surface circulation is reversed to pole ward forcing the northeast winter monsoon current to drive the waters from the Bay of Bengal to the Arabian Sea causing well oxygenated conditions in the region. The high continental precipitation and subsequent river runoff during summer monsoon influences the biological productivity in the coastal waters along the southwest coast of India (Jyothibabu et al., 2010). The coastal upwelling and river runoff maximize the biological productivity in the eastern boundary of Arabian Sea. Most of the primary production is associated with coastal waters and show high variability as these regions are under severe pressure due to multiple in situ and external factors of adjacent environments. The degradation of organic matter leads to oxygen deficiency in the sub-surface waters and a coastal sub-oxic zone is formed seasonally beneath the surface (Naqvi et al., 2000; Naqvi et al., 2006). In addition, because of the differential solubility of oxidized and reduced forms of metals, the sub-surface, sub-oxic water of the region plays a significant role in moderating the geochemical distribution of metals during the remineralization of organic matter. Strong oxygen minimum zones have substantial impacts on pelagic organisms, which in turn, may have consequences for carbon cycling along with vertical fluxes of trace metals. Further, a well developed perennial oxygen minimum zone (200–2000 m depth) is also observed in the offshore of eastern Arabian Sea (Naqvi et al., 2006). The upwelling period (June to October) of southwest monsoon is associated with algal blooms and the favourable productivity factors support large fisheries along the west coast, which contributes 60% to the total fish catches along the Indian coast (Naqvi et al., 2000).

There is evidence to show a considerable amount of aeolian and fluvial inputs of trace metals and other nutrient elements to the Arabian Sea from adjacent landmasses (Goldberg and Griffin, 1970). The terrigenous sediment supply to the Sea occurs at a higher rate as observed from the high carbonate content towards South India (Babu et al., 2002). It also provides an environment with sinking property which can absorb or release pollutants to both surfaces and organisms under changing conditions and contributes to the intense sedimentation rates of 15 mm 1000 year^{-1} (Ramaswamy et al., 1991). The coastal zones of Arabian Sea are seen in close association with estuaries, floodplains and wetlands, which are low lying and are flooded by storm tides during the summer monsoon. The coastal tracts undergo a significant ecological change due to its proximity towards the estuarine environment which receives huge discharges of untreated or partially treated industrial and domestic effluents, agricultural and aquacultural washloads. The sediments in this type of ecosystems are affected by multiple processes of material exchange through geological or anthropogenic perturbation, including riverine or airborne inputs, coastal and seafloor erosion, biological production, etc. So, different margins across the Arabian Sea experience widely different oceanographic conditions; hence a minor environmental disturbance can cause potentially large impact on the biogeochemical cycling and fluxes of numerous key elements.

2.1.2.1 Sampling Strategy

During summer monsoon, the continental shelf of Southeastern Arabian Sea, off Kerala was sampled in a series of eight transects running approximately perpendicular to the coastline (Table 2.3/Fig. 2.3) which extends from 08°23.03' to 12°50.86' N latitude and 73°20.35' to 76°29.45' E longitude. The sampling was carried out during two cruises, summer monsoon in July 2013 (Cruise No. 316) along four bathymetric transects including inner and outer shelf (30–200 m depth) off Trivandrum (TR22, TR23, TR24, TR25), Kollam (KO19, KO20, KO21), Alleppey (AL16, AL17, AL18) and Cochin (CO12, CO13, CO14, CO15) and August 2013 (Cruise No. 318) along four bathymetric transects including Valapad (VA9, VA10, VA11), Calicut (CA6, CA7, CA8), Kannur (KA3, KA4, KA5) and Mangalore (MA1, MA2). Sediments were collected onboard FORV Sagar Sampada (Cruise No. 316 and 318) using Smith-McIntyre grab sampler (0.2 m^2) in the Southeastern Arabian Sea along southwest coast of India, extending from Mangalore to Trivandrum.

Samples were preserved at −20°C, freeze dried and ground using agate mortar for further analyses.

Table 2.3: Location of sampling sites selected for the study in the continental shelf of Southeastern Arabian Sea off Kerala.

Transect	Stations	Depth	Latitude	Longitude
		m	°N	°E
Mangalore	MA1	20	12°51.57'	74°08.72'
	MA2	100	12°50.86'	73°20.35'
Kannur	KA3	30	12°05.38'	75°01.40'
	KA4	50	12°04.80'	74°53.98'
	KA5	100	12°04.00'	73°78.33'
Calicut	CA6	30	11°20.16'	75°33.95'
	CA7	50	11°20.13'	75°15.79'
	CA8	100	11°19.84'	74°54.09'
Valapad	VA9	30	10°33.24'	75°50.88'
	VA10	50	10°33.57'	75°41.07'
	VA11	100	10°33.18'	75°25.52'
Cochin	CO12	30	09°58.37'	76°01.24'
	CO13	46	09°58.22'	75°50.02'
	CO14	103	09°57.72'	75°38.25'
	CO15	213	09°57.92'	75°35.46'
Alleppey	AL16	30	09°29.89'	76°08.55'
	AL17	53	09°29.22'	76°02.84'
	AL18	105	09°29.92'	75°49.72'
Kollam	KO19	27	08°52.42'	76°29.06'
	KO20	50	08°52.93'	76°21.87'
	KO21	174	08°52.89'	75°59.95'
Trivandrum	TR22	35	08°32.33'	76°47.71'
	TR23	50	08°28.22'	76°42.59'
	TR24	83	08°25.62'	76°33.60'
	TR25	200	08°23.03'	76°29.45'

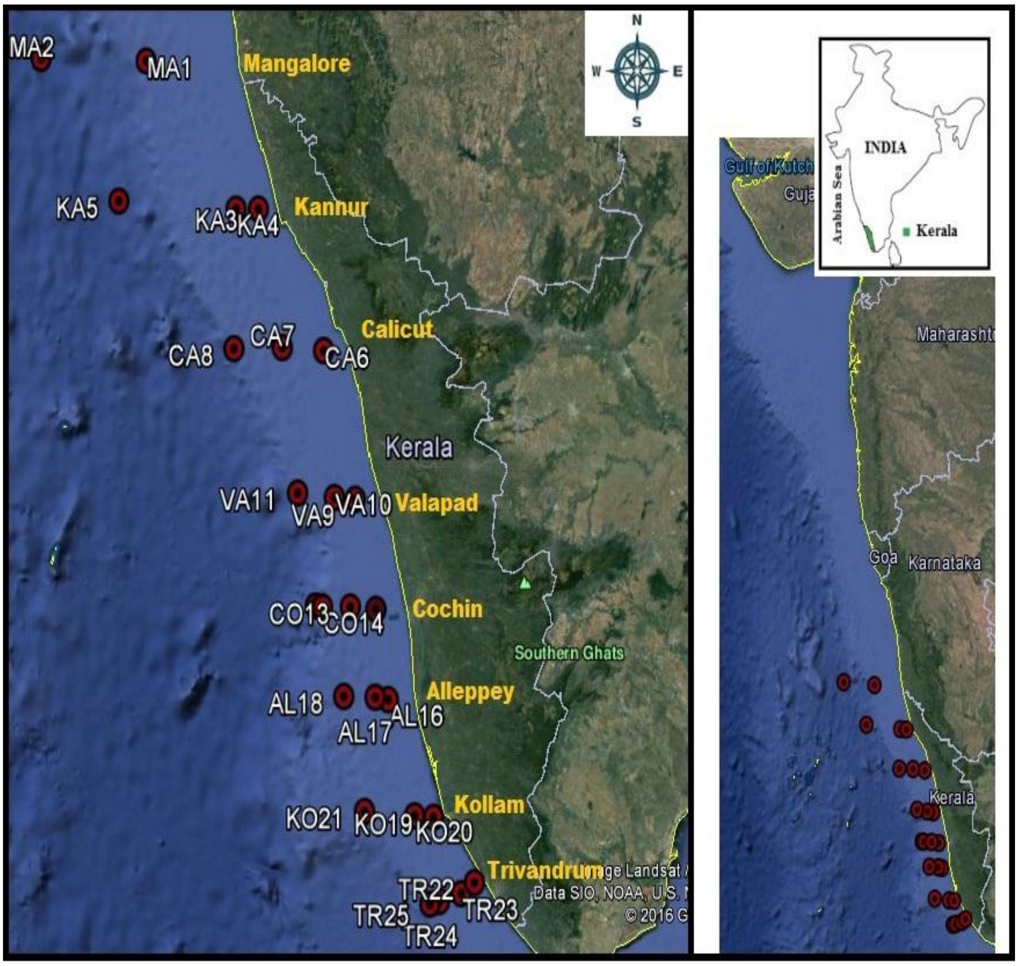

Fig. 2.3 Map of the study region and location of sampling sites during July-August 2013 (Cruise No. 316 & 318).

Another sampling was carried out during northeast monsoon (November-December 2014) and sediments were collected from eighteen stations in five transects coast-offshore in water depths 30 to 1000 m (transects A, B, C, D and E) running approximately perpendicular to the coast of Southern Kerala (Southwest India, Table 2.4/Fig. 2.4). Transect A with stations A1, A2, A3, A4 and A5 are located perpendicular to the coast of Cochin, the industrial capital of Kerala, South India. B1, B2 and B3 were the sampling points in transect B which borders Alleppey and Vembanad wetlands. Transect C includes C1, C2, C3 and C4, lies in the region of Kollam. Transect D and E lie in Trivandrum and Cape in the southern part of the study region with stations D1, D2, D3 and D4, and E1 and E2 respectively. Surface sediments were sampled onboard FORV Sagar Sampada (Cruise No. 332) using Smith-McIntyre grab sampler (0.2 m^2) and were transferred to polyethylene bags without any metal contamination. Samples were preserved at −20°C, freeze dried and ground using agate mortar for further analyses.

Table 2.4: Location of sampling sites selected for the study in the Arabian Sea off Southern Kerala.

Transect	Station code	Depth	Latitude	Longitude
		m	°N	°E
Cochin	A1	30	09°58.00'	75°59.78'
	A2	50	10°00.09'	75°49.63'
	A3	104	09°39.75'	75°43.80'
	A4	202	09°39.50'	75°39.52'
	A5	500	09°56.97'	75°32.85'
Alleppey	B1	30	09°30.38'	76°08.52'
	B2	53	09°30.69'	76°02.42'
	B3	215	09°32.96'	75°44.36'
Kollam	C1	30	08°59.67'	76°23.74'
	C2	50	09°00.31'	76°17.02'
	C3	300	09°01.42'	75°52.55'
	C4	400	09°00.08'	75°28.54'
Trivandrum	D1	30	08°31.49'	76°48.97'
	D2	100	09°58.67'	75°29.44'
	D3	490	08°30.90'	76°16.55'
	D4	1000	08°32.71'	75°59.11'
Cape	E1	30	07°59.43'	77°35.15'
	E2	50	07°47.45'	77°29.94'

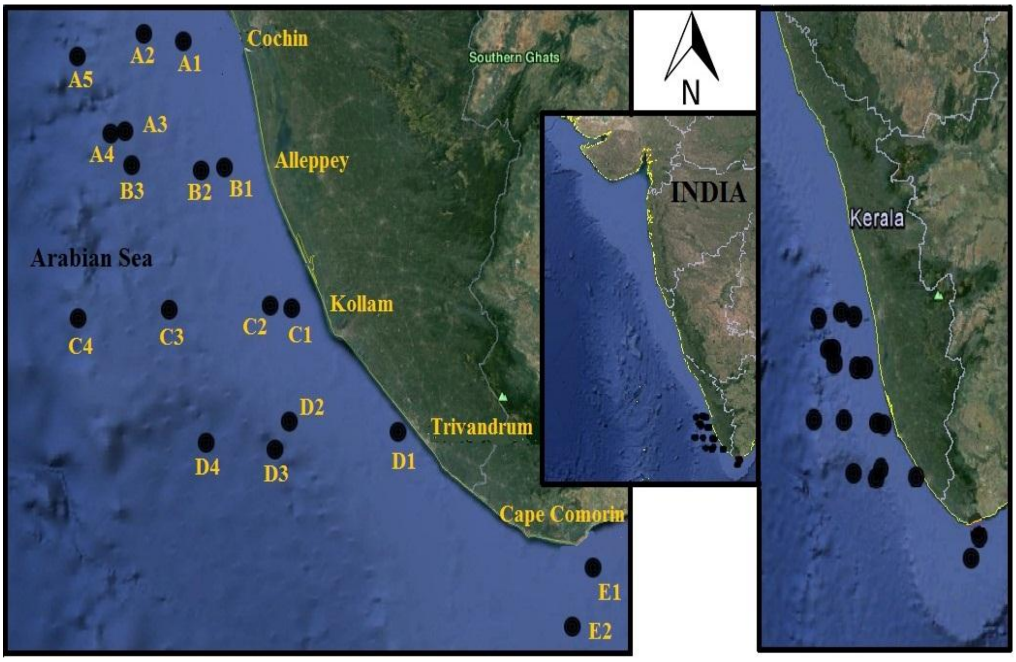

Fig. 2.4 Map of the study area and sampling locations during November-December 2014 (Cruise No. 332).

2.2 Analytical Methodology

2.2.1 Hydrographical Parameters

Hydrographical parameters such as temperature and dissolved oxygen profiles were recorded using a conductivity-temperature-depth (CTD) profiler (SBE 11 Plus, Sea-Bird, Redmond, WA, USA).

2.2.2 Nutrient Analysis

Water samples were analyzed for various nutrients (ammonia, nitrites, nitrates, phosphate and silicates) following the standard methods in Grasshoff et al. (1999). The ammonia in the seawater reacts in moderately alkaline solution with sodium hypochlorite and phenol in the presence of catalytic amount of nitroprusside ions and excess of hypochlorite to produce indophenol blue. The measurements were carried out spectrophotometrically at 630 nm (Analytik Jena Specord 200 plus). Nitrites were determined based on the reaction with sulphanilamide, leading to the formation of a diazonium compound which is then coupled with *N*-(1-Naphthyl)ethylenediamine dihydrochloride. The absorbance of the azo dye thus formed is measured spectrophotometrically at 543 nm. Nitrate in seawater is quantitatively reduced to nitrite by heterogeneous reduction involving copper-cadmium granules and determined as nitrite at 543 nm. Inorganic phosphate in seawater is determined by the reaction of ortho phosphate ions with an acidified molybdate reagent to yield a phosphomolybdate heteropoly acid, which is then reduced to a highly coloured blue complex and the absorbance is measured at 880 nm. Silicates were allowed to react with acid molybdate reagent resulting in the formation of silicomolybdate complex and get reduced to a blue reduction compound on treatment with reducing solution, containing ascorbic acid and oxalic acid. The absorbance of the compound is measured at 810 nm.

2.2.3 Texture Analysis

Sediment texture, broadly sand, silt and clay fractions were determined by pipette analysis using wet sediment samples after removing inorganic carbonates using 10% HCl and organic matter with 30% H_2O_2 (Folk, 1974). Sediment samples dispersed in sodium hexametaphosphate were wet sieved using a 63 μm sieve to determine the sand fraction. The remaining silt and clay fractions were estimated by the gravimetric separation of dispersed sediments.

2.2.4 Bulk Elemental Compositions

The bulk elemental compositions, total carbon (TC), total hydrogen (TH), total nitrogen (TN) and total sulphur (TS) were measured with a Vario EL III CHNS Analyzer. Total organic carbon (TOC) was evaluated after treating the sediments with 1M HCl to remove carbonates and analyzed using Elementar Vario Select TOC Analyzer. Samples were run with blank cups in order to correct the carbon and nitrogen associated with tin/silver cups.

Standard sediment supplied by Elementar Vario Select, Germany, was used for calibration in the TOC analyzer. Total inorganic carbon (TIC) was calculated as the difference between TC and TOC. Calcium carbonate ($CaCO_3$) was calculated by multiplying the TIC by 8.33, obtained from the difference of TC and TOC.

2.2.5 Phytopigments

Phytopigment analyses were carried out according to Lorenzen and Jeffrey (1980). Pigments were extracted with 90% acetone. In the extracts, chlorophyll-a (Chl-a), chlorophyll-b (Chl-b), chlorophyll-c (Chl-c) and carotenoids (Carot) were determined spectrophotometrically using standard equations. Their degradation products, the phaeopigments (Phaeo) were measured after acidification with 0.1N HCl (Plante-Cuny, 1974). The Chl-a/Chl-b, Chl-a/Chl-c, Chl-a/Carot and Chl-a/Phaeo ratios were also calculated.

2.2.6 Sedimentary Organic Matter and Trophic Status Evaluation

Total carbohydrates (CHO) were quantified colorimetrically by phenol-sulphuric acid method. The concentration was measured at 480 nm and expressed as glucose equivalents (Dubois et al., 1956). Total Protein (PRT) analysis was carried out following the sediment sample extraction with NaOH and expressed as bovine serum albumin (BSA) equivalents (Lowry et al., 1951). Total Lipids (LIP) from marine sediments were extracted by direct elution with chloroform and methanol. Absorbance measured at 440 nm (Barnes and Blackstock, 1973). All analyses were carried out in triplicate and determinations were done by spectrophotometric techniques (Analytik Jena Specord 200 plus). The concentrations of CHO, PRT and LIP were converted into carbon equivalents using conversion factors of 0.40, 0.49, and 0.75 of C g^{-1} respectively, and the sum of CHO, PRT and LIP carbon was referred as biopolymeric carbon (BPC; Fichez, 1991). Further, the algal contribution to

BPC was calculated as the percentage of chlorophyll-a to BPC concentrations, after converting chlorophyll-a concentrations into carbon equivalents using a mean value of 40 (Pusceddu et al., 2009). The PRT/CHO and LPD/CHO ratios were calculated and used as indicators of organic matter diagenesis (Dell'Anno et al., 2002).

The trophic status of the system was evaluated on the basis of both CHO and PRT values: hypertrophic (PRT > 4.0 mg g^{-1}; CHO > 7.0 mg g^{-1}; PRT/CHO > 1), eutrophic (PRT = 1.5–4.0 mg g^{-1}; CHO = 5.0–7.0 mg g^{-1}; PRT/CHO > 1) and meso-oligotrophic (PRT < 1.5 mg g^{-1}; CHO < 5.0 mg g^{-1}; PRT/CHO < 1) (Dell'Anno et al., 2002). Moreover, we assigned a trophic classification of the sampling locations based on BPC concentrations and the algal contribution to BPC following Pusceddu et al. (2011): eutrophic (BPC > 3 mg C g^{-1}; algal fraction < 12% of BPC), mesotrophic (BPC 1–3 mg C g^{-1}; algal fraction; 12–25% of BPC) and oligotrophic (BPC < 1 mg C g^{-1}; algal fraction > 25% of BPC).

2.2.7 Major and Trace Metal Analysis

For metal analysis, the sediments were dried at 50–60°C in an oven and disaggregated in an agate mortar. About 200 mg of sediment was digested with a solution of concentrated $HClO_4$-HNO_3-HF mixer nearly to dryness in a microwave digester (Anton Paar Multiwave 3000). The residue was diluted to 25 mL (Loring and Rantala, 1992). Blank acid mixtures were digested in the same manner. Trace metal concentrations (Cd, Co, Cu, Fe, Mg, Mn, Ni, Pb and Zn) were measured using a flame atomic absorption spectrophotometer (AAS) at specific wavelengths and appropriate hollow cathode lamps of each metal were used as light sources (Perkin Elmer 3110). Major and trace metal levels to study the geochemical influence in the surface sediments of Arabian Sea (Cruise No. 332) were determined using inductively coupled plasma-atomic emission spectroscopy (ICP-AES; Thermo Electron IRIS INTREPID II XSP DUO). All analyses were taken in triplicate and mean values were calculated. Detection limits for ICP-AES were 0.1% for Ca and Fe, 0.01% for Al and Mg, 0.01 mg kg^{-1} for Cd, Co, Cr, Cu, Mn and Zn, and 0.03 mg kg^{-1} for Pb.

2.3 Quality Assurance and Quality Control

Sediment cores were collected using a hand held PVC cores and sub-sectioned in the laboratory. Water samples were collected using a Niskin sampler (GO-FLO USA), and surface sediment samples were obtained using a Van Veen grab (0.042 m^2) and a Smith-McIntyre grab (0.2 m^2). Samples were taken from the central part of the grab sampler to avoid any metallic contamination from the metallic sampler. The samples were frozen at −20°C and stored until analysis. Freeze dried sediment samples were homogenized following the cone and quartering method and were ground, mixed, and powdered in an agate mortar (ASTM 230) before analytical procedures were conducted. Milli-Q water (Millipore 18.2 MΩ.cm) was used for preparing standards and reagents. All reagents used for the analysis of the samples were A.R Select grade or Suprapur grade (Merck). All the materials used in metal analysis were acid cleaned (dil. HNO_3) and washed several times with deionized water (Milli-Q). To ensure non-contamination of samples during analysis, a series of analytical blanks were measured. These blanks were treated in the same way as the samples and the results were blank corrected. In order to check the precision and accuracy of the measurements, certified reference materials were analyzed using the same protocol. Accuracy of the metal analysis was checked using standard reference material BCSS-I (standard reference material for marine and estuarine sediments). Triplicate analysis of quality control samples showed a good accuracy and the recovery rate ranged between 91.2% for Mn and 103.8% for Zn (Table 2.5).

Table 2.5: Analysis of standard reference materials BCSS-I for metals (mg kg^{-1} except Fe and Mg in %).

Metal	Cd	Co	Cu	Fe	Mg	Mn	Ni	Pb	Zn
Certified values	0.30	11.4	18.5	4.7	2.44	229	55.3	22.7	119
Measured values (n=3)	0.297	11.6	18.3	4.61	2.23	208.9	51.15	23.6	123.64

2.4 Geochemical Indices

2.4.1 Enrichment Factor

Enrichment factor (EF) is an important tool to assess metal enrichment and here, it is utilized for determining the anthropogenic and detrital metal evolution in the sediments and to predict the pollution status of the environment. EF is calculated as

$$EF = (M_s/N_s)/(M_b/N_b)$$

where M_s and M_b represent the metal concentration in the studied sample and the background respectively, and N_s and N_b are the metal concentration used for normalization in the studied sample and the background respectively. Al and Fe are the most commonly used conservative elements for normalization in geochemical studies. In this study, Al and Fe have been used as a conservative tracer to differentiate natural from anthropogenic components. The classification used to denote the degree of enrichment factor is given by Chen et al. (2007). It is categorized as $EF < 1$ indicates no enrichment, $EF < 2$ represent minor enrichment, EF = 2–5 implies moderate enrichment, EF = 5–10 shows moderately severe enrichment, EF = 10–25 display severe enrichment, EF = 25–50 represent very severe enrichment and $EF > 50$ shows extremely severe enrichment (Table 2.6).

2.4.2 Geoaccumulation Index

Geoaccumulation index (I_{geo}) is calculated to reveal the dominant source of metals to sediments and as indicators for anthropogenic activities, employing the equation (Müller, 1969).

$$I_{geo} = \log_2[C_n/(1.5B_n)]$$

where C_n is the concentration of metal analyzed, B_n is the background level of the metal and 1.5 is the background matrix correction factor due to lithogenic effects. I_{geo} consists of seven classes (Table 2.6) defined as : class I – $I_{geo} \leq 0$ (unpolluted), class II – $0 < I_{geo} \leq 1$ (unpolluted to moderately polluted), class III – $1 < I_{geo} \leq 2$ (moderately polluted), class IV – $2 < I_{geo} \leq 3$ (moderately to strongly polluted), class V – $3 < I_{geo} \leq 4$ (strongly polluted), class VI – $4 < I_{geo} \leq 5$ (strongly to extremely polluted) and class VII – $I_{geo} > 5$ (extremely polluted) (Müller, 1981).

Table 2.6: Range and classification of geochemical normalization methods and contamination indices.

Parameters	Range of values	Contamination category
Enrichment Factor (EF)	EF < 1	No enrichment
	EF < 2	Minor enrichment
	EF = 2–5	Moderate enrichment
	EF = 5–10	Moderately severe enrichment
	EF = 10–25	Severe enrichment
	EF = 25–50	Very severe enrichment
	EF > 50	Extremely severe enrichment
Geoaccumulation Index (I_{geo})	$I_{geo} \leq 0$	Unpolluted
	I_{geo} = 0–1	Unpolluted to moderately polluted
	I_{geo} = 1–2	Moderately polluted
	I_{geo} = 2–3	Moderately to strongly polluted
	I_{geo} = 3–4	Strongly polluted
	I_{geo} = 4–5	Strongly to extremely polluted
	$I_{geo} > 5$	Extremely polluted
Contamination Factor (CF)	CF < 1	Low contamination
	1 ≥ CF > 3	Moderate contamination
	3 ≥ CF ≥ 6	Considerable contamination
	CF > 6	Very high contamination
Pollution Load Index (PLI)	PLI < 1	Unpolluted area
	PLI = 1	Baseline level of pollutants
	PLI > 1	Polluted area

2.4.3 Contamination Factor

The level of contamination of sediment by a metal is often expressed in terms of a contamination factor calculated as:

$$CF = \frac{M_s}{M_b}$$

where M_s and M_b represent metal concentration in the sediment analyzed and background concentration of the respective metal. CF < 1 refers to low contamination, 1 ≥ CF ≥ 3 means moderate contamination, 3 ≥ CF ≥ 6 indicates considerable contamination and CF > 6 indicates very high contamination (Table 2.6).

2.4.4 Pollution Load Index

The assessment of contamination extent of metals in the sediments (Tomlinson et al., 1980) is further calculated using pollution load index (PLI). It provides a summative indication of the overall level of heavy metal pollution in a particular sample. PLI is evaluated using the equation,

$$PLI = \sqrt[n]{CF_1 \times CF_2 \times CF_3 \ldots\ldots\ldots\ldots\ldots . CF_n}$$

In the above equation, n is the number of metals for which the contamination factor (CF) is calculated as described above. The PLI provides simple but comparative means for assessing a site quality, where a value of PLI < 1 denotes unpolluted area; PLI = 1 presents baseline level of pollutants and PLI > 1 would indicate deterioration of site quality (Tomilson et al., 1980; Table 2.6).

2.5 Ecological Risk Assessment

2.5.1 Sediment Quality Guidelines

To evaluate the potential effects of metals to biota, sediment quality guideline variables, namely effective range low (ERL) and effective range medium (ERM) are applied based on Long et al. (1995). Sediment quality guideline variables, viz., namely effective range low (ERL) and effective range medium (ERM) compare the metal levels obtained in the present study. When the metal level is below ERL, the effects on biota would be rarely observed. At concentrations between ERL and ERM, the effect on biota occurs occasionally by the pollutant. If the metal concentration ≥ ERM, the effects would arise frequently (Table 2.7).

Table 2.7: Ecological risk assessment using different sediment quality guidelines proposed by Long et al. (1995).

Element (mg kg^{-1})	Cd	Cr	Cu	Ni	Pb	Zn
ERL	1.2	81	34	20.9	46.7	150
ERM	9.6	370	270	51.6	218	410

2.5.2 Potential Ecological Risk Assessment Index

The potential ecological risk assessment index describes the ecological risk associated with a single metal as Er_i and the overall potential risks of metals as RI (Håkanson, 1980). The Er_i and RI are calculated as follows:

$$Er_i = T_i(C_i/C_i{}^n)$$

$$RI = \sum Er_i = \sum T_i\ (C_i/C_i{}^n)$$

where Er_i is the potential ecological risk associated with metal i; C_i is the concentration of metal i; C_i^n is the background value of metal i; T_i is the toxicity coefficient of metal i and RI is the sum of potential risk factors for metals in sediment. The toxicity coefficients for Cd, Cr, Cu, Pb, Ni and Zn are given as 30, 2, 5, 5, 5 and 1, respectively (Håkanson, 1980). The Er_i is classified as $Er_i < 40$ poses a low risk, $40 \leq Er_i < 80$ indicates moderate risk, $80 \leq Er_i < 160$ gives considerable risk, $160 \leq Er_i < 320$ provides high risk and $Er_i \geq 320$ indicates very high risk. The RI classifications are RI < 150 indicates low risk, $150 \leq RI < 300$ gives moderate risk, $300 \leq RI < 600$ for considerable risk and $RI \geq 600$ for very high ecological risk (Table 2.8).

Table 2.8: Classification based on potential ecological risks of metals.

Risk index for single metal	Overall potential risk	Risk Classification
$Er_i < 40$	$RI < 150$	Low risk
$40 \leq Er_i < 80$	$150 \leq RI < 300$	Moderate risk
$80 \leq Er_i < 160$	$300 \leq RI < 600$	Considerable risk
$160 \leq Er_i < 320$	$RI \geq 600$	High risk
$Er_i \geq 320$		Very high risk

2.6 Data Treatment and Statistical Analysis

All the statistical analysis was performed using SPSS 13.0 for windows software. When the data sets did not conform to normality, the appropriate transformations were carried out before applying statistical methods. Physical and geochemical data were $\log_{10}(x+1)$ transformed to reduce the biasing effect of extremely low or high element concentrations (Chapman, 1996). Pearson correlation analysis was performed to find out the degree of relationship within the analyzed parameters for a better interpretation of trace metals and its associated factors. Principal component analysis (PCA) is an exploratory method of data analysis applied to reduce the number of variables into fewer linear latent factors of similar characteristics on the basis of correlations or covariances between them (Micó et al., 2006). The factors obtained are then rotated using varimax method, for extracting more appreciable information on the significance of the variables. Hierarchical cluster analysis (HCA) was performed as data reduction tool that creates sub clusters for finding easier inter-relationship than individual datum. The results were presented in a two dimensional plot called dendrogram showing clusters based on the linear pair coefficient of association between the variables.

References

Akhil, P.S., Sujatha, C.H., 2014. Spatial budgetary evaluation of organochlorine contaminants in the sediments of Cochin Estuary, India. Marine Pollution Bulletin, 78, 246–251.

Babu, C.P., Brumsack, H.J., Schnetger, B., Böttcher, M.E., 2002. Barium as a productivity proxy in continental margin sediments: a study from the eastern Arabian Sea. Marine Geology, 184, 189–206.

Barnes, H., Blackstock, J., 1973. Estimation of lipids in marine animal's tissues: Detailed investigation of the sulphophosphovanillin method for total lipids. Journal of Experimental Marine Biology and Ecology, 12, 103–118.

Bindu, K.R., Deepulal, P.M., Gireeshkumar, T.R., Chandramohanakumar, N., 2015. Evaluation of heavy metal enrichment in Cochin estuary and its adjacent coast: multivariate statistical approach. Environmental Monitoring and Assessment, 187, 519. doi: 10.1007/s10661-015-4749-2.

Burkill, P.H., Mantoura, R.F.C., Owens, N.J.P., 1993. Biogeochemical cycling in the north western Indian Ocean: a brief overview. Deep Sea Research Part II: Topical Studies in Oceanography, 40, 643–649.

Chapman, P.M., 1996. Presentation and interpretation of sediment Quality Triad data. Ecotoxicology, 5, 327–339.

Chen, C.W., Kao, C.M., Chen, C.F., Dong, C.D., 2007. Distribution and accumulation of heavy metals in the sediments of Kaohsiung Harbor, Taiwan. Chemosphere, 66, 1431-1440.

Ciji, P.P., Nandan, S.B., 2014. Toxicity of copper and zinc to *Puntius parrah* (Day, 1865). Marine Environmental Research, 93, 38–46.

Dell'Anno, A., Mei, M.L., Pusceddu, A., Danovaro, R., 2002. Assessing the trophic state and eutrophication of coastal marine systems: A new approach based on the biochemical composition of sediment organic matter. Marine Pollution Bulletin, 44, 611–622.

Dsikowitzky, L., Nordhaus, I., Sujatha, C.H., Akhil, P.S., Soman, K., Schwarzbauer, J., 2014. A combined chemical and biological assessment of industrial contamination in an estuarine system in Kerala, India. Science of the Total Environment, 485, 348–362.

Dubois, M., Gills, K.A., Hamilton, J.K., Roberts, P.A., Smith, F., 1956. Colorimetric method for the determination of sugars and related substances. Analytical Chemistry, 28, 350–356.

Fichez, R., 1991. Composition and fate of organic matter in submarine cave sediments; Implications for the biogeochemical cycle of organic carbon. Oceanologica Acta, 14, 369–377.

Folk, R.L., 1974. Petrology of sedimentary rocks. Hemphill publishing company, Austin, Texas.

Goldberg, E.D., Griffin, J.J., 1970. The sediments of the northern Indian Ocean. Deep Sea Research and Oceanographic Abstracts, 17, 513–537.

Gopalan, U.K., Vengayil, D.T., Udayavarma, P., Krishnankutty, M., 1983. The shrinking backwaters of Kerala. Journal of the Marine Biological Association of India, 25, 131–141.

Grasshoff, K., Ehrhardt, M., Kremling, K., (Eds.) 1999. Methods of seawater analysis. Verlag Chemie, Weinheim.

Green Peace, 2003. Status of Periyar's Health at Eloor Industrial Estate, Kerala, India–A Compilation of New Evidences.

Habeebrehman, H., Prabhakaran, M.P., Jacob, J., Sabu, P., Jayalakshmi, K.J., Achuthankutty, C.T., Revichandran, C., 2008. Variability in biological responses influenced by upwelling events in the Eastern Arabian Sea. Journal of Marine Systems, 74, 545−560.

Håkanson, L., 1980. An ecological risk index for aquatic pollution control: a sedimentological approach. Water Research, 14, 975–1001.

Hupe, A., Karstensen, J., 2000. Redfield stoichiometry in Arabian Sea subsurface waters. Global Biogeochemical Cycles, 14, 357–372.

Jyothibabu, R., Madhu, N.V., Habeebrehman, H., Jayalakshmy, K.V., Nair, K.K.C., Achuthankutty, C.T., 2010. Reevaluation of 'paradox of mesozooplankton' in the eastern Arabian Sea based on ship and satellite observations. Journal of Marine Systems, 81, 235–251.

Long, E.R., McDonald, D.D., Smith, S.L., Calder, F.D., 1995. Incidents of adverse biological effects within ranges of chemical concentrations in marine and estuarine sediments. Environmental Management, 19, 81–97.

Lorenzen C., Jeffrey, S.W., 1980. Determination of chlorophyll in sea water. UNESCO Technical Papers in Marine Science, 35, 1–20.

Loring, D.H., Rantala, R.T.T., 1992. Manual for geochemical analysis. Earth-Science Reviews, 32, 235–283.

Lowry, O.H., Rosebrough, N.J., Fart, A.L., Randall, R.J., 1951. Protein measurement with the Folin phenol reagent. The Journal of Biological Chemistry, 193, 265–275.

Marra, J., Barber, R.T., 2005. Primary productivity in the Arabian Sea: A synthesis of JGOFS data. Progress in Oceanography, 65, 159–175.

Martin, G.D., Nisha, P.A., Balachandran, K.K., Madhu, N.V., Nair, M., Shaiju, P., Joseph, T., Srinivas, K., Gupta, G.V.M., 2011. Eutrophication induced changes in benthic community structure of a flow-restricted tropical estuary (Cochin backwaters), India. Environmental Monitoring and Assessment, 176, 427–438.

Micó, C., Recatalá, L., Peris, M., Sánchez, J., 2006. Assessing heavy metal sources in agricultural soils of an European Mediterranean area by multivariate analysis. Chemosphere, 65, 863–872.

Müller, G., 1969. Index of geoaccumulation in the sediments of the Rhine River. The Journal of Geology, 2, 108–118.

Müller, G., 1981. The heavy metal pollution of the sediments of Neckars and its tributary. Chemiker-Zeitung, 105, 157–164.

Nandan, S.B., 2005. Fishery of selected prawn species in Kayamkulam backwater. Central Inland Fisheries Research Institute. CIFRI Bulletin No. 140.

Naqvi, S.W.A., Jayakumar, D.A., Narvekar, P.V., Naik, H., Sarma, V.V.S.S., D'Souza, W., Joseph, S., George, M.D., 2000. Increased marine production of N_2O due to intensifying anoxia on the Indian continental shelf. Nature, 408, 346–349.

Naqvi, S.W.A, Naik, H., Jayakumar, D.A., Shailaja, M.S., Narvekar, P.V., 2006. Seasonal oxygen deficiency over the western continental shelf of India. In: Neretin, l., (Ed.), Past and Present Water Column Anoxia. NATO Science Series, IV, Springer, Netherlands.

Plante-Cuny, M.R., 1974. Evaluation par spectrophotométrie des teneurs en chlorophylle a fonctionnelle et en phéopigments des substrats meubles marins. ORSTOM, Institut Français de Recherche Scientifique pour le Dévelopment en Coopération, Nosy-Bé, Madagascar, 45, 84.

Pusceddu, A., Dell'Anno, A., Fabiano, M., Danovaro, R., 2009. Quantity and bioavailability of sediment organic matter as signatures of benthic trophic status. Marine Ecology Progress Series, 375, 41–52.

Pusceddu, A., Bianchelli, S., Gambi, C., Danovaro, R., 2011. Assessment of benthic trophic status of marine ecosystems: Significance of meiofaunal rare taxa. Estuarine Coastal and Shelf Science, 93, 420–430.

Ramaswamy, V., Nair, R.R., Manganini, S., Haake, B., Ittekkot, V., 1991. Lithogenic fluxes to the deep Arabian Sea measured by sediment traps. Deep Sea Research Part A. Oceanographic Research Papers, 38, 169–184.

Rao, V.P., Rao, B.R., 1995. Provenance and distribution of clay minerals in the sediments of the western continental shelf and slope of India. Continental Shelf Research, 15, 1757–1771.

Salas, P.M., Sujatha, C.H., Kumar, C.S.R., Cheriyan, E., 2017. Heavy metal distribution and contamination status in the sedimentary environment of Cochin Estuary. Marine Pollution Bulletin, 119, 191–203.

Srinivas, K., Revichandran, C., Maheswaran, P.A., Asharaf, T.M., Murukesh, N., 2003. Propagation of tides in the Cochin estuarine system, southwest coast of India. Indian Journal of Marine Science, 32, 14–24.

Thamban, M., 1998. Changing depositional environments during the Late Quatrnary along the western continental margin of India. Journal Indian Association of Sedimentologists, 17, 147–156.

Tomlinson, D.L., Wilson, J.G., Harris, C.R. Jeffrey, D.W., 1980. Problems in the assessment of heavy metal levels in estuaries and the formation of a pollution index. Helgol Mar Res, 33, 566–575.

Wiggert, J.D., Hood, R.R., Banse, K., 2005. Monsoon-driven biogeochemical processes in the Arabian Sea. Progress in Oceanography, 65, 176–213.

Chapter

3 METAL DISTRIBUTION BACKGROUND USING SEDIMENT CORES

Contents

3.1 Introduction

Sediments are important carriers of trace metals as they bind to suspended particles and accumulate via sedimentation which serves as indicators of overlying water quality and its study is a useful tool in the assessment of changing environmental deterioration altered by anthropogenic disturbances. Rivers transport sediments which play a key role in the accumulation of trace metals and the ability of sediments to adsorb the metal species is related to the different geological structures of the drainage basin (Filho et al., 2015). Nevertheless, sediment cores are critical to identify, analyze and characterize the geological and human made components of the coastal sediments and to further assess the contamination in view of any past disturbance of the sediment column due to external factors such as sand mining, excavation, land reclamation, increased recreational activities and harbour operations (Morelli and Gasparon, 2015). The historical record of metal accumulation as a result of past pollution sources can be evaluated by studying sediment cores especially in urbanized coastal sediments (Buckley et al., 1995). Additionally, sediment cores can provide the knowledge of geochemical background of metal levels which is very important in the assessment of metal pollution using normalization indices at different environments of a particular region. The establishment of geochemical background of toxic metals is necessary to delineate natural and anthropogenic metal pollution and for suggesting environmental quality for waters, soils and sediments (Gałuszka and Migaszewski, 2011). Hence, this chapter aims to (1) quantify and estimate the vertical metal distribution profile at specific locations on the Kerala coast; (2) outline the natural and anthropogenic sources of metals by applying multivariate statistical analysis; (3) assess the vertical profile to outlay the background concentration of metals to describe the regional metal composition.

To generate background metal levels and to reveal the vertical distribution profile, sediment cores were sampled from a coastal and an estuarine site namely, Cape Comorin (CC1) and Cochin estuary (CE1). A PVC corer of 54 cm and 93 cm long were obtained from Cape Comorin and Cochin estuary respectively. CC1 is in the extreme south of the study area and exclusively representative of the coastal site. On the other hand, CE1 lies in the southern arm of the Cochin estuary.

3.2 Results and Discussion

3.2.1 Bulk Sediment Properties

Grain size is one of the basic attributes of sediments and its determination is essential to delineate the sedimentary environments. In general, the study of grain size distribution reveals the physical effects of the environment on deposition and the hydrodynamic conditions existing at the time of deposition. The distribution of sand, silt and clay fraction in the core sediments of Cape Comorin (CC1) and Cochin estuary (CE1) are depicted in Fig. 3.1.

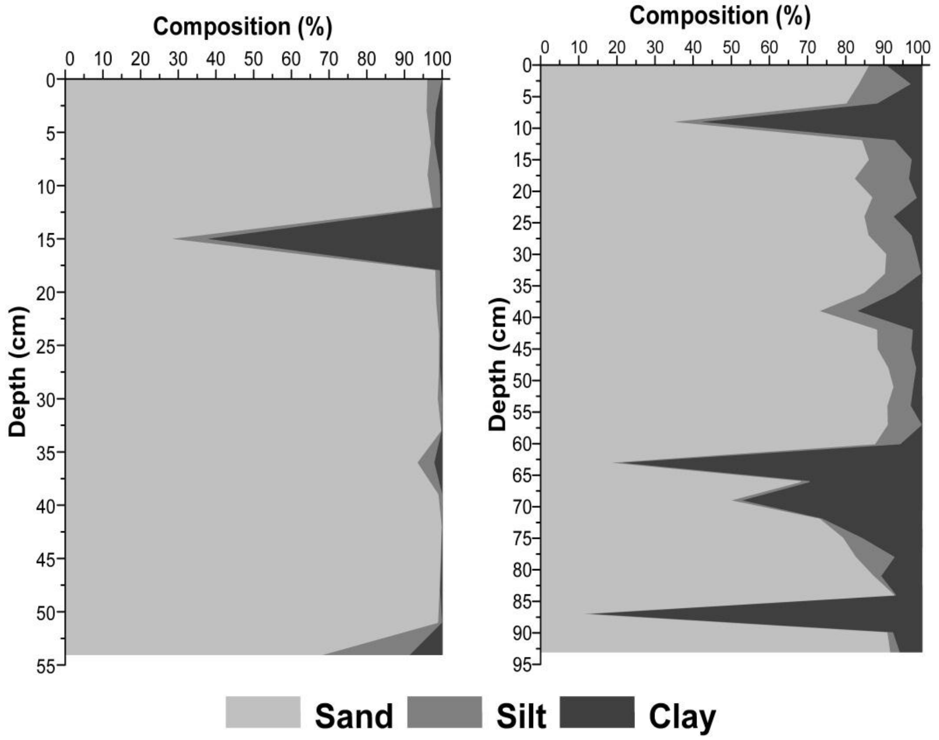

Fig. 3.1 Grain size composition downcore in the CC1 (left) and CE1 (right) core sediments.

The sand, silt and clay content varied between 27.05–99.80%, 0.02–23.12% and 0.07–63.44% in the core sediments of CC1 respectively. On the other hand, the sand content (> 63µm) varied from 8.84% to 92.58% showing the maximum at depth 84 to 87 cm in core CE1. The silt and clay content ranges from 0.46% to 14.26% and 0.16% to 89.31% respectively. Sediments at the depths 9–12, 63–66, 87–90 (cm) are majorly comprised of silt and clay rather than the sand fraction. Further, the silt and clay content together contributed 66.56%, 83.18% and 91.16% at depths 9–12, 63–66, 87–90 (cm) respectively. The distribution profile remarks the dominance of sand content in the core sediments. Overall fine sediment represented less than 25% in the entire length of the cores. The presence of coarser sediments such as sand and other particles (> 63µm) effectively dilutes the contaminant concentrations. The high sedimentation rate may be the factor responsible for the predominance of sandy nature in the sediments (Silver and Gowing, 1991). Sandy soils are well aerated and contain low organic matter content. These sediments are poor in organic matter preservation (Suthhof et al., 2000).

3.2.2 Vertical Distribution Profile of Major and Trace metals

3.2.2a. Cape Comorin

The vertical distribution profile of metals varied significantly from each other: Mg, 0.22–0.67% (average, 0.37%), Fe, 0.16–0.37% (average, 0.25%), Al, 0.03–0.10% (average, 0.06%), Mn, 17.14–48.47 mg kg^{-1} (average, 25.52 mg kg^{-1}), Zn, 3.59–16.82 mg kg^{-1} (average, 7.16 mg kg^{-1}), Cu, 0.05–10.65 mg kg^{-1} (average, 4.29 mg kg^{-1}), Cr, 0.89–9.12 mg kg^{-1} (average, 4.17 mg kg^{-1}), Pb, 0.20–6.88 mg kg^{-1} (average, 1.76 mg kg^{-1}), Ni, 0.05–1.59 mg kg^{-1} (average, 0.62 mg kg^{-1}) and Co, 0.03–0.44 mg kg^{-1} (average, 0.19 mg kg^{-1}). Cd was below detectable level in the entire section of the core. The distribution profile of major and trace metals revealed a significant enrichment in the upper portion of the core. Downcore metal variations are mainly affected by precipitation/dissolution processes at the redox boundary, adsorption/ desorption mechanisms and the degradation of organic matter (Du Laing et al., 2009; Beck et al., 2013). Pearson’s correlation analyses were applied to determine the relationships and interdependence of analyzed sedimentary parameters.

The average concentration of metals in Cape Comorin (CC1) core decreased in the following order: Mg > Fe > Al > Mn > Zn > Cu > Cr > Pb > Ni > Co (Table 3.1). Mg is an abundant element and a major constituent of clay minerals in the earth's crust. Besides, Fe is the most abundant metal in all sediments because it is one of the most common elements in the earth’s crust. Al is considered to be important as a conservative element since its natural abundance is not altered significantly and the metal is resistant to weathering and erosion (Wei et al., 2003). Mg content varied between 0.22% and 0.67% in the core sediments. Fe concentration ranged from 0.16% to 0.37% with an average of 0.25% whereas, Al varied from 0.03% to 0.10%. Mg and Fe had the highest concentrations than Al in the core sediments. Generally, the concentration of major metals viz., Al, Fe and Mg decreased towards the bottom of the core (Fig. 3.2). The vertical profile of Mg in the core sediments indicates that major portion is associated with geological sources. The correlation matrix employed to identify the potential metal interrelationships and thus geochemistry in the core sediments of CC1 is provided in Table 3.2. Significant positive correlations were observed between Al and most metals (Fe, Mg, Mn, Cr and Zn) suggesting the origin of these metals from terrigenous materials and not obtained from anthropogenic activities. Adsorption of the trace metals onto clay minerals containing major elements as constituents support the linear relationship of these metals with Al. The possibility of coupling of these metals to fine grained fractions can be ruled out since the downcore profile of sediment grain size predominantly composed of coarse grained texture.

Table 3.1: Major and trace metal concentrations in the Cape Comorin core sediments.

Depth	Al	Fe	Mg	Cd	Co	Cr	Cu	Mn	Ni	Pb	Zn
cm	%			mg kg^{-1}							
0–3	0.10	0.37	0.67	*BDL	0.37	9.12	2.56	48.47	1.49	0.66	16.82
3–6	0.09	0.34	0.61	BDL	0.44	8.11	2.34	37.56	0.68	0.20	6.85
6–9	0.09	0.37	0.58	BDL	0.17	5.47	0.32	37.32	1.59	2.00	10.87
9–12	0.07	0.30	0.39	BDL	BDL	5.58	1.06	22.45	0.53	6.88	9.65
12–15	0.07	0.29	0.42	BDL	0.11	5.01	0.05	25.42	0.57	2.72	6.82
15–18	0.07	0.28	0.40	BDL	0.25	5.84	0.15	24.50	0.50	1.95	6.99
18–21	0.08	0.33	0.51	BDL	0.07	2.90	1.56	30.98	0.32	1.31	5.82
21–24	0.07	0.32	0.47	BDL	0.11	1.64	0.91	32.40	0.24	2.05	7.89
24–27	0.05	0.25	0.27	BDL	0.07	1.12	0.60	22.51	0.80	1.19	4.41
27–30	0.05	0.20	0.28	BDL	0.28	0.89	1.59	20.43	0.55	0.38	5.05
30–33	0.03	0.16	0.27	BDL	0.04	4.69	5.77	17.89	0.58	1.43	3.59
33–36	0.03	0.17	0.31	BDL	BDL	5.86	5.98	18.93	1.16	1.40	5.45
36–39	0.04	0.16	0.24	BDL	0.03	3.98	5.85	17.89	0.21	1.51	3.72
39–42	0.05	0.23	0.35	BDL	0.28	4.26	8.59	27.75	0.58	1.14	14.28
42–45	0.04	0.24	0.26	BDL	BDL	3.10	6.15	22.61	0.36	1.85	5.03
45–48	0.04	0.19	0.22	BDL	0.17	1.99	8.72	18.67	BDL	1.47	7.19
48–51	0.05	0.23	0.32	BDL	0.12	3.08	10.65	21.77	0.61	2.00	6.16
51–54	0.05	0.23	0.29	BDL	0.32	3.93	9.08	20.28	0.05	1.72	5.07
54–57	0.04	0.18	0.26	BDL	BDL	2.60	9.55	17.14	0.40	1.64	4.40
Min	0.03	0.16	0.22	-	0.03	0.89	0.05	17.14	0.05	0.20	3.59
Max	0.10	0.37	0.67	-	0.44	9.12	10.65	48.47	1.59	6.88	16.82
Avg	0.06	0.25	0.37	-	0.19	4.17	4.29	25.52	0.62	1.76	7.16

*BDL: below detectable level

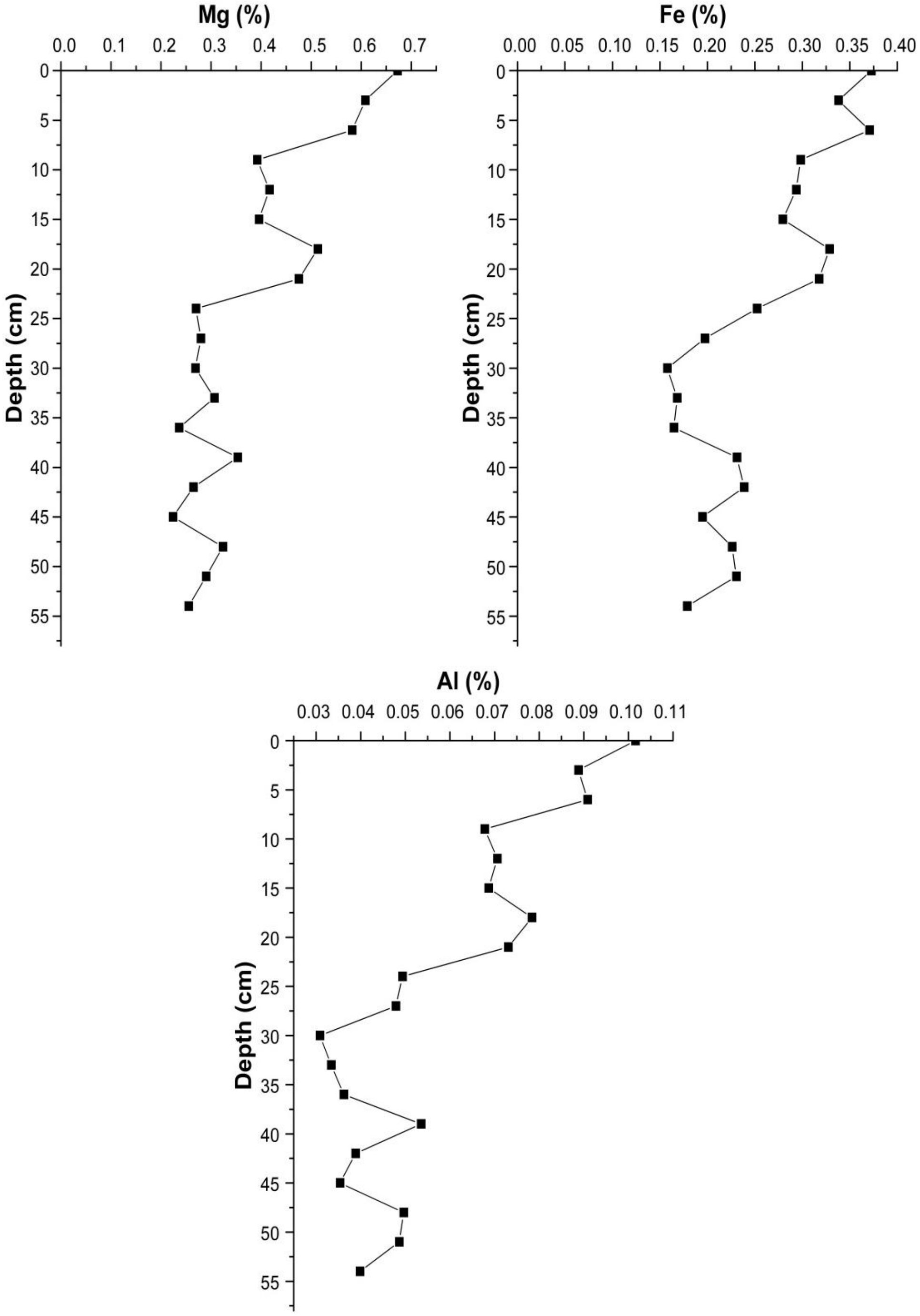

Fig. 3.2 Depth profile of Mg, Fe and Al in the CC1 core sediments.

Table 3.2: Pearson correlation coefficients for the metals and other sedimentary parameters analyzed in the Cape Comorin core sediments.

	Al	**Co**	**Cr**	**Cu**	**Fe**	**Mg**	**Mn**	**Ni**	**Pb**	**Zn**	**Sand**	**Silt**	**Clay**
Al	1												
Co	0.47	1											
Cr	*0.54*	*0.55*	1										
Cu	**−0.64**	0.03	−0.19	1									
Fe	**0.96**	0.37	0.45	**−0.64**	1								
Mg	**0.95**	0.45	**0.66**	*−0.56*	**0.91**	1							
Mn	**0.90**	0.50	**0.58**	*−0.47*	**0.88**	**0.95**	1						
Ni	0.41	0.24	*0.53*	−0.28	0.40	*0.54*	*0.56*	1					
Pb	0.06	*−0.56*	0.05	−0.17	0.13	−0.06	−0.20	−0.14	1				
Zn	**0.61**	0.50	*0.53*	−0.16	**0.59**	**0.64**	**0.74**	*0.56*	0.08	1			
Sand	−0.09	−0.14	−0.15	0.15	−0.01	0.00	0.09	0.12	−0.04	0.07	1		
Silt	−0.04	0.18	0.04	0.16	−0.14	−0.08	−0.15	−0.14	0.05	−0.10	**−0.65**	1	
Clay	0.12	0.13	0.17	−0.24	0.07	0.03	−0.05	−0.09	0.03	−0.04	**−0.96**	0.41	1

Note: Correlation significant at the 0.05 level is given in italics and correlation significant at the 0.01 level is given in bold.

Depth profile of Mn and Zn are shown in Fig. 3.3. Mn concentration varied from 17.14 mg kg^{-1} to 48.47 mg kg^{-1}. The downcore profile shows a decreasing trend with slight fluctuations towards the bottom of the core. Zn concentration in the core sediment varies between 3.59 mg kg^{-1} and 16.82 mg kg^{-1}. It shows a pronounced level at 39 cm depth (14.28 mg kg^{-1}). Mn shows positive association with Zn (r^2 = 0.74) and Ni (r^2 = 0.56). Further, Mn is a redox sensitive element and the distribution of Zn and Ni may be affected by the scavenging of Mn oxyhydroxides.

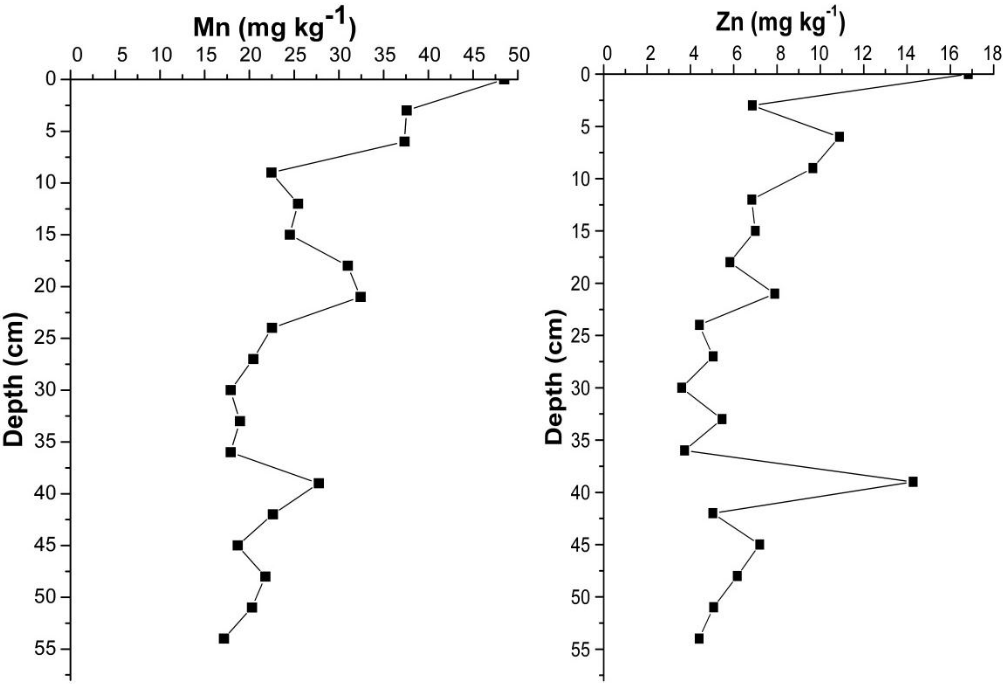

Fig. 3.3 Depth profile of Mn and Zn in the CC1 core sediments.

Cu concentrations increase with depth from 0.05 mg kg^{-1} to 10.65 mg kg^{-1} (Fig. 3.4). Cu concentrations in the top portion were much lower than the bottom of the core. It shows significant variation between the lower (5.77–10.65 mg kg^{-1}) and upper (0.05–2.56 mg kg^{-1}) part of the core. High concentration of metals below the sub-surface is generally due to the precipitation followed by downward diffusion but, limited to the top few cm of the sediment column. However, the authigenic enrichment of Cu towards the bottom of the core cannot be properly justified by this mechanism. On contrary, the enrichment pattern can be attributed to the biogeochemical changes occurred due to organic matter flux in the past and thereafter an alteration in the sedimentation processes as it is on the shoreline of the coast (Sundby et al., 2004). Further, Cu shows a negative correlation with the fraction of metals associated with source rocks such as Al, Fe, Mg and important metal adsorbing phase mainly Mn ($r^2 = -0.47$–-0.64).

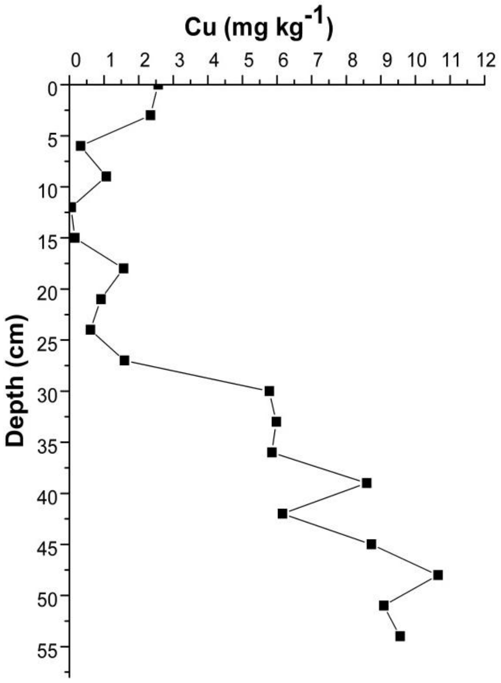

Fig. 3.4 Depth profile of Cu in the CC1 core sediments.

Depth profile of Cr, Pb, Ni and Co are depicted in Fig. 3.5. Cr varied in the range 0.89 mg kg^{-1} to 9.12 mg kg^{-1} with an average of 4.17 mg kg^{-1}. Further, Al is moderately correlated with Cr indicating a fraction of metal associated with siliciclastic sedimentary rocks. Pb concentration showed higher values in the top and substantially decreased with less significant variation towards the bottom of the core. It ranged from 0.20 mg kg^{-1} to 6.88 mg kg^{-1}. Pb levels varied less significantly below 24 cm of the core. Pb maxima (6.88 mg kg^{-1}) was observed at 9 cm of the core. Therefore, Pb levels revealed lithogenic fraction in the sediment column. In contrast to most metals, no significant correlations of Pb were observed except a moderate negative correlation with Co ($r^2 = -0.56$). Lower Pb content in the surface and sub-surface may be due to the release of metal from solid particles to pore water during sedimentary processes. Ni concentrations lie in a range of 0.05 mg kg^{-1} and 1.59 mg kg^{-1}. It averaged 0.62 mg kg^{-1} and showing a fluctuating trend throughout the depth profile. Co exhibits a varying pattern throughout the depth profile. It ranged between 0.03 mg kg^{-1} and 0.44 mg kg^{-1}. Co shows significant fluctuation in the downcore distribution.

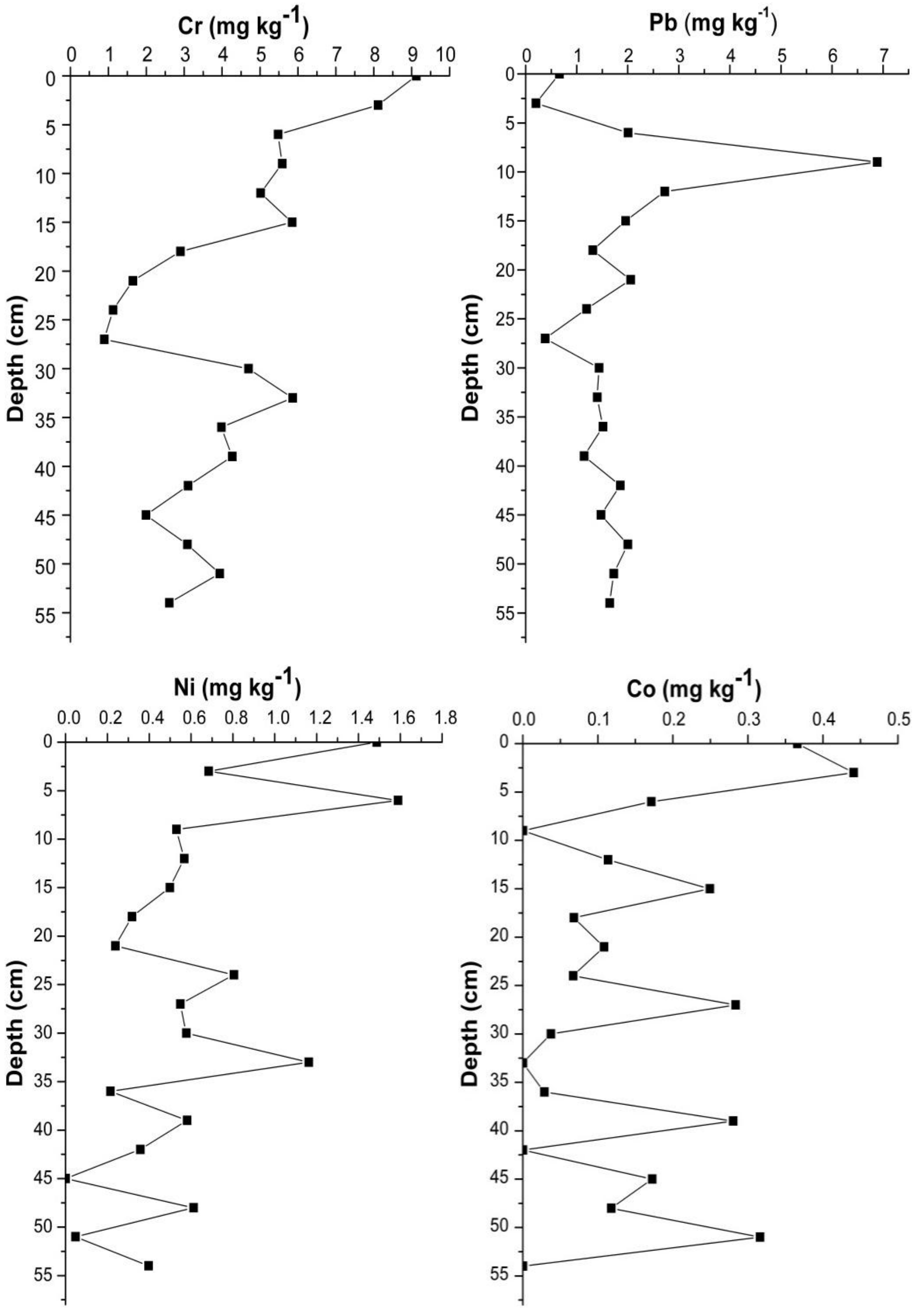

Fig. 3.5 Depth profile of Cr, Pb, Ni and Co analyzed in the CC1 core sediments.

3.2.2b. Cochin Estuary

The metal abundance in the CE1 sediments decreased in the order: Fe > Mg > Mn > Pb > Ni > Cu > Co > Zn > Cd. Fe was the most abundant heavy metal in the sediment, its concentration varying within a range of 0.04% to 1.12%. The lower values were observed at depths 39–42 cm whereas highest values recorded at depths 18–21 cm. The values suggest a lithogenic origin of metal in the sediments. The bottom of the core (60 to 96 cm) showed slight variation with values varied between 0.41% and 0.75% (Fig. 3.6). Thus, Fe in the bottom portion can be possibly generated from their source rocks and represent an area without wide redox fluctuations. Mg levels were next to Fe and the downcore profile showed slight variation from 0.12% and 0.38%. The average concentration of Mg was found to be 0.23% in the core sediments.

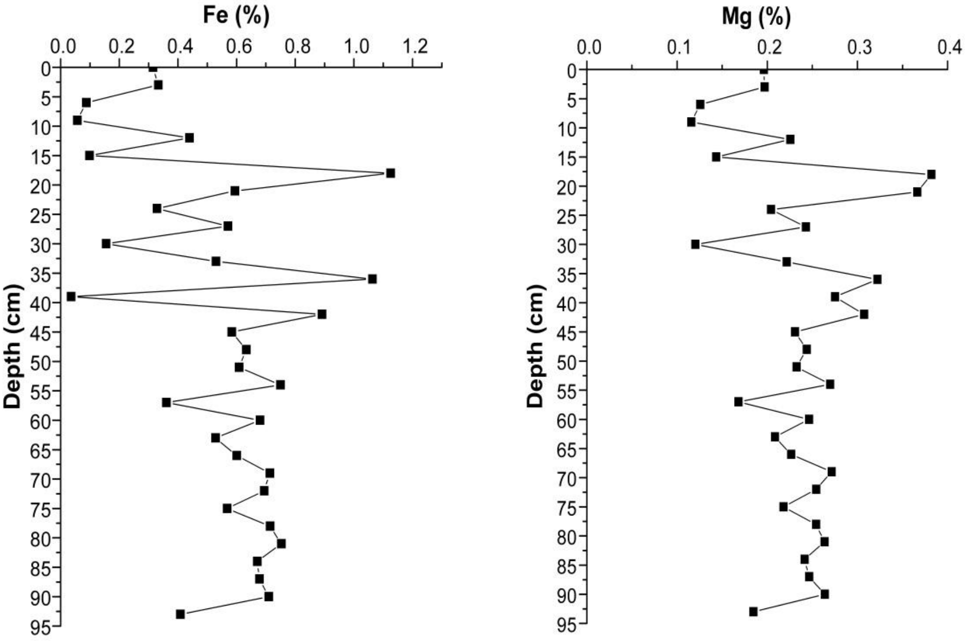

Fig. 3.6 Depth profile of Fe and Mg in the CE1 core sediments.

The mean concentrations of Cd, Co, Cu, Mn, Ni, Pb and Zn were 1.22 mg kg^{-1}, 6.65 mg kg^{-1}, 7.70 mg kg^{-1}, 35.51 mg kg^{-1}, 12.23 mg kg^{-1}, 21.23 mg kg^{-1} and 6.26 mg kg^{-1} respectively. Cd concentration was the lowest, varying from 0.25 to 2.50 mg kg^{-1} (Table 3.3).

Table 3.3: Down core metal variation in the Cochin estuary core sediments.

Depth	Fe	Mg	Cd	Co	Cu	Mn	Ni	Pb	Zn
cm	%		mg kg^{-1}						
0–3	0.31	0.20	0.61	3.65	16.06	32.61	3.16	BDL	13.99
3–6	0.33	0.20	*BDL	5.11	14.57	25.65	3.49	9.96	12.58
6–9	0.09	0.13	BDL	6.12	14.85	24.59	3.62	11.23	13.73
9–12	0.06	0.12	BDL	9.11	4.49	15.23	BDL	3.74	2.12
12–15	0.44	0.23	BDL	2.50	14.98	30.95	7.36	17.47	12.23
15–18	0.10	0.14	BDL	5.99	11.61	24.85	5.87	14.98	13.73
18–21	1.12	0.38	BDL	12.87	15.87	88.96	21.99	10.00	20.74
21–24	0.59	0.37	BDL	8.04	4.02	44.09	8.16	7.31	3.41
24–27	0.33	0.20	BDL	6.73	26.67	28.92	11.84	18.70	1.75
27–30	0.57	0.24	BDL	9.10	3.62	34.78	11.47	13.71	2.99
30–33	0.15	0.12	1.25	3.87	2.25	19.75	4.25	22.49	BDL
33–36	0.53	0.22	BDL	3.61	7.85	31.54	6.86	14.96	2.24
36–39	1.06	0.32	BDL	14.07	5.73	51.67	20.92	14.94	BDL
39–42	0.04	0.28	0.25	8.12	2.00	35.10	16.86	27.48	2.75
42–45	0.89	0.31	BDL	5.11	4.61	44.10	19.93	22.42	5.36
45–48	0.58	0.23	1.95	4.76	2.44	32.44	18.90	26.83	4.88
48–51	0.63	0.24	0.75	6.37	3.12	30.72	13.99	24.97	4.25
51–54	0.61	0.23	BDL	5.85	2.62	36.99	17.94	23.66	3.24
54–57	0.75	0.27	BDL	8.59	2.36	38.33	20.16	31.11	7.22
57–60	0.36	0.17	BDL	4.49	43.92	26.70	12.48	19.96	1.37
60–63	0.68	0.25	BDL	9.49	3.37	38.22	19.86	12.49	3.87
63–66	0.53	0.21	BDL	4.74	1.00	30.68	10.73	34.92	3.62
66–69	0.60	0.23	BDL	9.50	3.25	32.12	14.37	23.74	11.37
69–72	0.71	0.27	BDL	6.32	4.38	40.85	13.37	6.08	5.35
72–75	0.69	0.25	BDL	6.74	4.99	43.18	22.96	24.96	5.62
75–78	0.57	0.22	2.50	1.25	3.99	35.07	17.10	31.20	2.87
78–81	0.71	0.25	BDL	4.36	2.99	37.54	17.33	23.69	4.61
81–84	0.75	0.26	BDL	3.49	4.74	39.54	11.60	29.94	5.11
84–87	0.67	0.24	BDL	7.35	3.61	34.26	11.21	34.88	4.98
87–90	0.68	0.25	BDL	6.25	4.25	37.98	2.75	42.48	5.62
90–93	0.71	0.26	BDL	9.37	3.00	35.46	3.50	29.97	4.25
93–96	0.41	0.18	BDL	9.97	3.28	33.45	5.23	27.97	1.95
Min	0.04	0.12	0.25	1.25	1.00	15.23	2.75	3.74	1.37
Max	1.12	0.38	2.50	14.07	43.92	88.96	22.96	42.48	20.74
Avg	0.54	0.23	1.22	6.65	7.70	35.51	12.23	21.23	6.26

*BDL : below detectable level

Pearson's correlation coefficients indicating interrelationships and metal controlling factors among the variables of CE1 is shown in Table 3.4. Correlation analysis reveals that the trace metal concentration is not significantly influenced by grain size composition. Besides, Fe, Mg, Mn and Ni were positively correlated with each other (r^2 = 0.84–0.59) indicating their common origin from source rocks.

Table 3.4: Pearson correlation coefficients for metals in the core sediments of Cochin estuary.

	Cd	**Co**	**Cu**	**Fe**	**Mg**	**Mn**	**Ni**	**Pb**	**Zn**	**Sand**	**Silt**	**Clay**
Cd	1											
Co	*−0.42*	1										
Cu	−0.16	−0.15	1									
Fe	−0.11	0.34	−0.24	1								
Mg	−0.17	*0.41*	−0.24	**0.80**	1							
Mn	−0.14	**0.48**	−0.06	**0.78**	**0.84**	1						
Ni	0.12	0.23	−0.14	**0.62**	**0.60**	**0.59**	1					
Pb	0.18	−0.16	−0.32	0.21	0.06	−0.04	0.19	1				
Zn	−0.15	0.04	0.22	0.03	0.08	0.35	−0.07	−0.32	1			
Sand	0.13	0.00	0.19	0.08	0.11	0.09	0.24	−0.18	0.04	1		
Silt	0.01	0.07	0.30	−0.14	0.12	0.16	0.06	**−0.52**	0.25	0.31	1	
Clay	−0.12	−0.01	−0.23	−0.05	−0.13	−0.11	−0.24	0.25	−0.08	**−0.99**	**−0.46**	1

Note: Correlation significant at the 0.05 level is given in italics and correlation significant at the 0.01 level is given in bold.

Levels of metals (Mn, Pb, Ni and Cu) at different depth of CE1 core sediments are shown in Fig. 3.7. Mn profile showed the highest value of 88.96 mg kg^{-1} at a depth of 18 cm. Mn levels at other depths varied between 15.23 mg kg^{-1} and 51.67 mg kg^{-1}. The bottom layer of the core below 48 cm depth showed lesser variation of Mn ranging from 26.70 mg kg^{-1} to 43.18 mg kg^{-1} indicating crustal origin. Mn comprises about 0.1% of the earth's crust and found predominantly as crustal sources in nature.

The Pb levels in the core showed a random distribution in which the minimum and maximum concentrations of Pb were observed at a depth of 9–12 cm and 87–90 cm respectively. The average concentration of Pb was found to be 21.23 mg kg^{-1}. Possible pollution contributions would be for industrial wastes and also, in diffuse pollution from the combustion of leaded furnace fuels used in the industries (Adriano, 1986). The middle and bottom portion of the core recorded significantly higher values than the top portion suggesting the action of tides and waves exerting on sediments. Pb is negatively correlated to silt indicating external sources for the metal. Pb concentrations observed in the downcore profile can be attributed to different anthropogenic activities mainly dredging, operation of motorized vessels and monsoonal land run off. The Pb pollution is frequent in estuaries where marine traffic and industrial effluents present in immoderate levels. Ni concentration followed an irregular pattern with a mean concentration of 12.23 mg kg^{-1}. Ni content shows the maximum at a depth of 72–75 cm having a concentration of 22.96 mg kg^{-1} whereas lower value observed at 87–90 cm with 2.75 mg kg^{-1}. The middle portion of the core showed significant enrichment than the bottom and top portion suggesting its long term deposition. Ni is diminished towards the upper portion and then intensified throughout the depth profile in the Cochin estuary. In general, Cu concentration in the upper part of the core shows slightly higher values when compared to the lower part ranging from 1.00 mg kg^{-1} to 43.92 mg kg^{-1} with an average of 7.70 mg kg^{-1}. Cu is found to be diminished towards the bottom of the core indicates negligible anthropogenic influence and represents unpolluted samples with respect to the metal. The concentration of Cu in the upper part implies enrichment due to biological inputs.

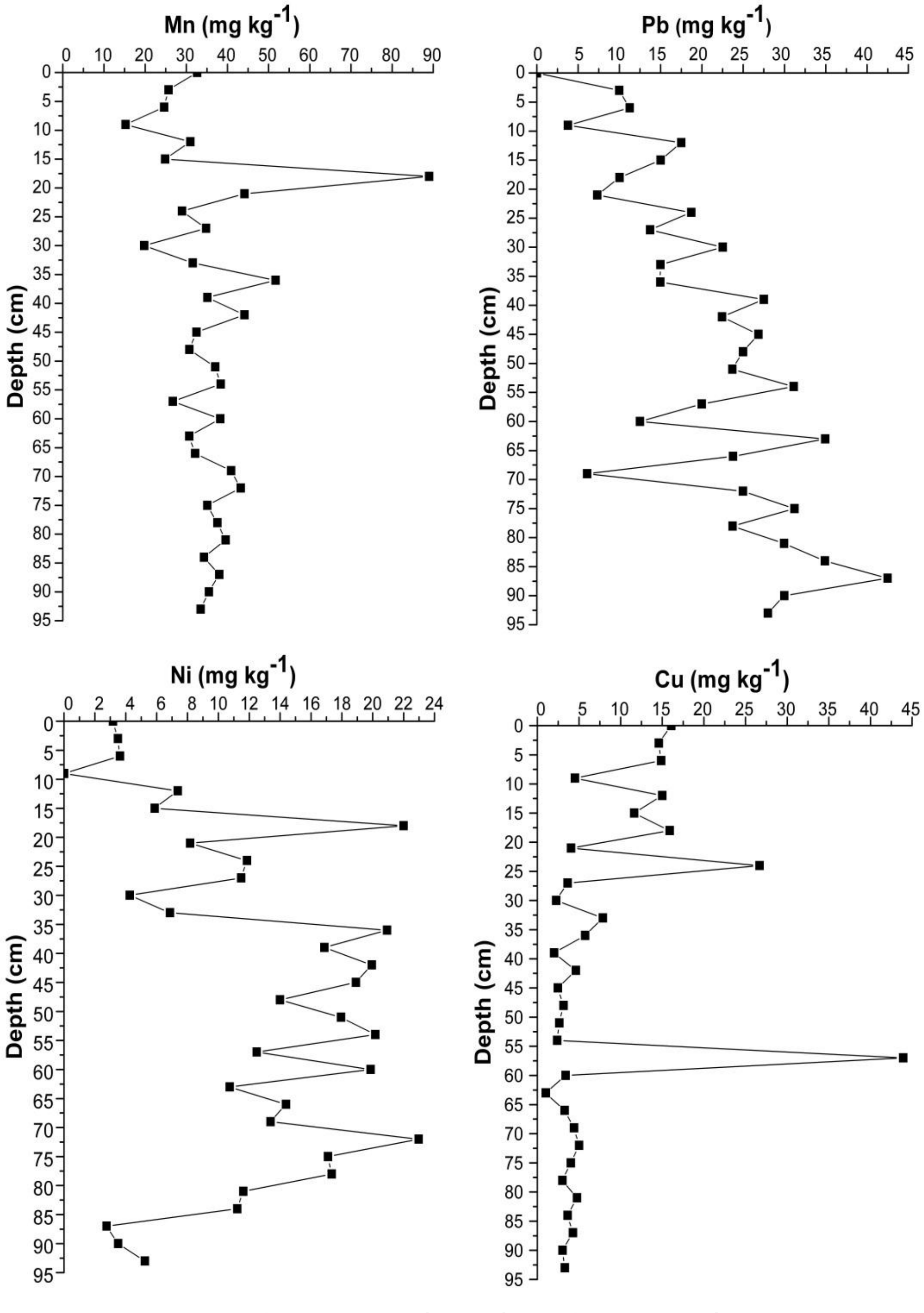

Fig. 3.7 Depth profile of Mn, Pb, Ni and Cu in the CE1 core sediments.

Downcore profile of Co and Zn are presented in Fig. 3.8. The downcore profile of Co ranged from 1.25 mg kg^{-1} to 14.07 mg kg^{-1}. It averaged 6.65 mg kg^{-1} and follows an irregular pattern throughout the depth profile. Co shows high concentration in the middle portion than the top and bottom of the core. Co is positively correlated to Mn and Mg suggests lithogenic origin and association to clay minerals. Hence, Co content in the Cochin estuary reveals lesser alteration with exogenic influences and accounts for lithogenic source of the metal. The downcore profile of Zn shows higher values in the top portion of the core with a mean concentration of 6.26 mg kg^{-1}. Zn recorded maximum concentration of 20.74 mg kg^{-1} at a depth of 18–21 cm whereas the lowest value of 1.37 mg kg^{-1} at 57 cm to 60 cm depth. The concentration of Zn in the top layers of Cochin estuarine core compared to bottom suggests the influence of anthropogenic sources in the study site.

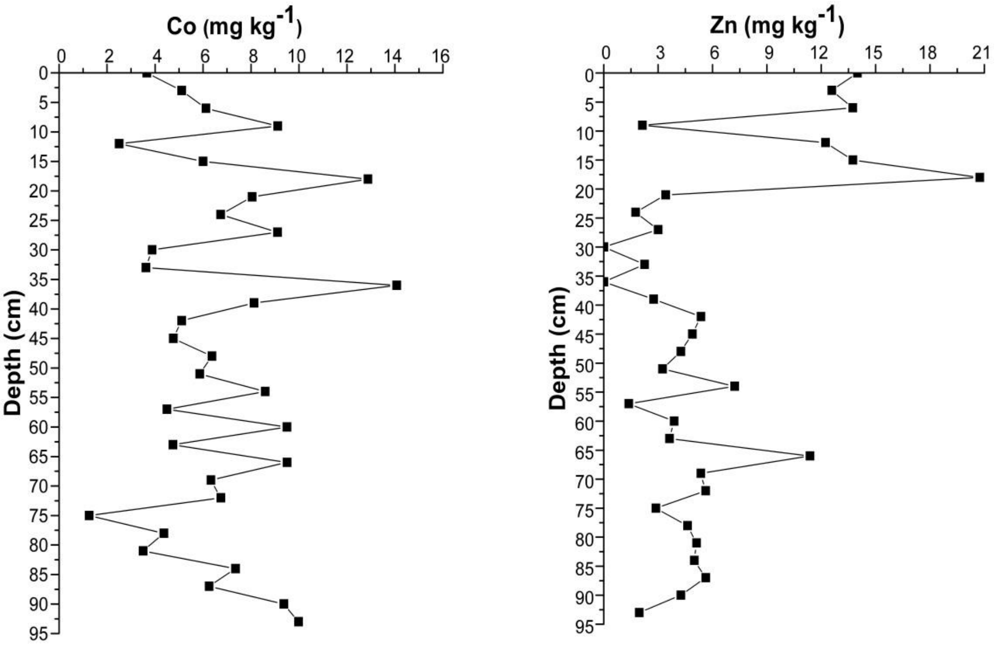

Fig. 3.8 Depth profile of Co and Zn in the CE1 core sediments.

The Cd concentration in the top five centimetres was much lower than those in the deeper core sediment samples (Fig. 3.9). The top section of the core contains Cd concentration of 0.61 mg kg^{-1}. The highest concentration of

Cd (2.50 mg kg^{-1}) was observed at the bottom portion of the core (75–78 cm depth). The depths 45–48 cm and 30–33 cm showed significant concentration of 1.95 mg kg^{-1} and 1.25 mg kg^{-1} respectively. Cd is not abundant in the crust and is found in the marine environment higher than normal levels as CdS. The weathering of parent rocks also attributes to Cd contamination in unpolluted regions (Fergusson, 1990). Contrary to this, the distribution profile of Cd in the Cochin estuary indicates anthropogenic subsidence caused by an increase in agriculture and aquaculture activities near the mangroves, and rapid industrialization in and around the estuarine zone. Furthermore, Cd is negatively correlated with Co ($r^2 = -0.42$) and did not show any significant association with the analyzed parameters signifies the unique anthropogenic enrichment of Cd in the region.

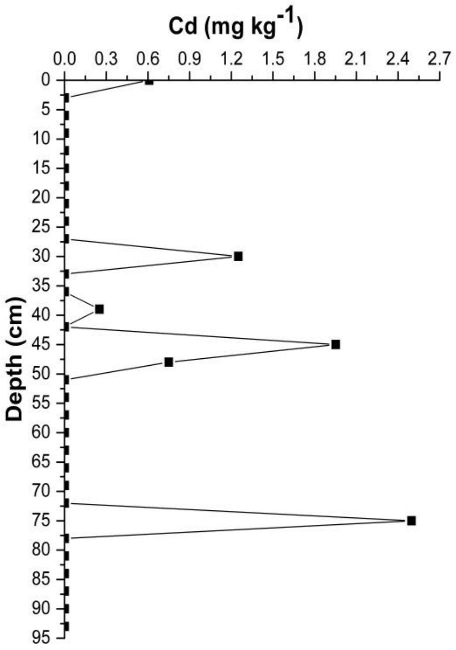

Fig. 3.9 Depth profile of Cd analyzed in the CE1 core sediments.

3.2.3 Multivariate Statistics - Principal Component Analysis

Principal component analysis was carried out on the analyzed variables to reduce the large data set into different factors with similar characteristics. Principal component analysis on studied metals and associated sedimentary parameters in the Cape Comorin core produced four factors with a total variance of 86.03% (Table 3.5).

Table 3.5: Results of PC analysis after varimax orthogonal rotation of Cape Comorin core sediment samples.

Variables	PC 1	PC 2	PC 3	PC4
Al	**0.92**	0.25	0.11	0.01
Co	0.37	0.15	**0.78**	0.28
Cr	0.44	0.33	0.05	**0.76**
Cu	−0.51	−0.44	0.20	**0.64**
Fe	**0.96**	0.14	0.03	−0.08
Mg	**0.94**	0.05	0.14	0.11
Mn	**0.96**	−0.01	0.18	0.12
Ni	**0.69**	−0.07	0.10	−0.01
Pb	−0.10	0.15	**−0.93**	0.06
Zn	**0.77**	−0.04	0.13	0.34
Sand	0.05	**−0.96**	0.01	0.01
Silt	0.18	**0.82**	−0.02	0.38
Clay	0.01	**0.96**	−0.02	−0.11
% Variance	40.48	22.64	12.33	10.58

Note: Factor loadings greater than ±0.60 are shown in bold.

The factor loadings greater than ±0.60 is considered as significant in the generated components. Factor 1 accounted for a variance of 40.48% with high positive loadings on Al, Fe, Mg, Mn, Ni and Zn. Thus factor 1 corresponds to lithogenic sources and insignificant granulometric dependence for these metals. Factor 2 accounts for 22.64% variance having positive loadings on silt and clay and negative loadings on sand. The third factor explains 12.33% variance with Co loaded positively while Pb loaded negatively. Cr and Cu loaded positively in factor 4 with a variance of 10.58%.

PCA generated four factors for CE1 core sediments after varimax rotation with a total variance of 74.21% (Table 3.6). Factor 1 accounted for a variance of 27.39% and positively loaded with Fe, Mg, Mn and Ni. It represents the lithogenic fractions controlling this factor. The second factor corresponds to 19.22% of variance having positive factor loadings on sand and silt and negative loadings on clay. Metals viz., Cu and Zn display positive loadings and Pb shows negative loading on factor 3 displaying a variance of 14.51%. Cu and Zn may exhibit an identical behaviour in sources and transport through biogenic particles. The factor 4 unveils 13.09% variance with positive loading on Co and high negative loading on Cd. The components of this factor are probably affected by exogenic influences. Further, the Cd concentrations may vary with respect to external human activities.

Table 3.6: Results of PCA after varimax orthogonal rotation of Cochin estuary core sediment samples.

Variables	1	2	3	4
Cd	−0.07	0.13	−0.22	**−0.81**
Co	0.14	0.01	−0.14	**0.89**
Cu	−0.16	0.37	**0.70**	0.04
Fe	**0.86**	−0.08	−0.09	0.03
Mg	**0.91**	0.02	−0.02	0.21
Mn	**0.93**	0.00	0.11	0.19
Ni	**0.80**	0.25	−0.25	−0.13
Pb	0.27	−0.16	**−0.67**	−0.14
Zn	0.22	−0.21	**0.78**	−0.08
Sand	0.17	**0.82**	0.03	−0.09
Silt	−0.15	**0.72**	0.21	0.01
Clay	−0.10	**−0.91**	0.05	0.06
% Variance	27.39	19.22	14.51	13.09

Note: Factor loadings greater than ±0.60 are shown in bold.

3.2.4 Anthropogenic Influence Assessment

For the calculation of geochemical indices such as EF, I_{geo}, CF and PLI, the metal background values were established from the crustal abundance reported by Taylor (1964). Metal levels obtained downcore were comparatively less than the crustal abundance and expected to have lesser contamination and geoaccumulation. On contrary, enrichment factor evaluates and remarks any variation or discrepancy in the lithogenic metal enrichment pattern caused by anthropogenic alterations or redox differences.

3.2.4.1 Enrichment Factor

The calculation of enrichment factors and different enrichment categories were detailed in Chapter 2. The EF value of metals studied in the CC1 core sediments were varied as 0.26–2.14 (mean of 1.02) for Co, 2.04–19.25 (mean of 8.33) for Cr, 0.11–36.93 (mean of 14.85) for Cu, 2.87–5.04 (mean of 3.94) for Mn, 0.11–3.82 (mean of 1.22) for Ni, 1.47–66.87 (mean of 21.96) for Pb and 8.73–31.36 (mean of 14.86) for Zn (Table 3.7). Cd was below the detectable limit and indicates no contamination in the core sediments. Cu shows very severe enrichment below 30 cm depth of the core while the top layer recorded only moderate enrichment of the metal. Cr, Pb and Zn show a similar pattern of enrichment down the core indicating a common source for metal accumulation (Fig. 3.10). Cr exhibits moderate enrichment at the top and moderately severe enrichment at the bottom in most of the samples. Pb shows the maximum enrichment of all the metals studied. On average, it displays severe enrichment at the top and very severe enrichment at the bottom of the core. Zn-EF value presents less significant variation, on average showing severe enrichment of the metal in the study region.

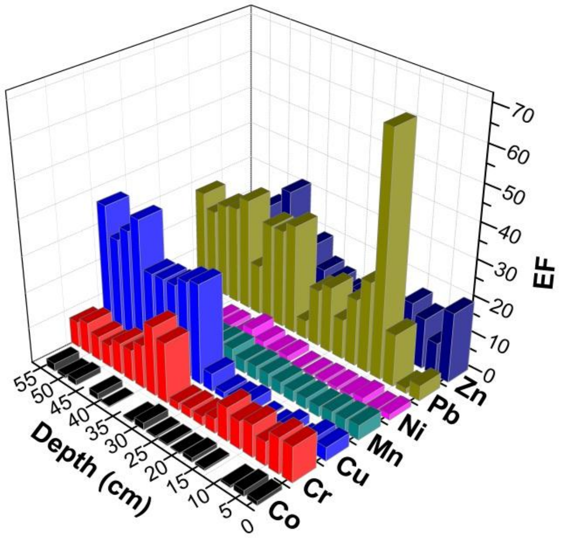

Fig. 3.10 Enrichment factor analyzed in the metals of Cape Comorin.

Table 3.7: Enrichment factors calculated in the Cape Comorin core sediments.

Depth	Enrichment Factor						
cm	Co	Cr	Cu	Mn	Ni	Pb	Zn
0–3	1.19	9.85	3.77	4.13	1.61	4.27	19.47
3–6	1.63	10.02	3.94	3.66	0.84	1.47	9.08
6–9	0.62	6.61	0.52	3.56	1.92	14.53	14.08
9–12	-	9.04	2.34	2.87	0.86	66.87	16.74
12–15	0.53	7.79	0.11	3.12	0.88	25.37	11.36
15–18	1.19	9.34	0.33	3.09	0.80	18.74	11.97
18–21	0.29	4.06	2.98	3.43	0.44	11.04	8.73
21–24	0.49	2.47	1.86	3.84	0.36	18.50	12.69
24–27	0.45	2.50	1.83	3.95	1.79	15.87	10.50
27–30	1.95	2.04	4.96	3.70	1.26	5.20	12.39
30–33	0.40	16.69	28.00	5.02	2.05	30.60	13.70
33–36	-	19.25	26.78	4.91	3.82	27.59	19.21
36–39	0.26	12.06	24.16	4.28	0.65	27.49	12.09
39–42	1.72	8.74	24.02	4.49	1.19	14.04	31.36
42–45	-	8.76	23.69	5.04	1.01	31.35	15.23
45–48	1.60	6.18	36.93	4.58	-	27.43	23.92
48–51	0.78	6.81	32.11	3.80	1.35	26.51	14.59
51–54	2.14	8.87	27.95	3.61	0.11	23.31	12.26
54–57	-	7.18	35.89	3.73	1.09	27.15	12.98
Min	0.26	2.04	0.11	2.87	0.11	1.47	8.73
Max	2.14	19.25	36.93	5.04	3.82	66.87	31.36
Avg	1.02	8.33	14.85	3.94	1.22	21.96	14.86

The EF calculated for CE1 core sediments is represented in Fig. 3.11. EF value of studied metals varied as 33.33–227.49 (mean of 122.10) for Cd, 0.50–51.83 (mean of 5.97) for Co, 0.19–17.47 (mean of 2.91) for Cu, 0.29–5.90 (mean of 0.67) for Mn, 0.30–35.89 (mean of 2.83) for Ni, 3.84–350.88 (mean of 32.78) for Pb and 0.31–12.69 (mean of 1.86) for Zn respectively (Table 3.8). Cd shows very high EF values at certain layers of the core clearly indicating the influence of human activities. Cd and Pb displayed enrichment above thirty (> 30) possibly due to the anthropogenic origin. The EF values of studied metals were maximum at a depth of 39–42 cm. It may be possibly contributed from intensive boat operations and direct effluent inputs carrying phosphate fertilizers originated from agricultural lands. Co showed EF values between 5 and 10 stipulate moderately severe enrichment compared to bottom layers. The mean EF value for Cu, Ni and Zn were below three (< 3) indicating minor enrichment of these metals. The mean EF value for Mn was less than one (< 1) suggesting a lithogenic source of the metal in the sediments. Depth profile of EF values of Co, Cu, Mn, Ni and Zn revealed high enrichment at the top portion compared to the bottom layer of the core.

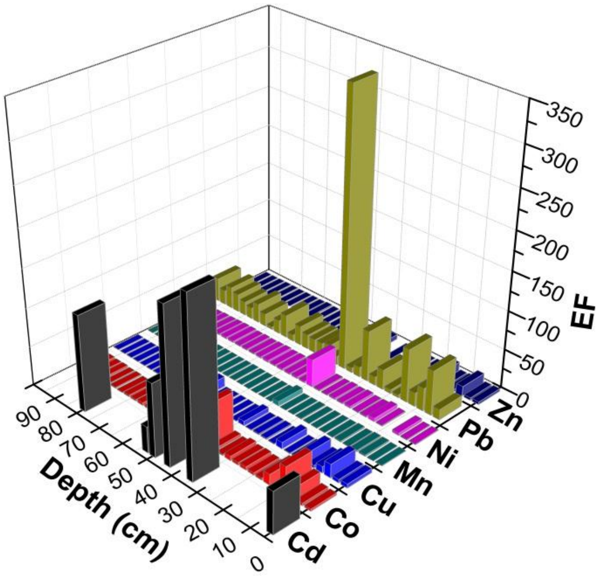

Fig. 3.11 Enrichment factor analyzed in the metals of Cochin estuary.

Table 3.8: Enrichment factors of metals analyzed in the core sediment of Cochin estuary.

Depth	Enrichment Factor						
cm	Cd	Co	Cu	Mn	Ni	Pb	Zn
0–3	54.40	2.61	5.22	0.61	0.75	-	3.57
3–6	-	3.46	4.48	0.46	0.79	13.48	3.04
6–9	-	15.82	17.47	1.67	3.12	58.12	12.69
9–12	-	36.34	8.15	1.60	-	29.87	3.02
12–15	-	1.28	3.49	0.42	1.26	17.93	2.24
15–18	-	13.82	12.17	1.51	4.51	69.08	11.31
18–21	-	2.58	1.44	0.47	1.47	4.00	1.48
21–24	-	3.05	0.69	0.44	1.03	5.54	0.46
24–27	-	4.62	8.32	0.52	2.71	25.66	0.43
27–30	-	3.60	0.65	0.36	1.51	10.84	0.42
30–33	227.49	5.64	1.49	0.76	2.06	65.52	-
33–36	-	1.54	1.52	0.35	0.97	12.72	0.34
36–39	-	2.98	0.55	0.29	1.48	6.33	-
39–42	199.36	51.83	5.80	5.90	35.89	350.88	6.27
42–45	-	1.29	0.53	0.29	1.68	11.33	0.48
45–48	94.18	1.84	0.43	0.33	2.43	20.72	0.67
48–51	33.33	2.27	0.51	0.29	1.66	17.78	0.54
51–54	-	2.17	0.44	0.36	2.21	17.53	0.43
54–57	-	2.58	0.32	0.30	2.02	18.70	0.77
57–60	-	2.81	12.48	0.44	2.60	24.96	0.31
60–63	-	3.14	0.51	0.33	2.19	8.28	0.46
63–66	-	2.02	0.19	0.34	1.53	29.80	0.55
66–69	-	3.56	0.55	0.32	1.80	17.82	1.52
69–72	-	2.00	0.63	0.34	1.41	3.84	0.60
72–75	-	2.19	0.74	0.37	2.49	16.21	0.65
75–78	123.81	0.50	0.72	0.37	2.26	24.76	0.41
78–81	-	1.38	0.43	0.31	1.82	14.94	0.52
81–84	-	1.05	0.64	0.31	1.16	17.92	0.55
84–87	-	2.47	0.55	0.30	1.26	23.45	0.60
87–90	-	2.08	0.64	0.33	0.30	28.24	0.67
90–93	-	2.97	0.43	0.30	0.37	19.02	0.48
93–96	-	5.51	0.82	0.49	0.96	30.90	0.38
Min	33.33	0.50	0.19	0.29	0.30	3.84	0.31
Max	227.49	51.83	17.47	5.90	35.89	350.88	12.69
Avg	122.10	5.97	2.91	0.67	2.83	32.78	1.86

3.2.4.2 Geoaccumulation Index

The different grades of geoaccumulation index were shown in Chapter 2. The I_{geo} values varied as follows: −10.36–−6.41 for Co, −6.98–−3.63 for Cr, −10.69–−2.95 for Cu, −6.38–−4.88 for Mn, −11.21–−6.15 for Ni, −6.56–−1.45 for Pb and −4.87–−2.64 for Zn. The negative I_{geo} values revealed negligible pollution by these metals in Cape Comorin (Table 3.9).

Table 3.9: Geoaccumulation index calculated in the Cape Comorin core sediments.

Depth	Geoaccumulation Index						
cm	Co	Cr	Cu	Mn	Ni	Pb	Zn
0–3	−6.68	−3.63	−5.01	−4.88	−6.24	−4.83	−2.64
3–6	−6.41	−3.79	−5.14	−5.25	−7.36	−6.56	−3.94
6–9	−7.78	−4.36	−8.02	−5.25	−6.15	−3.23	−3.27
9–12	-	−4.33	−6.28	−5.99	−7.73	−1.45	−3.44
12–15	−8.37	−4.49	−10.69	−5.81	−7.63	−2.78	−3.94
15–18	−7.23	−4.27	−9.07	−5.86	−7.82	−3.26	−3.91
18–21	−9.11	−5.28	−5.72	−5.52	−8.47	−3.84	−4.17
21–24	−8.44	−6.10	−6.51	−5.46	−8.89	−3.19	−3.73
24–27	−9.13	−6.65	−7.10	−5.98	−7.13	−3.98	−4.57
27–30	−7.05	−6.98	−5.70	−6.12	−7.68	−5.63	−4.38
30–33	−9.98	−4.58	−3.84	−6.32	−7.61	−3.71	−4.87
33–36	-	−4.26	−3.79	−6.23	−6.60	−3.74	−4.27
36–39	−10.36	−4.82	−3.82	−6.32	−9.04	−3.63	−4.82
39–42	−7.06	−4.72	−3.26	−5.68	−7.60	−4.04	−2.88
42–45	-	−5.18	−3.75	−5.98	−8.30	−3.34	−4.38
45–48	−7.77	−5.82	−3.24	−6.25	-	−3.67	−3.87
48–51	−8.32	−5.19	−2.95	−6.03	−7.52	−3.23	−4.09
51–54	−6.89	−4.84	−3.18	−6.13	−11.21	−3.44	−4.37
54–57	-	−5.43	−3.11	−6.38	−8.15	−3.51	−4.58
Min	−10.36	−6.98	−10.69	−6.38	−11.21	−6.56	−4.87
Max	−6.41	−3.63	−2.95	−4.88	−6.15	−1.45	−2.64
Avg	−8.04	−4.99	−5.27	−5.87	−7.84	−3.74	−4.01

The I_{geo} values of analyzed metals in the Cochin estuary is presented in Fig. 3.12. The I_{geo} values of studied metals were −0.26 to 3.06 (average 1.65) for Cd, −4.91 to −1.41 (average −2.64) for Co, −6.37 to −0.91 (average −4.00) for Cu, −6.55 to −4.00 (average −5.39) for Mn, −5.35 to −2.29 (average −3.46) for Ni, −2.32 to 1.18 (average 0.00) for Pb and −6.26 to −2.34 (average −4.42) for Zn respectively (Table 3.10). According to I_{geo} classification, Co, Cu, Mn, Ni and Zn can be considered as unpolluted in the study site. The I_{geo} values of Cd and Pb suggest its pollution mainly due to human activities.

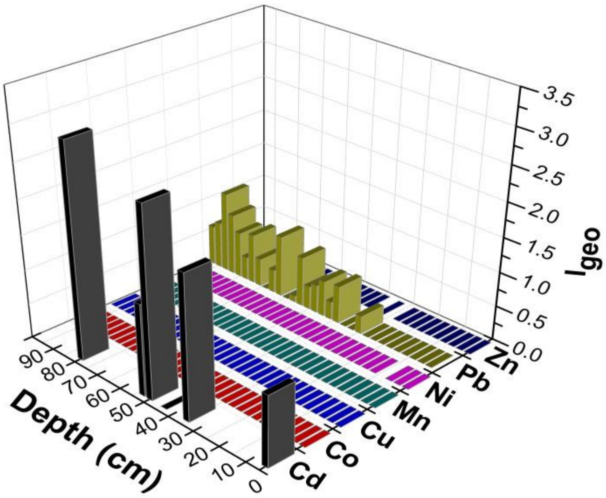

Fig. 3.12 Geoaccumulation index analyzed in the metals of Cochin estuary.

Table 3.10: Geoaccumulation index of metals analyzed in the core sediment of Cochin estuary.

Depth	Geoaccumulation Index						
cm	Cd	Co	Cu	Mn	Ni	Pb	Zn
0–3	1.02	−3.36	−2.36	−5.45	−5.15	-	−2.91
3–6	-	−2.88	−2.50	−5.80	−5.01	−0.91	−3.06
6–9	-	−2.62	−2.47	−5.86	−4.96	−0.74	−2.94
9–12	-	−2.04	−4.20	−6.55	-	−2.32	−5.63
12–15	-	−3.91	−2.46	−5.52	−3.93	−0.10	−3.10
15–18	-	−2.65	−2.83	−5.84	−4.26	−0.32	−2.93
18–21	-	−1.54	−2.38	−4.00	−2.35	−0.91	−2.34
21–24	-	−2.22	−4.36	−5.01	−3.79	−1.36	−4.94
24–27	-	−2.48	−1.63	−5.62	−3.25	0.00	−5.91

27–30	-	−2.04	−4.51	−5.36	−3.29	−0.45	−5.13
30–33	2.06	−3.27	−5.20	−6.17	−4.73	0.26	-
33–36	-	−3.37	−3.39	−5.50	−4.04	−0.33	−5.55
36–39	-	−1.41	−3.85	−4.79	−2.43	−0.33	-
39–42	−0.26	−2.21	−5.37	−5.34	−2.74	0.55	−5.26
42–45	-	−2.88	−4.16	−5.01	−2.50	0.26	−4.29
45–48	2.70	−2.98	−5.08	−5.46	−2.57	0.52	−4.43
48–51	1.32	−2.56	−4.72	−5.54	−3.01	0.41	−4.63
51–54	-	−2.68	−4.98	−5.27	−2.65	0.34	−5.02
54–57	-	−2.13	−5.12	−5.22	−2.48	0.73	−3.86
57–60	-	−3.06	−0.91	−5.74	−3.17	0.09	−6.26
60–63	-	−1.98	−4.61	−5.22	−2.50	−0.59	−4.76
63–66	-	−2.98	−6.37	−5.54	−3.39	0.90	−4.86
66–69	-	−1.98	−4.67	−5.47	−2.97	0.34	−3.21
69–72	-	−2.57	−4.24	−5.12	−3.07	−1.62	−4.29
72–75	-	−2.48	−4.05	−5.04	−2.29	0.41	−4.22
75–78	3.06	−4.91	−4.37	−5.34	−2.72	0.73	−5.19
78–81	-	−3.10	−4.78	−5.25	−2.70	0.34	−4.51
81–84	-	−3.42	−4.12	−5.17	−3.28	0.67	−4.36
84–87	-	−2.35	−4.51	−5.38	−3.33	0.90	−4.40
87–90	-	−2.59	−4.28	−5.23	−5.35	1.18	−4.22
90–93	-	−2.00	−4.78	−5.33	−5.01	0.68	−4.63
93–96	-	−1.91	−4.65	−5.41	−4.43	0.58	−5.75
Min	−0.26	−4.91	−6.37	−6.55	−5.35	−2.32	−6.26
Max	3.06	−1.41	−0.91	−4.00	−2.29	1.18	−2.34
Avg	1.65	−2.64	−4.00	−5.39	−3.46	0.00	−4.42

3.2.4.3 Contamination Factor

The classification of contamination factors were described in Chapter 2. The CF values of studied metals were 0.00–0.02 for Co, 0.01–0.12 for Cr, 0.00–0.19 for Cu, 0.02–0.05 for Mn, 0.00–0.02 for Ni, 0.02–0.55 for Pb and 0.05–0.24 for Zn (Table 3.11). All the metals analyzed show low contamination throughout the depth profile in CC1 core sediments (Fig. 3.13).

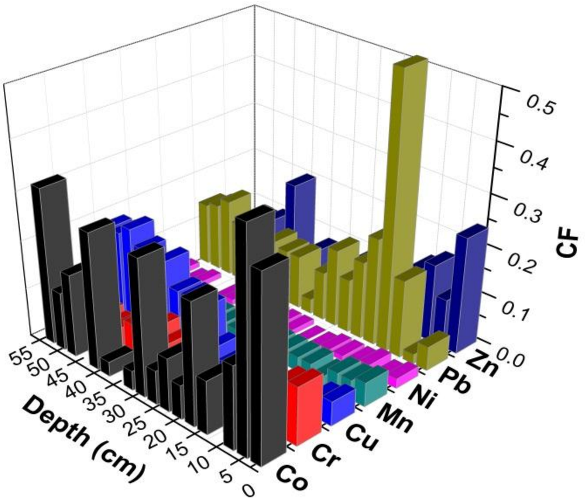

Fig. 3.13 Contamination factor analyzed in the metals of Cape Comorin.

Table 3.11: Contamination factors calculated in the Cape Comorin core sediments.

Depth	Contamination Factor						
cm	Co	Cr	Cu	Mn	Ni	Pb	Zn
0–3	0.37	0.12	0.05	0.05	0.02	0.05	0.24
3–6	0.44	0.11	0.04	0.04	0.01	0.02	0.10
6–9	0.17	0.07	0.01	0.04	0.02	0.16	0.16
9–12	-	0.07	0.02	0.02	0.01	0.55	0.14
12–15	0.11	0.07	0.00	0.03	0.01	0.22	0.10
15–18	0.25	0.08	0.00	0.03	0.01	0.16	0.10
18–21	0.07	0.04	0.03	0.03	0.00	0.11	0.08
21–24	0.11	0.02	0.02	0.03	0.00	0.16	0.11
24–27	0.07	0.01	0.01	0.02	0.01	0.10	0.06
27–30	0.28	0.01	0.03	0.02	0.01	0.03	0.07
30–33	0.04	0.06	0.10	0.02	0.01	0.11	0.05
33–36	-	0.08	0.11	0.02	0.02	0.11	0.08
36–39	0.03	0.05	0.11	0.02	0.00	0.12	0.05
39–42	0.28	0.06	0.16	0.03	0.01	0.09	0.20
42–45	-	0.04	0.11	0.02	0.00	0.15	0.07
45–48	0.17	0.03	0.16	0.02	-	0.12	0.10
48–51	0.12	0.04	0.19	0.02	0.01	0.16	0.09
51–54	0.32	0.05	0.17	0.02	0.00	0.14	0.07
54–57	-	0.03	0.17	0.02	0.01	0.13	0.06
Min	0.00	0.01	0.00	0.02	0.00	0.02	0.05
Max	0.02	0.12	0.19	0.05	0.02	0.55	0.24
Avg	0.01	0.06	0.08	0.03	0.01	0.14	0.10

CF values (Fig. 3.14) in the CE1 core revealed that contamination of Co, Cu, Mn, Ni and Zn were low (CF < 1). The CF values of Co, Cu, Mn, Ni and Zn averaged 0.27, 0.14, 0.04, 0.16 and 0.09 respectively (Table 3.12). This suggests that these metals originated, to a large extent from the earth's crust via weathering. On the other hand, Cd and Pb measured in the sediments originated from both natural and anthropogenic sources. The CF value of Cd ranged between 1.25 and 12.48 with an average of 6.09. However, the CF values were high for Cd and Pb which suggest pollution due to external discrete sources like land runoff and anthropogenic activities. Petroleum products and phosphate fertilizers are also a source of this metal in the coastal environment. The CF value of Pb varied between 0.30 and 3.40 with an average of 1.70. Moderate contamination was observed with respect to Pb. Pb emissions, mainly from petrol, to ambient air have caused considerable pollution and the use of Pb-based paints is also a source for Pb accumulation (Järup, 2003). Elements like Pb and Cd may exhibit extreme toxicity even at trace levels (Nicolau et al., 2006).

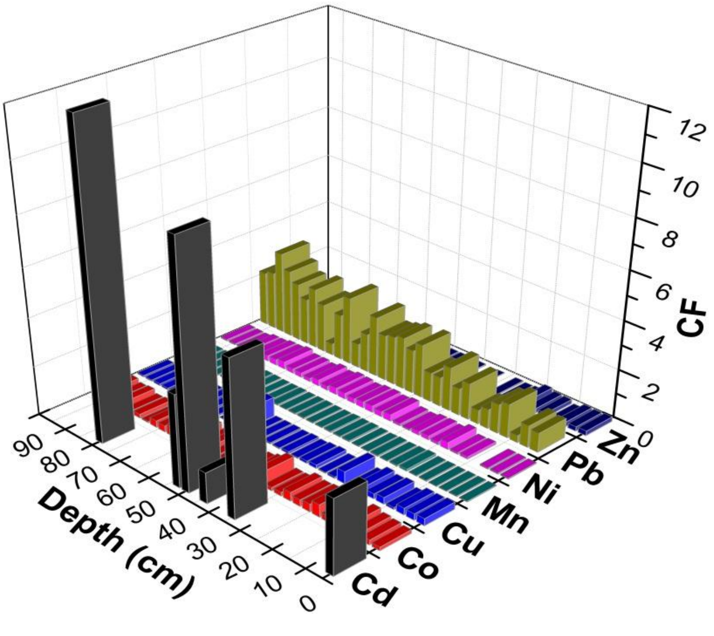

Fig. 3.14 Contamination factor analyzed in the metals of Cochin estuary.

Table 3.12: Contamination factors of metals analyzed in the core sediment of Cochin estuary.

Depth	Contamination Factor						
cm	**Cd**	**Co**	**Cu**	**Mn**	**Ni**	**Pb**	**Zn**
0–3	3.04	0.15	0.29	0.03	0.04	-	0.20
3–6	-	0.20	0.26	0.03	0.05	0.80	0.18
6–9	-	0.24	0.27	0.03	0.05	0.90	0.20
9–12	-	0.36	0.08	0.02	-	0.30	0.03
12–15	-	0.10	0.27	0.03	0.10	1.40	0.17
15–18	-	0.24	0.21	0.03	0.08	1.20	0.20
18–21	-	0.51	0.29	0.09	0.29	0.80	0.30
21–24	-	0.32	0.07	0.05	0.11	0.58	0.05
24–27	-	0.27	0.48	0.03	0.16	1.50	0.02
27–30	-	0.36	0.07	0.04	0.15	1.10	0.04
30–33	6.25	0.15	0.04	0.02	0.06	1.80	-
33–36	-	0.14	0.14	0.03	0.09	1.20	0.03
36–39	-	0.56	0.10	0.05	0.28	1.20	-
39–42	1.25	0.32	0.04	0.04	0.22	2.20	0.04
42–45	-	0.20	0.08	0.05	0.27	1.79	0.08
45–48	9.76	0.19	0.04	0.03	0.25	2.15	0.07
48–51	3.75	0.25	0.06	0.03	0.19	2.00	0.06
51–54	-	0.23	0.05	0.04	0.24	1.89	0.05
54–57	-	0.34	0.04	0.04	0.27	2.49	0.10
57–60	-	0.18	0.80	0.03	0.17	1.60	0.02
60–63	-	0.38	0.06	0.04	0.26	1.00	0.06
63–66	-	0.19	0.02	0.03	0.14	2.79	0.05
66–69	-	0.38	0.06	0.03	0.19	1.90	0.16
69–72	-	0.25	0.08	0.04	0.18	0.49	0.08
72–75	-	0.27	0.09	0.05	0.31	2.00	0.08
75–78	12.48	0.05	0.07	0.04	0.23	2.50	0.04
78–81	-	0.17	0.05	0.04	0.23	1.90	0.07
81–84	-	0.14	0.09	0.04	0.15	2.39	0.07
84–87	-	0.29	0.07	0.04	0.15	2.79	0.07
87–90	-	0.25	0.08	0.04	0.04	3.40	0.08
90–93	-	0.37	0.05	0.04	0.05	2.40	0.06
93–96	-	0.40	0.06	0.04	0.07	2.24	0.03
Min	1.25	0.05	0.02	0.02	0.04	0.30	0.02
Max	12.48	0.56	0.80	0.09	0.31	3.40	0.30
Avg	6.09	0.27	0.14	0.04	0.16	1.70	0.09

3.2.4.4 Pollution Load Index

The PLI values of CC1 were equal to zero indicating negligible contamination throughout the layer profile. PLI values of CE1 core varied from 0.01 to 0.19 showing slightly higher values than at Cape Comorin (Fig. 3.15). It is because the sediments of Cochin estuary has multiple sources mainly industrial and municipal effluents.

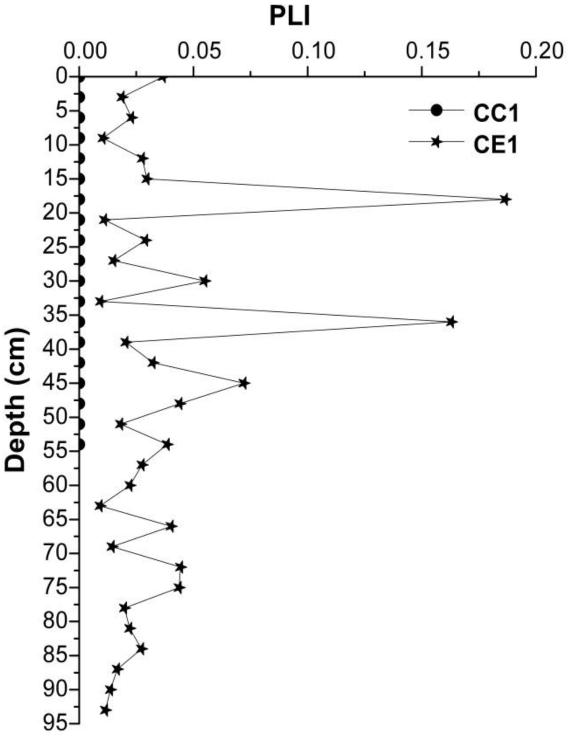

Fig. 3.15 Downcore pollution load index calculated for CC1 and CE1 core sediments.

3.3 Conclusions

The study was carried out to reveal the vertical distribution of metals and to estimate background concentration for determining anthropogenic influences in the region. Major and trace metal profile showed that the metal distribution is predominantly by background levels representing geological sources instead of human activities. Downcore metal abundance in the Cape

Comorin decreased in the following order: Mg > Fe > Al > Mn > Zn > Cu > Cr > Pb > Ni > Co. The metals in the core sediments of Cochin estuarine system occurred in the following ranking of abundance: Fe > Mg > Mn > Pb > Ni > Cu > Co > Zn > Cd. The vertical distribution profile of Fe, Mn, Cr, Zn and Ni in Cape Comorin revealed their authigenic phases associated with mineralogical fractions of clay and aluminosilicate minerals. Cu levels were differentiated from the lithogenic component by a surface minimum and an increase towards the bottom of the core. It signals the past accumulation of organic matter flux and further reworking of sediments. Pb profile suggests geologic sources for the metal. On the other hand, the mean concentrations of metals studied in Cochin estuary core had values representative of unpolluted sediments except for Cd and Pb. The most abundant metals in the sediments viz., Fe and Mg correspond to geological sources. The metals Co, Cu, Ni, Mn and Zn do not show pronounced anthropogenic intrusion. The various indices such as enrichment factor, geoaccumulation index and contamination factor indicate Cd as the primary element with high risk potential. The Cd concentration may be primarily attributed to phosphate fertilizers used in the catchments nearby and effluent washloads. The enrichment of Pb in the core sediments shows anthropogenic input from maritime traffic and industrial activities.

Vertical distribution profile presents a set of background values of metals that describe the regional sediment composition for the subsequent estimation of anthropogenic metal contamination in the riverine, brackish and marine sediments in the region. Further, this background metal data would provide a reference for the evaluation of metal contamination in the surface sediments along the Kerala coast and adjoining continental shelf of Southeastern Arabian Sea. It is important to combine the regional background and crustal background for a methodical understanding of the enrichment of metals in a particular region.

References

Adriano, D.C., 1986. Trace elements in the terrestrial environment. Springer-Verlag, New York.

Beck, M., Böning, P., Schückel, U., Stiehl, T., Schnetger, B., Rullkötter, J., Brumsack, H., 2013. Consistent assessment of trace metal contamination in surface sediments and suspended particulate matter: A case study from the Jade Bay in NW Germany. Marine Pollution Bulletin, 70, 100–111.

Buckley, D.E., Smith, J.N., Winters, G.V., 1995. Accumulation of contaminants metals in marine sediments of Halifax Harbour, Nova Scotia: Environmental factors and historical trends. Applied Geochemistry, 10, 175–195.

Du Laing, G., Rinklebe, J., Vandecasteele, B., Meers, E., Tack, F.M.G., 2009. Trace metal behaviour in estuarine and riverine floodplain soils and sediments: A review. Science of the Total Environment, 407, 3972–3985.

Fergusson, J.E., 1990. The heavy elements: chemistry, environmental impact and health effects. Oxford, Pergamon Press.

Filho, F.J.P., Marins, R.V., Lacerda, L.D., Aguiar, J.E., Peres, T.F., 2015. Background values for evaluation of heavy metal contamination in sediments in the Parnaíba River Delta estuary, NE/Brazil. Marine Pollution Bulletin, 91, 424–428.

Gałuszka, A., Migaszewski, Z.M., 2011. Geochemical background – an environmental perspective. Mineralogia, 42, 7–17.

Järup, L., 2003. Hazards of heavy metal contamination. British Medical Bulletin, 68, 167–182.

Morelli, G., Gasparon, M., 2015. Depositional variability of estuarine intertidal sediments and implications for metal distribution: An example from Moreton Bay (Australia). Continental Shelf Research, 108, 41–54.

Nicolau, R., Galera-Cunha, A., Lucas, Y., 2006. Transfer of nutrients and labile metals from the continent to the sea by a small Mediterranean river. Chemosphere, 63, 469–476.

Silver, M.W., Gowing, M.M., 1991. The particle flux: Origins and biological components. Progress in Oceanography, 26, 75–113.

Sundby, B., Martinez, P., Gobeil, C., 2004. Comparative geochemistry of cadmium, rhenium, uranium, and molybdenum in continental margin sediments. Geochimica et Cosmochimica Acta, 68, 2485–2493.

Suthhof, A., Jennerjahn, T.C., Schäfer, P., Ittekkot, V., 2000. Nature of organic matter in surface sediments from the Pakistan continental margin and the deep Arabian Sea: amino acids. Deep Sea Research Part II: Topical Studies in Oceanography, 47, 329–351.

Taylor, S.R., 1964. The abundance of chemical elements in the continental crust: a new table. Geochimica et Cosmochimica Acta, 28, 1273–1285.

Wei, G., Liu, Y., Li, X., Shao, L., Liang, X., 2003. Climatic impact on Al, K, Sc and Ti in marine sediments: Evidence from ODP Site 1144, South China Sea. Geochemical Journal, 37, 593–602.

Chapter

4

DISTRIBUTION, CONTROLLING FACTORS AND POTENTIAL RISK OF METALS IN THE KERALA COAST

Contents

4.1 Introduction

Heavy metals are found to be one of the major pollutants in highly industrialized coastal environments. These elements introduced from external sources may occur in the environment as dissolved phase, suspended particles or retained in the sediments (Vosoogh et al., 2016). Trace metals may be exchanged via chemical and biological processes, within the sedimentary compartment and back to the water column (Forstner and Wittmann, 1983; Tessier and Campbell, 1987). Human activities, directly and indirectly, are now the primary cause of ecological changes in coastal communities caused by overexploitation of aquatic resources such as overfishing, coastal development and pollution. The lack of efficient environment protection strategies and monitoring combined with rapid large scale industrial production and urban development in developed/developing countries caused an increase in anthropogenic metal discharges into the estuaries and coastal systems (Akele et al., 2016). The persistence of toxic metals in the aquatic systems led to a potential source of contamination in the overlying waters and further cause toxicity to biological organisms and humans. Trace metal contamination in sediment can effect the bio-assimilation and bio-accumulation of metals in marine sentinel organisms, resulting in long-term persistence and pose negative implications on lower trophic levels extending to human health and ecosystem. Hence, sediment and water quality along the coast is of utmost importance due to the extreme dependence on coastal resources. Effective monitoring is a necessity to distinguish and characterize the potential sources of trace metals to the aquatic environment due to their toxicity, persistence and non-degradable nature. Further to this, it is important to have a clear understanding of the depositional setting, distribution and potential sources of trace metal variability in the coastal transition zone to formulate and support any management strategies for the protection of coastal ecosystems. Hence, the main objective of this chapter is to (1) assess the distribution and levels of selected metals (Fe, Cd, Co, Cu, Mn, Ni, Pb and Zn) in the coastal and estuarine sediments along the Kerala coast; (2) to characterize the sources and factors influencing the concentration of metals; (3) determine the degree of metal contamination by normalizing with background metal levels determined in the field observations.

Thirteen stations were considered for the collection of surface sediment and water samples along the southern region of Kerala. The stations selected are broadly confined to two zones along the Southern Kerala coast representing the nearshore beach sites and estuarine sites with freshwater and marine water interactions respectively. The nearshore region includes Cape (C1 and C2), Kovalam (K3), Neendakara (N4), Purakkad (P8) and Nattika (N12). The estuarine stations are Ashtamudi (A5), Kayamkulam (K6), Kilimukkekadavu (K7), Aroorkutty (A9), Thevara (T10), Chennur (C11) and Chettuva (C13).

4.2 Data Analysis

To determine the contamination levels and differentiate the sources of metals in the study area, various indices such as enrichment factor (EF), geoaccumulation index (I_{geo}), contamination factor (CF) and pollution load index (PLI) were assessed. Generally, these indices are calculated based on the elemental concentration in the earth's crust or the abundance of the metal in the upper crust shale as the background value. Noteworthy, the estimation of contamination levels and thereafter interpretation of anthropogenic sources while applying average shale or crust composition is not always satisfactory because of the presence of local lithological anomalies (Zhou et al., 2014). So this calculation should be validated using a local regional background established from previous studies or analyzing the elemental content of sediment cores in the region (Xu et al., 2014). Here, the metal levels obtained were normalized based on two background references viz., the metal crustal background reported by Taylor (1964) and the regional background assessed in the previous chapter. The regional background comprises of the average metal levels of Cape Comorin (CC1) core sediment and that of Cochin estuary (CE1) core sediment referred for nearshore stations (C1, C2, K3, N4, P8 and N12) and estuarine stations (A5, K6, K7, A9, T10, C11 and C13) respectively (Table 4.1). Cd was below the detection limit in the CC1 core sediments and hence, EF, CF and I_{geo} of the metal were calculated using the Cd levels determined in the CE1 core sediment. EF_c and EF_r represent the EF for crustal and regional background respectively whereas, C-I_{geo} and R-I_{geo} representing crustal and regional background in the case of I_{geo}. CF of various trace metals using crustal and regional backgrounds are presented as CF_c and CF_r

respectively. PLIs are also calculated for crustal and regional background in the surface sediments.

Table 4.1: Background levels used for the calculation of geochemical indices.

Background	Cd	Cu	Co	Fe	Mg	Mn	Ni	Pb	Zn
mg kg^{-1}									
Crustal average	0.20	55	25	56300	23300	950	75	12.50	70
CC1	*BDL	4.29	0.19	2500	3700	25.52	0.62	1.76	7.16
CE1	1.22	7.70	6.65	5395	2333	35.51	12.23	21.23	6.26

*BDL: below detectable level

Note: CC1: Cape Comorin, CE1: Cochin estuary

Here, Fe has been utilized as normalizer to compensate the differences in sediment grain size and mineralogy (Schiff and Weisberg, 1999). The computation of enrichment factor (EF) has been carried out by employing the equation as follows

$$EF = (M_s/Fe_s)/(M_b/Fe_b)$$

where M_s and M_b represent the concentration of the analyzed metal in the sediment and the background respectively, and Fe_s and Fe_b are the concentration of Fe in the sediment and the background, respectively. Previous studies reported that when $0.5 \leq EF \leq 1.5$, traces of metal may be due to crustal materials or natural weathering processes (Zhang et al., 2007). Samples having EF value greater than 5 are considered to be contaminated with that particular element. Since, the bioavailability and toxicity of any trace metals in sediments depend on the chemical form and concentration of the metal (Kwon et al., 2001), it can be inferred that trace metals in sediment samples with high EF values, along with higher labile fractions in sediments are potential sources for mobility and bioavailability in the aquatic ecosystems.

4.3 Results and Discussion

4.3.1 Nutrient Dynamics

Nutrients are called biostimulants or fertilizers; include nitrates, nitrites, phosphates and silicates. If these chemical parameters exceed the optimum mark, then it will lead to various ecological consequences on the marine ecosystem. The main source of nutrients to the sea is rock weathering and runoff from land. Atmospheric inputs through precipitation (rain) also contribute a major extent in the nitrogen system (Grasshoff et al., 1999). The nutrient contents namely ammonium, nitrite, nitrate, phosphate and silicate along the sampling stations are given in Table 4.2.

Table 4.2: Nutrient dynamics along the Kerala coast.

Parameters	C1	K3	N4	A5	K6	K7	P8	A9	T10	C11	N12	C13
Ammonia (mg L^{-1})	48.61	48.61	50.71	6.65	3.47	10.13	60.76	3.18	1.74	10.42	14.47	14.18
Nitrite (µmol L^{-1})	0.87	0.62	1.86	0.10	1.52	1.10	0.44	1.38	3.01	1.59	1.36	1.93
Nitrate (µmol L^{-1})	0.21	0.21	0.14	0.11	8.72	0.64	0.16	2.76	6.40	10.09	1.27	0.80
Phosphate (µmol L^{-1})	1.82	0.47	0.65	1.68	7.20	4.50	2.24	9.14	11.53	3.03	1.81	1.22
Silicate (µmol L^{-1})	17.63	7.38	5.25	4.36	14.56	9.62	4.47	36.14	16.48	13.21	7.57	10.30

Ammonium concentration ranged from 1.74 mg L^{-1} to 60.76 mg L^{-1}. The transport of the effluent upstream by the tidal flux attributed higher ammonia content. The presence of excess ammonia in waters exhibits the balance between the production and utilization, and the reserves may play a vital role in the propagation and growth of marine organisms at a higher rate (Nair et al., 1990). Also, may be associated with the probability that the biological removal is not counter balanced by the ammonification processes. Rainfall and the resulting runoff carrying a large amount of detritus cause maximum input of ammonia-nitrogen (Indirani, 2010). Nitrite-N values varied between 0.10 µmol L^{-1} to 3.01 µmol L^{-1}. The lower values suggest its formation from organic matter and conversion into nitrate-nitrogen (Robin et al., 2011). Higher concentration may be due to several major and minor drainage channels loaded with waste products from municipal, industrial and fish processing units (Sujatha et al., 2009) and from non-point sources from the system itself (Devi et al., 1991). Nitrate-N is an essential nutrient but at high concentration it is toxic and capable of disturbing the aquatic environment. Nitrate-nitrogen values vary between 0.11 µmol L^{-1} to 10.09 µmol L^{-1}. The nitrate content may be very high due to the fact that nitrite-nitrogen will be oxidized to nitrate-nitrogen (Manikoth and Salih, 1974). The high amount of nitrates at C11 and T10 are generally indicative of pollution with respect to high domestic waste water load and human interference (Indirani, 2010).

Inorganic phosphate registered its peak value at station T10 (11.53 µmol L^{-1}) and lowest at station K3 (0.47 µmol L^{-1}). High phosphate value may be due to anthropogenic inputs, especially drainage effluents. The accumulation of condensed phosphate ions as $P_2O_7^{4-}$, rainfall, land runoff and other external disaster occurrence also attributes to phosphate concentration (Sujatha et al., 2009; Nath and Mudholkar, 1989). Similar trends were also noticed by Sankaranarayanan et al. (1969). The lower concentration of inorganic phosphate can be attributed to biological utilization (Balachandran, 2001). Lower values of phosphate with an increase in silicate indicates dilution with freshwater and to the great silt load that removes phosphorous from the marine environment (Lakshmanan et al., 1987).

Silicate is a biologically essential nutrient to marine organisms like diatoms, radiolarians and sponges for the growth and the formation of their skeletal materials. Inorganic silicates reported maximum at station A9 (36.14 µmol L^{-1}) and minimum at station A5 (4.36 µmol L^{-1}) respectively. The high value of silicate is mainly due to the addition of silicates which is caused by high fresh water input by rivers, streams, etc. into the coastal areas. However, when the marine organisms die and disintegrate, the silicate is rapidly liberated into the marine environment. Thus, as a consequence of its biological significance, silicate exhibits a strong seasonal dependence, reflecting the waxing and waning of the life processes (Balachandran, 2001). Silicate is also used as an important chemical tool in oceanography since the wide variability of its concentration can be used for tracing water masses in the seas (Richards, 1958). The decrease in silicate is evident in surface waters due to enhanced growth of silicate utilizing diatoms, subsequent removal of fixed biogenic silica via sedimentation and reduction in direct inputs from rivers (Ittekkot et al., 2000).

4.3.2 General Biogeochemical Properties

Results of sediment texture and organic carbon are listed in Table 4.3. The textural characteristics of coastal sediments are strongly influenced by several factors, like the nature of source rocks, climate, duration and energy of sediment transport and redox conditions of the depositional environments (Bhatia and Cook, 1986; Fralick and Kronberg, 1997). The textural parameters such as sand, silt and clay showed a significant spatial variation and is examined by the variation of sand (22.02–97.87%), silt (0.98–20.27%) and clay (0.66–63.71%) content in sediments. Textural characteristics revealed the dominance of sand content in the beach sediments except a decrease at stations C11, K7, P8 and T10. The decrease in grain size at estuarine stations viz., K7, T10 and C11 indicates the transport of sediments from the riverine region and settling of fine grained sediments as a result of biogeochemical processes (Nayar, 1992). TC% varied between 0.07–12.69 with an average of 0.93. TIC% ranges from 0.03 to 5.56. TOC% ranged between 0.03 and 7.13. TOC averaged 0.72% in the surface sediments. TOC content recorded the maximum at station K7 (7.13%).

Table 4.3: Results of elemental compositions, textural characteristics and biochemical degradation indices in the surface sediments along Kerala coast.

Stations	Sand	Silt	Clay	TC	TIC	TOC	CHO	PRT	LIP	PRT/CHO	LIP/CHO
	%						mg g^{-1}				
C1	97.73	1.55	0.72	1.19	1.14	0.05	2.02	0.02	0.01	0.01	0.00
C2	96.42	2.55	1.03	2.65	2.59	0.06	3.00	0.02	0.00	0.01	0.00
K3	94.98	2.2	2.82	0.11	0.06	0.05	0.67	0.28	0.81	0.42	1.21
N4	92.13	3.89	3.99	1.89	1.80	0.10	0.74	0.82	0.94	1.11	1.27
A5	97.87	1.12	1.01	0.14	0.11	0.03	1.88	0.01	0.00	0.00	0.00
K6	96.79	2.55	0.66	0.24	0.15	0.09	0.15	0.17	0.98	1.13	6.53
K7	71.91	3.55	24.54	12.69	5.56	7.13	49.39	1.05	2.61	0.02	0.05
P8	77.69	10.58	11.73	0.10	0.06	0.04	1.15	0.43	0.70	0.37	0.61
A9	97.39	1.55	1.06	0.51	0.10	0.41	4.13	0.11	0.13	0.03	0.03
T10	79.02	20.27	0.71	0.51	0.19	0.32	6.10	0.57	1.11	0.09	0.18
C11	22.02	14.26	63.71	*NA	NA	NA	0.60	3.84	0.13	6.40	0.22
N12	93.03	0.98	5.99	0.07	0.03	0.04	0.58	0.22	0.57	0.38	0.98
C13	97.62	1.55	0.83	1.90	1.57	0.33	4.68	0.06	0.13	0.01	0.03
Min	22.02	0.98	0.66	0.07	0.03	0.03	0.15	0.01	0.00	0.00	0.00
Max	97.87	20.27	63.71	12.69	5.56	7.13	49.39	3.84	2.61	6.40	6.53
Avg	85.74	5.12	9.14	1.83	1.11	0.72	5.78	0.58	0.62	0.77	0.85

* NA: not available

The biochemical composition of sedimentary organic matter and the biochemical degradation indices are presented in Table 4.3. Total carbohydrates (CHO) content varied between 0.15 mg g^{-1} and 49.39 mg g^{-1}. Maximum CHO and TOC content were observed at K7 which is actually a coconut husk retting station. Due to year round retting taking place at this station, the decayed organic debris would be deposited and preserved in the bottom sediments without much removal processes, enriching the organic content. Total proteins (PRT) and lipids (LIP) varied from 0.01 to 3.84 mg g^{-1} and 0.00 to 2.61 mg g^{-1} respectively in the surface sediments. PRT recorded maximum concentration at station C11 containing nutrient rich surface waters originated from riverine effluents. Protein to Carbohydrate ratio (PRT/CHO) and Lipid to Carbohydrate ratio (LIP/CHO) are used as an index to determine the age of sedimentary organic matter and give useful information about biochemical degradation processes (Danovaro, et al., 1993; Cividanes et al., 2002). High PRT/CHO ratios indicate living organic matter or newly generated detritus (Danovaro et al., 1993) and the role of proteins as potentially limiting factor for the benthic consumers (Fabiano et al., 1995). On the other hand, PRT/CHO < 1 has been attributed to more degraded organic matter (Danovaro et al., 1993). The lipid content and the LIP/CHO ratio have been used as good indexes to describe the energetic quality of the organic contents in the sediment (Grémare et al., 1997; Grémare et al., 2002; Fabiano and Pusceddu, 1998). PRT/CHO ratio ranged from 0.00 to 6.40. PRT/CHO ratio > 1 were recorded at stations C11 (6.40), K6 (1.13) and N4 (1.11). The PRT/CHO ratios > 1 indicates rapid detritus mineralization and enhanced protein content due to microbial processes. The bacterial activity and supply of anthropogenic wastes in the estuarine environments of C11 and K6 may cause the prevalence of fresh organic matter in the sediments. Low PRT/CHO ratios (< 1) at estuarine environment suggest low net mineralization rates and the detritus may be relatively nutrient poor and refractory in nature (Kristensen et al., 1995). LIP/CHO ratio ranges from 0.00 to 6.53. High LIP/CHO ratio at K6 (6.53) points to the high quality and nutritive aspect of labile organic matter in the region.

4.3.3 Metal Enrichment Geochemistry

The spatial distribution of trace metals in the sediments of Southern Kerala coast is given in Table 4.4. The distribution of trace metals in the coastal sediments decreased in the following order: Fe > Mn > Zn > Ni > Pb >

Cu > Co > Cd. Fe was the most abundant element in the sediment which indicates the natural capacity of the element to regulate and accumulate its concentration. Fe varied between 0.04% and 2.62%. Fe recorded significantly high values at the estuarine sites namely, C11, C13 and T10. High Fe content may be due to anthropogenic activities mainly dredging and boat operations occurring at C11 and T10. Pearson correlation coefficients for metals and other sedimentary parameters in the surface sediments along Kerala coast is presented in Table 4.5. The distribution trend and enrichment pattern of trace metals analyzed in this study are described below.

Table 4.4: Results of major and toxic trace metal concentrations in surface sediments.

Stations	Fe	Cd	Co	Cu	Mn	Ni	Pb	Zn
	%	mg kg^{-1}						
C1	0.16	1.71	7.75	8.17	13.40	9.62	0.70	3.62
C2	0.23	4.92	12.95	1.50	22.77	16.19	11.71	12.53
K3	0.57	1.44	1.83	1.86	31.03	1.29	17.57	8.31
N4	0.10	1.96	3.14	1.50	13.78	5.58	17.16	2.76
A5	0.04	0.44	*BDL	1.49	8.47	24.81	BDL	1.12
K6	0.22	1.22	3.38	5.95	37.43	3.93	10.45	13.71
K7	0.74	1.66	11.43	20.38	45.31	29.95	24.98	30.47
P8	0.93	2.42	7.96	6.27	84.46	6.41	39.66	19.36
A9	0.57	1.29	4.48	5.98	45.21	8.97	6.44	20.07
T10	1.06	1.77	8.06	6.80	36.85	16.61	4.86	8.04
C11	2.62	21.71	17.69	35.02	75.17	32.63	21.44	226.57
N12	0.66	1.73	3.33	4.74	27.51	4.91	0.25	8.05
C13	1.21	2.05	7.93	7.09	38.54	15.23	6.28	12.70
Min	0.04	0.44	1.83	1.49	8.47	1.29	0.25	1.12
Max	2.62	21.71	17.69	35.02	84.46	32.63	39.66	226.57
Avg	0.70	3.41	7.49	8.21	36.92	13.55	13.46	28.25
ERL		1.20		34		20.90	46.70	150
ERM		9.60		270		51.60	218	410

*BDL: below detectable level

Table 4.5: Pearson correlation coefficients for metals and other sedimentary parameters in the surface sediments along Kerala coast.

	Cd	Cu	Co	Fe	Mn	Ni	Pb	Zn	TC	TIC	TOC	Sand	Silt	Clay
Cd	1													
Cu	**0.82**	1												
Co	**0.75**	**0.76**	1											
Fe	**0.83**	**0.82**	*0.66*	1										
Mn	0.52	*0.60*	0.45	**0.74**	1									
Ni	0.55	**0.71**	**0.89**	0.51	0.20	1								
Pb	0.24	0.29	0.28	0.26	*0.70*	0.20	1							
Zn	**0.98**	**0.90**	**0.72**	**0.86**	*0.59*	*0.59*	0.28	1						
TC	0.11	**0.83**	0.56	0.12	0.10	*0.67*	0.30	*0.66*	1					
TIC	0.33	*0.69*	*0.66*	0.02	−0.04	*0.64*	0.25	0.54	**0.95**	1				
TOC	−0.07	**0.89**	0.45	0.19	0.19	*0.65*	0.33	**0.72**	**0.97**	**0.85**	1			
Sand	**−0.90**	**−0.92**	**−0.74**	**−0.87**	*−0.68*	*−0.64*	−0.45	**−0.93**	*−0.58*	−0.44	*−0.65*	1		
Silt	0.46	0.43	0.44	*0.62*	0.54	0.32	0.28	0.46	−0.09	−0.15	−0.03	*−0.65*	1	
Clay	**0.91**	**0.94**	**0.73**	**0.83**	*0.62*	*0.65*	0.44	**0.95**	**0.82**	*0.69*	**0.87**	**−0.97**	0.44	1

Note: Correlation significant at the 0.05 level is given in italics and correlation significant at the 0.01 level is given in bold.

4.3.3.1 Cadmium

Cd was found to be the least abundant element compared to other nutrient elements in sediments. The occurrence of Cd in the marine environment is rare, so Cd may be transported to the environment by metal mining and refining, phosphate fertilizers, operation of motor boats and industrial sewages (Nobi et al., 2010; Yuan et al., 2014). Cd recorded contamination in the beach sediments of Kerala which had been previously reported by Suresh et al. (2015) and considered Cd as a contaminant in this environment. In the present study, Cd concentration significantly varied between 0.44 mg kg^{-1} and 21.71 mg kg^{-1} (average 3.41 mg kg^{-1}). As per the calculated geochemical indices, Cd exhibits maximum contamination at C11 and C2 (Table 4.6). EF$_c$ of Cd displays very high values ranging from 46.91 to 597.18. EF$_r$ of Cd varied between 0.74 and 9.38. Using crustal background, EFs may generally show very high values for Cd whereas the regional background of the metal can be utilized to have a comprehend assumption on the enrichment pattern. Cd-EF_r shows moderately severe enrichment at C2 and N4 and moderate enrichment at K6, C11, A5 and C1. In general, Cd recorded higher values than background in the estuarine environment, especially at C11. The present enrichment of Cd is rather a result of anthropogenic activities other than source rocks or biological sources. Cd concentration at C11 (21.71 mg kg^{-1}) is very high due to industrial effluents. This station is situated in the lower arms of river Periyar where the large scale industries are located. Earlier reports suggest that the effluent treatment plants are directly emptying their treated effluents to the river channel and subsequent flow restrictions cause the deposition of pollutants at the lower reaches extending to Cochin estuary (Dsikowitzky et al., 2014). Therefore, the station C11 is heavily contaminated with pollutants, especially toxic metals. On the other hand, the high concentration of Cd observed at station C2 may be due to extensive harbour operations as well as transport of motorized boats. The enrichment of Cd at A5 and K6 may be preferably controlled by Fe-Mn oxyhydroxides. Most of the sampling stations along the coast are also active centres of fishing operations and hence, the enrichment of Cd can be attributed to anthropogenic activities. Cd, Co, Cu and Zn were found to be significantly correlated with each other (Table 4.5). It can be due to their similar sources in the surface sediments derived from human activities.

Table 4.6: Cd concentration and its corresponding EF, I_{geo} and CF with respect to crustal and regional background.

Stations	C1	C2	K3	N4	A5	K6	K7	P8	A9	T10	C11	N12	C13
Cd	1.71	4.92	1.44	1.96	0.44	1.22	1.66	2.42	1.29	1.77	21.71	1.73	2.05
EF_c	306.05	597.18	70.61	536.99	298.41	156.83	63.29	73.59	63.30	46.91	233.30	73.59	47.67
EF_r	4.81	9.38	1.11	8.44	4.69	2.46	0.99	1.16	0.99	0.74	3.66	1.16	0.75
C-I_{geo}	2.51	4.04	2.26	2.71	0.55	2.02	2.47	3.01	2.10	2.56	6.18	2.53	2.77
R-I_{geo}	−0.10	1.43	−0.35	0.10	−2.06	−0.58	−0.14	0.40	−0.50	−0.05	3.57	−0.08	0.16
CF_c	8.55	24.60	7.20	9.80	2.20	6.10	8.30	12.10	6.45	8.85	108.55	8.65	10.25
CF_r	1.40	4.03	1.18	1.61	0.36	1.00	1.36	1.98	1.06	1.45	17.80	1.42	1.68

C-I_{geo} of Cd ranged between 0.55 and 6.18. On average, Cd is found to be moderately polluted in the study region. Cd is moderately to strongly polluted at K6, A9, K3, K7, C1, N12, T10, N4 and C13, strongly polluted at P8, strongly to extremely polluted at C2 and extremely polluted at C11. Cd-R-I_{geo} ranged between −2.06 and 3.57. Accordingly, strong pollution of Cd is observed only at C11. Cd reported CF_c ranging from 2.20 to 108.55. CF_c of Cd revealed very high contamination in the studied samples. Cd shows CF_r values ranging from 0.36 and 17.80. CF_c for Cd indicates anthropogenic activity in the coastal areas.

4.3.3.2 Cobalt

The main source of Co is as a by product of metal mining processes. It is widely used in the production of uncorrosive high-strength alloys for automobiles. It is also used as a colouring in ceramics, glasses and inks. It is used as a key component in lithium batteries, as well as for industrial catalysts and electroplating. Co content was high at C11 (17.69 mg kg^{-1}) and lowest at K3 (1.83 mg kg^{-1}). Co shows high concentration at C11, C2 and K7 compared to other stations is an indication of additional sources for the metal enrichment (Table 4.7). Co-EF_c varied from 0.72 and 12.57. Considering EF_r, Co shows extremely severe enrichment at C1 and C2, very severe enrichment at N4, severe enrichment at P8 and moderately severe enrichment at P8 whereas EF_c displays severe enrichment at C1 and C2 and moderately severe enrichment at N4. The sites K6 and K7 reveal moderate enrichment with respect to crustal background. Co shows significant enrichment at coastal than estuarine sites which is a clear indication of the lithogenic mineral content of Co.

Table 4.7: Co concentration and its corresponding EF, I_{geo} and CF with respect to crustal and regional background.

Stations	C1	C2	K3	N4	A5	K6	K7	P8	A9	T10	C11	N12	C13
Co	7.75	12.95	1.83	3.14	*BDL	3.38	11.43	7.96	4.48	8.06	17.69	3.33	7.93
EF_c	11.10	12.57	0.72	6.88	-	3.48	3.49	1.94	1.76	1.71	1.52	1.13	1.48
EF_r	64.83	73.47	4.19	40.21	-	1.25	1.26	11.31	0.63	0.62	0.55	6.62	0.53
C-I_{geo}	−2.27	−1.53	−4.36	−3.58	-	−3.47	−1.71	−2.24	−3.07	−2.22	−1.08	−3.49	−2.24
R-I_{geo}	4.77	5.51	2.68	3.46	-	−1.56	0.20	4.80	−1.15	−0.31	0.83	3.55	−0.33
CF_c	0.31	0.52	0.07	0.13	-	0.14	0.46	0.32	0.18	0.32	0.71	0.13	0.32
CF_r	40.79	68.16	9.63	16.53	-	0.51	1.72	41.89	0.67	1.21	2.66	17.53	1.19

*BDL: below detectable level

C-I_{geo} of Co revealed negligible pollution of the metal in the study area. Co-R-I_{geo} ranges from −1.56 to 5.51 with an average of 1.87. Co is moderately to strongly polluted at K3, strongly polluted at N4 and N12, strongly to extremely polluted at C1 and P8 and extremely polluted at C2. Co shows CF_c values less than one indicating low contamination in the region. Co-CF_r unveils high values ranging from 0.51 and 68.16.

4.3.3.3 Copper

Cu is found in nature as mainly sulphides, sulphates and carbonates. The major mineral that contains copper is chalcopyrite ($CuFeS_2$), which constitutes 34% copper. It is widely dispersed in rocks and is concentrated in large Cu ore deposits. The element is also widely used in agriculture through bactericides, fungicides, and algaecides in water purification processes. The major contributors of possible pollution are thus the industrial processes and agriculture (Adriano, 1986). In this study, Cu concentration ranges from 1.49 mg kg^{-1} to 35.02 mg kg^{-1} (Table 4.8). The main source of Cu in the aquatic environment is waste incineration. Cu is used in paints to prevent seaweeds from becoming encrusted on the hulls of ships. Generally, Cu shows less significant variation and suggests geological sources for its origin in the environment. On contrary, Cu shows high values at C11 and K7 probably due to effluent inputs from the adjacent industries and agricultural washloads from non-point sources respectively. EF_c of Cu varied between 0.33 and 5.32. It shows moderate enrichment at K6, K7 and A5 and moderately severe enrichment at C1. Cu-EF_r varied from 0.19 to 3.03 showing moderate enrichment at A5 and C1. The enrichment of Cu at A5 and K6 may be preferably controlled by Fe-Mn oxyhydroxides. Cu concentration at C1 can be attributed to land discharges. Cu enrichment at the estuarine sites is indicative of land based terrestrial inputs containing high amounts of nutrient additives. Cu shows significant correlation with clay ($r^2 = 0.94$) indicating that the metal may be preserved in fine grained sediments as there is high clay percentage at the metal enriched sites.

Table 4.8: Cu concentration and its corresponding EF, I_{geo} and CF with respect to crustal and regional background.

Stations	C1	C2	K3	N4	A5	K6	K7	P8	A9	T10	C11	N12	C13
Cu	8.17	1.50	1.86	1.50	1.49	5.95	20.38	6.27	5.98	6.80	35.02	4.74	7.09
EF_c	5.32	0.66	0.33	1.49	3.67	2.78	2.83	0.69	1.07	0.66	1.37	0.73	0.60
EF_r	3.03	0.38	0.19	0.85	2.52	1.90	1.93	0.39	0.73	0.45	0.94	0.42	0.41
C-I_{geo}	−3.34	−5.78	−5.47	−5.78	−5.79	−3.79	−2.02	−3.72	−3.79	−3.60	−1.24	−4.12	−3.54
R-I_{geo}	0.34	−2.10	−1.79	−2.10	−2.95	−0.96	0.82	−0.04	−0.95	−0.76	1.60	−0.44	−0.70
CF_c	0.15	0.03	0.03	0.03	0.03	0.11	0.37	0.11	0.11	0.12	0.64	0.09	0.13
CF_r	1.90	0.35	0.43	0.35	0.19	0.77	2.65	1.46	0.78	0.88	4.55	1.10	0.92

C-I_{geo} of Cu revealed negligible pollution of the metal in the study area. R-I_{geo} of Cu varied from −2.95 to 1.60. It is unpolluted to moderately polluted at C1 and K7 and moderately polluted at C11 possibly by land based sources. Cu shows CF_c values less than one indicating low contamination in the region. CF_r of Cu varied from 0.19 to 4.55. It showed considerable contamination at C11.

4.3.3.4 Manganese

Mn is an essential element in the biological system. The major anthropogenic sources of Mn consist of municipal effluents, mineral processing and metal production industries and atmospheric deposition. Mn levels varied between 8.47 mg kg^{-1} and 84.46 mg kg^{-1} (Table 4.9). Mn is positively correlated with Fe (r^2 = 0.74) and clay (r^2 = 0.62) reflecting their inputs from lithogenic origin since it binds to major component of clay minerals. In addition to this, Mn poses moderate positive correlation with Pb and Zn (r^2 = 0.70 and 0.59 respectively). The EF_c and EF_r for Mn vary from 0.17 to 1.21 and 0.41 to 3.10 respectively in the surface sediments. EF_r revealed moderate enrichment of Mn at K6 and A5.

Table 4.9: Mn concentration and its corresponding EF, I_{geo} and CF with respect to crustal and regional background.

Stations	C1	C2	K3	N4	A5	K6	K7	P8	A9	T10	C11	N12	C13
Mn	13.4	22.77	31.03	13.78	8.47	37.43	45.31	84.46	45.21	36.85	75.17	27.51	38.54
EF_c	0.50	0.58	0.32	0.79	1.21	1.01	0.36	0.54	0.47	0.21	0.17	0.25	0.19
EF_r	0.83	0.96	0.53	1.31	3.10	2.60	0.93	0.89	1.20	0.53	0.44	0.41	0.48
C-I_{geo}	−6.73	−5.97	−5.52	−6.69	−7.39	−5.25	−4.97	−4.08	−4.98	−5.27	−4.24	−5.69	−5.21
R-I_{geo}	−1.51	−0.75	−0.30	−1.47	−2.65	−0.51	−0.23	1.14	−0.24	−0.53	0.50	−0.48	−0.47
CF_c	0.01	0.02	0.03	0.01	0.01	0.04	0.05	0.09	0.05	0.04	0.08	0.03	0.04
CF_r	0.53	0.89	1.22	0.54	0.24	1.05	1.28	3.31	1.27	1.04	2.12	1.08	1.09

C-I_{geo} of Mn revealed negligible pollution of the metal in the study area. R-I_{geo} of Mn ranged from −2.65 to 1.14 showing moderate pollution at P8. Mn shows CF_c values less than one indicating low contamination in the region. Considerable contamination of Mn (CF_r = 3.31) was obtained at P8 with CF_r ranged between 0.24 and 3.31. Moderate contamination of Mn at the estuarine sediments explains the control of Fe-Mn oxyhydroxides.

4.3.3.5 Nickel

Nickel is used in the manufacturing processes of alloys (mainly stainless steel), electroplating, Ni-Cd batteries and electronic components. The main sources of possible nickel pollution are industries refining nickel into alloys, sewage sludge, phosphate fertilizers and Ni content in phosphate rocks (Alloway, 1990; Adriano, 1986). Ni content ranged between 1.29 mg kg^{-1} and 32.63 mg kg^{-1} (Table 4.10) in the surface sediments. EF$_c$ and EF$_r$ of Ni varied from 0.17 to 44.87 and 0.55 to 28.15 respectively. Ni-EF$_c$ revealed very severe enrichment at A5. EF$_r$ of Ni displays very severe enrichment at C2 and A5 and severe enrichment at N4 and C1. Ni-EF$_r$ shows moderate enrichment at P8 and N12. The enrichment of Ni at estuarine stations may be contributed through organic matter inputs. High enrichment of Ni was observed at coastal sediments may be of geological origin.

Table 4.10: Ni concentration and its corresponding EF, I$_{geo}$ and CF with respect to crustal and regional background.

Stations	C1	C2	K3	N4	A5	K6	K7	P8	A9	T10	C11	N12	C13
Ni	9.62	16.19	1.29	5.58	24.81	3.93	29.95	6.41	8.97	16.61	32.63	4.91	15.23
EF$_c$	4.59	5.24	0.17	4.08	44.87	1.35	3.05	0.52	1.17	1.17	0.94	0.56	0.94
EF$_r$	24.66	28.15	0.91	21.90	26.37	0.79	1.79	2.79	0.69	0.69	0.55	2.99	0.55
C-I$_{geo}$	−3.55	−2.80	−6.45	−4.33	−2.18	−4.84	−1.91	−4.13	−3.65	−2.76	−1.79	−4.52	−2.88
R-I$_{geo}$	3.37	4.12	0.47	2.58	0.44	−2.22	0.71	2.79	−1.03	−0.14	0.83	2.40	−0.27
CF$_c$	0.13	0.22	0.02	0.07	0.33	0.05	0.40	0.09	0.12	0.22	0.44	0.07	0.20
CF$_r$	15.52	26.11	2.08	9. 00	2.03	0.32	2.45	10.34	0.73	1.36	2.67	7.92	1.25

C-I$_{geo}$ of Ni revealed negligible pollution of the metal in the study area. Ni-R-I$_{geo}$ ranged between −2.22 and 4.12 with an average of 1.08. It is unpolluted to moderately polluted at A5, K3, K7 and C11. Ni shows CF$_c$ values less than one indicating low contamination in the region. Ni-CF$_r$ contamination levels ranged between 0.32 and 26.11. Moderate to strong pollution of Ni was observed at N12, N4 and P8, strong pollution at C1 and strong to extreme pollution at C2 in the study region. Subsequently, the metal shows very high contamination at coastal sediments.

4.3.3.6 Lead

The main users of lead are in the construction and automotive industries. Other uses of lead are as a shielding agent for radioactive material, batteries, soldering products and fuel additive. Lead arsenate is widely used in pesticides, but it has been banned for this use. In the present study, Pb concentration was highest at P8 (39.66 mg kg^{-1}) and lowest at N12 (0.25 mg kg^{-1}). The accumulation of Pb at estuarine stations is mainly from municipal effluents, atmospheric emissions, etc. Heavy marine traffic is frequent along the coast because shipping and fishing harbours, fish processing industries and chemical plants are situated primarily in the study area. Pb-EF_c shows extremely severe enrichment at N4 and severe enrichment at K3, K7, P8, K6 and C2. EF_r of Pb reveals severe enrichment at N4 and moderately severe enrichment at P8 and C2 (Table 4.11).

Table 4.11: Pb concentration and its corresponding EF, I_{geo} and CF with respect to crustal and regional background.

Stations	C1	C2	K3	N4	A5	K6	K7	P8	A9	T10	C11	N12	C13
Pb	0.70	11.71	17.57	17.16	*BDL	10.45	24.98	39.66	6.44	4.86	21.44	0.25	6.28
EF_c	2. 00	22.74	13.78	75.22	-	21.49	15.24	19.3	5.06	2.06	3.69	0.17	2.34
EF_r	0.63	7.17	4.35	23.72	-	1.21	0.86	6.09	0.29	0.12	0.21	0.05	0.13
C-I_{geo}	−4.74	−0.68	−0.09	−0.13	-	−0.84	0.41	1.08	−1.54	−1.95	0.19	−6.23	−1.58
R-I_{geo}	−1.92	2.15	2.73	2.70	-	−1.61	−0.35	3.91	−2.31	−2.71	−0.57	−3.40	−2.34
CF_c	0.06	0.94	1.41	1.37	-	0.84	2. 00	3.17	0.52	0.39	1.72	0.02	0.50
CF_r	0.40	6.65	9.98	9.75	-	0.49	1.18	22.53	0.30	0.23	1.01	0.14	0.30

*BDL: below detectable level

C-I_{geo} of Pb varied between −6.23 and 1.08. Pb is unpolluted to moderately polluted at C11 and K7 and moderately polluted at P8. R-I_{geo} revealed moderate to strong pollution of Pb in the study area varying from

−3.40 to 3.91. It shows strong pollution at P8 and moderately to strongly polluted at C2, N4 and K3. Pb-CF$_c$ ranged between 0.02 and 3.17. It displayed moderate contamination at N4, K3, C11 and K7 and considerable contamination at P8. CF$_r$ of Pb varied between 0.14 and 22.53. Pb-CF$_r$ shows significantly high CF (22.53) at P8 compared to C2, N4 and K3 with values 6.65, 9.75 and 9.98 respectively. It shows moderate contamination at K7 and C11 and low contamination at other estuarine stations. Pb shows significant contamination at N4 and P8 may be due to the scavenging of Fe-Mn oxyhydroxides onto fine grained particles.

4.3.3.7 Zinc

Zn is used as a pigment in paints, a micronutrient in fertilizers, batteries and hardening agents in concrete and cement. Smaller amounts are also used in the manufacture of disinfectant solutions and cosmetic products. The main contributors to possible pollution are industrial wastes, over fertilization and sewage sludge (Adriano, 1986). Also, Zn is employed as a metal and alloy protective agent against corrosion. Zn showed values in the range 1.12–226.57 mg kg^{-1} with an average of 28.25 mg kg^{-1} (Table 4.12). Zn levels recorded maximum concentration at C11 indicating the discharge of industrial effluents consisting of trace elements. Zn shows less enrichment compared to EF$_c$ and EF$_r$. EF$_c$ of Zn varied from 0.61 to 6.96 and Zn-EF$_r$ ranged between 0.65 and 7.45 displaying moderately severe enrichment at K6 and C11. Zn shows positive association with Fe and Mn (Table 4.5) indicating the preferential adsorption to Fe and Mn oxyhydroxides in the sedimentary environment.

Table 4.12: Zn concentration and its corresponding EF, I_{geo} and CF with respect to crustal and regional background.

Stations	C1	C2	K3	N4	A5	K6	K7	P8	A9	T10	C11	N12	C13
Zn	3.62	12.53	8.31	2.76	1.12	13.71	30.47	19.36	20.07	8.04	226.57	8.05	12.7
EF_c	1.85	4.35	1.16	2.16	2.17	5.04	3.32	1.68	2.81	0.61	6.96	0.98	0.84
EF_r	0.80	1.89	0.51	0.94	2.33	5.40	3.56	0.73	3.01	0.65	7.45	0.42	0.90
C-I_{geo}	−4.86	−3.07	−3.66	−5.25	−6.55	−2.94	−1.78	−2.44	−2.39	−3.71	1.11	−3.71	−3.05
R-I_{geo}	−1.57	0.22	−0.37	−1.96	−3.07	0.55	1.70	0.85	1.10	−0.22	4.59	−0.42	0.44
CF_c	0.05	0.18	0.12	0.04	0.02	0.20	0.44	0.28	0.29	0.11	3.24	0.12	0.18
CF_r	0.51	1.75	1.16	0.39	0.18	2.19	4.87	2.70	3.21	1.28	36.19	1.12	2.03

C-I_{geo} of Zn revealed negligible pollution of the metal in the study area. Besides, Zn is moderately polluted at C11 compared to crustal background. R-I_{geo} of Zn varies between −3.07 and 4.59 showing negligible to moderate pollution at C2, K6 and C13. Moderate pollution of Zn was observed at A9 and K7 whereas strong to extreme pollution at C11. Zn shows considerable contamination at C11 with respect to crustal background. Zn-CF_r ranges from 0.18 to 36.19. Moderate contamination of Zn was noticed at N12, K3, T10, C2, C13, K6 and P5 whereas considerable contamination at A9 and K7. Zn recorded CF value of 36.19 at C11 revealing very high contamination. The results suggest that the estuarine stations show high contamination of Zn compared to coastal stations. Further, it is estimated that about 550 m^3 d^{-1} wastewaters containing trace elements (especially Zn and Pb) are discharged into the Periyar River from a single industrial establishment located in the industrial belt (KSPCB, 2000; Nasir, 2010; Dsikowitzky et al., 2014). The common occurrence of Zn is from harbour and shipyard sectors of world coasts.

4.3.4 Biological and Ecological Risks

To evaluate the potential effects of metals to biota, sediment quality guideline variables, namely effective range low (ERL) and effective range medium (ERM) based on Long et al. (1995) and potential ecological risk assessment index suggested by Håkanson (1980) were applied on the observed metal data.

Sediment quality guideline variables, viz., effective range low (ERL) and effective range medium (ERM) compare the toxic metal threshold levels with those obtained in the present study. All the mean concentrations of Cd metal were between ERL and ERM, except at station C11, which is greater than ERM. Hence, biota may be occasionally exposed to the toxic effects of the metal, Cd. Cu and Zn concentration exceeded the ERL value at C11 whereas the Ni levels exceeded the ERL value at A5, K7 and C11. Here also, an occasional threat to biota is likely to occur with respect to these metals.

Potential ecological risk assessment index was calculated based on two background references viz., crustal and regional background as shown in Table 4.13. According to crustal background, the Er_i values varied from 66–3256.50 for Cd (average 511.38), 0.15–3.20 for Cu (average 0.75), 0.10–2.20 for Ni (average 0.91), 0.10–15.85 for Pb (average 5.39) and 0.02–3.24 for Zn (average 0.41). On average, Cd posed very high risk while Cu, Ni, Pb and Zn show low risk in the region. RI values range from 67.82 to 3273.74 showing considerable risk associated with the metals.

Based on regional background, the Er_i values varied from 10.80–534 for Cd (average 83.84), 0.95–22.75 for Cu (average 6.28), 1.60–130.55 for Ni (average 31.45), 0.70–112.65 for Pb (average 22.07) and 0.18–36.19 for Zn (average 4.43). Cd poses moderate risk at stations K7, C1, N12, T10, N4, C13 and P8, considerable risk at C2 and very high risk at C11. Ni poses moderate risk at N4, P8 and C1 and considerable risk at C2. On the other hand, Pb reveals moderate risk at N4 and K3 whereas considerable risk at P8. The RI values varied from 22.08 to 611.34, indicating moderate risk at P8 and C2. The station C11 recorded very high ecological risk showing RI value of 611.34. On average, the study area can be classified as low risk according to the regional background (Table 4.13). Hence, the application of metal ecological risk using crustal and regional background has helped to generate better results to attain solid inferences.

Table 4.13: Ecological risk associated with a single metal (Er_i) and the overall potential risk of metals (RI) in the surface sediments.

Stations	Cd	Cu	Ni	Pb	Zn	RI	Cd	Cu	Ni	Pb	Zn	RI
	Er_i (crustal background)						**Er_i (regional background)**					
C1	256.50	0.75	0.65	0.30	0.05	258.25	42.00	9.50	77.60	2.00	0.51	131.61
C2	738.00	0.15	1.10	4.70	0.18	744.13	120.90	1.75	130.55	33.25	1.75	288.20
K3	216.00	0.15	0.10	7.05	0.12	223.42	35.40	2.15	10.40	49.90	1.16	99.01
N4	294.00	0.15	0.35	6.85	0.04	301.39	48.30	1.75	45.00	48.75	0.39	144.19
A5	66.00	0.15	1.65	-	0.02	67.82	10.80	0.95	10.15	-	0.18	22.08
K6	183.00	0.55	0.25	4.20	0.20	188.20	30.00	3.85	1.60	2.45	2.19	40.09
K7	249.00	1.85	2.00	10.00	0.44	263.29	40.80	13.25	12.25	5.90	4.87	77.07
P8	363.00	0.55	0.45	15.85	0.28	380.13	59.40	7.30	51.70	112.65	2.70	233.75
A9	193.50	0.55	0.60	2.60	0.29	197.54	31.80	3.90	3.65	1.50	3.21	44.06
T10	265.50	0.60	1.10	1.95	0.11	269.26	43.50	4.40	6.80	1.15	1.28	57.13
C11	3256.50	3.20	2.20	8.60	3.24	3273.74	534.00	22.75	13.35	5.05	36.19	611.34
N12	259.50	0.45	0.35	0.10	0.12	260.52	42.60	5.50	39.60	0.70	1.12	89.52
C13	307.50	0.65	1.00	2.50	0.18	311.83	50.40	4.60	6.25	1.50	2.03	64.78
Min	66.00	0.15	0.10	0.10	0.02	67.82	10.80	0.95	1.60	0.70	0.18	22.08
Max	3256.50	3.20	2.20	15.85	3.24	3273.74	534.00	22.75	130.55	112.65	36.19	611.34
Avg	511.38	0.75	0.91	5.39	0.41	518.42	83.84	6.28	31.45	22.07	4.43	146.37

4.3.5 Pollution Load Index

The calculation and categories of pollution load index (PLI) were described in chapter 2. The PLI provides simple but comparative means for assessing a site quality, where a value of PLI < 1 denotes unpolluted area; PLI = 1 presents baseline level of pollutants and PLI > 1 would indicate deterioration of site quality (Tomilson et al., 1980). The decreasing order of PLI is as follows: C11 > K7 > P8 > C13 ≥ C2 > T10 > A9 > K6 > C1 ≥ N4 ≥ K3 ≥ A5 > N12 and P8 > C11 > C2 > K7 > C1 > K3 > N4 > N12 > C13 > T10 > A9 > K6 > A5 for crustal and regional background respectively. According to the crustal background, PLI of stations were below one except for stations K7 and C11 (Table 4.14). The PLI recorded values of 1.07 and 21.40 for stations K7 and C11 respectively. On contrary, the PLI generated very high values for the regional background. It varied between 0.39 and 2143.73 recording minimum at A5 and maximum at P8.

Table 4.14: Pollution Load Index for different stations along the Kerala coast.

Stations	PLI	
	crustal background	regional background
C1	0.01	67.69
C2	0.12	482.43
K3	0.01	66.38
N4	0.01	61.64
A5	0.01	0.39
K6	0.04	2.65
K7	1.07	73.67
P8	0.38	2143.73
A9	0.07	4.96
T10	0.08	5.62
C11	21.40	1475.73
N12	0.00	30.83
C13	0.12	8.56
Min	0.00	0.39
Max	21.40	2143.73
Avg	1.79	340.33

4.3.6 Multivariate Statistics

4.3.6a. Principal Component Analysis

Principal component analysis generated five factors with a total variance of 92.33% (Table 4.15). The first component accounted for 30.51%

variance with high positive loadings on Ni, Co, TC, TIC and TOC. It suggests that the metal content may be preferably controlled by organic matter inputs. Factor 2 describes 21.10% of variance and shows positive loadings on Fe, Mn and Zn. This factor explains the control of Fe-Mn hydroxides in the region and adsorption of Zn onto these metal scavengers. The third factor displays positive loading of Pb and clay with a variance of 15.68%. It can be assigned as the clay controlled factor. Variance of 12.57% with significant positive and negative loadings of Cd and Cu respectively were observed in factor 4. Factor 5 reveals positive and negative loadings on silt and sand respectively with a variance of 12.47%.

Table 4.15: Principal component analysis generated after varimax orthogonal rotation.

Variables	1	2	3	4	5
Cd	0.35	−0.06	−0.01	**0.88**	0.09
Cu	0.52	0.47	−0.05	**−0.64**	0.15
Co	**0.82**	0.27	−0.14	0.33	0.29
Fe	0.02	**0.83**	−0.04	−0.17	0.24
Mn	−0.12	**0.92**	0.28	−0.04	0.22
Ni	**0.92**	0.22	−0.15	0.06	0.23
Pb	−0.01	0.21	**0.82**	0.33	0.19
Zn	0.26	**0.87**	0.33	0.01	−0.12
TC	**0.91**	−0.11	0.36	−0.03	−0.10
TIC	**0.88**	−0.25	0.31	0.13	−0.14
TOC	**0.71**	0.24	0.48	−0.42	0.00
Sand	−0.36	−0.30	−0.49	0.24	**−0.68**
Silt	−0.02	0.13	0.14	0.12	**0.95**
Clay	0.21	0.17	**0.76**	−0.25	0.15
% Variance	30.51	21.10	15.68	12.57	12.47

Note: Factor loadings greater than ±60 are shown in bold.

4.3.6b. Cluster Analysis

Cluster analysis was performed to reveal the similar association of sampling stations based on the analyzed parameters. It generated three prominent clusters for thirteen sampling stations analyzed in the study (Fig.4.1). The first cluster comprises of stations A9, C13, K6, K3 and N12. This cluster represents unpolluted area with respect to metal concentrations. The second cluster consists of stations C1, N4, C2 and T10. It represents stations of moderate metal contamination. The third cluster composed of four stations namely, K7, P8, A5 and C11. These stations can be considered as the most polluted, tolerating high enrichment of trace metals.

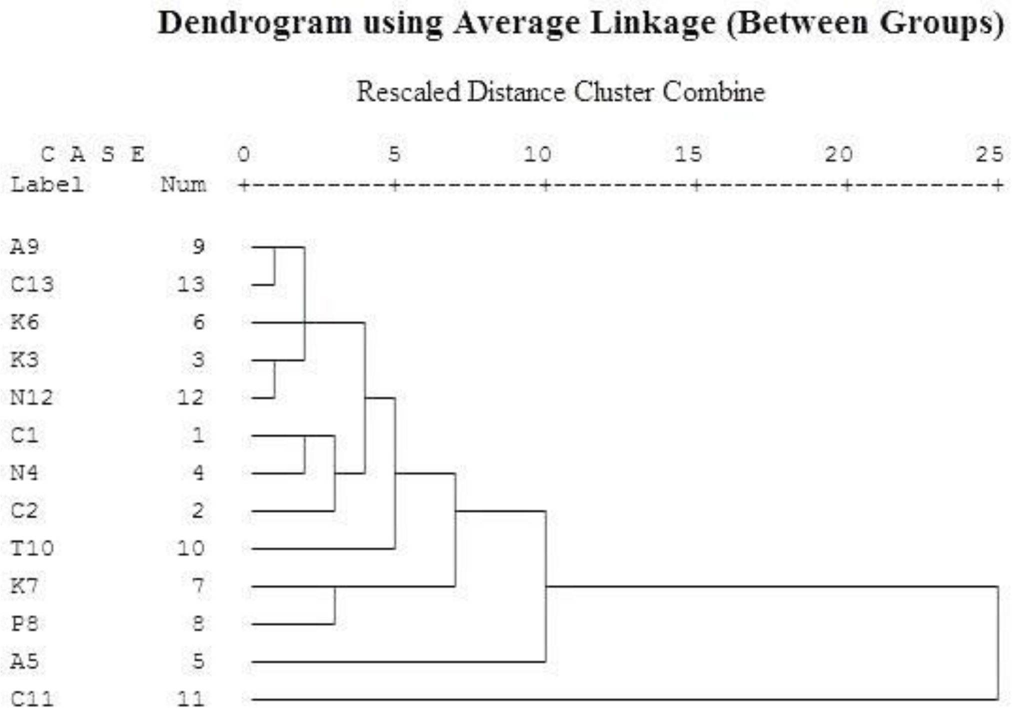

Fig. 4.1 Dendrogram showing cluster of sampling stations from the Kerala coast.

4.4 Conclusions

Present study focussed on the possible sources and potential enrichment of metals in the coastal and estuarine environments of Kerala associated with the impact of urbanization and industrialization. The levels and distribution of trace metals (Fe, Cd, Co, Cu, Mn, Ni, Pb and Zn) at thirteen stations were determined. Distribution of trace metals in the surface sediments decreased in the following order: Fe > Mn > Zn > Ni > Pb > Cu > Co > Cd. Concentration range of trace metals in sediments were the following (mg kg^{-1}): Mn (8.47 to 84.46), Zn (1.12 to 226.57), Ni (1.29 to 32.63), Pb (0.25 to 39.66), Cu (1.49 to 35.02), Co (1.83 to 17.69) and Cd (0.44 to 21.71). The station C11 in the Cochin estuary is found to be the most polluted and anthropogenically altered compared to other sampling points. The local uniqueness in the metal enrichment of Chennur is likely due to the anthropogenic sources originating from direct points of industrial units in the region. Moreover, the high hazardous trace element concentrations at station C11 (Chennur) can, therefore, be explained by the industrial inputs into the northern arm of the estuary, which is located in the immediate vicinity of the industrial hub. This deviation in the metal behaviour can be well explained by previous literature and data sets. The general metal enrichment pattern can be explained as follows: (i) Cd is introduced into the environment by anthropogenic activities whereas Cu accumulation is due to non-point sources nearby the estuarine region; (ii) Ni and Co concentration is preferably controlled by lithogenic fractions; (iii) Pb content may be increased due to the adsorption onto clay particles; (iv) Cu, Zn and slightly Ni concentrations are influenced by organic carbon content and (v) Lithogenic origin of Fe and Mn and the adsorption of Zn on their surfaces enrich Zn concentration in the sediments. Potential ecological risk index and sediment quality guidelines indicated that, on average, Cd posed considerable risk and Cu, Ni, Pb and Zn had low risk. Generally, no widespread contamination is found but, the study identified specific localized areas of potential concern and their point sources of contamination where the concentration exceeded threshold levels.

References

Adriano, D.C., 1986. Trace elements in the terrestrial environment. Springer-Verlag, New York.

Akele, M.L., Kelderman, P., Koning, C.W., Irvine, K., 2016. Trace metal distributions in the sediments of the Little Akaki River, Addis Ababa, Ethiopia. Environmental Monitoring and Assessment, 188, 389. doi: 10.1007/s10661-016-5387-z.

Alloway, B.J., 1990. Heavy metals in soils. Blackie and Son Ltd., London, UK.

Balachandran, K.K., 2001. Chemical oceanographic studies of the coastal waters of Cochin. Cochin University of Science and Technology, Cochin, India. (Ph.D. thesis).

Bhatia, M.R., Cook, K.A.W., 1986. Trace element characteristics of graywackes and tectonic setting discrimination of sedimentary basins. Contributions to Mineralogy and Petrology, 92, 181–193.

Cividanes, S., Incera, M., López, J., 2002. Temporal variability in the biochemical composition of sedimentary organic matter in an intertidal flat of the Galician coast (NW Spain). Oceanologica Acta, 25, 1–12.

Danovaro, R., Fabiano, M., Della Croce, N., 1993. Labile organic matter and microbial biomasses in deep-sea sediments (Eastern Mediterranean Sea). Deep Sea Research Part I: Oceanographic Research Papers, 40, 953–965.

Devi, K.S., Sankaranarayanan, V.N., Venugopal, P., 1991. Distribution of nutrients in the Periyar estuary. Indian Journal of Marine Sciences, 20, 49–54.

Dsikowitzky, L., Nordhaus, I., Sujatha, C.H., Akhil, P.S., Soman, K., Schwarzbauer, J., 2014. A combined chemical and biological assessment of industrial contamination in an estuarine system in Kerala, India. Science of the Total Environment, 485, 348–362.

Fabiano, M., Danovaro, R., Fraschetti, S., 1995. A three-year time series of elemental and biochemical composition of organic matter in subtidal sandy sediments of the Ligurian Sea (northwestern Mediterranean). Continental Shelf Research, 15, 1453−1469.

Fabiano, M., Pusceddu, A., 1998. Total and hydrolizable particulate organic matter (carbohydrates, proteins and lipids) at a coastal station in Terra Nova Bay (Ross Sea, Antarctica). Polar Biology, 19, 125–132.

Forstner, U., Wittmann, G.T.W., 1983. Metal pollution in aquatic environment. Springer-Verlag, New York.

Fralick, P.W., Kronberg, B.I., 1997. Geochemical discrimination of clastic sedimentary rock sources. Sedimentary Geology, 113, 111–124.

Grasshoff, K., Ehrhardt, M., Kremling, K., 1999. Methods of sea water analysis. 3rd edition, Verlag Chemie, Weinheim, Germany.

Grémare, A., Amouroux, J.M., Charles, F., Dinet, A., Riaux-Gobin, C., Baudart, J., Medernach, L., Bodiou, J.Y., Vetion, G., Colomines, J.C., Albert, P., 1997. Temporal changes in the biochemical composition and nutritional value of the particulate organic matter available to surface deposit-feeders: a two year study. Marine Ecology Progress Series, 150, 195–206.

Grémare, A.L., Medernach, F., deBovee, J. M., Amoroux, G., Vetion, Albert, P., 2002. Relationships between sedimentary organics and benthic meiofauna on the continental shelf and the upper slope of the Gulf of Lions (NW Mediterranean). Marine Ecology Progress Series, 234, 85–94.

Håkanson, L., 1980. An ecological risk index for aquatic pollution control: a sedimentological approach. Water Research, 14, 975–1001.

Indirani, B., 2010. Studies on ammonia, nitrate and phosphate content of Pazhayar river, Kanyakumari district-Tamilnadu, India. Journal of Basic and Applied Biology, 4, 221–225.

Ittekkot, V., Humborg, C., Schäfer, P., 2000. Hydrological alterations and marine biogeochemistry: A silicate issue. BioScience, 50, 776–782.

Kerala State Pollution Control Board (KSPCB)., 2000. Environmental Status Report 2000.

Kristensen, E., Ahmed, S.I., Devol, A.H., 1995. Aerobic and anaerobic decomposition of organic matter in marine sediment: Which is fastest?. Limnology and Oceanography, 40, 1430–1437.

Kwon, Y.T., Lee, C.W., Ahn, B.Y., 2001. Sedimentation pattern and sediments bioavailability in a wastewater discharging area by sequential metal analysis. Microchemical Journal, 68, 135–141.

Lakshmanan, P.T., Shynamma, C.S., Balachand, A.N., Nambisan, P.N.K., 1987. Distribution and variability of nutrients in Cochin backwaters, south west coast of India. Indian Journal of Marine Sciences, 16, 99–102.

Long, E.R., McDonald, D.D., Smith, S.L., Calder, F.D., 1995. Incidents of adverse biological effects within ranges of chemical concentrations in marine and estuarine sediments. Environmental Management, 19, 81–97.

Manikoth, S., Salih, K.Y.M., 1974. Distribution characteristics of nutrients in the estuarine complex of Cochin. Indian Journal of Marine Sciences, 3, 125–130.

Nair, S.M., Balchand, A.N., Nambisan, P.N.K., 1990. Metal concentrations in recently deposited sediments of Cochin backwaters, India. Science of the Total Environment, 97–98, 507–524.

Nasir, U.P., 2010. Water quality assessment and isotope studies of Vembanad Wetland system. Calicut University, Calicut, India. (Ph.D. thesis).

Nath, B.N., Mudholkar, A.V., 1989. Early diagenetic processes affecting nutrients in the pore waters of central Indian Ocean cores. Marine Geology, 86, 57–66.

Nayar, T.V., 1992. Biogeoorganics in the sedimentary environments of Cochin estuary. Cochin University of Science and Technology, Cochin, India. (Ph.D. thesis).

Nobi, E.P., Dilipan, E., Thangaradjou, T., Sivakumar, K., Kannan, L., 2010. Geochemical and geo-statistical assessment of heavy metal concentration in the sediments of different coastal ecosystems of Andaman Islands, India. Estuarine Coastal and Shelf Science, 87, 253–264.

Richards, F.A., 1958. Dissolved silicate and related properties of some western north Atlantic and Caribbean waters. Journal of Marine Resources, 17, 449–465.

Robin, R.S., Pradipta, R., Muduli, K., Vardhan, V., Rao, G.N., Balasubramanian, T., 2011. Seasonal variation of nutrient concentration in a tropical estuary, south west coast of India. PIET, Rourkela, 49–54.

Sankaranarayanan, V.N., Qasim, S.Z., 1969. Nutrients of the Cochin Backwater in relation to environmental characteristics. Marine Biology, 2, 236–247.

Schiff, K.C., Weisberg, S.B., 1999. Iron as a reference element for determining trace metal enrichment in southern California coastal shelf sediments. Marine Environmental Research, 48, 161–176.

Sujatha, C.H., Benny, N., Raveendran, R., Fanimol, C.L., Samantha, N.K., 2009. Nutrient dynamics in the two lakes of Kerala, India. Indian Journal of Geo-Marine Sciences, 38, 451–456.

Suresh, G., Ramasamy, V., Sundarrajan, M., Paramasivam, K., 2015. Spatial and vertical distributions of heavy metals and their potential toxicity levels in various beach sediments from high-background-radiation area, Kerala, India. Marine Pollution Bulletin, 91, 389–400.

Taylor, S.R., 1964. The abundance of chemical elements in the continental crust: a new table. Geochimica et Cosmochimica Acta, 28, 1273–1285.

Tessier, A., Campbell, P.G.C., 1987. Partitioning of trace metals in sediments: Relationships with bioavailability. Hydrobiologia, 149, 43–52.

Tomlinson, D.L., Wilson, J.G., Harris, C.R. Jeffrey, D.W., 1980. Problems in the assessment of heavy metal levels in estuaries and the formation of a pollution index. Helgol Mar Res, 33, 566–575.

Vosoogh, A., Saeedi, M., Lak, R., 2016. Heavy metals relationship with water and size-fractionated sediments in rivers using canonical correlation analysis (CCA) case study, rivers of south western Caspian Sea. Environmental Monitoring and Assessment, 188, 603. doi: 10.1007/s10661-016-5611-x.

Xu, G., Liu, J., Pei, S., Kong, X., Hu, G., 2014. Distribution and source of heavy metals in the surface sediments from the near-shore area, north Jiangsu Province, China. Marine Pollution Bulletin, 83, 275–281.

Yuan, Z., Taoran, S., Yan, Z., Tao, Y., 2014. Spatial distribution and risk assessment of heavy metals in sediments from a hypertrophic plateau lake Dianchi, China. Environmental Monitoring and Assessment, 186, 1219–1234.

Zhang, L., Ye, X., Feng, H., Jing, Y., Ouyang, T., Yu, X., Liang, R., Gao, C., Chen, W., 2007. Heavy metal contamination in western Xiamen Bay sediments and its vicinity, China. Marine Pollution Bulletin, 54, 974–982.

Zhou, G., Sun, B., Zeng, D., Wei, H., Liu, Z., Zhang, B., 2014. Vertical distribution of trace elements in the sediment cores from major rivers in east China and its implication on geochemical background and anthropogenic effects. Journal of Geochemical Exploration, 139, 53–67.

Chapter

5

SOURCE ASSESSMENT OF METALS IN THE SOUTHEASTERN ARABIAN SEA

Contents

5.1 Introduction

Marine and terrestrial pollution sources have caused a considerable deterioration of coastal and marine ecosystems worldwide. The coastal zones are platforms of significant ecological importance that link marine and terrestrial environments. The coastal margins are seen to be potential sources of hazardous trace elements, as the effluents are discharged into water bodies and finally flushed out to the open ocean. Coastal construction, urbanization and port activities may increase the impact of human activities on the coastal ecosystems (Bianchi et al., 2014; Piggott et al., 2015; Nepote et al., 2017). Fluvial inputs through rivers are considered to be the primary source of elements to the Sea and the process is more effective in the land-sea margins exclusively in the coastal environment. The geochemical nature of trace elements supplied to ocean waters would depend on complexation potential, pH, organic matter, local geography and anthropogenic inputs, and become attached to fine-grained components, such as oxides of Fe and Mn, sulphides, organic constituents and clay minerals (de Andrade Passos et al., 2010; Luís et al., 2011; Benson et al., 2016). Sediments are more useful tracers than water as they control processes such as adsorption, complexation of metals to organic ligands, clay and mineral surfaces. It is important that the dynamic processes taking place in the sediments can contribute to the understanding of biogeochemical cycles.

The Arabian Sea along the southwest coast of India experiences seasonal upwelling causing resuspension of bottom waters and surface sediments, revoking a considerable impact on the physico-chemical processes of the water body. The upwelled waters bring nutrients into the surface and consequently enormous biological production occurs in the surface water. Most of the organic matter in the marine sediments is derived from biological productivity of the water. Although the environmental factors favour the accumulation of marine derived organic matter; a previous study by Acharya et al. (2015), accounted for the transport of terrestrial matter into the shelf. The assessment of bulk organic geochemical techniques through interrelated parameters such as TOC, TN, and C/N provide substantial support of source specification of organic matter (Bianchi et al., 2002; Ramaswamy et al., 2008; Dubois et al., 2012; Zhang et al., 2014; Rasiq et al., 2016; Acharya and Panigrahi, 2016). The assessment of preliminary source using sedimentary indicators such as TOC/TN would help to explain and support the complex biogeochemical processes occurring in the Arabian Sea. The accumulation and preservation of organic matter is controlled by numerous factors such as productivity and oxygen content of the waters, grain size, water depth, sedimentation rates, lateral transport of surface waters, bacterial degradation and sediment mixing (Paropkari, 1990; Calvert et al., 1995; Hedges and Keil, 1995; Hartnett et al., 1998). The extent of primary production and export flux of organic matter together with aeolian or land derived fluvial inputs results in water column particle scavenging that can greatly regulate the complexation level of metals both in water and sediments (Cowie, 2005). The binding and release of trace metals in the sediments occur at different rates in which humic substances are an important component for controlling the transport of metals (Jalali and Moradi, 2013). The redox conditions persisting in the deeper layers significantly alter the degradation pattern of organic matter and its subsequent accumulation in the sediments (Rasiq et al., 2016). The signals of diagenesis of organic matter certainly affect the rate of organic geochemical reactions and transport of elements in the surrounding environment. The sedimentation of organic matter through water removes inorganic pollutants from the water column (Mackereth, 1965). Thus organic matter is a key factor influencing the metal accumulation and the study of sources, degradation state and quality of sedimentary organic matter is important and essential in elucidating the geochemical characteristics of an aquatic system. Furthermore, the biological productivity directs the export of organic matter giving rise to oxygen depleted conditions and pose stress to marine flora and fauna (Wainright and Hopkinson Jr, 1997).

To successfully evaluate the sources of metals in the Southeastern Arabian Sea, this chapter focuses to (1) investigate the spatial variability in sources and nature of organic matter supplied to the shelf sediments; (2) study the spatial distribution of major and environmentally relevant trace elements content in the sediments during an upwelling event; (3) ascertain the association of metals by correlating the metal levels with bulk sediment properties using multivariate statistical methods.

The continental shelf of Arabian Sea, along the Kerala coast was sampled in a series of eight transects running approximately perpendicular to the coastline which extends from 08°23.03' to 12°50.86' N latitude and 73°20.35' to 76°29.45' E longitude. The sampling was carried out during two cruises, summer monsoon in July 2013 (Cruise No. 316) along four bathymetric transects including inner and outer shelf off Trivandrum (TR22, TR23, TR24, TR25), Kollam (KO19, KO20, KO21), Alleppey (AL16, AL17, AL18) and Cochin (CO12, CO13, CO14, CO15) and August 2013 (Cruise No. 318) along four bathymetric transects including Valapad (VA9, VA10, VA11), Calicut (CA6, CA7, CA8), Kannur (KA3, KA4, KA5) and Mangalore (MA1, MA2).

5.2 Data Analysis

To evaluate the magnitude of contamination in the environment, EF is computed relative to the abundance of species in source material to that found in the earth's crust and it is a convenient measure of geochemical trends and is adopted for making comparison between areas (Sinex and Helz, 1981). It is calculated by comparing the studied metal, suspected to be polluted, with respect to non-polluted samples of similar texture, chemical and mineralogical composition. Fe has been chosen as normalization element because of its origin being exclusively lithospheric (Bloundi et al., 2009). Further, the Fe geochemistry is similar to that of many trace metals both in oxic and anoxic environments. These properties justify its use as a normalizer (Kumar et al., 2010; Sreekanth et al., 2015). EF is calculated as follows:

$$EF = (M_s/Fe_s)/(M_b/Fe_b)$$

where M_s and M_b represent the concentration of the analyzed metal in the sediment and the background respectively, and Fe_s and Fe_b are the concentration of Fe in the sediment and the background, respectively. For a critical geochemical evaluation of EF, CF and I_{geo}, regional background values of metals were used in place of average earth crust values to normalize the metal concentrations. The regional background values of metals (except Cd and Mg) were obtained from Varghese (2004), reported in the western continental shelf of India (Eastern Arabian Sea). Cd and Mg were not analyzed in the study and hence, the geochemical indices were not applied to these metals. It should be however noted that many of these values exceed the corresponding earth crust levels.

5.3 Results and Discussion

5.3.1 General Biogeochemical Properties

5.3.1.1 Sediment Texture

Textural parameters such as sand, silt and clay showed a significant spatial variation throughout all stations may be due to the strong seasonality in particle flux (Table 5.1). The physical settings and hydrodynamic conditions of the environment would be always reflected in the sediment grain size distribution. Sand content varied from 3.93–96.08% and was found maximum at TR22 (96.08%) and minimum at MA1 (3.93%). The dominance of sand fraction may be due to coastal rock formation and other hydrodynamic factors (Rao and Wagle, 1997). The distribution of sand and mud contents showing higher concentration of coarse sediments is due to tidal effects (Raj and Jayaprakash, 2008). The silt content in the surface sediments ranged from 2.95% (KO20) to 45.83% (KO21). Clay content ranged from 0.84% to 65.08%. Maximum clay content was recorded at MA1, while the lowest was observed at TR22. The granulometric analysis revealed the predominance of sand fraction in all stations except at KO21, CA6, KA4, KA3, MA2, MA1 and TR25. The stations MA1, MA2, KA3, KA4 and CA6 dominated by clay and silt content for which the fine grained sediments have been derived from the nearby estuarine region. Consequently, the increase in fine grained sediments along the coast is an indication of fresh water input with finer particles that settle to the bottom when current and wind speeds reduce (Stephen-Pichaimani et al., 2007). This is consistent with the many studies of nearshore sediments throughout the world (Sweeney and Naidu, 1989). On contrary, the sediments of station KO19 is clayey sand which may be derived from the adjacent Ashtamudi lagoon. The textural feature of sediments along Cochin, Alleppey, Kollam and Trivandrum transects generally reveals a relative decrease of sand content in shelf sediments compared to the nearshore regions. Similarly, Rao and Veerayya (2000) have observed the dominance of silt-clay fraction in the outer shelf of Arabian Sea.

Table 5.1: Grain size fractions (sand, silt and clay percentages) in the surface sediments of Southeastern Arabian Sea.

Transect	Stations	Sand	Silt	Clay	Nomenclature
		%			
Mangalore	MA1	3.93	30.98	65.08	Silty clay
	MA2	8.61	31.62	59.77	Silty clay
Kannur	KA3	20.16	29.04	50.80	Silty clay
	KA4	24.73	11.21	64.06	Sandy clay
	KA5	52.69	16.36	30.95	Clayey sand
Calicut	CA6	28.61	25.89	45.50	Sandy clay
	CA7	92.31	3.61	4.08	Sand
	CA8	77.62	7.73	14.65	Sand
Valapad	VA9	80.44	9.10	10.47	Sand
	VA10	63.20	5.21	31.59	Clayey sand
	VA11	80.80	7.83	11.37	Sand
Cochin	CO12	93.20	5.50	1.30	Sand
	CO13	95.04	3.47	1.49	Sand
	CO14	88.77	8.80	2.43	Sand
	CO15	76.54	14.72	8.74	Silty sand
Alleppey	AL16	93.82	4.32	1.86	Sand
	AL17	88.15	6.93	4.92	Sand
	AL18	93.63	5.36	1.01	Sand
Kollam	KO19	60.09	16.56	23.35	Clayey sand
	KO20	95.56	2.95	1.49	Sand
	KO21	38.04	45.83	16.13	Sandy silt
Trivandrum	TR22	96.08	3.08	0.84	Sand
	TR23	94.40	3.85	1.75	Sand
	TR24	54.26	30.65	15.09	Silty sand
	TR25	44.66	40.25	15.09	Silty sand
Min		3.93	2.95	0.84	
Max		96.08	45.83	65.08	
Avg		65.81	14.83	19.35	

5.3.1.2 Elemental Compositions

The bulk composition of elements such as C, H, N and S in sediments and their elemental ratios (C/N, C/S) provide valuable information about the origin, degree of degradation and transport of organic matter in accordance with primary production, remineralization and diagenesis. The elemental composition in the sediment samples followed the order: C > H > S > N (Table 5.2). TC% in the sediments ranged between 0.92% (AL16) and 11.60% (KO21). TIC% varies from 0.02% (MA1) to 7.27% (CA8). TOC% of sediments ranged from 0.12% (TR22) to 6.81% (KO21) with the lowest value recorded at the near shore station TR22 and the highest value found at KO21. TOC% averaged 2.09% in the sediments of Southeastern Arabian Sea. TOC% was higher than 1% at most of the stations implies the transport of organic matter from the surface layers to the shelf during primary production. Higher TOC content accounts for lesser dilution with terrigenous matter with high phytoplankton production typical of upwelling region and the supply of detrital organic matter to the shelf. López-Sánchez et al. (1996) observed that both anthropogenic and natural processes have resulted in elevated concentrations of organic carbon in sediments. Also, high content of TOC was observed at outer shelf stations where higher proportions of fine-grained sediment, predominantly silt and clay fractions (< 63 µm), are confronted. Earlier studies on organic carbon preservation (Suess and Muller, 1980) have also indicated the influence of sediment grain size as a controlling factor. Higher TOC content in the fine-grained sediments are due to the higher retention capability of cohesive sediments which observed in the Arabian Sea, has been noted in other marine and coastal systems (Hedges and Keil, 1999). Comparatively, high TOC values in the nearby coastal areas (MA1, MA2, KA3 and CA6) indicate that, they are moderately influenced by the input and deposition of organic debris from local industrial sources where a higher terrestrial and anthropogenic input is always expected due to the relative proximity of rivers that drain into the Arabian Sea (Rajamanickam and Shetty, 1973). The preservation of sinking organic matter in these stations may be enhanced by the adsorption to clay minerals. Low values of TOC were found near the coastal regions. It can be attributed to the presence of organic poor sand sized sediments. TOC was negatively correlated with sand proving the control of fine grained sediments in the preservation of organic matter. It also enunciates the similar hydrodynamic property of clay–silt and organic fragments (Hedges and Keil, 1995). According to the correlation coefficients calculated, an inverse relationship between TOC and grain size was observed in this study.

Total hydrogen (TH%) ranged between 0.11% and 1.52% with an average of 0.60%. The variational trend of TN% in the sediments is similar to the TOC% distribution. TN% varied between 0.03% and 0.84% displaying higher values at KO21 and a lower one at the near shore region namely, TR22. The TN content is depleted in the sediments may be due to the utilization of nitrogen by phytoplankton and the subsequent depletion in the overlying water column activates the release of sedimentary nitrogen at an increased rate. The scatter plot of TOC vs. TN (Fig. 5.1) shows that the regression line passes through the origin indicating that the fraction of inorganic nitrogen in the sediments is negligible and hence, the TN represents a major fraction of organic nitrogen. These results are in agreement with the data reported by Jacob et al. (2009) in the western continental shelf of India.

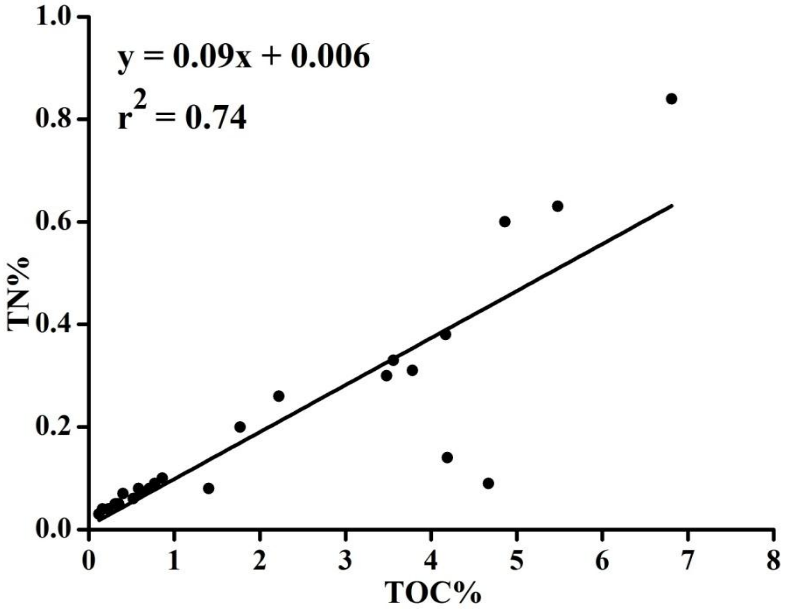

Fig. 5.1 Scatter plot of TOC vs. TN in the sediments.

The percentage of TS in the sediments recorded highest value at MA1 (1.98%) and lowest at KO20 (0.07%) with a mean of 0.42%. The highest value was observed in the nearshore region of MA1 influenced by terrestrial sources. Sediment texture, biological productivity, land runoff and terrestrial sources are the important factors that regulate the organic matter in the shelf sediments. Further, TN ($r^2 = 0.94$, $p < 0.01$) and TS ($r^2 = 0.77$, $p < 0.01$) show positive correlations with silt and clay content respectively in the sediments.

Table 5.2: Elemental compositions (C, H, N and S), TOC/TN, TOC/TS in sediments.

Stations	TC	TIC	TOC	TH	TN	TS	TOC/TN	TOC/TS
	%							
MA1	3.80	0.02	3.78	1.42	0.31	1.98	12.19	1.91
MA2	3.75	0.27	3.48	1.48	0.30	1.78	11.60	1.96
KA3	3.74	0.18	3.56	1.45	0.33	1.09	10.79	3.27
KA4	1.57	1.17	0.40	0.35	0.07	0.22	5.71	1.82
KA5	8.55	4.36	4.19	0.57	0.14	0.26	29.93	16.12
CA6	4.35	0.18	4.17	1.52	0.38	0.86	10.97	4.85
CA7	3.84	3.53	0.31	0.30	0.05	0.11	6.20	2.82
CA8	8.67	7.27	1.40	0.53	0.08	0.18	17.50	7.78
VA9	1.04	0.27	0.77	0.80	0.09	0.32	8.56	2.41
VA10	4.44	3.58	0.86	0.71	0.10	0.12	8.60	7.17
VA11	10.40	5.73	4.67	0.57	0.09	0.19	51.89	24.58
CO12	1.00	0.65	0.35	0.21	0.05	0.10	7.72	3.52
CO13	2.61	1.90	0.71	0.30	0.08	*ND	9.18	ND
CO14	5.79	5.21	0.58	0.45	0.08	0.11	7.69	5.50
CO15	5.17	3.41	1.77	1.01	0.20	0.14	8.77	12.83
AL16	0.92	0.40	0.52	0.32	0.06	0.13	8.26	4.10
AL17	2.35	1.75	0.60	0.13	0.07	ND	9.11	ND
AL18	1.26	1.09	0.16	0.35	0.04	0.19	4.55	0.86
KO19	3.26	1.04	2.22	1.05	0.26	0.52	8.53	4.24
KO20	0.98	0.64	0.33	0.19	0.05	0.07	6.97	5.08
KO21	11.60	4.78	6.81	0.32	0.84	0.14	8.12	48.42
TR22	1.99	1.87	0.12	0.15	0.03	ND	4.59	ND
TR23	3.07	2.84	0.23	0.11	0.04	ND	5.76	ND
TR24	11.08	6.22	4.86	0.23	0.60	0.21	8.05	23.35
TR25	9.65	4.17	5.48	0.52	0.63	0.15	8.66	36.82
Min	0.92	0.02	0.12	0.11	0.03	0.07	4.55	0.86
Max	11.60	7.27	6.81	1.52	0.84	1.98	51.89	48.42
Avg	4.60	2.50	2.09	0.60	0.20	0.42	11.20	10.45

*ND: not detectable

5.3.1.3 Sources and Diagenetic State of Sedimentary Organic Matter

Bulk properties such as TOC/TN can be used to identify the origin and sources of sedimented organic matter. In general, marine autogenic organic matter and terrestrial organic matter have TOC/TN ratio of 5–8 and > 15, respectively (Meyers, 1997). TOC/TN ratios are commonly used to differentiate marine from terrestrial organic matter (Perdue and Koprivnjak, 2007) i.e. the ratio indicates whether the source of organic matter is autochthonous or allochthonous. If the origin of organic matter is from a terrestrial source, the ratio of TOC/TN would generally be greater than 20. In this study, TOC/TN ratio varied from 4.55 to 51.89 with an average of 11.20 (Table 5.2). It suggests that marine algae derived organic matter is present in the shelf sediments of Southeastern Arabian Sea. Besides, the strong correlation between TOC and TN indicates the dominance of marine derived organic matter. Moreover, the TOC and TOC/TN ratio indicates the production and export of marine organic matter having both labile and refractory compounds. Higher TOC/TN ratios were observed at stations KA5 and VA11, are not indicative of terrestrial organic matter, but may be due to the deposition of degraded organic matter after effective remineralization during sinking. The nitrogen is preferentially mineralized relative to carbon and this processes greatly reflected in the TOC/TN ratio of KA5 and VA11. The sediment samples (MA1 and CA6) show high TOC/TN ratio, which presumably represents greater input of eroded material from the surrounding land. Also, the wastewater drainage from nearby industries and agricultural activities results in relatively high accumulation of terrestrial organic matter in these regions.

TOC/TS ratio is generally used as diagenetical proxy to distinguish oxic and anoxic environments. The TOC/TS ratio, varying from 0.86 to 48.42 (Table 5.2). TOC/TS ratio lower than 2.8 are indicative of sediments tending to anoxic conditions (Berner, 1989). The present value of TOC/TS ratio indicates oxic condition in the sediments except at AL18, KA4, MA1, MA2 and VA9.

5.3.1.4 Biochemical Degradation Indices Based Trophic Status

Biochemical compositional difference between the three main constituents of sedimentary organic matter in the coastal and shelf sediments of the Southeastern Arabian Sea is presented in Table 5.3. Total carbohydrates (CHO) was the most abundant characterized component of organic matter (1.10–16.67 mg g^{-1}) followed by total proteins (PRT; 0.03–6.72 mg g^{-1}) and total lipids (LIP; 0.27–1.94 mg g^{-1}). The biopolymeric carbon (BPC) ranged between 0.74 mg C g^{-1} and 9.70 mg C g^{-1} and did not display a significant variation. On average CHO (74.40%) is the dominant contributor to BPC followed by LIP (18.07%) and PRT (7.53%). The high concentrations of CHO in sediments display the contribution of autochthonous biogenic matter as a result of biological productivity. The PRT accumulation and concentration in the sediments purely depend on the remineralization mechanism existing in the water column. No correlation observed for PRT with TOC and TN confirms that little amount of PRT is adsorbed onto organic matter settling down the water column and thereby mineralization of proteins. The CHO and PRT concentration is high for MA1, MA2, KA3, CA6, CA8, VA9 and KO19 compared to other sites pointing to the contribution of organic matter from autochthonous and allochthonous sources. It can be observed that MA2 showed high concentrations of LIP (1.94 mg g^{-1}) for which the sediments composed by more than 50% of silt and clay. The lowest concentration (0.27 mg g^{-1}) from AL18 can be attributed to the presence of coarse sediments (> 90%). The deep sea sediments showed low concentration due to distance of the main sources of lipids. Lower concentrations of LIP observed may be due to the dilution of organic matter of sediment by matter of poor lipid content or the utilization of lipid as an energy source by the heterotrophic organisms (Ittekkot et al., 1984). Proliferation of minerals may also influence the degradation of lipids into other compounds. The sedimentary organic matter fractions show positive association with finer sediments which can be attributed to the similar hydraulic equivalence of both organic and clay particles.

Table 5.3: Bulk sedimentary organic matter composition, PRT/CHO, BPC and the evaluation of trophic status in sediments.

Stations	CHO	PRT	LIP	PRT/CHO	BPC	Trophic status
	mg g^{-1}				mg C g^{-1}	
MA1	15.16	3.32	0.80	0.22	8.29	*MO
MA2	11.83	3.48	1.94	0.29	7.89	MO
KA3	16.67	3.84	0.64	0.23	9.03	MO
KA4	3.47	1.80	0.93	0.52	2.97	MO
KA5	6.64	2.54	0.98	0.38	4.63	MO
CA6	13.72	6.72	1.24	0.49	9.70	MO
CA7	9.88	1.80	1.21	0.18	5.74	MO
CA8	12.15	0.53	0.42	0.04	5.43	MO
VA9	11.53	0.79	0.95	0.07	5.71	MO
VA10	7.40	0.95	1.01	0.13	4.18	MO
VA11	6.48	0.27	1.15	0.04	3.59	MO
CO12	2.86	0.37	0.33	0.13	1.58	MO
CO13	4.90	0.68	0.33	0.14	2.54	MO
CO14	4.41	0.48	0.36	0.11	2.27	MO
CO15	4.61	0.34	0.31	0.07	2.24	MO
AL16	6.22	0.41	0.33	0.07	2.94	MO
AL17	4.19	0.47	0.30	0.11	2.14	MO
AL18	2.19	0.11	0.27	0.05	1.13	MO
KO19	11.51	1.39	0.37	0.12	5.56	MO
KO20	2.81	0.21	0.36	0.07	1.50	MO
KO21	1.10	0.11	0.33	0.10	0.74	MO
TR22	1.73	0.03	0.35	0.02	0.97	MO
TR23	1.53	0.07	0.33	0.04	0.89	MO
TR24	2.00	0.07	0.35	0.03	1.10	MO
TR25	1.46	0.12	0.42	0.08	0.96	MO
Min	1.10	0.03	0.27	0.02	0.74	
Max	16.67	6.72	1.94	0.52	9.70	
Avg	6.66	1.24	0.64	0.15	3.75	

*MO: meso-oligotrophic

Protein to Carbohydrate ratio (PRT/CHO) is used as an index to determine the age of sedimentary organic matter (Danovaro, et al., 1993; Cividanes et al., 2002; Dell'Anno et al., 2002). Dominance of carbohydrates and lower PRT/CHO ratio (< 1) is a typical feature of detrital heterotrophic environments (Danovaro, 1996) since bacteria use proteins more readily than carbohydrates (Newell and Jordan, 1983). In both deep and shallow depths of the Arabian Sea, the CHO concentration is always exceed PRT content and the PRT/CHO ratio varied between 0.02 and 0.52 with less significant variation, which implies the presence of aged (less degradable) organic matter. This result supports the earlier observation made by Jacob et al. (2009). The PRT/CHO ratio is decreasing from the north to the south along the Kerala coast. The PRT/CHO ratio confirmed the role of rapidly utilized PRT's as a potentially limiting element for the growth of benthic organisms. CHO in sediments has been ascribed to the accumulation of aged organic detritus due to the faster utilization of proteins than carbohydrates by bacteria (Joseph et al., 2008). Moreover, the dominance of carbohydrates over lipids and proteins indicate its lower nutritive aspect and their aged and refractory nature (Grémare et al., 2003). The high concentration of carbohydrates observed in the marine system can be due to the combined effect of several contributory factors: high productivity, transport of organic matter (estuarine and terrestrial), anthropogenic input, high rate of sedimentation and decomposition (both aerobic and anaerobic), and subsequent preservation due to the ambient condition prevalent in the ecosystem such as pH, salinity, dissolved oxygen, Eh, etc. In addition to this, large water column in the shelf region contributed to an increase in concentration of carbohydrates.

The trophic status was evaluated based on Dell'Anno et al. (2002) and the CHO and PRT concentrations averaged 6.66 mg g^{-1} and 1.24 mg g^{-1}

respectively and BPC averaged 3.75 mg C g^{-1} (Table 5.3). On the basis of PRT/CHO ratio, all the stations were categorized as meso-oligotrophic (PRT/CHO < 1). Usually oligotrophic systems are characterized by extreme utilization of organic nitrogen resulting in lower PRT/CHO ratios and low BPC values (Vezzulli and Fabiano, 2006).

5.3.2 Autochthonous Domain on Metals

The total metal concentrations represented in Table 5.4 followed the order: Fe > Mg > Mn > Ni > Pb > Co > Cu > Zn > Cd. The mean concentrations of Fe, Mg, Cd, Co, Cu, Mn, Ni, Pb and Zn were measured to be 2.79 %, 1.21%, 5.66 mg kg^{-1}, 21.41 mg kg^{-1}, 15.56 mg kg^{-1}, 62.16 mg kg^{-1}, 49.08 mg kg^{-1}, 40.95 mg $kg^{-1}$and 12.18 mg kg^{-1} respectively. Of the nine metals studied Fe was found to be the most abundant metal present in the sediment. Fe concentration varied from 0.58% to 9.35%. Pearson's correlation analysis presented in Table 5.5 was performed on the measured data to determine the relationship between metals and other sedimentary parameters, as well as to explore the source of metals. Fe was moderately correlated with Co, Cu and Ni (r^2 = 0.42, 0.41 and 0.47 respectively). In addition, Fe was significantly correlated with metals viz., Mg and Mn and biochemical components viz., CHO and BPC (r^2 = 0.53–0.62). The positive association between Fe and Mn suggests their detrital origin and a relevant carrier phase for sedimentary burial of trace elements (Balachandran et al., 2003). Hence, it may be derived from crustal background rather than anthropogenic influence. Magnesium was found to be the second most abundant metal in the study region. It showed a maximum value at TR25 (3.36%) and a minimum at KO20 (0.21%). Mg was positively correlated with Fe, Co, Ni and Pb (r^2 = 0.55–0.80). Further, it was significantly associated with TOC, TN and silt (r^2 = 0.65, 0.61 and 0.63 respectively). So, there may be some common geochemical processes controlling their spatial variability. It can be due to their similar origin and analogous property of transport in the marine environment.

The Cd concentration revealed high values significantly above the crustal average of 0.1 mg kg^{-1} (Wedepohl, 1995). The maximum concentration of Cd was 18.95 mg kg^{-1} (VA11) and a minimum of 1.12 mg kg^{-1} (VA10). Ten concentrations greater than 5 mg kg^{-1} were observed at CO14, CA7, CA6, TR24, KA3, CO15, CA8, KA5, KO21, TR25 and VA11. Significant correlations between TOC and trace metals (Co, Mg, Cd and Ni) were observed, suggesting the increase in adsorption capacity of organic matter and their similar transport in the aquatic environment (Ottosen and Villumsen, 2006). The Cd content also follows an enrichment pattern similar to that of TOC (Pailler et al., 2002). The maximum Cd content was observed at station V11 where it encounters the highest organic matter accumulation. Accordingly, the presence of Cd was accompanied by an increase in the accumulation of organic carbon in the sediments. Further, Cd is highly enriched in sediments and is considerably contributed to sediments by direct influx through biogenic detritus linked with surface productivity. In addition, the metal data confirms that Cd was depleted with decrease in the organic carbon content. The TIC has a strong association with Cd, Pb and Ni shows that variable amounts of shell/skeleton act as scavengers for these metals.

Co concentration ranged from 3.11 mg kg^{-1} to 41.05 mg kg^{-1}. It shows high value than regional background at majority of the sampling stations in the Southeastern Arabian Sea. During the study, the levels of Cu varied between 4.73 mg kg^{-1} and 41.13 mg kg^{-1}. Cu shows significant positive correlation with TS, BPC, CHO, PRT and clay and a significant negative correlation with sand and TIC ($r^2 = -0.49$ and -0.52). Sedimentary organic matter vs. Cu correlations can be observed and the Cu may be associated with organic matter as organometal complexes (Tribovillard et al., 2008). Besides, the concentration of Cu has been controlled by regional influence at MA1 (38.04 mg kg^{-1}) and MA2 (35.18 mg kg^{-1}) showing values above the regional background. The reducing environment in MA1 and MA2 favours the precipitation of Cu as Cu sulphides and cause a relative increase in concentration in the sediments. Furthermore, the correlation of Cu with total sulphur ($r^2 = 0.74$) indicates that the reducing environment along the sediment-water interface cause the precipitation of Cu as sulphides.

Low levels of Mn enrichment were observed at all sampling stations where it varied from 1.00 mg kg^{-1} to 173.82 mg kg^{-1}. Mn is sensitive towards oxidizing and reducing conditions. Moreover, Fe and Mn are macro elements that can be used to assess diagenetic changes (Álvarez-Iglesias et al., 2003). In the case of Mn, background level was not exceeded indicating no contamination and confirms its utility as diagenetic indicator. Comparably low Mn contents are typically for oxygen minimum zones in upwelling regions (Lewis and Luther III, 2000). The upwelling in the Arabian Sea favours settling of organic matter down the water column and the subsequent oxygen consumption for decomposition induces changes in the redox conditions. Mn can be used as electron acceptor in the bacterial oxidation of organic matter and may get easily reduced to more soluble form thereby exported to adjacent waters. So, Mn is remobilized to the water column and found to be low in the surface sediments. Mn showed significant correlations with Ni and Zn ($r^2 = 0.64$ and 0.59, $p < 0.01$) may be due to the scavenging of Ni and Zn by Mn oxides. It may be a potential factor affecting the geochemical nature of Ni and Zn in the local environment.

Ni concentrations vary between 6.86 mg kg^{-1} and 87.63 mg kg^{-1} for stations AL16 and MA1 respectively. Ni was found to be enriched compared to background values. In the present study, Ni and organic matter show a similar trend of enrichment. The complexation of Ni with organic matter exported with greater residence time settles to the bottom and enriches its concentration in the surface sediments. Anthropogenic Ni inputs are mainly derived from phosphate fertilizers, industrial effluents, pesticides, etc. Ni associated to goethite and hematite minerals also enriches its presence in the sediments. Further, organic matter shows high metal affinity for Ni especially in systems having high primary production flux.

Pb concentration varied from 9.96 mg kg^{-1} to 94.61 mg kg^{-1}. Pb and Co were positively correlated with each other, Ni was positively correlated with Co and these three elements (Co, Ni and Pb) were well correlated with Mg. Moreover, Mg is a major component of clay minerals and these trace elements may be associated with clay minerals. Zn values varied from 1.00–110.97 mg kg^{-1} showing less significant spatial variation except at VA11 (110.97 mg kg^{-1}). There are natural sources as the element comprises 0.008% of the crust (Taylor and McLennon, 1985). Zn concentration was found to be high at VA11 (110.97 mg kg^{-1}) may be contributed along biodetritus reaching the sediment floor. Significant correlation of Zn with Cd ($r^2 = 0.72$) indicates same point source or transport mechanism for these two metals influenced by the supply of biogenic detritus. Zn is found to have high complexing capacity with organic matter. But, no correlation of Zn vs. TOC was observed, probably the Zn incorporated onto organic matter, could have released during sub-surface decay while settling through the water column. Previous literature suggests that low concentration of Zn is preferably caused by remobilization in the water column during change in bioturbation and remineralization of biogenic detritus, before reaching the sediments (Saito et al., 2004).

Table 5.4: Spatial variation of metals analyzed in sediment samples in the Southeastern Arabian Sea.

Stations	Fe	Mg	Cd	Co	Cu	Mn	Ni	Pb	Zn
	%		mg kg^{-1}						
MA1	5.00	1.67	2.31	33.18	38.04	152.89	87.63	40.11	16.41
MA2	5.02	1.59	4.37	25.45	35.18	135.35	60.5	23.7	13.10
KA3	4.65	1.57	6.99	19.34	29.19	88.32	43.66	22.46	12.60
KA4	1.04	0.38	*BDL	3.11	8.71	16.8	22.15	9.96	1.00
KA5	2.11	1.17	10.33	22.41	17.55	80.93	73.46	34.86	6.23
CA6	4.53	1.52	6.24	22.97	29.71	93.36	62.03	24.96	13.23
CA7	1.56	0.87	5.98	25.05	7.48	BDL	56.95	BDL	3.74
CA8	3.12	1.53	7.41	28.91	12.03	99.61	84.31	38.87	5.34
VA9	7.42	0.61	4.61	21.19	19.32	138.09	53.46	21.19	13.21
VA10	4.31	1.62	1.12	13.99	8.37	BDL	64.06	43.71	6.24
VA11	2.53	1.65	18.95	20.2	11.85	173.82	75.44	41.15	110.97
CO12	1.10	0.33	1.95	9.51	9.51	27.30	20.84	32.90	4.51
CO13	1.24	0.65	2.49	17.08	7.98	20.07	28.55	48.62	4.36
CO14	1.65	1.05	5.73	25.39	12.32	45.55	56.63	54.76	17.30
CO15	9.35	3.31	7.34	37.45	14.56	57.49	62.47	57.24	18.54
AL16	1.17	0.39	3.99	5.48	41.13	1.00	6.86	38.64	4.86
AL17	1.46	0.47	2.24	8.35	8.60	BDL	17.82	34.89	5.11
AL18	0.74	0.35	2.87	15.60	8.74	14.85	17.48	26.21	3.62
KO19	3.66	1.41	3.77	27.34	17.38	72.43	57.60	55.90	12.64
KO20	0.58	0.21	2.86	6.84	9.58	6.47	11.45	32.35	4.36
KO21	1.07	1.69	9.86	38.68	7.11	22.33	54.65	66.12	4.62
TR22	1.33	0.68	3.48	21.78	5.35	BDL	26.26	48.53	5.72
TR23	0.94	0.51	4.23	7.84	BDL	47.81	BDL	12.45	4.98
TR24	0.64	1.59	6.35	36.97	4.73	2.37	72.83	94.61	4.23
TR25	3.57	3.36	10.48	41.05	9.11	8.61	60.89	78.61	7.49
Min	0.58	0.21	1.12	3.11	4.73	1.00	6.86	9.96	1.00
Max	9.35	3.36	18.95	41.05	41.13	173.82	87.63	94.61	110.97
Avg	2.79	1.21	5.66	21.41	15.56	62.16	49.08	40.95	12.18
Regional background	5.08	**NA	NA	10.38	29.30	430	45.40	11.81	68.67

*BDL: below detectable limit, **NA: not available

Table 5.5: Pearson correlation coefficients for metal concentrations, TIC, TOC, TN, TS, sedimentary organic matter and grain size composition of sediments.

	Cd	Co	Cu	Fe	Mg	Mn	Ni	Pb	Zn	TIC	TOC	TN	TS	CHO	PRT	LIP	BPC	Sand	Silt	Clay
Cd	1																			
Co	*0.42*	1																		
Cu	−0.09	−0.03	1																	
Fe	0.08	*0.42*	*0.41*	1																
Mg	*0.48*	**0.80**	0.07	**0.62**	1															
Mn	0.33	0.20	*0.46*	**0.58**	0.20	1														
Ni	*0.48*	**0.74**	0.13	*0.47*	**0.66**	**0.64**	1													
Pb	0.25	**0.71**	−0.37	−0.05	**0.55**	−0.32	0.34	1												
Zn	**0.73**	0.08	0.05	0.16	0.23	**0.59**	0.34	0.01	1											
TIC	**0.58**	*0.46*	**−0.53**	−0.17	0.38	−0.06	**0.53**	**0.57**	0.26	1										
TOC	**0.64**	**0.69**	0.18	0.18	**0.65**	0.25	**0.60**	*0.47*	0.31	0.31	1									
TN	0.33	**0.72**	0.05	0.12	**0.61**	−0.11	0.40	**0.61**	−0.07	0.22	**0.87**	1								
TS	−0.20	0.19	**0.74**	0.38	0.15	**0.59**	0.32	−0.28	0.02	*−0.49*	0.30	0.20	1							
CHO	−0.03	0.14	**0.69**	**0.56**	0.15	**0.73**	*0.45*	−0.33	0.12	−0.31	0.15	−0.01	**0.69**	1						
PRT	−0.02	0.06	**0.63**	0.35	0.12	*0.45*	0.29	−0.38	−0.03	*−0.43*	0.30	0.17	**0.69**	**0.74**	1					
LIP	0.22	0.02	0.40	0.34	0.11	**0.68**	0.39	−0.39	0.29	−0.16	0.24	−0.00	*0.51*	**0.54**	**0.64**	1				
BPC	0.00	0.12	**0.71**	**0.53**	0.15	**0.72**	*0.44*	−0.39	0.11	−0.36	0.22	0.04	**0.75**	**0.97**	**0.87**	**0.67**	1			
Sand	−0.16	−0.38	*−0.49*	−0.36	*−0.44*	−0.36	*−0.46*	0.03	0.02	0.18	**−0.66**	**−0.61**	**−0.76**	*−0.50*	**−0.68**	**−0.52**	−0.60	1		
Silt	0.32	**0.70**	0.27	0.26	**0.63**	0.10	*0.46*	*0.42*	−0.04	0.07	**0.88**	**0.94**	*0.47*	0.19	0.36	0.18	0.25	**−0.80**	1	
Clay	0.03	0.11	**0.53**	0.36	0.24	*0.45*	0.37	−0.29	−0.00	−0.30	*0.40*	0.29	**0.77**	**0.60**	**0.75**	**0.62**	**0.70**	**−0.93**	**0.53**	1

Note: Correlation significant at the 0.01 level is given in bold and correlation significant at the 0.05 level is given in italics.

Texture is an important factor controlling the diagenetic reactions of trace metals and organic matter in a particular area and indicative of the kinetic energy at the sea floor (Liu et al., 2015). Most of the metals showed negative correlation with sand particles may be of the low surface area. Elevated metal concentrations were observed at stations MA1, MA2, CO15, KO19, TR25, CO14, TR24 and KO21. As seen from the textural peculiarities of sediments, the metal enrichment can be attributed to the decrease in sediment grain size (Abrahim et al., 2007). The accumulation process is more intense in silt and clay fractions rather than the sand dominated regions as the negatively charged clay minerals and organic components adsorb positively charged metal ions. Co, Mg and Cu show strong affinity to silt and clay, whereas they show a negative correlation with sand. This suggests their bounding nature to fine grained sediments (< 63 µm) because of its high surface area to grain size ratio and the ionic attraction (Yu et al., 2010). Cu and Ni were also negatively correlated with sand indicating that these elements are ion exchanged easily on the negatively charged surfaces of Mn oxides (Acharya et al., 2015).

5.3.3 Anthropogenic and Terrestrial Influences on Metals

The coastal transects are an area of intense shipping lines with respect to extensive port activities with rapid industrialization. Apart from natural origin and preservation of fine grained sediments, enrichment of certain trace metals viz., Cd, Pb, Zn, etc. can also be attributed to substantial anthropogenic inputs from ship wastes as well as from the anti-corrosive paints applied on ships because of heavy marine traffic observed in the study zones. The land based input of fertilizers and pesticides from agricultural activities is also a contributing factor for Cd enrichment in the coastal zones. The Cochin transect showed metal accumulation which is in agreement with earlier studies by Sudhanandh et al. (2011) and Balachandran et al. (2003). Usually, the anthropised coastal margins compared to other offshore stations are subjected to extreme stress from different pollution sources. This may be due to the effluent discharge from various industries which consist of fertilizers, refinery and smelters, harbour activities, heavy marine traffic and dredging that take place in the coastal zones. The distributional trend may be well consistent with anthropogenic influence originating frequently from urban and industrial effluents to drive sedimentary enrichment.

Enrichment factor (EF) values of metals studied were varied as 1.40–28.18 (average of 5.81) for Co, 0.27–6.10 (average of 1.31) for Cu, 0.01–0.81 (average of 0.27) for Mn, 0.66–12.69 (average of 2.73) for Ni, 1.23–63.39 (average of 11.54) for Pb and 0.07–3.24 (average of 0.39) for Zn (Table 5.6). The stations with high EF values are indicative of anthropogenic contribution such as industrialization, urbanization and others, but some natural sources can also contribute towards the observed metal enrichment. On average, Pb and Co revealed significant enrichment whereas Ni and Cu showed moderate and minimal enrichment respectively, in the study region. Mn-EF values were less than one (< 1) indicating negligible enrichment of the metal. Zn shows moderate enrichment only at station VA11. The characteristic distribution of Mn and Zn in these sediments indicates a majority of lithogenic fragments with minor contributions from anthropogenic sources. The concentration of Co ranged from 3.11 mg kg^{-1} to 41.05 mg kg^{-1} in the sediments. EF values of Co unveil very high enrichment at TR24, significant enrichment at KA5, CO13, CO14, CA7, AL18 and KO21, and moderate enrichment at KA3, AL16, MA2, AL17, CA6, MA1, KO19, VA11, TR23, CO12 and CA8. The surface enrichment may also due to the retention of Co in the sediment during the decomposition or diffusion of carrier phases out of the sedimentary column. Trivandrum and Cochin transect shows the maximum concentration of Co. It may be enriched due to channels carrying industrial and municipal sewage to the Sea and land runoff mainly by river discharge. EF values of Cu show minimum enrichment along the coast except at AL18, KO20 and AL16. It revealed moderate enrichment at AL18 (2.05) and KO20 (2.87) whereas significant enrichment at AL16 (6.10). The significant enrichment of Cu suggests anthropogenic contribution. The Cu concentration recorded appreciably high value at station AL16. This can be primarily due to the terrestrial discharge containing fertilizers, algaecides, fungicides, molluscicides which originate predominantly from agricultural activities and other economic sectors. The coast and intertidal zones of Alleppey and Kollam are contrasting regions of mariculture activities like coconut husk retting, fishing operations discharging untreated effluents and expanding tourism on the shores. Ni shows significant enrichment at KO21 and TR24, while moderate enrichment at CO12, KO20, TR22, KA4, CO13, AL18, CA8, VA11, CO14, KA5 and CA7. Pb shows extremely high enrichment at TR24, very high enrichment at KO20 and KO21 and significant enrichment at CA8, TR23, VA11, KA5, TR25, AL17, CO12, AL16, CO14, AL18, TR22 and CO13. Moderate enrichment of Pb was observed at MA2, KA3, CA6, CO15, MA1, KA4 and VA10.

Table 5.6: Enrichment factor calculated using regional background in the studied samples.

Stations	Co	Cu	Mn	Ni	Pb	Zn
MA1	3.25	1.32	0.36	1.96	3.45	0.24
MA2	2.48	1.22	0.32	1.35	2.03	0.19
KA3	2.03	1.09	0.22	1.05	2.08	0.20
KA4	1.46	1.45	0.19	2.38	4.11	0.07
KA5	5.21	1.45	0.45	3.90	7.12	0.22
CA6	2.48	1.14	0.24	1.53	2.37	0.22
CA7	7.88	0.83	-	4.10	-	0.18
CA8	4.53	0.67	0.38	3.02	5.35	0.13
VA9	1.40	0.45	0.22	0.81	1.23	0.13
VA10	1.59	0.34	-	1.66	4.36	0.11
VA11	3.90	0.81	0.81	3.33	6.98	3.24
CO12	4.23	1.50	0.29	2.12	12.87	0.30
CO13	6.76	1.12	0.19	2.58	16.92	0.26
CO14	7.52	1.29	0.33	3.83	14.25	0.77
CO15	1.96	0.27	0.07	0.75	2.63	0.15
AL16	2.30	6.10	0.01	0.66	14.22	0.31
AL17	2.80	1.02	-	1.37	10.30	0.26
AL18	10.32	2.05	0.24	2.64	15.24	0.36
KO19	3.66	0.82	0.23	1.76	6.57	0.26
KO20	5.78	2.87	0.13	2.21	24.01	0.56
KO21	17.75	1.16	0.25	5.73	26.67	0.32
TR22	8.04	0.70	-	2.22	15.74	0.32
TR23	4.08	-	0.60	-	5.69	0.39
TR24	28.18	1.28	0.04	12.69	63.39	0.49
TR25	5.63	0.44	0.03	1.91	9.48	0.16
Min	1.40	0.27	0.01	0.66	1.23	0.07
Max	28.18	6.10	0.81	12.69	63.39	3.24
Avg	5.81	1.31	0.27	2.73	11.54	0.39

Geoaccumulation index (I_{geo}) values of studied metals were −2.32 to 1.40 (average 0.21) for Co, −3.22 to −0.10 (average −1.78) for Cu, −9.34 to −1.89 (average −4.26) for Mn, −3.31 to 0.36 (average −0.73) for Ni, −0.83 to 2.42 (average 1.03) for Pb and −6.69 to 0.11 (average −3.80) for Zn (Table 5.7). The negative I_{geo} values of the different metals indicate that the region has not been polluted by these metals. The negative I_{geo} values reported for Cu, Mn and Zn (except at V11), shows that the surface sediments are not polluted by these metals. In general, the study sites are unpolluted to moderately polluted with respect to metals. I_{geo} values of Co were less than two ($I_{geo} < 2$), indicating that the region is unpolluted to moderately polluted by this metal. The stations KA4, AL16, KO20, TR23, AL17, CO12, VA10 and AL18 are unpolluted with respect to Co. Ni displayed moderate contamination (0.15–1.93) in the region except at TR23, AL16, KO20, CO12, AL18, AL17, KA4, TR22, KA3 and CO13. Ni show I_{geo} values between class I ($I_{geo} < 0$) and class II ($0 \leq I_{geo} < 1$) at stations TR24, KA5, VA11, CA8 and MA1. Pb is unpolluted to moderately polluted at stations VA9, KA3, MA2, CA6, AL18, KO20, CO12, KA5 and AL17, and unpolluted at TR23 and KA4. The I_{geo} values of Pb revealed moderate to strong pollution at TR25 and TR24 whereas moderate pollution at stations CA8, AL16, MA1, VA11, VA10, TR22, CO13, CO14, KO19, CO15 and KO21.

Table 5.7: Geoaccumulation index calculated using regional background in the studied samples.

Stations	Co	Cu	Mn	Ni	Pb	Zn
MA1	1.09	−0.21	−2.08	0.36	1.18	−2.65
MA2	0.71	−0.32	−2.25	−0.17	0.42	−2.98
KA3	0.31	−0.59	−2.87	−0.64	0.34	−3.03
KA4	−2.32	−2.34	−5.26	−1.62	−0.83	−6.69
KA5	0.53	−1.32	−2.99	0.11	0.98	−4.05
CA6	0.56	−0.56	−2.79	−0.13	0.49	−2.96
CA7	0.69	−2.55	-	−0.26	-	−4.78
CA8	0.89	−1.87	−2.69	0.31	1.13	−4.27
VA9	0.44	−1.19	−2.22	−0.35	0.26	−2.96
VA10	−0.15	−2.39	-	−0.09	1.30	−4.05
VA11	0.38	−1.89	−1.89	0.15	1.22	0.11
CO12	−0.71	−2.21	−4.56	−1.71	0.89	−4.51
CO13	0.13	−2.46	−5.01	−1.25	1.46	−4.56
CO14	0.71	−1.83	−3.82	−0.27	1.63	−2.57
CO15	1.27	−1.59	−3.49	−0.12	1.69	−2.47
AL16	−1.51	−0.10	−9.34	−3.31	1.13	−4.41
AL17	−0.90	−2.35	-	−1.93	0.98	−4.33
AL18	0.00	−2.33	−5.44	−1.96	0.57	−4.83
KO19	0.81	−1.34	−3.15	−0.24	1.66	−3.03
KO20	−1.19	−2.20	−6.64	−2.57	0.87	−4.56
KO21	1.31	−2.63	−4.85	−0.32	1.90	−4.48
TR22	0.48	−3.04	-	−1.38	1.45	−4.17
TR23	−0.99	-	−3.75	-	−0.51	−4.37
TR24	1.25	−3.22	−8.09	0.10	2.42	−4.61
TR25	1.40	−2.27	−6.23	−0.16	2.15	−3.78
Min	−2.32	−3.22	−9.34	−3.31	−0.83	−6.69
Max	1.40	−0.10	−1.89	0.36	2.42	0.11
Avg	0.21	−1.78	−4.26	−0.73	1.03	−3.80

Contamination factor (CF) of various trace metals in the surface sediments are presented in Table 5.8. On average, Mn, Zn and Cu showed very low contamination whereas; Co gave moderate contamination and Pb shows considerable contamination (CF > 3) in the study area. Mn poses low contamination having CF values between 0.00 and 0.40. Zn (0.01−1.62) revealed low contamination in the region except at VA11 (1.62) with an average of 0.18. Cu-CF averaged 0.53, showing minimum at TR24 (0.16) and maximum contamination at AL16 (1.40). CF values of Co averaged 2.06, ranging from 0.30 to 3.95. Co shows considerable contamination at MA1, TR24, CO15, KO21 and TR25. Pb exhibit significant contamination at TR25 (6.66) and TR24 (8.01) and the CF values varied between 0.84 and 8.01 showing an average of 3.47. The high selectivity of Pb towards fine grained muddy sediments, active vertical mixing and factors favouring sedimentation enriches its concentration in the shelf. Industrial and sewage effluents discharged from adjacent regions in addition to water traffic also add to the pollution phenomena. The Pb levels were high in the seawater and zooplankton as suggested by Robin et al., 2012. So, Pb forms colloids in the water column and may get adsorbed onto biogenic debris which might have settled along with these particles.

Table 5.8: Contamination factor calculated using regional background in the studied samples.

Stations	Co	Cu	Mn	Ni	Pb	Zn
MA1	3.20	1.30	0.36	1.93	3.40	0.24
MA2	2.45	1.20	0.31	1.33	2.01	0.19
KA3	1.86	1.00	0.21	0.96	1.90	0.18
KA4	0.30	0.30	0.04	0.49	0.84	0.01
KA5	2.16	0.60	0.19	1.62	2.95	0.09
CA6	2.21	1.01	0.22	1.37	2.11	0.19
CA7	2.41	0.26	-	1.25	-	0.05
CA8	2.79	0.41	0.23	1.86	3.29	0.08
VA9	2.04	0.66	0.32	1.18	1.79	0.19
VA10	1.35	0.29	-	1.41	3.70	0.09
VA11	1.95	0.40	0.40	1.66	3.48	1.62
CO12	0.92	0.32	0.06	0.46	2.79	0.07
CO13	1.65	0.27	0.05	0.63	4.12	0.06
CO14	2.45	0.42	0.11	1.25	4.64	0.25
CO15	3.61	0.50	0.13	1.38	4.85	0.27
AL16	0.53	1.40	0.00	0.15	3.27	0.07
AL17	0.80	0.29	-	0.39	2.95	0.07
AL18	1.50	0.30	0.03	0.38	2.22	0.05
KO19	2.63	0.59	0.17	1.27	4.73	0.18
KO20	0.66	0.33	0.02	0.25	2.74	0.06
KO21	3.73	0.24	0.05	1.20	5.60	0.07
TR22	2.10	0.18	-	0.58	4.11	0.08
TR23	0.76	-	0.11	-	1.05	0.07
TR24	3.56	0.16	0.01	1.60	8.01	0.06
TR25	3.95	0.31	0.02	1.34	6.66	0.11
Min	0.30	0.16	0.00	0.15	0.84	0.01
Max	3.95	1.40	0.40	1.93	8.01	1.62
Avg	2.06	0.53	0.14	1.08	3.47	0.18

5.3.4 Multivariate Statistics

5.3.4a. Principal Component Analysis

PCA is widely employed to reduce original variables and analyze their sources (Zaharescu et al., 2009; Gong et al., 2009). The variables were subjected to logarithmic data transformation before the PC analysis. According to the results obtained after varimax orthogonal rotation, the original variables were reduced to four components with eigen values greater than 1, which accounted for 83.72% of the total variance (Table 5.9). Factor 1 accounted for 36.23% of total variance with high positive loadings for the sedimentary organic matter chiefly CHO, PRT, LIP, BPC, TS and Cu, and significant negative loadings on TIC, Pb and sand. It can be assessed as a link between preservation and sedimentation of marine organic matter with phytobenthic contribution controlling the factor. In factor 2, high positive loading has been observed for Co, Mg, silt, clay, TN and TOC with a total variance of 29.67%. This factor points to the metal enrichment through adsorption onto clay minerals and organic matter inputs. The factor 3 with 17.82% variance showing significant loadings for Cd, Mn, Ni and Zn which describes the distinct accumulation pattern of these metals through important carrier phase namely Mn oxyhydroxides.

Table 5.9: Principal components generated after varimax orthogonal rotation for analyzed variables.

Variables	1	2	3
Cd	−0.34	0.38	**0.68**
Co	−0.10	**0.80**	0.44
Cu	**0.88**	−0.08	0.03
Fe	0.57	0.23	0.57
Mg	0.01	**0.79**	0.52
Mn	0.57	0.07	**0.69**
Ni	0.12	0.65	**0.66**
Pb	**−0.72**	0.51	0.01
Zn	0.26	0.01	**0.78**
TIC	**−0.78**	0.24	0.46
TOC	0.08	**0.88**	0.28
TN	−0.13	**0.94**	−0.17
TS	**0.88**	0.39	−0.04
CHO	**0.86**	−0.09	0.35
PRT	**0.90**	0.24	0.08
LIP	**0.70**	0.16	0.38
BPC	**0.90**	0.01	0.33
Sand	**−0.70**	**−0.62**	0.11
Silt	0.19	**0.97**	0.05
Clay	0.59	**0.72**	0.29
%Variance	36.23	29.67	17.82

Note: Factor loadings greater than ±0.60 are shown in bold.

5.3.4b. Cluster Analysis

Cluster analysis was performed and dendrogram was generated based on average linkage between groups to explore the association between sampling sites (spatial variability). The sites with more similar spatial attributes or elements with more similar source or properties will be clustered into one group at a closer distance. The hierarchical clustering performed on the standardized data set generates a dendrogram as shown in Fig. 5.2. For the spatial cluster, twenty five sampling sites were grouped into four clusters at the distance of 25. Cluster 1 included stations MA1, MA2, KA3 and CA6 characterized by comparatively high levels of trace metals viz., Fe, Mn, Pb, etc. indicating the control of Fe-Mn oxyhydroxides and granulometric properties. The second cluster formed consists of stations KO21, TR24 and TR25 having high organic matter deposition to the bottom sediments. The third group comprises of stations namely, CA8, VA10, KA5, KO19, VA9, CO15 and VA11. Finally, cluster 4 consists of stations CO12, AL18, KO20, TR22, TR23, AL16, AL17, CO13, CA7, CO14 and KA4.

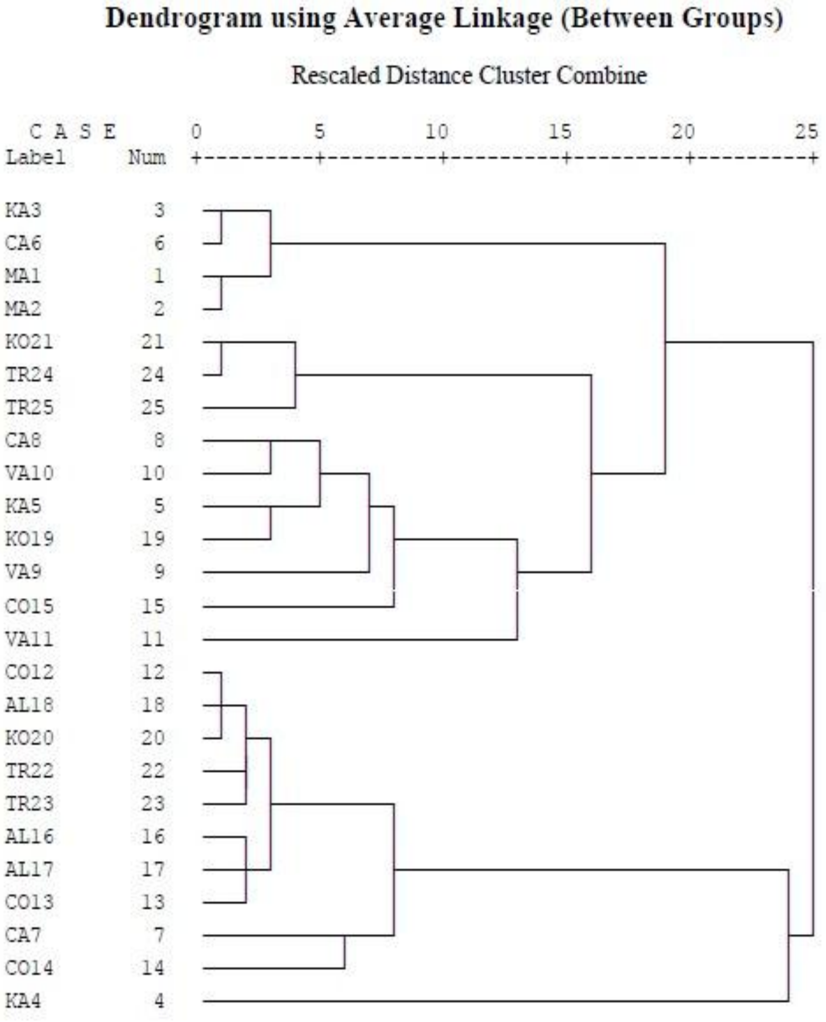

Fig. 5.2 Dendrogram showing the cluster of sampling stations in the Southeastern Arabian Sea.

5.4 Conclusions

Coastal zone, especially including the Indian exclusive economic zone (EEZ), is a region of foremost significance in terms of economic and societal cardinal that includes fishing, petroleum exploration, tourism establishments, waste dumping and marine resources preservation. So it is worthwhile accounting the anthropogenic and lithogenic sources of trace metals and the geochemical processes controlling their distribution in the shelf of Southeastern Arabian Sea. A detailed investigation on general geochemical characteristics was carried out using biogeochemical proxies for the assessment of environmental quality and organic matter sources. Correlation, principal component analysis (PCA) and cluster analysis (CA) were used to confirm the origin information of metals and the nature of organic matter composition. The geochemical distribution of trace metals is mainly controlled by different complexation phases such as Fe-Mn oxyhydroxides, organic matter and fine grained sediments. High biological productivity associated with upwelling leads to significant accumulation of Cd than crustal abundance in the shelf region. The geochemical analysis revealed the enrichment of Pb and Co in the environment which can be attributed to anthropogenic contributions mainly discharge from industrial activities, shipping zone and atmospheric input. Cu enrichment observed close to major urban sectors, initiated by the precipitation as Cu sulphides. The sediment grain size plays a key role in the enrichment of trace metals. Metals viz., Pb, Co and Ni show higher enrichment, evidenced by the association through adsorption of iron-manganese nodules onto clay minerals. Low levels of Zn, preferably display scavenging by Fe/Mn metal oxides. The ratios among various biogeochemical parameters such as total organic carbon/total nitrogen ($TOC/TN < 10$), protein/carbohydrate ($PRT/CHO < 1$) displayed that the organic matter deposited in sedimentary systems is of marine origin and relatively old with potentially low nutritional value. The high primary productivity leads to higher biogenic detritus from the surface layer to intermediate water depths, promoting microbial respiration, causing oxygen depletion and ultimately remineralization of labile organic matter, along with a large residence time of sinking biogenic matter accounts for the refractory nature of organic matter in the sediments. Biochemical degradation indices indicated meso-oligotrophic conditions with a higher microphytobenthic contribution to biopolymeric carbon in the surface sediments.

References

Abrahim, G.M.S., Parker, R.J., Nichol, S.L., 2007. Distribution and assessment of sediment toxicity in Tamaki Estuary, Auckland, New Zealand. Environmental Geology, 52, 1315–1323.

Acharya, S.S., Panigrahi, M.K., Gupta, A.K., Tripathy, S., 2015. Response of trace metal redox proxies in continental shelf environment: The Eastern Arabian Sea scenario. Continental Shelf Research, 106, 70−84.

Acharya, S.S., Panigrahi, M.K., 2016. Evaluation of factors controlling the distribution of organic matter and phosphorus in the Eastern Arabian Shelf: A geostatistical reappraisal. Continental Shelf Research, 126, 79–88.

Álvarez-Iglesias, P., Rubio, B., Vilas, F., 2003. Pollution in intertidal sediments of San Simón Bay (Inner Ría de Vigo, NW of Spain): total heavy metal concentrations and speciation. Marine Pollution Bulletin, 46, 491–506.

Balachandran, K.K., Joseph, T., Nair, M., Sankaranarayanan, V.N., Kesavadas, V., Sheeba, P., 2003. Geochemistry of surficial sediments along the central southwest coast of India: Seasonal changes in regional distribution. Journal of Coastal Research, 19, 664–683.

Benson, N.U., Asuquo, F.E., Williams, A.B., Essien, J.P., Ekong, C.I., Akpabio, O., Olajire, A.A., 2016. Source evaluation and trace metal contamination in benthic sediments from equatorial ecosystems using multivariate statistical techniques. PloS one, 11, e0156485.

Berner, R.A., 1989. Biogeochemical cycles of carbon and sulfur and their effect on atmospheric oxygen over Phanerozoic time. Palaeogeography Palaeoclimatology Palaeoecology, 75, 97–122.

Bianchi, T.S., Mitra, S., McKee, B.A., 2002. Sources of terrestrially-derived organic carbon in lower Mississippi River and Louisiana shelf sediments: implications for differential sedimentation and transport at the coastal margin. Marine Chemistry, 77, 211–223.

Bianchi, C.N., Corsini-Foka, M., Morri, C., Zenetos, A., 2014. Thirty years after: Dramatic change in the coastal marine ecosystems of Kos Island (Greece), 1981–2013. Mediterranean Marine Science, 15, 482–497.

Bloundi, M.K., Duplay, J., Quaranta, G., 2009. Heavy metal contamination of coastal lagoon sediments by anthropogenic activities: the case of Nador (East Morocco). Environmental Geology, 56, 833–843.

Calvert, S.E., Pedersen, T.F., Naidu, P.D., von Stackelberg, U., 1995. On the organic carbon maximum on the continental slope of the eastern Arabian Sea. Journal of Marine Research, 53, 269–296.

Cividanes, S., Incera, M., López, J., 2002. Temporal variability in the biochemical composition of sedimentary organic matter in an intertidal flat of the Galician coast (NW Spain). Oceanologica Acta, 25, 1–12.

Cowie, G., 2005. The biogeochemistry of Arabian Sea surficial sediments: A review of recent studies. Progress in Oceanography, 65, 260–289.

Danovaro, R., Fabiano, M., Della Croce, N., 1993. Labile organic matter and microbial biomasses in deep-sea sediments (Eastern Mediterranean Sea). Deep Sea Research Part I: Oceanographic Research Papers, 40, 953–965.

Danovaro, R., 1996. Detritus-bacteria-meiofauna interactions in a seagrass bed (*Posidonia oceanica*) of the NW Mediterranean. Marine Biology, 127, 1–13.

de Andrade Passos, E., Alves, J.C., dos Santos, I.S., Jose do Patrocínio, H.A., Garcia, C.A.B., Costa, A.C.S., 2010. Assessment of trace metals contamination in estuarine sediments using a sequential extraction technique and principal component analysis. Microchemical Journal, 96, 50–57.

Dell'Anno, A., Mei, M.L., Pusceddu, A., Danovaro, R., 2002. Assessing the trophic state and eutrophication of coastal marine systems: A new approach based on the biochemical composition of sediment organic matter. Marine Pollution Bulletin, 44, 611–622.

Dubois, S., Savoye, N., Gremare, A., Charlier, K., Beltoise, A., Blanchet, H., 2012. Origin and composition of sediment organic matter in a coastal semi-enclosed ecosystem: An elemental and isotopic study at the ecosystem space scale. Journal of Marine Systems, 94, 64–73.

Gong, M., Wu, L., Bi, X., Ren, L., Wang, L., Ma, Z., Bao, Z., Li, Z., 2009. Assessing heavy metal contamination and sources by GIS-based approach and multivariate analysis of urban-rural top soils in Wuhan, central China. Environmental Geochemistry and Health, 32, 59–72.

Grémare, A., Medernach, L., DeBovee, F., Amouroux, J.M., Charles, F., Dinet, A., Vetion, G., Albert, P., Colomines, J.C., 2003. Relationships between sedimentary organics and benthic fauna within the Gulf of Lions: Synthesis on the identification of new biochemical descriptors of sedimentary organic nutritional value. Oceanologica Acta, 26, 391–406.

Hartnett, H.E., Keil, R.G., Hedges, J.I., Devol, A.H., 1998. Influence of oxygen exposure time on organic carbon preservation in continental margin sediments. Nature, 391, 572–575.

Hedges, J.I., Keil, R.G., 1995. Sedimentary organic matter preservation: an assessment and speculative synthesis. Marine Chemistry, 49, 81–115.

Hedges, J.I., Keil, R.G., 1999. Organic geochemical perspectives on estuarine processes: sorption reactions and consequences. Marine Chemistry, 65, 55–65.

Ittekkot, V., Deuser, W.G., Degens, E.T., 1984. Seasonality in the fluxes of sugars, amino acids, and amino sugars to the deep ocean: Sargasso Sea. Deep Sea Research Part A. Oceanographic Research Papers, 31, 1057–1069.

Jacob, J., Jayaraj, K.A., Habeebrehman, H., Chandramohanakumar, N., Balachandran, K.K., Raveendran, T.V., Joseph, T., Nair, M., Achuthankutty, C.T., 2009. Biogeochemical characteristics of the surface sediments along the western continental shelf of India. Chemistry and Ecology, 25, 135–149.

Jalali, M., Moradi, F., 2013. Competitive sorption of Cd, Cu, Mn, Ni, Pb and Zn in polluted and unpolluted calcareous soils. Environmental Monitoring and Assessment, 185, 8831–8846.

Joseph, M.M., Kumar, C.S.R., Kumar, T.R.G., Renjith, K.R., Chandramohanakumar, N., 2008. Biogeochemistry of surficial sediments in the intertidal systems of a tropical environment. Chemistry and Ecology, 24, 247–258.

Kumar, C.S.R., Joseph, M.M., Kumar, T.R.G., Renjith, K.R., Manju, M.N., Chandramohanakumar, N., 2010. Spatial variability and contamination of heavy metals in the inter-tidal systems of a tropical environment. International Journal of Environmental Research, 4, 691–700.

Lewis, B., Luther III, G.W., 2000. Processes controlling the distribution and cycling of manganese in the oxygen minimum zone of the Arabian Sea. Deep Sea Research Part II: Topical Studies in Oceanography, 47, 1541–1562.

Liu, D., Li, X., Emeis, K., Wang, Y., Richard, P., 2015. Distribution and sources of organic matter in surface sediments of Bohai Sea near the Yellow River Estuary, China. Estuarine Coastal and Shelf Science, 165, 128–136.

López-Sánchez, J.F., Rubio, R., Samitier, C., Rauret, G., 1996. Trace metal partitioning in marine sediments and sludges deposited off the coast of Barcelona (Spain). Water Research, 30, 153–159.

Luís, A.T., Teixeira, P., Almeida, S.F.P., Matos, J.X., da Silva, E.F., 2011. Environmental impact of mining activities in the Lousal area (Portugal): Chemical and diatom characterization of metal-contaminated stream sediments and surface water of Corona stream. Science of the Total Environment, 409, 4312–4325.

Mackereth, F.J.H., 1965. Chemical investigation of lake sediments and their interpretation. Proceedings of the Royal Society of London, Series B, Biological Sciences, 161, 295–309.

Meyers, P.A., 1997. Organic geochemical proxies of paleoceanographic, paleolimnologic and paleoclimatic processes. Organic Geochemistry, 27, 213–250.

Nepote, E., Bianchi, C.N., Morri, C., Ferrari, M., Montefalcone, M., 2017. Impact of a harbour construction on the benthic community of two shallow marine caves. Marine Pollution Bulletin, 114, 35–45.

Newell, R.I., Jordan, S.J., 1983. Preferential ingestion of organic material by the American oyster *Crassostrea virginica*. Marine Ecology Progress Series, 13, 47–53.

Ottosen, L.M., Villumsen, A., 2006. High Cu and Cd pollution in sediments from Sisimiut, Greenland. Adsorption to organic matter and fine particles. Environmental Chemistry Letters, 4, 195–199.

Pailler, D., Bard, E., Rostek, F., Zheng, Y., Mortlock, R., van Green, A., 2002. Burial of redox sensitive metals and organic matter in the equatorial Indian Ocean linked to precession. Geochimica et Cosmochimica Acta, 66, 849–865.

Paropkari, A.L., 1990. Geochemistry of sediments from the Mangalore-Cochin shelf and upper slope off southwest India: Geological and environmental factors controlling dispersal of elements. Chemical Geology, 81, 99−119.

Perdue, E.M., Koprivnjak, J.F., 2007. Using the C/N ratio to estimate terrigenous inputs of organic matter to aquatic environments. Estuarine Coastal and Shelf Science, 73, 65−72.

Piggott, J.J., Townsend, C.R., Matthaei, C.D., 2015. Reconceptualizing synergism and antagonism among multiple stressors. Ecology and Evolution, 5, 1538–1547.

Raj, S.M., Jayaprakash, M., 2008. Distribution and enrichment of trace metals in marine sediments of Bay of Bengal, off Ennore, southeast coast of India. Environmental Geology, 56, 207–217.

Rajamanickam, G.V., Setty, M.G.A.P., 1973. Distribution of phosphorus and organic carbon in the nearshore sediments of Goa. Indian Journal of Marine Science, 2, 84–89.

Ramaswamy, V., Gaye, B., Shirodkar, P.V., Rao, P.S., Chivas, A.R., Wheeler, D., Thwin, S., 2008. Distribution and sources of organic carbon, nitrogen and their isotopic signatures in sediments from the Ayeyarwady (Irrawaddy) continental shelf, northern Andaman Sea. Marine Chemistry, 111, 137–150.

Rao, P., Wagle, B.G., 1997. Geomorphology and surficial geology of the western continental shelf and slope of India: A review. Current Science, 73, 330–350.

Rao, B.R., Veerayya, M., 2000. Influence of marginal highs on the accumulation of organic carbon along the continental slope of western India. Deep Sea Research Part II: Topical Studies in Oceanography, 47, 303–327.

Rasiq, K.T., Kurian, S., Karapurkar, S.G., Naqvi, S.W.A., 2016. Sedimentary pigments and nature of organic matter within the oxygen minimum zone (OMZ) of the Eastern Arabian Sea (Indian margin). Estuarine Coastal and Shelf Science, 176, 91–101.

Robin, R.S., Muduli, P.R., Vardhan, K.V., Ganguly, D., Abhilash, K.R., Balasubramanian, T., 2012. Heavy metal contamination and risk assessment in the marine environment of Arabian Sea, along the southwest coast of India. American Journal of Chemistry, 2, 191–208.

Saito, M.A., Moffett, J.W., DiTullio, G.R., 2004. Cobalt and nickel in the Peru upwelling region: A major flux of labile cobalt utilized as a micronutrient. Global Biogeochemical Cycles, 18, 1−9.

Sinex, S.A., Helz, G.R., 1981. Regional geochemistry of trace elements in Chesapeake Bay sediments. Environmental Geology, 3, 315–323.

Sreekanth, A., Mrudulrag, S.K., Cheriyan, E., Sujatha, C.H., 2015. Trace metal enrichment and organic matter sources in the surface sediments of Arabian Sea along southwest India (Kerala coast). Marine Pollution Bulletin, 101, 938–946.

Stephen-Pichaimani, V., Jonathan, M.P., Srinivasalu, S., Rajeshwara-Rao, N., Mohan, S.P., 2007. Enrichment of trace metals in surface sediments from the northern part of Point Calimere, SE coast of India. Environmental Geology, 55, 1811–1819.

Sudhanandh V.S., Udayakumar, P., Ouseph, P.P., Amaldev, S., Babu, K.N., 2011. Dispersion and accumulation trend of heavy metals in coastal and estuarine sediments and its textural characteristics, a case study in India. Journal of Human Ecology, 36, 85–90.

Suess, E., Muller, P.J., 1980. Productivity, sedimentation rate and sedimentary organic matter in the oceans II. - elemental fractionation. Colloques Internationaux du C.N.R.S., 293, 17–26.

Sweeney, M.D., Naidu, A.S., 1989. Heavy metals in sediments of the inner shelf of the Bean Fort Sea, Northern Arctic Alaska. Marine Pollution Bulletin, 20, 140–143.

Taylor, S.R., McLennon, S.M., 1985. The continental crust, its composition and evolution: An examination of the geochemical record preserved in sedimentary rocks. Blackwell, Oxford, UK.

Tribovillard, N., Bout-Roumazeilles, V., Algeo, T., Lyons, T.W., Sionneau, T., Montero-Serrano, J.C., Riboulleau, A., Baudin, F., 2008. Paleodepositional conditions in the Orca Basin as inferred from organic matter and trace metal contents. Marine Geology, 254, 62−72.

Varghese, S., 2004. Geochemistry of rare earth elements and trace metals along the western continental shelf of India. Cochin University of Science and Technology, Cochin, India. (Ph.D. thesis).

Vezzulli, L., Fabiano, M., 2006. Sediment biochemical and microbial variables for the evaluation of trophic status along the Italian and Albanian continental shelves. Journal of the Marine Biological Association of the United Kingdom, 86, 27–37.

Wainright, S.C., Hopkinson Jr, C.S., 1997. Effects of sediment resuspension on organic matter processing in coastal environments: A simulation model. Journal of Marine Systems, 11, 353–368.

Wedepohl, K.H., 1995. The composition of the continental crust. Geochimica et Cosmochimica Acta, 59, 217–239.

Yu, F., Zong, Y., Lloyd, J.M., Huang, G., Leng, M.J., Kendrick, C., Lamb, A.L., Yim, W.W.S., 2010. Bulk organic $\delta^{13}C$ and C/N as indicators for sediment sources in the Pearl River delta and estuary, southern China. Estuarine Coastal and Shelf Science, 87, 618–630.

Zaharescu, D.G., Hood, P.S., Soler, A.P., Fernandez, J., Burghelea, C.I., 2009. Trace metals and their source in the catchment of the high altitude Lake Respomuso, Central Pyrenees. Science of the Total Environment, 407, 3546–3553.

Zhang, Y., Kaiser, K., Li, L., Zhang, D., Ran, Y., Benner, R., 2014. Sources, distributions, and early diagenesis of sedimentary organic matter in the Pearl River region of the South China Sea. Marine Chemistry, 158, 39–48.

Chapter

6

GEOCHEMISTRY OF TRACE METAL ENRICHMENT IN THE ARABIAN SEA OFF SOUTHERN KERALA

Contents

6.1 Introduction

Coastal ecosystem sustains large ecological and biological diversity which in turn supports nutrient balance, sedimentation processes, ion exchange and other hydrological functions. Although together occupying only 8% of the total surface, they account for 20–25% of global plant growth. The coastal zone is also a dynamic fragile area with many cyclic and random processes owing to a variety of resources and habitats. Contaminants from the terrestrial environment enter the estuarine, coastal and shelf sediments affecting the ecosystem balance and pose severe threat to aquatic biota (Williams and Block, 2015). In addition to this, the tropical regions are subjected to heavy seasonal rainfall and intense fluvial inputs which may alter the geochemical behaviour of trace elements. Preliminary studies showed that the coast and shelf of Kerala are more apparent to anthropogenic inputs due to regular human activities. This region of the Arabian Sea along Southwest India is characterized by seasonal reversal of winds and the changes in circulation pattern induce intense upwelling and biological productivity in the coastal margins. The phenomenon of upwelling in combination with southwest monsoon significantly alters the material transport in the Sea linking to the land. Organic matter and nutrient sources play a key role in understanding the ecosystem functioning as a whole and connectivity of wetlands with riverine and coastal environments. The organic matter in marine sediments is profound and plays a pivotal role in the chemistry of oceans not only on the sediment which provides a significant reservoir in the global carbon cycle, but also organic matter drives in the early diagenesis. As organic matter is a principle fuel for biogeochemical reactions, it is intimately associated with the fluxes and cycling of other chemical elements in the sediments. Analysis of sediment organic matter outweighs the changes in the environmental chemical pattern and this organic matter vocabulary is significant as it exerts a strong control on the diagenetic alterations in the sediment.

Enrichment of metals is affected by regional mineralogy and source rocks and in most cases, the metal pollution is estimated using normalization procedures in relation with a conservative element such as Al, Fe, Cs and Li (Jesus et al., 2010; Felja et al., 2016). It is important to note that the geochemical interpretation of a given area depends on the selection of the background level (Rubio et al., 2000; Prego and Cobelo-García, 2003). First of all, the constituent chosen for background normalization should be associated with finer particles (related to grain size) and its concentration should not be anthropogenically altered. Al and Fe are the most commonly used conservative elements for normalization in geochemical studies. In this study, Al is considered for normalization because it is a major element of clay minerals and its concentration is not significantly altered in diagenetic environments and anthropogenic factors, thus being the best suitable element for grain size normalization and has been successfully used by several workers (Zhang et al., 2007; Duman et al., 2012; Beck et al., 2013; Pang et al., 2015). Furthermore, previous investigations carried out in this region used only a single background value may be from the crustal or regional background, whereas the present study aimed at a combination of three level background parameters to set up a good agreement in interpreting the enrichment of major and trace elements. Such information providing a comparative assessment of environmental pollution by trace metals are essential and adequate to reexamine the metal geochemistry and anthropogenic impact in densely populated coastal regions susceptible to contamination in the upwelling zone of southern continental shelf of India. In this context, the chapter aims to (1) explore the geochemistry of trace metal enrichment in the shelf and slope sediments; (2) compare the calculated geochemical indices with different background reference values to better understand the mechanisms of metal enrichment; (3) account for variations in the flux of terrigenous material using Al as a normalizing element; (4) compute ecological risk assessment factor of toxic metals to assess the potential effects to biota.

Sediments were collected from eighteen stations in five transects coast-offshore in water depths 30 to 1000 m (transects A, B, C, D and E) running approximately perpendicular to the coast of Southern Kerala (Southwest India) during November-December 2014 (northeast monsoon). Transect A with stations A1, A2, A3, A4 and A5 are located perpendicular to the coast of Cochin, the industrial capital of Kerala, South India. B1, B2 and B3 were the sampling points in transect B which borders Alleppey and Vembanad wetlands. Transect C includes C1, C2, C3 and C4, lies in the region of Kollam, an area enriched with heavy mineral deposits (Ramasamy et al., 2013).

Transect D and E lies in Trivandrum and Cape Comorin in the southern part of the study region with stations D1, D2, D3 and D4, and E1 and E2 respectively.

6.2 Data Analysis

Enrichment factor (EF) is an important tool to assess metal enrichment and here, it is utilized for determining the geochemistry of metal evolution along the Southwest Indian continental shelf sediments in the Arabian Sea. EF is calculated as

$$EF = (M_s/Al_s)/(M_b/Al_b)$$

where M_s and M_b represent the metal concentration in the studied sample and the background respectively, and Al_s and Al_b are the Al concentration in the studied sample and the background respectively. The background values were established from Taylor (1964), Varghese (2004) (Western continental shelf of India) and the average metal levels in the core sediment (54 cm) retrieved from Cape Comorin for a critical evaluation of the geochemical behaviour of trace elements in the upwelling sediments.

EFs calculated were given by EF_c for crust, EF_r for regional and EF_{cs} for core sediment background respectively. C-I_{geo}, R-I_{geo} and CS-I_{geo} represent I_{geo} values for crust, regional and core sediment background respectively.

6.3 Results and Discussion

6.3.1 Background Geochemical Characteristics

6.3.1.1 Hydrographical Conditions

Bottom water temperatures and oxygen concentrations followed a similar trend with increasing depths along the five transects (Table 6.1). Temperatures varied from 28.86°C at 50 m depth to 7.18°C at 1000 m depth offshore. Bottom oxygen concentrations ranged between 0.24 mL L^{-1} and 4.26 mL L^{-1}. The dissolved oxygen was found to be less than 1 mL L^{-1} at greater water depths (Depths ≥ 200 m). Suboxic conditions (2 mL $L^{-1} < O_2 > 0.2$ mL L^{-1}) were observed at stations A4 (0.24 mL L^{-1}), B3 (0.26 mL L^{-1}), C3 (0.37 mL L^{-1}), C4 (0.40 mL L^{-1}), D3 (0.40 mL L^{-1}), D4 (0.78 mL L^{-1}) and A3 (1.56 mL L^{-1}). This observed oxygen content was very much close to anoxic condition during the northeast monsoon. A major factor causing low oxygen in the waters may be the decomposition of organic matter in the water column. Offshore sediments receive higher amounts of biodetritus and thus increase the oxygen consumption, generating suboxic conditions at these sites. On the other hand, the inner shelf stations show well oxygenated conditions.

6.3.1.2 Sediment Texture

The spatial trend of sediment texture (Table 6.1) shows that the sediment consists of sand followed by clay fraction. Sand, silt and clay content ranges from 2.53–96.43% (average 57.72%), 0.44–52.05% (average 15.51%) and 3.13–70.51% (average 26.77%) respectively. Sand particle shows a decreasing trend from inner to the outer shelf at transects A and D while it followed an increasing trend in transects B and E. It decreased from 94.60% (A1) to 10.30% (A5) and 96.43% (D1) to 2.53% (D4) in transects A and D respectively. In transect B, the sand content increases seaward from 38.66–84.62%. Silt content increased towards offshore in transects A, C and D. Station D4 (52.05%) has been recorded maximum silt concentration and minimum at D1 (0.44%). The silt content varies from 0.58–44.10%, 0.68–24.40% and 0.44–52.05% in transects A, C and D respectively. Clay fraction exhibits increasing trend towards offshore at transects A and D whereas decreasing trend at transects B and E respectively. Maximum clay content is observed at C1 (70.51%) and lower at D1 (3.13%). The spatial trend of sediment texture reveals that the outer shelf and slope are composed of clayey silt and sandy on the inner coastal shelf. The weak surface currents compared to southwest monsoon period may intensify the accumulation of fine grained sediments in the outer shelf region.

6.3.1.3 Elemental Compositions

The composition of carbon, nitrogen and sulphur (Table 6.1) followed the order: C > N > S. Total carbon (TC) varies from 0.69% to 13.59%. Distribution of total organic carbon (TOC) content averages 3.25% in the surface sediments. It ranged between 0.16% (A1) and 9.34% (D3). The offshore stations recorded higher values of TOC. Low levels of TOC may be due to reduced preservation in oxygen rich bottom waters. Contrastingly, high organic carbon values at station D1 may be due to the input of terrigenous materials including urban effluents. $CaCO_3$ content varied from 1.10% to 74.68%. It averaged 30.62% and a significant amount of $CaCO_3$ content was observed at E1 and E2 (Cape). $CaCO_3$ is a major component of particulate matter in the Arabian Sea and finally, gets deposited to the Sea surface. High $CaCO_3$ levels are mainly derived from the deposition of biogenic calcareous shells and the skeletal remains of benthic organisms. Higher $CaCO_3$ concentration (> 30%) in the outer shelf sediments exclusively indicate pelagic carbonates with a lesser dilution of the terrigenous matter. TN% ranges from 0.03% to 1.64%. TOC/TN differs from 5.28 to 13.37. TOC/TN ratio also showed that terrestrial inputs are not pronounced with increasing water depths. It indicates that the sediments are derived from vertical settling through the overlying water column rather than lateral advection of terrigenous matter. Significant correlation between TOC and TN (Fig. 6.1) confirmed the dominance of marine-derived organic matter. This is because the coast and shelf are major upwelling regions with high biological productivity and biogenic matter supply which suppress and dilute the terrigenous organic particles supplied from the adjacent landmasses.

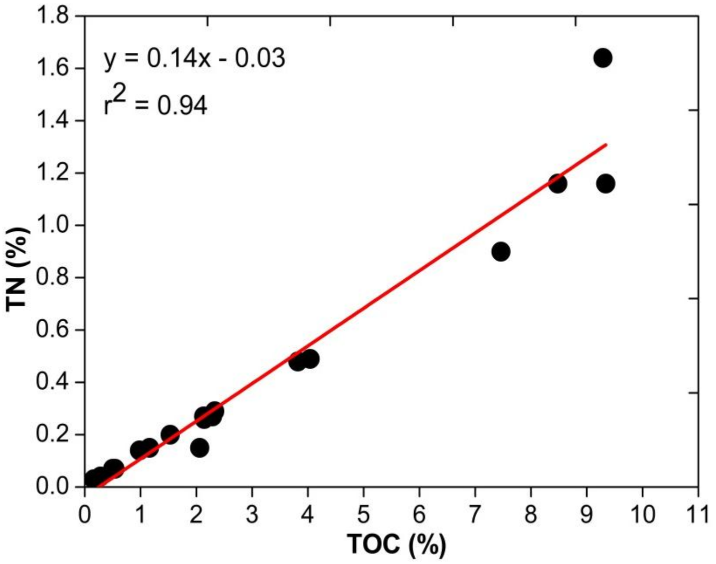

Fig. 6.1 Scatter plot of TOC vs. TN.

Total sulphur percentage recorded low concentrations ranging from 0.02% to 2.82% with an average of 1.03%. The TOC/TS ratio ranges from 1.09 to 60.56 with an average of 10.65 (Table 6.1). TOC/TS ratio is utilized to characterize oxic and anoxic conditions prevailing in the sediments and this ratio lower than 2.8 are generally indicative of sediments likely to be anoxic (Berner, 1989). The TOC/TS ratio indicates anoxic condition in the sediments of sites A4 and C3.

Table 6.1: Hydrographical parameters, texture and elemental composition and their ratios in the study region

Stations	Depth	Bottom Temperature	Bottom O_2	Sand	Silt	Clay	Texture	TC	TOC	$CaCO_3$	TN	TS	TOC/TN	TOC/TS
	m	°C	$mL\,L^{-1}$	%				%						
A1	30	28.71	3.94	94.60	0.58	4.82	Sand	0.69	0.16	4.40	0.03	**BDL	5.28	-
A2	50	28.86	3.18	91.15	2.73	6.12	Sand	2.46	0.54	15.97	0.07	0.02	7.49	33.47
A3	104	23.91	1.56	74.68	10.04	15.27	Sand-silt-clay	8.14	2.13	50.08	0.27	0.44	8.02	4.81
A4	202	13.14	0.24	54.82	12.13	33.05	Clayey sand	7.83	2.06	48.08	0.15	1.81	13.37	1.14
A5	500	*NA	NA	10.30	44.11	45.59	Silty clay	9.77	8.48	10.75	1.16	2.16	7.31	3.92
B1	30	28.50	3.89	38.66	22.53	38.81	Sand-silt-clay	2.42	2.29	1.10	0.27	0.20	8.43	11.51
B2	53	28.77	3.28	81.20	2.20	16.60	Sand	3.37	1.16	18.40	0.15	BDL	7.80	-
B3	215	13.74	0.26	84.62	4.49	10.89	Sand	6.32	0.50	48.50	0.07	0.06	6.79	7.80
C1	30	28.51	3.73	28.81	0.68	70.51	Sandy clay	2.92	2.14	6.52	0.26	0.47	8.14	4.56
C2	50	28.76	3.53	91.28	2.51	6.21	Sand	1.67	0.28	11.61	0.04	0.02	6.50	13.93
C3	300	12.10	0.37	47.24	21.45	31.32	Sand-silt-clay	6.93	2.33	38.32	0.29	2.13	8.00	1.09
C4	400	11.04	0.40	36.16	24.40	39.44	Sand-silt-clay	8.51	4.04	37.22	0.49	1.08	8.16	3.75
D1	30	28.55	4.12	96.43	0.44	3.13	Sand	10.75	7.46	27.35	0.90	1.82	8.33	4.10
D2	100	25.49	2.27	45.93	23.23	30.84	Clayey sand	10.37	3.82	54.58	0.48	0.77	7.94	4.97
D3	490	10.45	0.40	27.32	32.34	40.33	Silty clay	9.76	9.34	3.52	1.16	2.50	8.04	3.73
D4	1000	7.18	0.78	2.53	52.05	45.42	Clayey silt	13.59	9.29	35.82	1.64	2.82	5.66	3.30
E1	30	27.57	4.26	55.24	15.31	29.44	Clayey sand	9.24	1.53	64.25	0.20	0.20	7.55	7.77
E2	50	28.60	3.93	77.99	7.95	14.06	Sand	9.94	0.98	74.68	0.14	0.02	7.03	60.56
Min		7.18	0.24	2.53	0.44	3.13		0.69	0.16	1.10	0.03	0.02	5.28	1.09
Max		28.86	4.26	96.43	52.05	70.51		13.59	9.34	74.68	1.64	2.82	13.37	60.56
Avg		21.99	2.36	57.72	15.51	26.77		6.93	3.25	30.62	0.43	1.03	7.77	10.65

*NA: not available, **BDL: below detectable level

6.3.1.4 Phytopigment Based Proxies

Chl-a in the sediments has been widely used as productivity related indicator in estuarine and shallow coastal systems (Dell'Anno et al., 2002). Chl-a and Carot are well known as biogeochemical fossils and appear to be universally present in fresh, marine and estuarine sediments. Further, the pigments in the sediment are directly related to aquatic productivity. Generally, the surface sediment layers sustain all of the recently suspended particles that are deposited from the water column. The variation of pigments in the shallow region indicates the input of nutrient rich sewage effluents and agricultural wash loads from the surrounding urban settlements. In the present study, Chl-a concentration significantly varied in the range 0.87 mg kg^{-1} to 67.84 mg kg^{-1} along the sediments and was found maximum at A5 (Table 6.2). Chl-b and Chl-c recorded a less pronounced variation of 0.35–5.94 mg kg^{-1} and 0.43–11.74 mg kg^{-1} respectively. Carotenoids varied between 0.84 mg kg^{-1} and 76.41 mg kg^{-1} with an average of 15.82 mg kg^{-1}. Phaeo pigments are decomposition products of chlorophyll, varied between 0.95 mg kg^{-1} and 101.07 mg kg^{-1}. Several authors have suggested that the deposition trend of organic matter in the depth profile is affected by productivity, rainfall, industrial waste and other non-point sources of nutrient inputs (Galois et al., 2000; Moreno and Niell, 2004). In addition, the texture of the sediments influenced by hydrodynamic processes played an important role in preserving the pigments. Chlorophyll degradation products such as Phaeo found to be dominated due to high microbial mineralization rate of organic matter and reveal the effective formation of detrital chlorophyll in the productive shelf region.

Table 6.2: Phytopigments (Chl-a, Chl-b, Chl-c, Carot and Phaeo) and their ratios in the surface sediments.

Stations	Chl-a	Chl-b	Chl-c	Carot	Phaeo	Chl-a/Chl-b	Chl-a/Chl-c	Chl-a/Carot	Chl-a/Phaeo
	mg kg^{-1}								
A1	2.40	0.75	1.07	2.58	3.53	3.19	2.23	0.93	0.68
A2	7.56	1.75	2.47	8.46	11.92	4.33	3.06	0.89	0.63
A3	8.14	1.34	1.91	8.97	13.49	6.05	4.25	0.91	0.60
A4	2.93	0.49	0.71	3.08	4.69	5.97	4.13	0.95	0.62
A5	67.84	5.94	11.14	76.41	101.07	11.43	6.09	0.89	0.67
B1	15.53	2.61	3.82	16.80	24.67	5.95	4.07	0.92	0.63
B2	11.21	2.78	3.87	12.40	17.12	4.04	2.90	0.90	0.65
B3	2.03	0.45	0.69	2.19	3.13	4.54	2.94	0.93	0.65
C1	14.88	2.55	2.99	13.33	22.04	5.84	4.98	1.12	0.68
C2	4.37	1.00	1.52	4.82	6.68	4.38	2.88	0.91	0.65
C3	12.67	1.75	2.85	13.22	20.34	7.23	4.45	0.96	0.62
C4	8.04	1.48	1.89	8.37	12.90	5.44	4.24	0.96	0.62
D1	0.87	0.35	0.43	0.84	0.95	2.49	2.02	1.04	0.92
D2	8.30	1.44	2.19	9.11	13.11	5.76	3.78	0.91	0.63
D3	31.16	4.63	7.57	33.57	47.52	6.73	4.11	0.93	0.66
D4	61.92	5.45	11.74	58.69	92.82	11.37	5.27	1.05	0.67
E1	5.24	1.27	1.69	6.52	7.61	4.13	3.11	0.80	0.69
E2	4.64	0.99	1.38	5.36	6.16	4.67	3.36	0.87	0.75
Min	0.87	0.35	0.43	0.84	0.95	2.49	2.02	0.80	0.60
Max	67.84	5.94	11.74	76.41	101.07	11.43	6.09	1.12	0.92
Avg	14.98	2.06	3.33	15.82	22.76	5.75	3.77	0.94	0.67

The degree of organic matter degradation is evaluated using different pigment ratio proxies as shown in Table 6.2. The ratios of Chl-a/Chl-b and Chl-a/Chl-c ranged between 2.49–11.43 and 2.02–6.09 respectively. High ratios of phytopigments suggest the productive nature of the region. The higher values confirm the major source of organic matter as autochthonous and the minor influence of terrestrial organic matter. The land runoff to the coastal environment cannot be discarded completely in the light of sedimentary indicators but should be realized that the influence of allochthonous fraction is suppressed by the surface productivity in the Arabian Sea.

Chl-a/Carot ratio varied between 0.80 and 1.12. It averaged 0.94, showing less significant variation. The ratio can be used as an index to the quality of organic matter preservation and for the assessment of relative input of terrestrially derived organic matter. It implies the general behaviour of processes altering the accumulation and preservation of organic matter in the sediments. Furthermore, low values are indicative of better preservation of settling biogenic matter and less contribution of terrestrial derived organic matter to the sedimentary pool. The present study pointed out that the state of high surface production is reflected in the observed Chl-a/Carot ratio and the preservation enhanced by silty clay or clayey silt fractions in the sediments. The factor of degradation and preservation should be compared as a co-varying process and play their roles in the fate of organic matter. The terrestrially derived matter may be less significant considering the productivity in the coastal region of Southeastern Arabian Sea.

Chl-a/Phaeo ratio varied between 0.60 and 0.92. The ratio averaged 0.67, showing less significant variation. Phaeo pigments can reflect the “status” of the algae in the sediments, that is, a high Chl-a/Phaeo ratio means that the algae is in a good physiological state at the sampling time. This ratio has also been used as an indicator of phytoplankton growth, cellular senescence and zooplankton grazing. Chl-a/Phaeo ratio around 2 for freshly deposited chlorophylls and 1.0 for chemically degraded refractory organic matter (Venturini et al., 2012). Chl-a/Phaeo ratios < 1 were obtained at the sampling stations indicate the prevalence of unreactive detritus in primary material in the sediments and might come under the influence of biological activity which brought about the conversion of chlorophyll to phaeo pigments. Comparison of the pigment ratio and relative amount of chlorophyll and degradation products showed that the sediments generally contained more phaeo pigments than chlorophyll. According to Dell'Anno et al. (2002), the predominance of phaeo pigments may be attributed to high turbidity, chemical contamination or other factors affecting photosynthetic potential of primary producers.

6.3.1.5 Benthic Trophic Status Classification

Main constituents of organic matter and their trophic status classification in the sediments are presented in Table 6.3. CHO was found to be the most abundant biochemical component of organic matter (4.80–45.30 mg g^{-1}) followed by PRT (0.66–5.40 mg g^{-1}) and LIP (0.01–0.30 mg g^{-1}). The significant correlation observed for PRT with TOC and TN ($r^2 = 0.81$ and 0.84 respectively) confirms that PRT is adsorbed onto organic matter settling down the water column and thereafter the mineralization of labile organic matter. Based on total carbohydrate (CHO) concentrations, the majority of stations were categorized as hypertrophic, whereas the protein (PRT) content showed a different trend consisting of hypertrophic, eutrophic and meso-oligotrophic conditions in the sampling stations. The PRT/CHO ratio has been utilized to determine the age of sedimentary organic matter as suggested by Dell'Anno et al. (2002). PRT/CHO varied between 0.07 and 0.24 with an average of 0.15. The CHO concentration was always greater than PRT and the PRT/CHO ratio varied between 0.07 and 0.24 with less significant variation infers the presence of refractory (less labile) organic matter in the sediments (Grémare et al., 2003). The PRT/CHO ratio indicated meso-oligotrophic conditions in all the stations. On contrary, the BPC and CChl-a% concentration showed eutrophic conditions in most of the sampling stations.

Table 6.3: Bulk sedimentary organic matter composition, PRT/CHO, BPC, algal contribution to BPC (CChl-a) and the evaluation of trophic status (TS) in sediments. H: hypertrophic; E: eutrophic; MO: meso-oligotrophic; M: mesotrophic; O: oligotrophic.

Stations	CHO	TS	PRT	TS	PRT/CHO	TS	BPC	TS	CChl-a	TS	LIP
	mg g^{-1}		mg g^{-1}				mg C g^{-1}		%		mg g^{-1}
A1	4.80	MO	1.04	MO	0.22	MO	2.47	M	3.88	E	0.06
A2	8.32	H	2.01	E	0.24	MO	4.37	E	6.93	E	0.07
A3	12.92	H	1.73	E	0.13	MO	6.03	E	5.39	E	0.02
A4	9.75	H	0.92	MO	0.09	MO	4.36	E	2.69	E	0.02
A5	45.30	H	5.40	H	0.12	MO	20.94	E	12.96	M	0.23
B1	16.68	H	2.47	E	0.15	MO	7.91	E	7.85	E	0.05
B2	13.29	H	2.01	E	0.15	MO	6.33	E	7.08	E	0.04
B3	7.95	H	0.66	MO	0.08	MO	3.56	E	2.29	E	0.07
C1	14.73	H	1.83	E	0.12	MO	6.81	E	8.74	E	0.02
C2	6.62	E	1.19	MO	0.18	MO	3.29	E	5.32	E	0.08
C3	18.13	H	1.71	E	0.09	MO	8.12	E	6.24	E	0.03
C4	21.92	H	1.46	MO	0.07	MO	9.50	E	3.38	E	0.02
D1	21.41	H	2.94	E	0.14	MO	10.06	E	0.35	E	0.08
D2	8.22	H	1.17	MO	0.14	MO	3.86	E	8.60	E	0.01
D3	17.50	H	2.80	E	0.16	MO	8.43	E	14.78	M	0.08
D4	39.60	H	4.63	H	0.12	MO	18.33	E	13.51	M	0.30
E1	5.20	E	1.03	MO	0.20	MO	2.62	M	7.99	E	0.05
E2	5.96	E	1.26	MO	0.21	MO	3.06	E	6.07	E	0.07
Min	4.80		0.66		0.07		2.47		0.35		0.01
Max	45.30		5.40		0.24		20.94		14.78		0.30
Avg	15.46		2.01		0.15		7.23		6.89		0.07

6.3.2 Geochemistry of Metal Enrichment in the Shelf and Slope

The distribution of major and trace metals from five transects in the shelf sediments of Arabian Sea are shown in Table 6.4. The concentration of major elements in the sediments followed the order: Ca > Fe > Al > Mg. The mean concentrations of Ca, Fe, Al and Mg were found to be 7.85%, 1.67%, 1.34% and 0.78% respectively. Sedimentary Ca ranged from 1.29% (C1) to 23.27% (A4), Fe concentration varied between 0.11% (D2) and 5.48% (A4), Al in the sediment samples varied from 0.07% (D2) to 4.67% (A5) and Mg concentration from 0.11% (C1) to 3.08% (A4). Transect A (Cochin) recorded highest values for the major elements and the average concentrations of Ca, Al, Fe and Mg were 11.73%, 2.26%, 2.22% and 1.27% respectively. Overall, the station A4 (Transect A) showed the maximum concentration and C4 (Transect C) recorded minimum value for major elements in the study. Mg is a major constituent of clay minerals and absorption of Mg ions from seawater enriches its concentration in the sediments. Comparing the Mg levels, high values were encountered at sites bearing greater carbonate contents. It gives the implication of a considerable amount of biogenic material in the outer shelf sediments (Limmer et al., 2012). Correlation coefficients between major and trace metals, elemental compositions and texture in the Arabian Sea sediments is shown in Table 6.5. Mg shows positive association with Ca and Fe which suggests that scavenging and absorption take place in the sediments as a result Mg-rich calcite is formed. Ca shows moderate correlation with $CaCO_3$ (r^2 = 0.55) describes that the element is almost present as biogenic $CaCO_3$. The poor correlation of metals with $CaCO_3$ indicates that the carbonate is not a carrier phase in the accumulation of trace elements. The insignificance of $CaCO_3$ as a carrier phase may be due to the fact that hydrous Fe oxides and organic matter are abundant to form highly stable metal complexes rather than coprecipitation with carbonates (Li et al., 2000). Al concentration and $CaCO_3$ was negatively correlated implies the dilution of biogenic carbonates by aluminosilicate fragment in the sediments (Nameroff et al., 2004). High Ca content indicates the dominance of calcareous marine planktons in the overlying water column as a result of productivity in the region.

Table 6.4: Variation of major and trace element concentrations, crustal, regional and core sediment background values in sediments.

Stations	Al	Ca	Fe	Mg	Cd	Co	Cr	Cu	Mn	Ni	Pb	Zn
	%				mg kg^{-1}							
A1	1.80	2.35	0.76	0.19	*BDL	5.29	30.64	1.59	165.64	88.72	14.97	12.91
A2	1.61	4.25	1.04	0.51	0.12	7.14	54.84	8.19	184.86	96.13	11.32	20.50
A3	1.64	18.62	1.15	1.34	0.17	3.18	63.61	9.84	105.29	99.70	2.14	22.00
A4	1.56	23.27	5.48	3.08	0.41	4.34	119.23	10.97	128.93	90.67	6.71	34.29
A5	4.67	10.16	2.68	1.25	0.38	8.61	154.10	40.16	98.72	97.84	4.83	54.05
B1	3.90	2.43	2.65	0.76	0.16	8.43	138.05	12.47	136.33	86.17	21.51	36.12
B2	2.19	7.64	1.87	0.86	0.22	5.99	80.32	5.85	99.37	95.45	25.95	19.91
B3	0.67	6.86	3.36	1.64	0.53	11.56	84.51	3.20	206.23	91.25	19.56	25.49
C1	0.93	1.29	1.28	0.11	BDL	4.98	51.43	1.99	77.94	113.09	10.98	19.12
C2	0.53	1.69	0.47	0.16	BDL	2.65	41.78	0.38	34.62	91.07	5.78	7.62
C3	0.79	5.60	3.54	0.65	0.23	1.33	165.46	13.18	18.92	82.20	17.16	44.99
C4	1.24	6.19	2.63	0.31	0.32	2.41	161.80	17.06	54.53	95.01	23.40	29.14
D1	0.93	15.26	1.49	0.77	0.47	2.10	114.32	11.59	20.31	85.83	0.31	23.43
D2	0.07	2.52	0.11	0.23	0.06	0.44	6.85	0.27	7.45	102.55	BDL	28.64
D3	0.25	3.11	0.46	0.14	0.19	0.84	41.98	4.14	4.89	112.20	0.53	31.76
D4	0.70	4.60	0.45	0.12	0.24	2.82	44.42	14.95	22.00	112.39	BDL	39.19
E1	0.27	11.83	0.24	1.01	0.04	1.43	20.46	1.32	36.06	71.88	2.71	7.45
E2	0.32	13.60	0.35	0.97	0.06	1.96	23.42	0.55	49.70	94.91	4.48	13.29
Min	0.07	1.29	0.11	0.11	0.04	0.44	6.85	0.27	4.89	71.88	0.31	7.45
Max	4.67	23.27	5.48	3.08	0.53	11.56	165.46	40.16	206.23	113.09	25.95	54.05
Avg	1.34	7.85	1.67	0.78	0.24	4.20	77.62	8.76	80.65	94.84	10.77	26.11
Crustal	8.23	4.15	5.63	2.33	0.20	25	100	55	950	75	12.50	70
Regional	7.14	-	5.08	-	-	10.38	99.59	29.3	430	45.4	11.81	68.67
Core sediment	0.06	-	0.25	0.37	BDL	0.19	4.17	4.29	25.52	0.62	1.76	7.16

*BDL: below detectable level

Table 6.5: Pearson's correlation coefficient for major and trace metals, elemental compositions and texture in the Arabian Sea sediments.

	Cd	Co	Cr	Cu	Mn	Ni	Pb	Zn	Al	Ca	Fe	Mg	TOC	CaCO$_3$	TN	TS	Sand	Silt	Clay
Cd	1																		
Co	0.46	1																	
Cr	*0.59*	0.30	1																
Cu	0.42	0.30	**0.72**	1															
Mn	0.31	**0.85**	0.12	0.04	1														
Ni	−0.03	−0.05	−0.26	0.04	−0.15	1													
Pb	0.12	0.46	0.40	0.01	0.42	−0.11	1												
Zn	0.39	0.19	**0.67**	**0.79**	−0.07	0.23	0.14	1											
Al	0.21	**0.63**	*0.56*	**0.72**	0.46	−0.09	0.26	*0.49*	1										
Ca	0.27	−0.09	0.20	0.20	0.06	−0.29	−0.43	0.03	0.05	1									
Fe	**0.66**	0.43	**0.78**	0.43	0.40	−0.27	0.38	*0.52*	0.40	0.40	1								
Mg	0.44	0.32	0.32	0.21	0.41	−0.34	−0.12	0.19	0.23	**0.81**	**0.72**	1							
TOC	0.23	−0.24	0.19	*0.55*	*−0.51*	0.46	−0.41	**0.61**	0.10	0.01	−0.10	−0.19	1						
CaCO$_3$	−0.20	−0.34	−0.20	−0.22	−0.20	−0.27	−0.20	−0.17	*−0.48*	*0.55*	0.01	0.41	−0.18	1					
TN	0.18	−0.21	0.12	*0.53*	*−0.49*	*0.49*	−0.40	**0.59**	0.08	−0.05	−0.17	−0.25	**0.97**	−0.16	1				
TS	0.34	−0.28	0.35	*0.53*	−0.45	0.31	−0.23	**0.72**	0.08	0.10	0.21	−0.01	**0.84**	−0.20	**0.82**	1			
Sand	0.07	0.11	−0.24	*−0.51*	0.37	−0.46	−0.00	**−0.68**	−0.21	0.18	−0.09	0.13	**−0.65**	0.112	**−0.67**	*−0.60*	1		
Silt	−0.05	−0.13	0.22	**0.61**	−0.38	0.33	−0.09	**0.73**	0.22	−0.11	0.00	−0.11	**0.75**	−0.01	**0.80**	**0.69**	**−0.86**	1	
Clay	−0.08	−0.06	0.20	0.32	−0.28	*0.47*	0.06	*0.49*	0.15	−0.20	0.14	−0.11	0.42	−0.17	0.42	0.37	**−0.90**	*0.56*	1

Note: Correlations significant at 0.01 and 0.05 levels are shown in bold and italics respectively.

Table 6.6: Range of EF and I_{geo} calculated for crustal, regional and core sediment background respectively in the studied samples.

Indices	Fe	Mg	Cd	Co	Cr	Cu	Mn	Ni	Pb	Zn
EF										
EF_c	0.61–7.29	0.37–13.05	1.63–38.25	0.55–5.65	1.40–17.15	0.11–3.20	0.17–2.65	2.30–170	0.22–19.13	0.84–50.87
EF_r	0.59–7.01	-	-	1.15–11.81	1.22–14.94	0.18–5.22	0.32–5.08	3.29–243.64	0.20–17.56	0.74–44.99
EF_{cs}	0.10–1.20	0.02–0.60	-	0.53–5.42	0.24–3.00	0.01–0.30	0.05–0.72	2.03–149.92	0.01–0.99	0.06–3.63
I_{geo}										
C-I_{geo}	−6.29–−0.62	−4.99–−0.18	−2.80–0.82	−6.41–−1.70	−4.45–0.14	−8.27–−1.04	−8.19–−2.79	−0.65–0.01	−5.92–0.47	−3.82–−0.96
R-I_{geo}	−6.15–−0.48	-	-	−5.14–−0.43	−4.45–0.15	−7.36–−0.13	−7.04–−1.65	0.08–0.73	−5.84–0.55	−3.79–−0.93
CS-I_{geo}	−1.80–3.87	−2.33–2.47	-	0.63–5.34	0.13–4.73	−4.59–2.64	−2.97–2.43	6.27–6.93	−3.09–3.30	−0.53–−2.33

The range of EF and I_{geo} calculated for crustal, regional and core sediment background respectively for metals in the studied samples are given in Table 6.6. The respective values of these indices are presented in Table A1.1 and Table A1.2 (Appendix I). EF_c and EF_r values of Fe and Mg displayed moderately severe enrichment at A4, C3 (not for Mg) and B3 (Fig. 6.2). The EF_c value unveils severe enrichment of Mg at E2, D2 and E1. The EF_{cs} of Mg averaged 0.18 and possess negligible enrichment. Fe shows negative I_{geo} values (Class I) indicating a negligible level of pollution with respect to C-I_{geo} and R-I_{geo} in the study region. CS-I_{geo} of Fe varied from −1.80 to 3.87. Fe is strongly polluted at stations B3, C3 and A4 and moderately to strongly polluted at B2, C4, B1 and A5. According to CS-I_{geo}, Mg is moderately to strongly polluted at A4 (2.47). A very similar paradigm of enrichment was obtained for EF and I_{geo} values calculated for Fe and Mg. Fe concentration was slightly higher at deeper depths (A4, B3 and C3) whereas Al concentration did not vary significantly at different depths. The intense chemical weathering in the precambrian rocks and laterites rich in iron oxide content and the predominance of authigenic Fe-rich clays (Kumar, 2005) may initiate the present enrichment of Fe at the above sites, due to the significant spatial variation and the enrichment shown by Fe associated trace elements in the study.

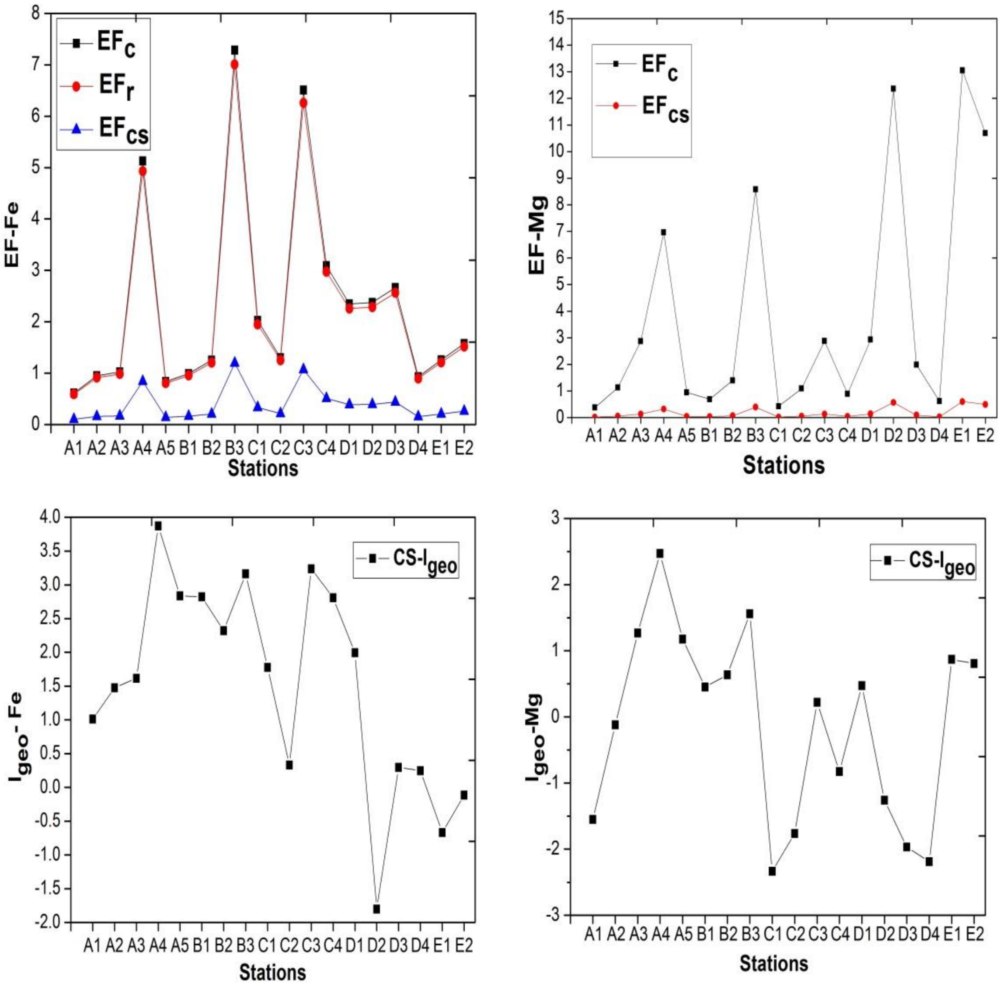

Fig. 6.2 Enrichment factors and geoaccumulation index calculated for Fe and Mg.

6.3.2.1 Cadmium

Cd concentration averaged 0.24 mg kg^{-1} showing minimum at E1 (0.04 mg kg^{-1}) and maximum at B3 (0.53 mg kg^{-1}). The Cd level in the outer shelf sediments shows high values except at D4 (0.24 mg kg^{-1}; Table 6.4). Cd shows moderate enrichment with EF_c values 3.20 at A2, 3.36 at A5, 4.12 at B2 and 4.24 at A3 (Fig. 6.3). Moderately severe enrichment of Cd was observed at E1 (6.47) and E2 (7.30) whereas, severe enrichment at A4, C4, C3, D4 and

D1 ranging between 10.69 and 20.88. Stations D3, B3 and D2 exhibit very severe enrichment of Cd with EF_c values 31.06, 32.34 and 38.25 respectively. Since the regional background of Cd was not available, EF_r and EF_{cs} cannot be calculated for these metals. C-I_{geo} of Cd varied from −2.80 to 0.82 with an average of −0.67. The sites C4, A5, A4, B3 and D1 were unpolluted to moderately polluted with respect to Cd.

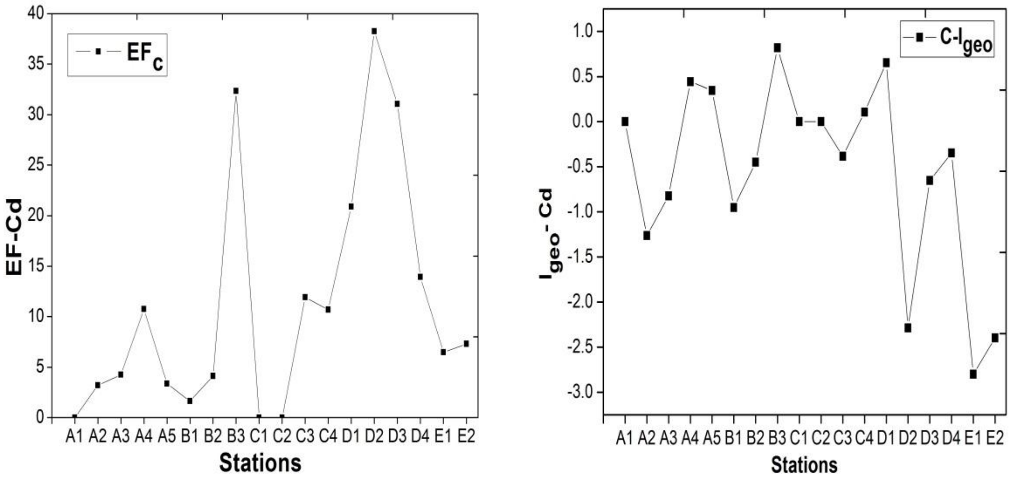

Fig. 6.3 Enrichment factor and geoaccumulation index calculated for Cd.

Cd showing high values above the crustal average in deep sediment samples is not representative of anthropogenic activities, but significantly contributed by upwelling phenomenon and subsequently preserved in the sedimentary environment. Cd enrichment towards the offshore cannot be ascribed to anthropogenic contamination from land. Apart from human activities, Cd in this type of marine environments could be possibly derived from high biological productivity associated with upwelling or precipitation as Cd sulphides during complexation with sulphur compounds (Collier and Edmond, 1984; Rosenthal et al., 1995; Cheriyan et al., 2015). At present, the lack of significant correlation between Cd, and TOC, TS and carbonates suggests the fluctuating influx of Cd through biogenic detritus. However, the abundant Fe oxyhydroxides in the water column preferably scavenge Cd to its surface and sink to the bottom sediments. Furthermore, the Cd levels markedly for the offshore sites would reflect the retainment of the metal in the sedimentary material effected sufficiently through biological productivity coupled with the formation of inorganic complexes.

6.3.2.2 Chromium

The concentration of Cr varied between 6.85 mg kg^{-1} (D2) and 165.46 mg kg^{-1} (C3). It averaged about 77.62 mg kg^{-1} with higher values than crustal background (100 mg kg^{-1}) at C3 (165.46 mg kg^{-1}), C4 (161.80 mg kg^{-1}), A5 (154.10 mg kg^{-1}), B1 (138.05 mg kg^{-1}), A4 (119.23 mg kg^{-1}) and D1 (114.32 mg kg^{-1}). Cr shows significant correlation with Al suggesting that the lithic and non-lithic fractions of these elements may be strongly bound to the fine grained aluminosilicate minerals. Cr was found to be high in clayey and silty regions and likely, the significant association of Cr with Al indicates that the element is exchanged with Al in clastic clays. Besides, Cr was depleted in nearshore regions mainly composed of sand sized particles.

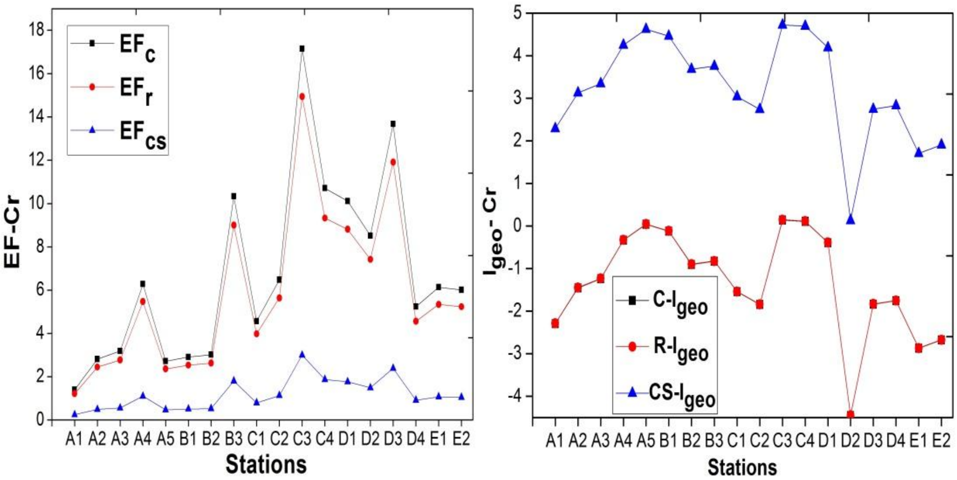

Fig. 6.4 Enrichment factor and geoaccumulation index calculated for Cr.

According to crustal background, Cr shows severe enrichment at D1, B3, C4, D3 and C3 (10.11–17.15) whereas moderately severe enrichment was observed at D4, E2, E1, A4, C2 and D2 (5.24–8.52). Moderate enrichment of Cr was recorded with EF values ranged between 2.71 and 4.56 at stations A5, A2, B1, B2, A3 and C1. Cr-EF_r shows severe enrichment at D3 (11.91) and C3 (14.94) and moderately severe enrichment was observed at E2, E1, A4, C2, D2, D1, B3 and C4 (5.23–9.33). Moderate enrichment of Cr was recorded with EF values ranged between 2.36 and 4.56 at A5, A2, B1, B2, A3, C1 and D4. EF_{cs} value of Cr varied between 0.24 and 3.00 reveals moderate enrichment at D3 and C3, and minor enrichment at stations E1, E2, A4, C2, D2, D1, B3 and C4. Cr shows C-I_{geo} values ranging from −4.45 to 0.14 and the metal is unpolluted to moderately polluted at A5, C4 and C3. R-I_{geo} of Cr varied between −4.45 and 0.15. Based on R-I_{geo}, Cr is unpolluted to moderately polluted at stations A5, C4 and C3. CS-I_{geo} values of Cr averaged 3.24 whereas it varied from 0.13 to 4.73 in the surface sediments (Fig. 6.4). CS-I_{geo} value suggests that Cr is strongly to extremely polluted at D1, A4, B1, A5, C4 and C3, strongly polluted at C1, A2, A3, B2 and B3 and moderately to strongly polluted at A1, C2, D3 and D4. Cr may be associated with sand and silt fractions and significant enrichment may be observed in coarse grained sediments (Schnetger et al., 2000). In this study, the Cr enrichment seawards may be attributed to the binding nature of source rocks preferably aluminosilicate minerals.

6.3.2.3 Copper and Zinc

Cu content in the sediments varied from 0.27 mg kg^{-1} to 40.16 mg kg^{-1} displaying less significant enrichment. EF_c value of Cu suggests moderate enrichment at C4, D3, C3 and D4 (2.05–3.20) and minor enrichment at A4, A5 and D1 (1.05–1.86). EF_r of Cu suggests moderately severe enrichment at D4

(5.22) and moderate enrichment at A5, D1, C4, D3 and C3 (Fig. 6.5). The EF_{cs} of Cu averaged 0.10 respectively, and possess negligible enrichment. Cu shows negative I_{geo} values (Class I) indicating a negligible level of pollution with respect to C-I_{geo} and R-I_{geo} of these metals. Considering CS-I_{geo}, Cu is moderately to strongly polluted at A5 (2.64) and moderately polluted at C3 (1.03), D4 (1.22) and C4 (1.41) respectively.

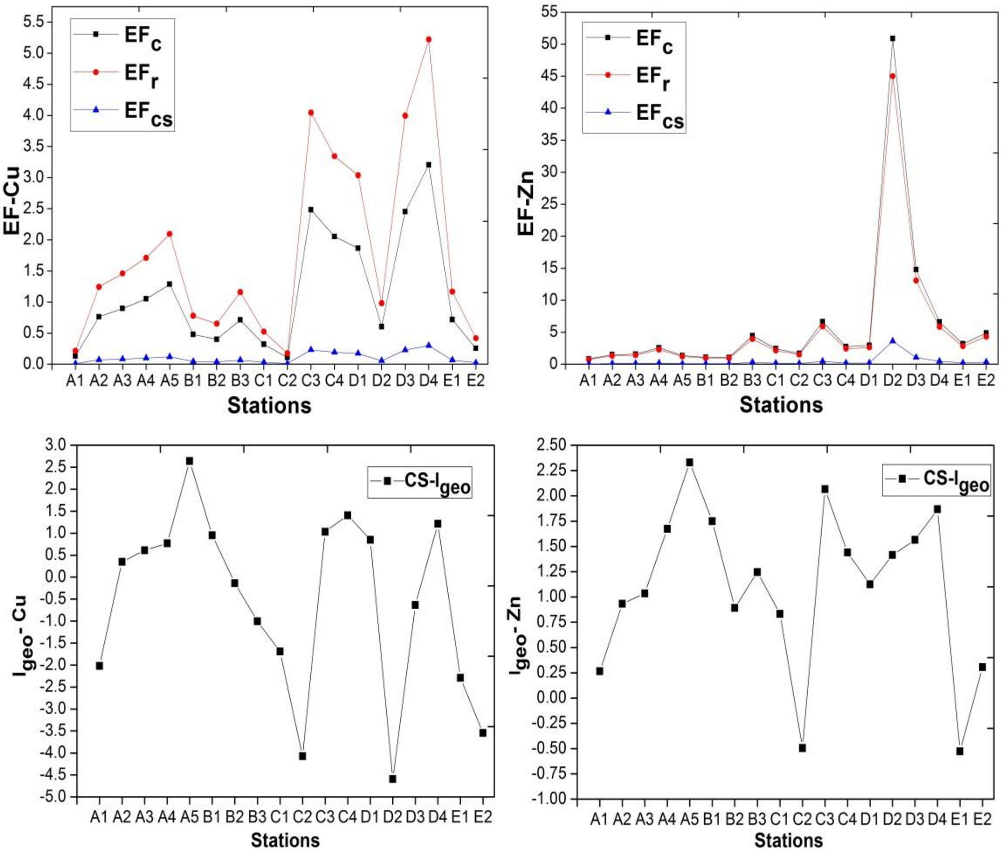

Fig. 6.5 Enrichment factor and geoaccumulation index calculated for Cu and Zn.

Zn averaged 26.11 mg kg^{-1} in the sediments showing very low enrichment in the study region. Zn-EF_c recorded extremely severe enrichment at D2 whereas, very severe enrichment compared to EF_r. EF_c and EF_r of Zn revealed severe enrichment at D3 and moderately severe enrichment at D4 and

C3 (Fig. 6.5). Zn-EF_{cs} exhibits moderate enrichment at D2 and rest of the stations were impoverished with respect to the metal. Zn shows negative I_{geo} values (Class I) indicating a negligible level of pollution with respect to C-I_{geo} and R-I_{geo} of these metals in the study region. CS-I_{geo} of Zn varied from −0.53 to 2.33 with an average of 1.10. Moderate to strong pollution of Zn was recorded at C3 and A5.

Organic matter may affect negatively or positively the metal enrichment as a result of the formation of metal incorporated complexes in productive marine environments (Mellis et al., 2004). Association of organic matter with these metals is through biological uptake and adsorption with subsequent incorporation into refractory organic degradation products, such as humic substances (Panda et al., 2006). Cu shows higher affinity to form complex with organic matter than Fe/Mn oxyhydroxide phases because of the high formation constants of organic-Cu compounds (Stumm and Morgan, 1981; Chakraborty et al., 2015). Cu and Zn act as micronutrients that show a positive association with organic matter and its correlation coefficients has been presented in Table 6.5 and 6.7. Cu and Zn were significantly correlated with organic carbon. Further, Cu and Zn show significant positive correlation with TN, TS, CHO, PRT, Chl-a, Chl-b, Chl-c, Carot, Phaeo and silt, and a significant negative correlation with sand. The significant correlation between Cu and Zn with silt content implies a similar depositional pattern and the significant role of fine grained particles in the preservation of these metals. Positive correlations were observed with different metals such as Cr-Cu, Cu-Zn and Cr-Zn (r^2 = 0.67–0.79). The significant correlation of Cu with Zn (r^2 = 0.79) is primarily due to uptake by marine planktons since these elements behave as micronutrients for their growth (Ergin et al., 1996). Zn correlates with TOC suggest that the element is mainly associated with organic matter (Sreekanth et al., 2015). Zn (r^2 = 0.72) and Cu (r^2 = 0.53) moderately correlated with TS indicate its deposition associated with sulphide phases (Lo Monaco et al., 2002), that the reducing environment along the sediment-water interface can induce their precipitation as sulphides. The association between organic carbon, Cu and Zn may reflect a direct influx of biogenic material enriched in these metals from the upwelled water column.

Table 6.7: Pearson's correlation coefficient for Cu, Ni, Zn, biochemical composition and chlorophyll pigments in Arabian Sea sediments.

	Cu	**Ni**	**Zn**	**CHO**	**PRT**	**LIP**	**Chl-a**	**Chl-b**	**Chl-c**	**Carot**	**Phaeo**
Cu	1										
Ni	0.04	1									
Zn	**0.79**	0.22	1								
CHO	**0.85**	0.36	**0.76**	1							
PRT	**0.76**	0.39	**0.64**	**0.92**	1						
LIP	*0.54*	0.31	0.43	**0.77**	**0.82**	1					
Chl-a	**0.69**	*0.49*	**0.67**	**0.89**	**0.91**	**0.86**	1				
Chl-b	*0.58*	*0.56*	**0.60**	**0.80**	**0.86**	**0.72**	**0.94**	1			
Chl-c	**0.60**	*0.53*	**0.63**	**0.84**	**0.89**	**0.83**	**0.98**	**0.98**	1		
Carot	**0.73**	0.45	**0.68**	**0.88**	**0.91**	**0.83**	**0.99**	**0.94**	**0.97**	1	
Phaeo	**0.70**	*0.49*	**0.68**	**0.89**	**0.90**	**0.85**	**1.00**	**0.95**	**0.98**	**0.99**	1

Note: Correlations significant at 0.01 and 0.05 levels are shown in bold and italics respectively.

6.3.2.4 Manganese and Cobalt

Mn is a redox sensitive element which exhibited low concentration throughout the sampling sites ranging from 4.89 mg kg^{-1} to 206.23 mg kg^{-1}. Mn-EF_c displays minor enrichment at A2, E1 and E2, and moderate enrichment at B3 (2.65). Mn shows moderately severe enrichment at B3 (EF_r =

5.08) and moderate enrichment at E1 and E2 (EF_r = 2.18 and 2.57 respectively; Fig. 6.6). The EF_{cs} of Mn averaged 0.19, and possess negligible enrichment. Mn shows negative I_{geo} values (Class I) indicating a negligible level of pollution with respect to C-I_{geo} and R-I_{geo}. The CS-I_{geo} of Mn averaged 0.46 ranging from −2.97 to 2.43. Sites A1, A2 and B3 show moderate to strong pollution and rest of the stations in Cochin and Alleppey transect show moderate pollution of Mn.

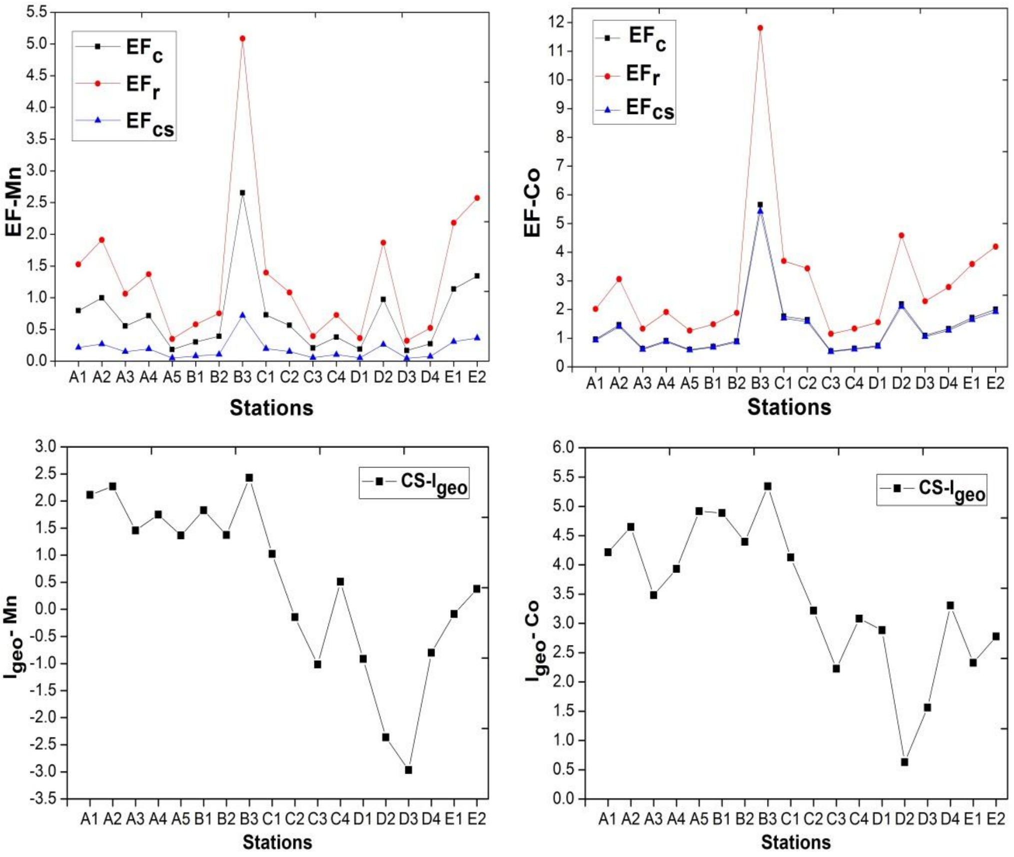

Fig. 6.6 Enrichment factor and geoaccumulation index calculated for Mn and Co.

Co recorded low values below background level ranging from 0.44 mg kg^{-1} to 11.56 mg kg^{-1} with an average of 4.20 mg kg^{-1}. Co-EF_c varied between 0.55 and 5.65 shows moderately severe enrichment at B3. The EF_r

value of Co averaged 2.96 ranging between 1.15 and 11.81. Maximum enrichment was observed at B3. Moderate enrichment of Co ranging from 2.02 to 4.58 was observed at A1, D3, D4, A2, C2, E1, C1, E2 and D2 and the rest of the stations recorded minor enrichment (except B3). Based on EF_{cs}, Co shows moderately severe enrichment at B3 and moderate enrichment at D2. Minor enrichment of Co was observed at D3, D4, A2, C2, E1, C1 and E2. EF of Co showed a significant value at B3 where it is 5.42 for EF_{cs}, 5.65 for EF_c and 11.81 for EF_r (Fig. 6.6). Noteworthy, the EF_c and EF_{cs} of Co also exhibited a similar enrichment sequence and shows extreme value at site B3. Moreover, the Co concentration was slightly enriched compared to other metals at B3 and it can be attributed to geological sources.

Co shows negative I_{geo} values (Class I) indicating a negligible level of pollution with respect to C-I_{geo} and R-I_{geo}. CS-I_{geo} values of Co averaged 3.44 whereas it varied from 0.63 to 5.34 in the surface sediments. Co is extremely polluted at B3 and strongly to extremely polluted at C1, A1, B2, A2, B1 and A5. It is strongly polluted at C4, C2, D4, A3 and A4 and moderately to strongly polluted at C3, E1, E2 and D1.

Mn levels at sites confronting low organic carbon content have to be considered as background Mn below the crustal and regional averages, whereas the overall Mn concentration in the region is affected by the low oxygen content of bottom waters due to remineralization of organic matter rich particles. The Mn concentration was found to decrease with an increase in the organic carbon flux to the sediments. This was confirmed by the inverse correlation of Mn and TOC because the high organic carbon content favours Mn oxide reduction over oxidation and the dissolution of Mn to the overlying water column (Aller, 1994). The positive correlation of Co with Mn shows their similar behaviour of mobilization effected by the scavenging of Mn oxyhydroxides. Concurrently, Mn and Co show low enrichment caused by the remobilization of these metals while sinking through a suboxic water column (Böning et al., 2004). Co scavenged onto Mn oxyhydroxides is also remobilized during the vertical transport and shows minor enrichment except at B3. Co shows significant correlation with Al suggesting that the fractions of these elements may be strongly bound to fine grained aluminosilicate minerals.

6.3.2.5 Nickel

In the study, Ni shows significant enrichment than that of background values for which maximum concentration was observed at C1 (113.09 mg kg^{-1}) and minimum at E1 (71.88 mg kg^{-1}). Ni-EF$_c$ and Ni-EF$_r$ values ranged from 2.30 to 170 and 3.29 to 243.64 respectively. Ni-EF$_{cs}$ values ranged from 2.03 to 149.92 with an average of 20.04. Comparing the three background references, extremely severe enrichment of Ni was observed at D2. EF$_c$ and EF$_{cs}$ displayed a very severe enrichment of Ni at D3, E1 and E2, and severe enrichment at B3, C1, C2, C3 and D4. Ni-EF$_r$ recorded extremely severe enrichment at D3 and very severe enrichment at C2, D4, E1 and E2. In transect A, EF$_c$ and EF$_r$ show moderately severe enrichment of Ni whereas moderate enrichment at A5. Based on C-I$_{geo}$, Ni is unpolluted except at C1 (0.01). R-I$_{geo}$ values of Ni in the entire sampling site falls in class II, from 0.08 to 0.73 with an average of 0.47. The CS-I$_{geo}$ values of Ni lies in class VII (I$_{geo}$ > 5) indicating that the metal is extremely polluted in the study area.

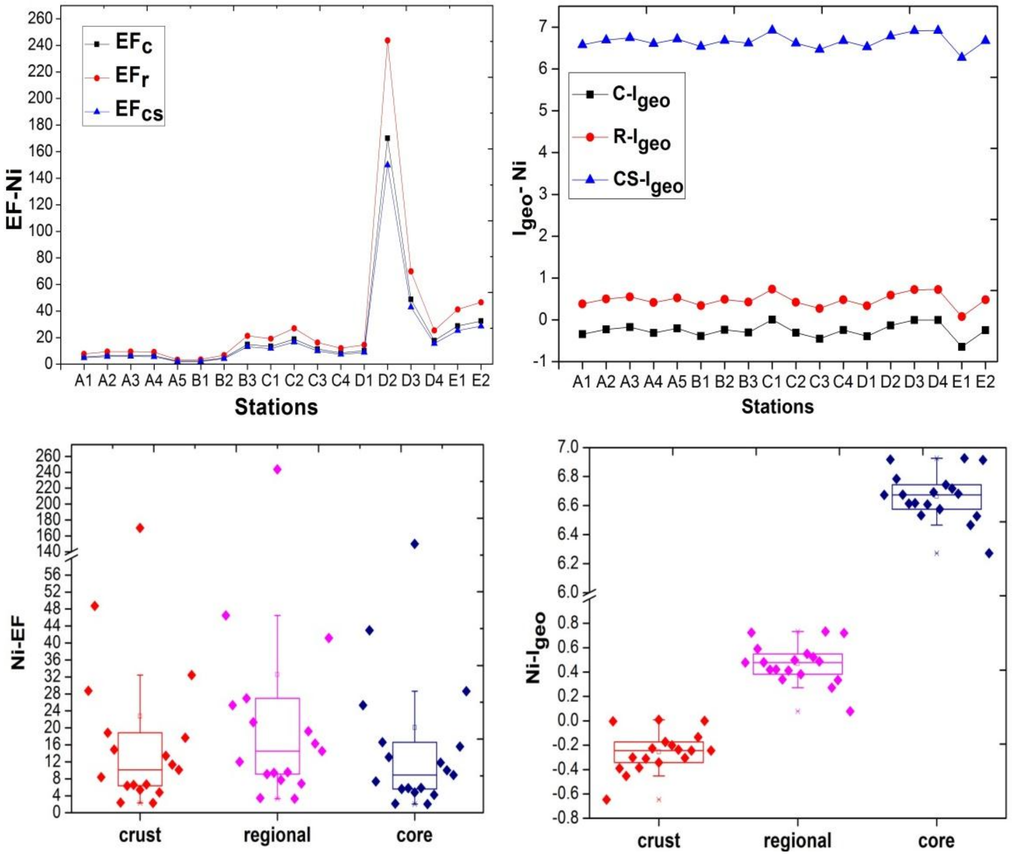

Fig. 6.7 Enrichment factor and geoaccumulation index calculated for Ni and their representation in box whisker plots.

Ni shows a very similar range of variation for the EF and I_{geo} indices compared to other metals (Fig. 6.7). In comparison, with Cu and Zn, Ni generated a partial correlation with chlorophyll pigments and total nitrogen. Hence, the overall metal enrichment mainly Ni at site D2 can be explained by the occurrence of marine algae mainly diatoms dominated during productivity periods and the metal may be retained onto refractory compounds for prolonged time scales in the sediments (Algeo and Maynard, 2004; Böning et al., 2015). Further, Ni does not show a significant association with TOC and hence an additional source other than primary production should be assessed (Table 6.5). Excess Ni is often incorporated within its silicate lattice rather than as separate grains in contaminated sediments (Adamo et al., 1996). So it cannot be extracted by general diacid digestion unless causing the dissolution of silicates. Therefore, the sample digestions were carried out using hydrofluoric acid to extract the metal bound to silicates and hence, the excess Ni incorporated were precisely measured. R-I_{geo} and CS-I_{geo} values suggest moderate and extreme pollution of Ni in the surface sediments respectively. These values show a less significant variation within a short range (CS-I_{geo} = 6.27–6.93) in all the sampling sites. Also, on account of the EF_c and EF_{cs} values shown by Ni, it is hypothesized that an anthropogenic source of Ni is less likely to occur while the accumulation is analogous to authigenic enrichment in the sediments apart from productivity sources. This finding is in agreement with the study by Rao and Rao (1995), suggested that surface sediments of South India are mainly composed of the weathering products of precambrian gneissic rocks and laterites, as a source of Ni.

6.3.2.6 Lead

Pb averaged 10.77 mg kg^{-1} in the sediments showing very low enrichment in the study region. Pb-EF_c values averaged 6.49 ranging from 0.22 to 19.13. EF_r of Pb ranged between 0.20 and 17.56. EF_c and EF_r results of Pb suggest severe enrichment at C4, C3 and B3, and moderately severe enrichment at A1, E1, C2, C1, B2 and E2 (Fig. 6.8). The EF_{cs} of Pb averaged 0.34 respectively and possess negligible enrichment. C-I_{geo} values of Pb ranged from −5.92 to 0.47 and the stations B3, B1, C4 and B2 are unpolluted to moderately polluted with respect to Pb. Pb shows R-I_{geo} values ranging from −5.84 to 0.55. It is found to be unpolluted to moderately polluted at transect B and at station C4. C-I_{geo} and R-I_{geo} suggest that the sites B1, B2, B3 and C4 are unpolluted to moderately polluted with respect to Pb. CS-I_{geo} of Pb ranges from −3.09 to 3.30. It is strongly polluted at B1, B2 and C4 whereas moderately to strongly polluted at C1, A2, A1, C3 and B3.

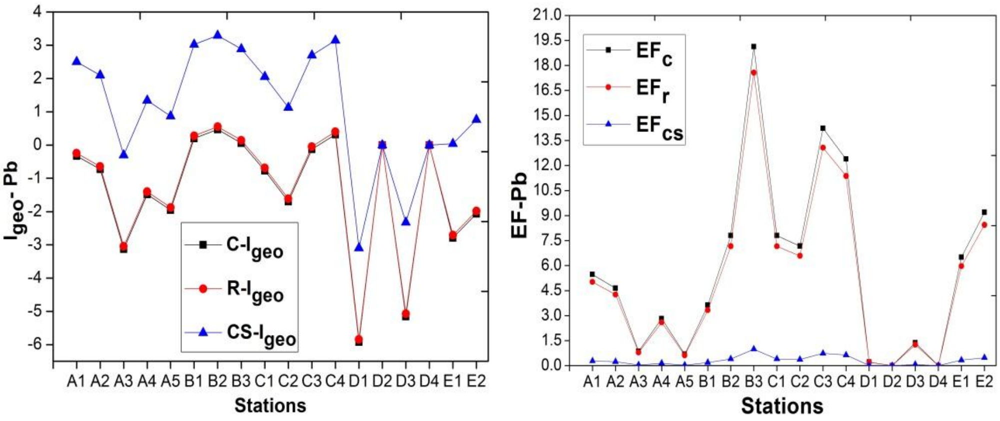

Fig. 6.8 Enrichment factor and geoaccumulation index calculated for Pb.

6.3.3 Principal Component Analysis

PCA produced five factors accounting for a total variance of 86.63% for the analyzed organic and inorganic variables (Table 6.8). Factor 1 shows high positive loadings on TOC, TN, TS, silt and clay, whereas a negative loading on sand fraction, which accounts for 22.55% of variance. This factor implies the production and preservation of organic matter on fine grained biogenic sediments, which exert a strong control on the redox status of the sediments. Factor 2 (18.72% variance) accounts for significant positive loadings on Cd, Cr, Cu and Fe. It suggests that these bioelements transported as a result of biological productivity may be scavenged by Fe oxyhydroxides. Biochemical components viz., CHO, PRT and LIP were positively loaded in factor 3 explaining a variance of 18.43%. It describes the dominance of refractory products in the sediments due to the effective remineralization of organic matter in the water column. Metals namely, Co, Mn and Al show significant positive loadings on factor 4 indicating the influence of Mn oxyhydroxides on Co mobilization and the lithogenic metal content associated with aluminosilicate minerals. Finally, factor 5 consists of positively loaded major metals (Ca and Mg) together with $CaCO_3$ having a variance of 13.30%. It can be designated as the pelagic carbonates controlled factor.

Table 6.8: Results of the principal component analysis carried out on the analyzed parameters in the study.

Variables	1	2	3	4	5
Cd	0.18	**0.64**	0.37	0.06	0.50
Co	−0.08	0.34	−0.09	**0.89**	−0.07
Cr	0.09	**0.91**	0.03	0.27	0.10
Cu	0.49	**0.71**	0.20	0.27	0.21
Mn	−0.26	0.25	−0.31	**0.84**	0.11
Ni	0.44	−0.16	0.27	0.00	−0.49
Pb	−0.34	0.55	−0.56	0.37	−0.19
Zn	0.61	0.62	0.26	−0.05	0.01
Al	0.03	0.60	−0.01	**0.74**	−0.03
Ca	0.03	0.18	0.11	0.05	**0.93**
Fe	−0.05	**0.91**	−0.04	0.35	0.12
Mg	−0.15	0.36	−0.09	0.23	**0.80**
TOC	**0.70**	0.19	0.57	−0.32	0.03
$CaCO_3$	0.01	−0.22	−0.08	−0.28	**0.78**
TN	**0.75**	0.03	0.56	−0.19	−0.02
TS	**0.80**	−0.01	0.39	0.36	0.01
CHO	0.22	0.06	**0.86**	−0.06	−0.26
PRT	0.20	0.02	**0.91**	−0.11	−0.08
LIP	−0.12	0.16	**0.92**	−0.02	0.18
Sand	**−0.93**	0.03	−0.19	−0.07	0.17
Silt	**0.85**	0.10	−0.19	−0.30	0.19
Clay	**0.73**	0.19	−0.15	−0.23	−0.21
% Variance	22.55	18.72	18.43	13.63	13.30

Note: Factor loadings greater than ±60 are shown in bold.

6.3.4 Site Specific Enrichment Pattern of Metals

Trace metal concentrations reveal significant spatial variation in all the transects. The concentrations of Cd, Cr, Cu and Zn in transect A and the concentrations of Ni and Zn in transect D generally increased with increasing water depth.

Generally, the metal enrichment followed a particular trend in the following stations. (i) Fe, Mg, Cd, Cr and Ni show marked enrichment at A4 (Cochin 202 m), (ii) Fe, Mg, Cd, Co, Cr, Ni and Pb display high enrichment at B3 (Alleppey 215 m), (iii) Fe, Cd, Cr, Ni, Pb and Zn showed observable enrichment at C3 (Kollam 300 m) and (iv) Cd, Cr, Ni and Pb reveal possible enrichment at C4 (Kollam 400 m). From these results it is clear that, high metal enrichment were obtained at sites A4, B3, C3 and C4 compared to other sites in the study region. In accordance, these sites mainly A4 and C3 tend to be anoxic and they contain the lowest PRT/CHO ratios of 0.07 to 0.09. Low ratios indicate the faster degradation of more labile particles and the accumulation of refractory products during organic matter recycling in the environment. In the case of Cu, Cr, Co and Zn, the observed metal enrichment is possibly due to reducing conditions induced by the degradation of labile fractions and thus, the metal could have further released/tend to adsorb onto the refractory fraction ultimately, retained on the sediments. On the other hand, Cd and Pb enrichment may be due to the precipitation of metal as their metal sulphides as a result of reductive diagenesis in the sediment water interface. Cu enrichment was observed at sites where high organic matter accumulation was witnessed. So its transport and accumulation pattern in the region is associated with the sinking biogenic matter deposited in the sediments.

Another significant trend of metal enrichment was at transect D, where Cd, Cr, Ni and Zn show notable enrichment. Cd may be contributed by detrital carbonates and significantly preserved in fine grained sediments. Cr enrichment in transects C and D are consistent with increasing fine grained clay content, which is having increased metal adsorption sites. Clayey sediments provide high specific surface area as active sites for binding with the metals (Beck et al., 2013). Ni and Zn enrichment are caused by the effective trapping of metals onto clay minerals which enhances its preservation in the surface sediments.

6.3.5 Cluster Analysis

Out of eighteen sampling sites, the dendrogram generated four clusters with atleast three stations in a cluster (Fig. 6.9). Accordingly, cluster 1 consists of stations namely E1, E2 and D2. These stations are marked by the presence of productivity related pelagic carbonates. Cluster 2 comprises of sites viz., C4, C3, A2, B2, A4, A3 and B3. On analyzing the trace metal concentration, these stations reveal significant enrichment associated with principal metal carriers and biogenic matter. The third cluster includes four inner shelf stations (A1, C2, C1 and D1). It can be categorized as those stations having low enrichment of trace elements. Cluster 4 contains four stations specifically D4, D3, A5 and B1 characterized by high accumulation and preservation of organic matter in the surface sediments.

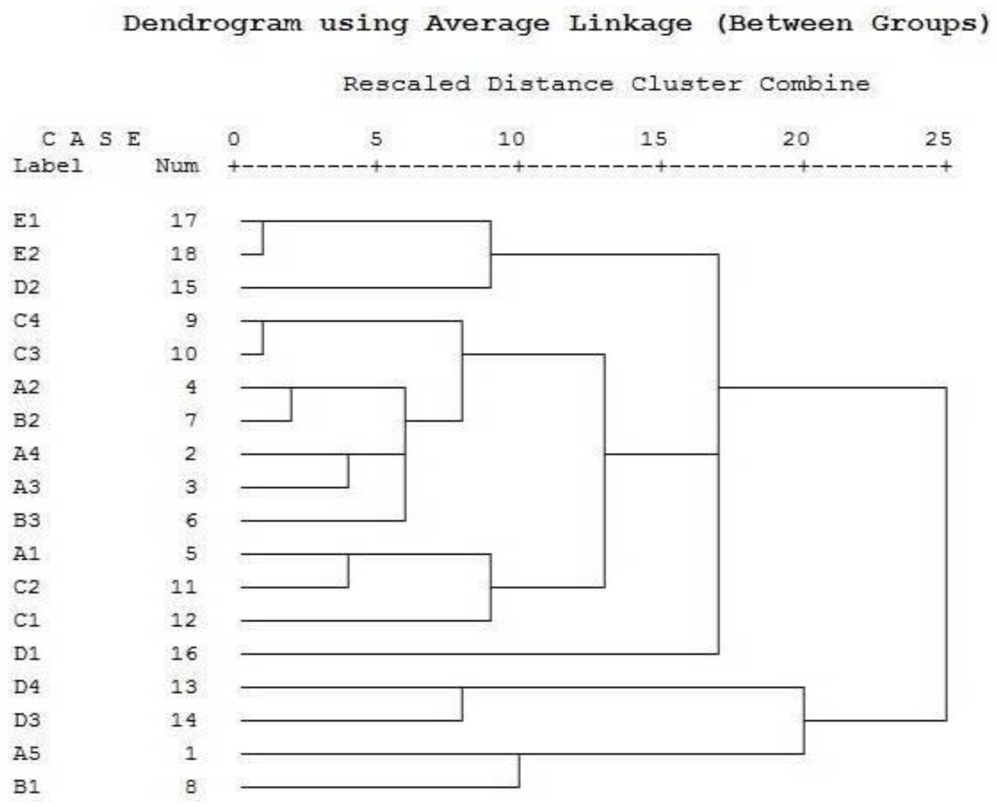

Fig. 6.9 Dendrogram showing the cluster of sampling stations.

6.3.6 Biological and Ecological Risks

To evaluate the potential effects of metals to biota, sediment quality guideline variables (SQGs), namely effective range low (ERL) and effective range medium (ERM) were applied based on Long et al. (1995). Cd, Pb and Zn concentration were below the ERL value and hence, adverse effects of these metals would rarely observed on biota. Cu levels exceeded the ERL value (34 mg kg^{-1}) at A5 (40.16 mg kg^{-1}) posing occasional threat to biota. Cr concentration was between ERL (81 mg kg^{-1}) and ERM value (370 mg kg^{-1}) at B3, D1, A4, B1, A5, C4 and C3 indicating incidental toxicity to biota. The proposed ERL and ERM value of Ni is 20.9 mg kg^{-1} and 51.6 mg kg^{-1} respectively. In this study, Ni concentration ranged between 71.88 mg kg^{-1} and

113.09 mg kg^{-1} showing higher values than ERM at all sampling stations. So, Ni concentration revealed that a frequent prevalence of Ni toxicity to biota in the area.

To further assess and validate the negative effects of toxic metals to biota, potential ecological risk assessment index suggested by Håkanson (1980) was calculated based on crustal and regional backgrounds. According to crustal background, the Er_i values varied from 6.47–79.39 for Cd (average 36.02), 0.14–3.31 for Cr (average 1.55), 0.02–3.65 for Cu (average 0.80), 4.79–7.54 for Ni (average 6.32), 0.12–10.38 for Pb (average 4.31) and 0.11–0.77 for Zn (average 0.37) respectively. Er_i value does not show a significant difference when calculated using regional background and its range of variation is shown in Table 6.9. Er_i of Cd was not calculated since regional background data was not available for Cd. Based on regional background, the Er_i values varied as follows: Cr, 0.14–3.32; Cu, 0.05–6.85; Ni, 7.92–12.45; Pb, 0.13–10.99; Zn, 0.11–0.79.

The results suggest that Cr, Cu, Ni, Pb, and Zn poses a low ecological risk ($Er_i < 40$), while Cd poses a moderate risk ($40 \leq Er_i < 80$) at stations C4, A5, A4, D1 and B3 (48.45–79.39; crustal background). Moreover, the metal enrichment observed on account of EF values provide elementary support for the potential ecological risk associated with these metals particularly stations at which Cd poses moderate risk factor (Liu and Shen, 2014; Lin et al., 2016). The overall potential metal risk (RI) values ranged from 9.36 to 95.64 (crustal background) and 13.49 to 100.34 (regional background) exhibiting low ecological risk (RI < 150) in the region (Table 6.9). The conclusions drawn on employing two different assessment methods such as SQGs and Er_i produced useful results that SQGs suggest adverse effects on biota by Ni, whereas Cd poses potential ecological risk based on Er_i values.

Table 6.9: Potential risk index of a single metal (Er_i) and the overall potential risk index (RI) at various stations with respect to crustal and regional background in the sediments.

Stations	Cd	Cr	Cu	Ni	Pb	Zn	RI	Cd	Cr	Cu	Ni	Pb	Zn	RI
	Er_i (Crustal background)							Er_i (Regional background)						
A1	-	0.61	0.14	5.91	5.99	0.18	12.84	-	0.62	0.27	9.77	6.34	0.19	17.18
A2	18.75	1.10	0.74	6.41	4.53	0.29	31.82	-	1.10	1.40	10.59	4.79	0.30	36.92
A3	25.42	1.27	0.89	6.65	0.86	0.31	35.41	-	1.28	1.68	10.98	0.91	0.32	40.59
A4	61.20	2.38	1.00	6.04	2.68	0.49	73.80	-	2.39	1.87	9.99	2.84	0.50	78.79
A5	57.24	3.08	3.65	6.52	1.93	0.77	73.20	-	3.09	6.85	10.78	2.05	0.79	80.80
B1	23.27	2.76	1.13	5.74	8.60	0.52	42.03	-	2.77	2.13	9.49	9.11	0.53	47.29
B2	32.93	1.61	0.53	6.36	10.38	0.28	52.10	-	1.61	1.00	10.51	10.99	0.29	57.33
B3	79.39	1.69	0.29	6.08	7.83	0.36	95.64	-	1.70	0.55	10.05	8.28	0.37	100.34
C1	-	1.03	0.18	7.54	4.39	0.27	13.41	-	1.03	0.34	12.45	4.65	0.28	18.75
C2	-	0.84	0.03	6.07	2.31	0.11	9.36	-	0.84	0.07	10.03	2.45	0.11	13.49
C3	34.52	3.31	1.20	5.48	6.87	0.64	52.02	-	3.32	2.25	9.05	7.27	0.66	57.07
C4	48.45	3.24	1.55	6.33	9.36	0.42	69.35	-	3.25	2.91	10.46	9.91	0.42	75.41
D1	70.81	2.29	1.05	5.72	0.12	0.33	80.33	-	2.30	1.98	9.45	0.13	0.34	85.00
D2	9.23	0.14	0.02	6.84	-	0.41	16.64	-	0.14	0.05	11.29	-	0.42	21.12
D3	28.61	0.84	0.38	7.48	0.21	0.45	37.97	-	0.84	0.71	12.36	0.22	0.46	43.20
D4	35.40	0.89	1.36	7.49	-	0.56	45.70	-	0.89	2.55	12.38	-	0.57	51.80
E1	6.47	0.41	0.12	4.79	1.08	0.11	12.98	-	0.41	0.22	7.92	1.15	0.11	16.28
E2	8.54	0.47	0.05	6.33	1.79	0.19	17.37	-	0.47	0.09	10.45	1.90	0.19	21.65
Min	6.47	0.14	0.02	4.79	0.12	0.11	9.36	-	0.14	0.05	7.92	0.13	0.11	13.49
Max	79.39	3.31	3.65	7.54	10.38	0.77	95.64	-	3.32	6.85	12.45	10.99	0.79	100.34
Avg	36.02	1.55	0.80	6.32	4.31	0.37	42.89	-	1.56	1.50	10.44	4.56	0.38	47.95

6.3.7 Comparison with Indian and Other Coastal Systems

The metal concentrations in the present study were in good agreement with other regions around the world (Table 6.10). The levels of Cd, Cu, Mn and Pb were found to be lower than the Bay of Bengal (Raj and Jayaprakash, 2008). Co concentration was comparable with other regions namely, Bay of Bengal (Raj and Jayaprakash, 2008), Yellow Sea (Jiang et al., 2014) and Mediterranean Shelf (Duman et al., 2012). The concentration of Ni was found to be high in comparison with other coastal regions in India and across the world. Cr levels were closest to those reported in Kerala coast (Srinivas et al., 2017; Udayakumar et al., 2014), Moroccan coast (Omar et al., 2015) and Southeast Brazil (Abreu et al., 2016). Cd concentrations were less than those surveyed from Northern Chile (Valdés et al., 2005) and Yellow Sea (Jiang et al., 2014). In the case of Mn, the recorded concentrations were lower than those reported from Moroccan coast (Omar et al., 2015), Southeast Brazil (Abreu et al., 2016), Yellow Sea (Jiang et al., 2014) and Mediterranean Shelf (Duman et al., 2012).

Table 6.10: Comparison of metal concentrations (mg kg^{-1}) with marine and other coastal systems around the world.

Location	Cd	Co	Cr	Cu	Mn	Ni	Pb	Zn	Reference
Southeastern Arabian Sea	0.04–0.53	0.44–11.56	6.85–165.46	0.27–40.16	4.89–206.23	71.88–113.09	0.31–25.95	7.45–54.05	Present study
Kerala coast	-	-	96–288	18–51	-	34–119	25–50	22–71	Srinivas et al. (2017)
Southwest coast of India	0.08–3.60	-	34–217.80	15–67	-	14–134	7.4–38	25–219	Udayakumar et al. (2014)
Bay of Bengal	4.6–7.5	5.80–11.80	148.6–243.2	385–657	284–460	19.8–53.4	24.9–40	71.3–201	Raj and Jayaprakash (2008)
Gulf of Mannar	-	-	0.00–452.48	0.04–555.29	120.04–179.96	29.14–450.57	0.44–2091.16	0.00–186.73	Krishnakumar et al. (2017)
South Korean coast	-	1.60–33.30	3.80–99.60	1.30–310.80	-	3.0–44.9	11.20–229.30	6–595	Song and Choi (2017)
Northern Chile	3–38	-	-	-	20–138	2–36	-	10–62	Valdés et al. (2005)
Gulf of Oman	0.02–0.21	0.10–45.20	3.36–303	0.60–48.30	13.20–360	0.74–1010	0.43–99	1.57–52.20	de Mora et al. (2004)
Moroccan coast	0.14–0.27	18.06–31.70	88.40–160.97	4.09–29.12	256.56–651.66	34.19–79.89	33.11–47.97	64.82–110.77	Omar et al. (2015)
Southern Caspian Sea	0.27–0.82	-	31.66–90.22	1.16–28.16	-	13.58–28.52	0.32–6.20	32.63–58.63	Jamshidi and Bastami (2017)
Southeast Brazil	0.47–1.80	-	24.6–157	-	141–1363	1.11–15.9	14.6–107	89.0–456	Abreu et al. (2016)
Yellow Sea	0–8.21	4.11–13.30	-	4.95–26.1	84.7–1593	8.31–32.40	4.31–21.9	18.80–96.20	Jiang et al. (2014)
East China Sea	0.09–0.21	-	-	18.8–49.2	-	-	24.4–53.0	80.2–140.5	Liu et al. (2011)
Dumai coast, Indonesia	0.46–1.89	-	-	1.61–13.84	-	7.26–19.97	14.63–84.90	31.49–87.11	Amin et al. (2009)
Western shelf of Mediterranean	-	12.20–17	14.0–38	39.50–73.60	342–443	11.20–25.80	1.60–12.80	36.0–78.0	Duman et al. (2012)
Bohai Bay, China	0.12–0.66		60.1–224.50	20.1–62.9	-	23.4–52.7	20.9–66.4	55.3–457.30	Gao and Chen (2012)

6.4 Conclusions

The study analyzed the geochemical variation of major and trace elements in the sediments of the Southwest Indian continental shelf of Arabian Sea to evaluate the metal enrichment status applying Al normalization using crustal, regional and core sediment background levels and organic matter variability. Our results suggest low terrigenous influx, but high contents of organic carbon and pelagic carbonates reflecting biological productivity in the outer shelf sediments. Low organic carbon values in the inner shelf due to reduced inputs from biological production concurrent with the existence of oxic depositional environments. Biochemical descriptors classified the trophic status as hypertrophic, eutrophic and meso-oligotrophic in the sediments. The metal enrichment is influenced by biogenic sources, metal oxides and reducing conditions with minimal anthropogenic footprints, reflecting significant processes viz., (i) biological productivity induced oxygen depleted conditions and adsorption to Fe oxyhydroxides concurrently cause Cd enrichment, (ii) depletion of metals (Mn and Co) due to scavenging and remobilization in the sediment water interface, (iii) Cu and Zn possess a definite association with organic matter, chlorophyll pigments and its degradation products and (iv) detrital origin of Ni from source rocks. Cd and Ni are primarily assessed as a threat to biota and their bioavailability results in adverse effects to marine species. The present study employed three background references and provides insight to different enrichment processes unravelling the fate and transport of trace metals and its associated factors in the South Indian continental shelf.

References

Abreu, I.M., Cordeiro, R.C., Soares-Gomes, A., Abessa, D.M.S., Maranho, L.A., Santelli, R.E., 2016. Ecological risk evaluation of sediment metals in a tropical Euthrophic Bay, Guanabara Bay, Southeast Atlantic. Marine Pollution Bulletin, 109, 435–445.

Adamo, P., Dudka, S., Wilson, M.J., McHardy, W.J., 1996. Chemical and mineralogical forms of Cu and Ni in contaminated soils from the Sudbury mining and smelting region, Canada. Environmental Pollution, 91, 11–19.

Algeo, T.J., Maynard, J.B., 2004. Trace-element behavior and redox facies in core shales of Upper Pennsylvanian Kansas-type cyclothems. Chemical Geology, 206, 289–318.

Aller, R.C., 1994. The sedimentary Mn cycle in Long Island Sound: Its role as intermediate oxidant and the influence of bioturbation, O_2 and C_{org} flux on diagenetic reaction balances. Journal of Marine Research, 52, 259–295.

Amin, B., Ismail, A., Arshad, A., Yap, C.K., Kamarudin, M.S., 2009. Anthropogenic impacts on heavy metal concentrations in the coastal sediments of Dumai, Indonesia. Environmental Monitoring and Assessment, 148, 291–305.

Beck, M., Böning, P., Schückel, U., Stiehl, T., Schnetger, B., Rullkötter, J., Brumsack, H., 2013. Consistent assessment of trace metal contamination in surface sediments and suspended particulate matter: A case study from the Jade Bay in NW Germany. Marine Pollution Bulletin, 70, 100–111.

Berner, R.A., 1989. Biogeochemical cycles of carbon and sulfur and their effect on atmospheric oxygen over Phanerozoic time. Palaeogeography, Palaeoclimatology, Palaeoecology, 75, 97–122.

Böning, P., Brumsack, H., Böttcher, M.E., Schnetger, B., Kriete, C., Kallmeyer, J., Borchers, S.L., 2004. Geochemistry of Peruvian near-surface sediments. Geochimica et Cosmochimica Acta, 21, 4429–4451.

Böning, P., Shaw, T., Pahnke, K., Brumsack, H.J., 2015. Nickel as indicator of fresh organic matter in upwelling sediments. Geochimica et Cosmochimica Acta, 162, 99–108.

Chakraborty, P., Ramteke, D., Chakraborty, S., 2015. Geochemical partitioning of Cu and Ni in mangrove sediments: Relationships with their bioavailability. Marine Pollution Bulletin, 93, 194–201.

Cheriyan, E., Sreekanth, A., Mrudulrag, S.K., Sujatha, C.H., 2015. Evaluation of metal enrichment and trophic status on the basis of biogeochemical analysis of shelf sediments of the southeastern Arabian Sea, India. Continental Shelf Research, 108, 1−11.

Collier, R., Edmond, J., 1984. The trace element geochemistry of marine biogenic particulate matter. Progress in Oceanography, 13, 113–199.

Dell’Anno, A., Mei, M.L., Pusceddu, A., Danovaro, R., 2002. Assessing the trophic state and eutrophication of coastal marine systems: A new approach based on the biochemical composition of sediment organic matter. Marine Pollution Bulletin, 44, 611–622.

de Mora, S., Fowler, S.W., Wyse, E., Azemard, S., 2004. Distribution of heavy metals in marine bivalves, fish and coastal sediments in the Gulf and Gulf of Oman. Marine Pollution Bulletin, 49, 410–424.

Duman, M., Kucuksezgin, F., Atalar, M., Akcali, B., 2012. Geochemistry of the northern Cyprus (NE Mediterranean) shelf sediments: Implications for anthropogenic and lithogenic impact. Marine Pollution Bulletin, 64, 2245–2250.

Ergin, M., Kazan, B., Ediger, V., 1996. Source and depositional controls on heavy metal distribution in marine sediments of the Gulf of Iskenderun, Eastern Mediterranean. Marine Geology, 133, 223–239.

Felja, I., Romić, M., Romić, D., Bakić, H., Pikelj, K., Juračić, M., 2016. Application of empirical model to predict background metal concentration in mixed carbonate-alumosilicate sediment (Adriatic Sea, Croatia). Marine Pollution Bulletin, 106, 190–199.

Galois, R., Blanchard, G., Seguignes, M., Huet, V., Joassard, L., 2000. Spatial distribution of sediment particulate organic matter on two estuarine intertidal mudflats: a comparison between Marennes-Oleron Bay (France) and the Humber Estuary (UK). Continental Shelf Research, 20, 1199-1217.

Gao, X., Chen, C.T.A., 2012. Heavy metal pollution status in surface sediments of the coastal Bohai Bay. Water Research, 46, 1901–1911.

Grémare, A., Medernach, L., DeBovee, F., Amouroux, J.M., Charles, F., Dinet, A., Ve- tion, G., Albert, P., Colomines, J.C., 2003. Relationships between sedimentary organics and benthic fauna within the Gulf of Lions: synthesis on the identification of new biochemical descriptors of sedimentary organic nutritional value. Oceanologica Acta, 26, 391–406.

Håkanson, L., 1980. An ecological risk index for aquatic pollution control: a sedimentological approach. Water Research, 14, 975–1001.

Jamshidi, S., Bastami, K.D., 2017. Preliminary assessment of metal distribution in the surface sediments along the coastline of the southern Caspian Sea. Marine Pollution Bulletin, 116, 462–468.

Jesus, C.C., de Stigter, H.C., Richter, T.O., Boer, W., Mil-Homens, M., Oliveira, A., Rocha, F., 2010. Trace metal enrichments in Portuguese submarine canyons and open slope: Anthropogenic impact and links to sedimentary dynamics. Marine Geology, 271, 72–83.

Jiang, X., Teng, A., Xu, W., Liu, X., 2014. Distribution and pollution assessment of heavy metals in surface sediments in the Yellow Sea. Marine Pollution Bulletin, 83, 366–375.

Krishnakumar, S., Ramasamy, S., Chandrasekar, N., Peter, T.S., Gopal, V., Godson, P.S., Magesh, N.S., 2017. Trace element concentrations in reef associated sediments of Koswari Island, Gulf of Mannar biosphere reserve, southeast coast of India. Marine Pollution Bulletin, 117, 515–522.

Kumar, A.A., 2005. Palaeoclimatic and palaeoceanographic studies on the sediment cores of the northwestern continental margin of India. Goa University, Goa, India. (Ph.D. thesis).

Li, X., Shen, Z., Wai, O.W.H., Li, Y., 2000. Chemical partitioning of heavy metal contaminants in sediments of the Pearl River Estuary. Chemical Speciation & Bioavailability, 12, 17–25.

Limmer, D.R., Böning, P., Giosan, L., Ponton, C., Köhler, C.M., Cooper, M.J., Tabrez, A.R., Clift, P.D., 2012. Geochemical record of Holocene to Recent sedimentation on the Western Indus continental shelf, Arabian Sea. Geochemistry, Geophysics, Geosystems, 13, Q01008. doi: 10.1029/2011GC003845.

Lin, Q., Liu, E., Zhang, E., Li, K., Shen, J., 2016. Spatial distribution, contamination and ecological risk assessment of heavy metals in surface sediments of Erhai Lake, a large eutrophic plateau lake in southwest China. Catena, 145, 193–203.

Liu, S., Shi, X., Liu, Y., Zhu, Z., Yang, G., Zhu, A., Gao, J., 2011. Concentration distribution and assessment of heavy metals in sediments of mud area from inner continental shelf of the East China Sea. Environmental Earth Sciences, 64, 567–579.

Liu, E., Shen, J., 2014. A comparative study of metal pollution and potential eco-risk in the sediment of Chaohu Lake (China) based on total concentration and chemical speciation. Environmental Science and Pollution Research, 21, 7285–7295.

Lo Monaco, S., Lopez, L., Rojas, H., Garcia, D., Premovic, P., Briceno, H., 2002. Distribution of major and trace elements in La Luna Formation, Southwestern Venezuelan Basin. Organic Geochemistry, 33, 1593–1608.

Long, E.R., McDonald, D.D., Smith, S.L., Calder, F.D., 1995. Incidents of adverse biological effects within ranges of chemical concentrations in marine and estuarine sediments. Environmental Management, 19, 81–97.

Mellis, E.V., da Cruz, M.C.P., Casagrande, J.C., 2004. Nickel adsorption by soils in relation to pH, organic matter and iron oxides. Scientia Agricola, 61, 190–195.

Moreno, S., Niell, F.X., 2004. Scales of variability in the sediment chlorophyll content of the shallow Palmones River Estuary, Spain. Estuarine Coastal and Shelf Science, 60, 49–57.

Nameroff, T.J., Calvert, S.E., Murray, J.W., 2004. Glacial-interglacial variability in the eastern tropical North Pacific oxygen minimum zone recorded by redox-sensitive trace metals. Paleoceanography, 19. doi: 10.1029/2003PA000912.

Omar, M.B., Mendiguchía, C., Er-Raioui, H., Marhraoui, M., Lafraoui, G., Oulad-Abdellah, M.K., García-Vargas, M., Moreno, C., 2015. Distribution of heavy metals in marine sediments of Tetouan coast (North of Morocco): natural and anthropogenic sources. Environmental Earth Sciences, 74, 4171–4185.

Panda, U.C., Rath, P., Sahu, K.C., Majumdar, S., Sundaray, S.K., 2006. Study of geochemical association of some trace metals in the sediments of Chilika lake: a multivariate statistical approach. Environmental Monitoring and Assessment, 123, 125–150.

Pang, H., Lou, Z., Jin, A., Yan, K., Jiang, Y., Yang, X., Chen, C.A., Chen, X., 2015. Contamination, distribution, and sources of heavy metals in the sediments of Andong tidal flat, Hangzhou bay, China. Continental Shelf Research, 110, 72–84.

Prego, R., Cobelo-García, A., 2003. Twentieth century overview of heavy metals in the Galician Rias (NW Iberian Peninsula). Environmental Pollution, 121, 425–452.

Ramasamy, V., Sundarrajan, M., Paramasivam, K., Meenakshisundaram, V., Suresh, G., 2013. Assessment of spatial distribution and radiological hazardous nature of radionuclides in high background radiation area, Kerala, India. Applied Radiation and Isotopes, 73, 21–31.

Raj, S.M., Jayaprakash, M., 2008. Distribution and enrichment of trace metals in marine sediments of Bay of Bengal, off Ennore, south-east coast of India. Environmental Geology, 56, 207–217.

Rao, V.P., Rao, B.R., 1995. Provenance and distribution of clay minerals in the sediments of the western continental shelf and slope of India. Continental Shelf Research, 15, 1757–1771.

Rosenthal, Y., Lam, P., Boyle, E.A., Thomson, J., 1995. Authigenic cadmium enrichments in suboxic sediments: Precipitation and postdepositional mobility. Earth and Planetary Science Letters, 132, 99–111.

Rubio, B., Nombela, M.A., Vilas, F., 2000. Geochemistry of major and trace metals in sediments of the Ria de Vigo (NW Spain), an assessment of metal pollution. Marine Pollution Bulletin, 40, 968–980.

Schnetger, B., Brumsack, H.J., Schale, H., Hinrichs, J., Dittert, L., 2000. Geochemical characteristics of deep-sea sediments from the Arabian Sea: a high-resolution study. Deep Sea Research Part II: Topical Studies in Oceanography, 47, 2735–2768.

Song, Y., Choi, M.S., 2017. Assessment of heavy metal contamination in sediments along the coast of South Korea using Cs-normalized background concentrations. Marine Pollution Bulletin, 117, 532–537.

Sreekanth, A., Mrudulrag, S.K., Cheriyan, E., Sujatha, C.H., 2015. Trace metal enrichment and organic matter sources in the surface sediments of Arabian Sea along southwest India (Kerala coast). Marine Pollution Bulletin, 101, 938–946.

Srinivas, R., Shynu, R., Sreeraj, M.K., Ramachandran, K.K., 2017. Trace metal pollution assessment in the surface sediments of nearshore area, off Calicut, southwest coast of India. Marine Pollution Bulletin. doi: 10.1016/j.marpolbul.2017.05.028.

Stumm, W., Morgan, J.J., 1981. Aquatic chemistry: An introduction emphasizing chemical equilibria in natural waters. 2nd edition, John Wiley & Sons, New York.

Taylor, S.R., 1964. Abundance of chemical elements in the continental crust: a new table. Geochimica et Cosmochimica Acta, 28, 1273–1285.

Udayakumar, P., Jose, J.J., Krishnan, K.A., Kumar, C.S.R., Manju, M.N., Salas, P.M., 2014. Heavy metal accumulation in the surficial sediments along southwest coast of India. Environmental Earth Sciences, 72, 1887–1900.

Valdés, J., Vargas, G., Sifeddine, A., Ortlieb, L., Guinez, M., 2005. Distribution and enrichment evaluation of heavy metals in Mejillones Bay (23°S), Northern Chile: Geochemical and statistical approach. Marine Pollution Bulletin, 50, 1558–1568.

Varghese, S., 2004. Geochemistry of rare earth elements and trace metals along the western continental shelf of India. Cochin University of Science and Technology, Cochin, India. (Ph.D. thesis).

Venturini, N., Pita, A.L., Brugnoli, E., García-Rodríguez, F., Burone, L., Kandratavicius, N., Hutton, M., Muniz, P., 2012. Benthic trophic status of sediments in a metropolitan area (Rio de la Plata estuary): Linkages with natural and human pressures. Estuarine Coastal and Shelf Science, 112, 139–152.

Williams, N., Block, K.A., 2015. Spatial and vertical distribution of metals in sediment cores from Río Espíritu Santo estuary, Puerto Rico, United States. Marine Pollution Bulletin, 100, 445–452.

Zhang, L., Ye, X., Feng, H., Jing, Y., Ouyang, T., Yu, X., Liang, R., Gao, C., Chen, W., 2007. Heavy metal contamination in western Xiamen Bay sediments and its vicinity, China. Marine Pollution Bulletin, 54, 974–982.

SUMMARY AND CONCLUSIONS

This is the first study that has developed a comprehensive assessment of environmentally relevant trace metals in the sediments of estuarine, coastal and shelf region of Kerala coast. Geochemistry of trace metal enrichment was studied by a different approach to predict the geochemical signature affected by different physical, chemical and biological processes in the marine environment along South India. This research work includes the determination of background metal level in the region using sediment cores, assessing the trace metal enrichment in the estuarine and coastal regions of Kerala coast utilizing the core sediment data, evaluating the origin of organic matter and estimation of trace element sources in the continental shelf of Southeastern Arabian Sea with respect to a regional metal background. Further, a comparative approach using different metal background levels fruitfully explains the geochemistry of trace metal enrichment in the Arabian Sea off Kerala. The observed trace metal concentrations were compared with background concentrations using Al as a normalizing element to account for variations in the flux of terrigenous material. The present study used a very extensive data composed of several types of variables which helps to perceive the factors contribute to the enrichment of metals in this region and if this enrichment could constitute a risk for the living organisms. From the available data and calculated indices, the thesis discusses the possible processes and mechanisms that may result in the observed enrichment of trace metals. The work tends to gloss over urgent points regarding the need for conservation of regional marine ecosystems and demonstrate a strong command over the literature that has been referenced.

Geochemical and ecological risk assessment indexes were also accounted. Five different indices were used to assess the pollutant level and toxicological status of the sediments: enrichment factor, geoaccumulation index, contamination factor; pollution load index and potential ecological risk assessment. The most important contribution, however, in the understanding of the source characterization and variability of metal in this study comes from the incorporation of the regional background to reveal human pressures and contamination status. The addition of metal regional background has provided a different dimension to explain the metal enrichment on a spatial scale and certainly to predict the variation in response to anthropogenic disturbances. Moreover, the novelty of geochemical indices established and the data generated in this study provide a strong bias for the geochemical interpretation focused on variable aspects of the marine system. For example, a new set of metal enrichment factors were calculated based on the background trace metal levels in the region. The magnitude of calculated enrichment factors is inherently tied to the choice of the chosen background reference values, thereby illustrating one of the issues with interpreting enrichment factors in terms of mechanisms of enrichment. It is thus useful to compare different background values, to better understand the uncertainty on the calculated enrichment factors. The indices have been compared with one another both as a function of metal and as a function of sampling station. They are used to test whether these give similar or different information: for instance whether indicators of pollution and the indicator of ecological risk are related to one another. It can be seen that these values would better represent and explain the pollution status of the coastal environment and provide insightful observations on metal enrichment. However, the geoaccumulation index and ecological risk factor are presented as robust calculations of geochemically important parameters. Thus the study employed different assessment methods accounting regional influences to minimize the dilemma of single assessment strategy to provide a methodical understanding of trace metal enrichment in upwelling sediments.

One of the key goals of the study was to establish a set of background trace metal concentrations that describe the regional sediment composition in the absence of anthropogenic inputs. These levels are considered to represent background conditions and it can be used to evaluate the contamination in the coastal sediments. This is the first study to provide region specific background concentration ranges for trace metals in the core sediments of the southern tip of peninsular India (Cape Comorin) which have never been surveyed or included in the calculation reports available in the literature. Out of the trace metals studied for background concentrations, Cd was below detectable limit in the core sediment of Cape Comorin. All the metal concentrations (average: Mg > Fe > Al > Mn > Zn > Cu > Cr > Pb > Ni > Co) were observed without any anthropogenic intervention. At the same time, the core sediment used to generate background levels in the Cochin estuary was found to vary in several respects. However, the anthropogenic impact is considerable in the Cochin estuarine system due to the extremely high urbanization and industrialization which causes concern. In addition, the increased monsoonal supply of materials together with previously deposited sediments is mainly a factor for this increased metal contamination. The behaviour of trace metals in the estuary is complex, and the natural impact on the coastal environment is clearly reflected by their concentrations. It should be concluded that the metal content in the estuarine environment is more vulnerable to natural and anthropogenic sources and tend to be different in all aspects. Cd and Pb show enrichment in the core sediments, clearly originated from anthropogenic activities. It should be further stated that the levels were taken as background for Cd and Pb since the estuarine environment receives metals from multiple sources such as municipal effluents, river discharges, agricultural sources, atmospheric emissions, industrial units, etc. (Range: Fe > Mg > Mn > Zn > Ni > Pb > Cu > Co > Cd).

Furthermore, the study highlights the contamination and spatial distribution of sediment organic matter and trace metals in selected stations of Kerala coast and focuses on the different spatial correlation pattern of trace metal enrichment. The spatial distribution of trace metals in the coastal and estuarine environment along the Kerala coast presents a unique pattern for certain trace elements. The distribution of trace metals in the surface sediments decreased in the following order: Fe > Mg > Mn > Pb > Zn > Ni > Co > Cu > Cd. The metal concentrations increased marginally on the northern arm of the Cochin estuary, central Kerala exactly at the lower reaches of river Periyar. Noteworthy were the concentrations of Cd and Zn at Chennur (Cochin estuary) and the levels were much higher than elsewhere in the entire study region. This metal accumulation is linked to uncontrolled and diffuse discharges associated with industrial manufacturing units. With the exception of this source, the sampling locations did not indicate any massive industrial inputs. On the other hand, present enrichment of metals at these stations is caused by local sources such as discharge from rivers, municipal sewage effluents, aquaculture/agricultural catchments, fishing and harbour activities.

The Arabian Sea along the west coast of India (Southeastern Arabian Sea off Kerala termed in this thesis) is well known as region where summer monsoon induced upwelling provides availability of nutrients which stimulates higher levels of biological production in the coast and shelf. The bulk elemental composition and elemental ratios viz., C/N and C/S have been used to indicate the sources of organic matter and redox status existing in the sediments. Organic carbon data suggests notable input of organic matter seawards and subsequent preservation in the outer shelf sediments. Generally, the C/N ratio ranged between 5 and 15 indicating marine origin of organic matter. High biological productivity in the Arabian Sea helps to dominate autochthonous organic matter in the marine environment than terrestrial signals. However, comparison of organic carbon and nitrogen values at certain coastal stations namely, Kollam (30 m depth) near to Ashtamudi lagoon suggests remarkable input of estuarine discharges, municipal sewage and terrestrial materials.

Besides, the biochemical composition of sedimentary organic matter and photosynthetic pigments in the Southeastern Arabian Sea were analyzed and describe the applicability in assessing the trophic status of the marine coastal environment. Of the three biochemical components, carbohydrates (CHO) show high values compared to proteins (PRT) and lipids (LIP). As such, the biochemical descriptors in sediments indicated hypertrophic, eutrophic and meso-oligotrophic conditions with a higher microphytobenthic contribution to biopolymeric carbon. The numerous marine resources substantiate the consumption of fresh and labile organic components and deposition of detritus in primary materials. Nevertheless, grain size has been identified as a relevant factor controlling the distribution and preservation of organic matter in the shelf sediments.

To conclude the behaviour of organic matter deposited in the sediments of Southeastern Arabian Sea, it is stated as the ratios among various biogeochemical parameters such as total organic carbon/total nitrogen (TOC/TN < 10), protein/carbohydrate (PRT/CHO < 1) displayed that the organic matter deposited in sedimentary systems is of marine origin and relatively old with potentially low nutritional value. Both these processes are ultimately linked to surface biological productivity.

Trace elements were determined along the continental shelf of Southeastern Arabian Sea, an upwelling margin in the Southwest India (Kerala coast). The study suggests that marine autochthonous biological production initiated biogenic matter and abundant binding sites mainly Fe and Mn oxyhydroxides are the crucial factors, apart from terrestrial inputs influencing metal variability in the shelf. In the inner shelf, the water column never turned anoxic but the redox state of the sediment has fluctuated between oxic and mildly suboxic conditions. Offshore sites comprise organic carbon-metal abundant surface prevailing on fine grained biogenic carbonate rich sediments. High biological productivity associated with upwelling leads to significant accumulation of Cd than crustal abundance in the shelf region. Cd may be probably associated with settling marine biogenic material. Enrichment of Cd is evidenced by fluctuating biogenic source besides preferable scavenging by Fe oxyhydroxide surfaces. The behaviour of Co shows remobilization induced by the mobilization of Mn hydroxides in the sediment-water interface. Depositional pattern and fate of Cr is not influenced by anthropogenic activities, but consistent with biological scavenging during organic matter accumulation thereafter found to be exchanged with Al in clastic clays. Cu enrichment observed close to major urban sectors, initiated by the precipitation as Cu sulphides. Cu and Zn are adsorbed onto refractory organic particles preserved on negatively charged detrital minerals while Ni shows detrital accumulation in the surface sediments. Multivariate statistical analyses of geochemical variables were used to confirm the origin information and the processes controlling the trace element concentrations. The concentration of certain elements is affected by biological production because the organic matter degradation consumes a sequence of oxidants viz., oxygen, nitrate, iron and manganese oxides, etc. Pb, Co and Ni show higher enrichment, evidenced by the association through adsorption of iron-manganese nodules onto clay minerals. The geochemical distribution of trace metals is mainly controlled by different complexation phases such as association to Fe-Mn oxyhydroxides, TOC and fine grained sediments.

Sediment quality guidelines in comparison with metal concentration revealed adverse effects, possibly occurring in marine benthic species. Potential ecological risk index related to toxic metals, Cd and Ni suggesting negative effects are possible to occur on marine biota. The potential toxic effects of Cd and Ni occurring on biota possess a wide concern over the highly productive fishery zone along the Kerala coast, Southwest India.

Vertical distribution profile helped to establish a background level for the subsequent estimation of anthropogenic metal contamination in the surface sediments along the Kerala coast. These regional background levels were used to assess the geochemical indices in the coastal, estuarine and shelf sediments of Kerala coast in addition to the application of crustal background. The enrichment factors calculated by conventional methods using crustal background may not be able to account for an adequate characterization of pollution sources. Nevertheless, the comparative assessment method adopted in this study gives better results on the interpretation of pollution indices which is essential for anthropised coastal regions. Altogether, the scientific basis for choosing this location to examine trace metal biogeochemistry is interesting that the Arabian Sea accounts for a wide range of biogeochemical properties such as hypertrophic, eutrophic, meso-oligotrophic, upwelling and oxygen minimum conditions as a result of circulation, climate and geology. The study provides vital information about sediment biogeochemistry and metal contamination from a potential fishery zone of Indian exclusive economic zone. Besides, the present study recommends extensive monitoring on bioavailability and mobility of trace elements which would be a great help for the effective management of this fragile coastal environment. This study has taken to the extent of collecting more data over a range of temporal-spatial variation relating to the anthropogenic vs. geologic intervention in this type of sensitive ecosystems. Hence, it provides clear evidence of the need and value for region specific management tools in support of intervention actions to protect and conserve the valuable resources in the coastal ecosystems.

PUBLICATIONS

1. **Eldhose Cheriyan**, Athira Sreekanth, Mrudulrag, S.K., Sujatha, C.H., 2015. Evaluation of metal enrichment and trophic status on the basis of biogeochemical analysis of shelf sediments of the southeastern Arabian Sea, India. *Continental Shelf Research*, 108, 1–11.
2. Athira Sreekanth, Mrudulrag, S.K., **Eldhose Cheriyan**, Sujatha, C.H., 2015. Trace metals enrichment and organic matter sources in the surface sediments of Arabian Sea along southwest India (Kerala coast). *Marine Pollution Bulletin*, 101, 938–946.
3. Ragi, A.S., Leena, P.P., **Eldhose Cheriyan**, Nair, S.M., 2017. Heavy metal concentrations of some gastropods and bivalves collected from the fishing zone of South India. *Marine Pollution Bulletin*, 118, 452–458.
4. Sanil Kumar, K.S., Nair, S.M., Salas, P.M., **Eldhose Cheriyan**., 2017. Distribution and sources of sedimentary organic matter in Chitrapuzha, a tropical tidal river, southwest coast of India. *Environmental Forensics*, 18, 135–146.
5. Salas, P.M., Sujatha, C.H., Ratheesh Kumar, C.S., **Eldhose Cheriyan**., 2017. Heavy metal distribution and contamination status in the sedimentary environment of Cochin Estuary. *Marine Pollution Bulletin*, 119, 191–203.

6. **Eldhose Cheriyan**, Mrudulrag S.K, Athira Sreekanth, Sujatha C.H., 2017. Distribution, sources and geochemistry of metal enrichment in a tropical upwelling margin of Arabian Sea along Southwest India. *Marine Pollution Bulletin*. (Under review).
7. **Eldhose Cheriyan**, Athira Sreekanth, Sujatha, C.H., Jyothishkumar, T., Mrudulrag, S.K., 2013. Distributional dynamics of nutrients along Kerala coast, India. Paper presented at the Symposium on Coastal Oceanographic Studies: Modelling and Observations (COSMOS 2013), Cochin, India, 207–213.
8. Athira Sreekanth, **Eldhose Cheriyan**, Sujatha, C.H., 2013. Distribution of trace metals and organic matter in the surface sediments along Kerala coast, India. Paper presented at the National Conference of Ocean Society of India on Role of Oceans in Earth System (OSICON 2013), Pune, India, 316–319.

APPENDICES

Appendix I

Results of Geochemical Indices

The following section lists the metal EF and I_{geo} values for crustal, regional and core sediment background presented in Chapter 6.

Table A1.1: Metal EF values for crustal, regional and core sediment background.

Stations	Fe			Mg		Cd	Co			Cr		
	crust	regional	core	crust	core	crust	crust	regional	core	crust	regional	core
A1	0.61	0.59	0.10	0.37	0.02	-	0.97	2.02	0.93	1.40	1.22	0.24
A2	0.95	0.91	0.16	1.12	0.05	3.20	1.46	3.06	1.40	2.81	2.45	0.49
A3	1.02	0.98	0.17	2.87	0.13	4.24	0.64	1.33	0.61	3.19	2.77	0.56
A4	5.13	4.93	0.84	6.96	0.32	10.74	0.91	1.91	0.88	6.28	5.47	1.10
A5	0.84	0.81	0.14	0.95	0.04	3.36	0.61	1.27	0.58	2.71	2.36	0.47
B1	0.99	0.95	0.16	0.69	0.03	1.63	0.71	1.48	0.68	2.91	2.54	0.51
B2	1.25	1.20	0.21	1.39	0.06	4.12	0.90	1.88	0.86	3.02	2.63	0.53
B3	7.29	7.01	1.20	8.58	0.39	32.34	5.65	11.81	5.42	10.33	9.00	1.81
C1	2.03	1.95	0.33	0.42	0.02	-	1.77	3.69	1.69	4.56	3.98	0.80
C2	1.30	1.25	0.21	1.09	0.05	-	1.64	3.43	1.58	6.48	5.64	1.13
C3	6.51	6.26	1.07	2.88	0.13	11.93	0.55	1.15	0.53	17.15	14.94	3.00
C4	3.09	2.97	0.51	0.89	0.04	10.69	0.64	1.33	0.61	10.71	9.33	1.87
D1	2.35	2.26	0.39	2.92	0.13	20.88	0.74	1.55	0.71	10.11	8.81	1.77
D2	2.38	2.29	0.39	12.36	0.57	38.25	2.19	4.58	2.10	8.52	7.42	1.49
D3	2.66	2.56	0.44	1.98	0.09	31.06	1.10	2.29	1.05	13.67	11.91	2.39
D4	0.93	0.90	0.15	0.62	0.03	13.92	1.33	2.78	1.28	5.24	4.56	0.92
E1	1.26	1.21	0.21	13.05	0.60	6.47	1.72	3.58	1.65	6.13	5.34	1.07
E2	1.58	1.52	0.26	10.69	0.49	7.30	2.01	4.19	1.92	6.01	5.23	1.05
Min	0.61	0.59	0.10	0.37	0.02	1.63	0.55	1.15	0.53	1.40	1.22	0.24
Max	7.29	7.01	1.20	13.05	0.60	38.25	5.65	11.81	5.42	17.15	14.94	3.00
Avg	2.34	2.25	0.38	3.88	0.18	13.34	1.42	2.96	1.36	6.73	5.87	1.18

Stations	Cu			Mn			Ni			Pb		
	crust	regional	core	crust	regional	core	crust	regional	core	crust	regional	core
A1	0.13	0.21	0.01	0.80	1.53	0.22	5.40	7.74	4.76	5.47	5.02	0.28
A2	0.76	1.24	0.07	1.00	1.91	0.27	6.57	9.41	5.79	4.64	4.26	0.24
A3	0.90	1.46	0.08	0.55	1.06	0.15	6.66	9.54	5.87	0.86	0.79	0.04
A4	1.05	1.71	0.10	0.71	1.37	0.19	6.37	9.12	5.61	2.83	2.60	0.15
A5	1.29	2.09	0.12	0.18	0.35	0.05	2.30	3.29	2.03	0.68	0.63	0.04
B1	0.48	0.78	0.04	0.30	0.58	0.08	2.42	3.47	2.14	3.63	3.33	0.19
B2	0.40	0.65	0.04	0.39	0.75	0.11	4.78	6.85	4.22	7.80	7.16	0.40
B3	0.71	1.16	0.07	2.65	5.08	0.72	14.87	21.31	13.11	19.13	17.56	0.99
C1	0.32	0.52	0.03	0.73	1.40	0.20	13.38	19.18	11.80	7.80	7.16	0.40
C2	0.11	0.18	0.01	0.56	1.08	0.15	18.82	26.98	16.60	7.17	6.58	0.37
C3	2.48	4.04	0.23	0.21	0.40	0.06	11.36	16.28	10.02	14.23	13.07	0.74
C4	2.05	3.34	0.19	0.38	0.73	0.10	8.38	12.01	7.39	12.39	11.38	0.64
D1	1.86	3.04	0.17	0.19	0.36	0.05	10.12	14.51	8.93	0.22	0.20	0.01
D2	0.60	0.98	0.06	0.97	1.87	0.26	170.00	243.64	149.92	-	-	-
D3	2.45	3.99	0.23	0.17	0.32	0.05	48.73	69.84	42.97	1.37	1.26	0.07
D4	3.20	5.22	0.30	0.27	0.52	0.07	17.67	25.33	15.58	-	-	-
E1	0.72	1.17	0.07	1.14	2.18	0.31	28.73	41.18	25.34	6.50	5.97	0.34
E2	0.26	0.42	0.02	1.34	2.57	0.36	32.46	46.52	28.63	9.19	8.44	0.48
Min	0.11	0.18	0.01	0.17	0.32	0.05	2.30	3.29	2.03	0.22	0.20	0.01
Max	3.20	5.22	0.30	2.65	5.08	0.72	170.00	243.64	149.92	19.13	17.56	0.99
Avg	1.10	1.79	0.10	0.70	1.34	0.19	22.72	32.57	20.04	6.49	5.96	0.34

Stations	Zn		
	crust	regional	core
A1	0.84	0.74	0.06
A2	1.50	1.33	0.11
A3	1.57	1.39	0.11
A4	2.58	2.28	0.18
A5	1.36	1.20	0.10
B1	1.09	0.96	0.08
B2	1.07	0.94	0.08
B3	4.45	3.94	0.32
C1	2.42	2.14	0.17
C2	1.69	1.49	0.12
C3	6.66	5.89	0.47
C4	2.75	2.44	0.20
D1	2.96	2.62	0.21
D2	50.87	44.99	3.63
D3	14.78	13.07	1.05
D4	6.60	5.84	0.47
E1	3.19	2.82	0.23
E2	4.87	4.31	0.35
Min	0.84	0.74	0.06
Max	50.87	44.99	3.63
Avg	6.18	5.47	0.44

Table A1.2: Metal I_{geo} values for crustal, regional and core sediment background.

Stations	Fe			Mg		Cd	Co			Cr		
	crust	regional	core	crust	core	crust	crust	regional	core	crust	regional	core
A1	−3.48	−3.33	1.01	−4.20	−1.55	-	−2.83	−1.56	4.21	−2.29	−2.29	2.29
A2	−3.02	−2.87	1.48	−2.77	−0.12	−1.26	−2.39	−1.12	4.65	−1.45	−1.45	3.13
A3	−2.88	−2.73	1.62	−1.39	1.27	−0.82	−3.56	−2.29	3.48	−1.24	−1.23	3.35
A4	−0.62	−0.48	3.87	−0.18	2.47	0.44	−3.11	−1.84	3.93	−0.33	−0.33	4.25
A5	−1.66	−1.51	2.84	−1.48	1.17	0.35	−2.12	−0.85	4.92	0.04	0.04	4.62
B1	−1.67	−1.52	2.82	−2.20	0.45	−0.95	−2.15	−0.89	4.89	−0.12	−0.11	4.46
B2	−2.17	−2.02	2.32	−2.02	0.64	−0.45	−2.65	−1.38	4.39	−0.90	−0.90	3.68
B3	−1.33	−1.18	3.16	−1.09	1.56	0.82	−1.70	−0.43	5.34	−0.83	−0.82	3.76
C1	−2.72	−2.57	1.78	−4.99	−2.33	-	−2.91	−1.65	4.13	−1.54	−1.54	3.04
C2	−4.16	−4.01	0.33	−4.42	−1.76	-	−3.82	−2.55	3.22	−1.84	−1.84	2.74
C3	−1.26	−1.11	3.24	−2.43	0.22	−0.38	−4.82	−3.55	2.22	0.14	0.15	4.73
C4	−1.68	−1.54	2.81	−3.48	−0.83	0.11	−3.96	−2.69	3.08	0.11	0.12	4.69
D1	−2.50	−2.35	1.99	−2.18	0.47	0.65	−4.16	−2.89	2.88	−0.39	−0.39	4.19
D2	−6.29	−6.15	−1.80	−3.92	−1.26	−2.29	−6.41	−5.14	0.63	−4.45	−4.45	0.13
D3	−4.20	−4.05	0.30	−4.62	−1.97	−0.65	−5.48	−4.21	1.56	−1.84	−1.83	2.75
D4	−4.25	−4.10	0.25	−4.85	−2.19	−0.35	−3.73	−2.46	3.31	−1.76	−1.75	2.83
E1	−5.16	−5.01	−0.67	−1.78	0.87	−2.80	−4.71	−3.44	2.33	−2.87	−2.87	1.71
E2	−4.61	−4.46	−0.12	−1.85	0.81	−2.40	−4.26	−2.99	2.78	−2.68	−2.67	1.90
Min	−6.29	−6.15	−1.80	−4.99	−2.33	−2.80	−6.41	−5.14	0.63	−4.45	−4.45	0.13
Max	−0.62	−0.48	3.87	−0.18	2.47	0.82	−1.70	−0.43	5.34	0.14	0.15	4.73
Avg	−2.98	−2.83	1.51	−2.77	−0.12	−0.67	−3.60	−2.33	3.44	−1.35	−1.34	3.24

Stations	Cu			Mn			Ni			Pb		
	crust	regional	core	crust	regional	core	crust	regional	core	crust	regional	core
A1	−5.70	−4.79	−2.02	−3.10	−1.96	2.11	−0.34	0.38	6.58	−0.33	−0.24	2.50
A2	−3.33	−2.42	0.35	−2.95	−1.80	2.27	−0.23	0.50	6.69	−0.73	−0.65	2.10
A3	−3.07	−2.16	0.61	−3.76	−2.61	1.46	−0.17	0.55	6.74	−3.13	−3.05	−0.30
A4	−2.91	−2.00	0.77	−3.47	−2.32	1.75	−0.31	0.41	6.61	−1.48	−1.40	1.35
A5	−1.04	−0.13	2.64	−3.85	−2.71	1.37	−0.20	0.52	6.72	−1.96	−1.87	0.87
B1	−2.73	−1.82	0.95	−3.39	−2.24	1.83	−0.38	0.34	6.53	0.20	0.28	3.03
B2	−3.82	−2.91	−0.14	−3.84	−2.70	1.38	−0.24	0.49	6.68	0.47	0.55	3.30
B3	−4.69	−3.78	−1.01	−2.79	−1.65	2.43	−0.30	0.42	6.62	0.06	0.14	2.89
C1	−5.37	−4.46	−1.69	−4.19	−3.05	1.03	0.01	0.73	6.93	−0.77	−0.69	2.06
C2	−7.75	−6.84	−4.07	−5.36	−4.22	−0.14	−0.30	0.42	6.61	−1.70	−1.62	1.13
C3	−2.65	−1.74	1.03	−6.23	−5.09	−1.02	−0.45	0.27	6.47	−0.13	−0.05	2.70
C4	−2.27	−1.36	1.41	−4.71	−3.56	0.51	−0.24	0.48	6.67	0.32	0.40	3.15
D1	−2.83	−1.92	0.85	−6.13	−4.99	−0.91	−0.39	0.33	6.53	−5.92	−5.84	−3.09
D2	−8.27	−7.36	−4.59	−7.58	−6.44	−2.36	−0.13	0.59	6.78	-	-	-
D3	−4.32	−3.41	−0.64	−8.19	−7.04	−2.97	0.00	0.72	6.91	−5.15	−5.07	−2.32
D4	−2.46	−1.56	1.22	−6.02	−4.87	−0.80	0.00	0.72	6.92	-	-	-
E1	−5.97	−5.06	−2.29	−5.30	−4.16	−0.09	−0.65	0.08	6.27	−2.79	−2.71	0.04
E2	−7.23	−6.32	−3.55	−4.84	−3.70	0.38	−0.25	0.48	6.67	−2.07	−1.98	0.76
Min	−8.27	−7.36	−4.59	−8.19	−7.04	−2.97	−0.65	0.08	6.27	−5.92	−5.84	−3.09
Max	−1.04	−0.13	2.64	−2.79	−1.65	2.43	0.01	0.73	6.93	0.47	0.55	3.30
Avg	−4.24	−3.34	−0.56	−4.76	−3.62	0.46	−0.26	0.47	6.66	−1.57	−1.49	1.26

Stations	Zn		
	crust	regional	core
A1	−3.02	−3.00	0.27
A2	−2.36	−2.33	0.93
A3	−2.25	−2.23	1.03
A4	−1.61	−1.59	1.67
A5	−0.96	−0.93	2.33
B1	−1.54	−1.51	1.75
B2	−2.40	−2.37	0.89
B3	−2.04	−2.01	1.25
C1	−2.46	−2.43	0.83
C2	−3.78	−3.76	−0.49
C3	−1.22	−1.20	2.07
C4	−1.85	−1.82	1.44
D1	−2.16	−2.14	1.13
D2	−1.87	−1.85	1.42
D3	−1.72	−1.70	1.56
D4	−1.42	−1.39	1.87
E1	−3.82	−3.79	−0.53
E2	−2.98	−2.95	0.31
Min	−3.82	−3.79	−0.53
Max	−0.96	−0.93	2.33
Avg	−2.19	−2.17	1.10